

# **Phytochemical and Pharmacological Studies on *Hibiscus sabdariffa* and *Polygonum salicifolium***

A thesis presented in fulfilment of the requirements for the  
degree of

**Doctor of Philosophy**

By

**Ahmed Mohammed Zheoat**

**2019**

Strathclyde Institute of Pharmacy and Biomedical Science

**University of Strathclyde  
Glasgow, United Kingdom**

## **Declaration**

This thesis is the result of the author's original research. It has been composed by the author and has not been previously submitted for examination which has led to the award of a degree.

The copyright of this thesis belongs to the author under the terms of the United Kingdom copyright Acts as qualified by University of Strathclyde Regulation 3.49.

Due acknowledgement must always be made of the use of any material contained in, or derived from, this thesis.

Signed:

Date:

*Dedicated to my family*

\*\*\*\*\*

## Acknowledgements

First and foremost, I would like to express my gratitude to Allah (SWT) for blessing me and giving me strength to complete this study. I would like to express my sincere gratitude and appreciation to my Supervisors: *Dr. Valerie Ferro, Dr. Robert Drummond, and Prof. Alexander Gray*, for their inspiration, moral support and encouragement, during the entire period of this research and also for their guidance, and patience during this project, perseverance which paved a successful way for my work. My sincere thanks also goes to *Prof. John Igoli* for his valuable time, knowledge and support. I would also like to thank my lab members for their support and encouragement during the project work. I am grateful to *Dr. Alan Kennedy* for carrying out the X-Ray crystallography of the compounds isolated in this study, and for his help in the publication of the paper. Great thanks to *Dr. Tong Zhang* and *Dr. Christopher Lawson* for their assistance in MS experiments. I am also grateful to all members of the BPU for their efforts to provide us with experimental material. I am grateful to *Mr. Craig Irving* for helping me out with NMR experiments.

My acknowledgements also go to the Ministry of Higher Education and Scientific Research in Iraq for awarding me the scholarship and providing me with the opportunity to study abroad to undertake my PhD degree in the United Kingdom. My deepest gratitude and sincere deep thanks goes to my Wife for her moral support and tolerating the pressure with me. Finally, I would like to express my deepest gratitude to all members of my family in particular my brother for strong encouragement of my academic endeavours over the years and supporting me at all times.

## Abstract

Medicinal plants are an important resource for the discovery of new and potent therapeutic compounds. *Hibiscus sabdariffa* (Malvaceae) is a plant that is widely recognised for its antihypertensive properties; however the constituent(s) responsible for this biological activity are presently unknown. The aim of this study was to identify the potential compounds that are responsible for the vasorelaxant activity of *Hibiscus sabdariffa*. A second aim was to determine whether the aquatic plant, *Polygonum salicifolium* (Polygonaceae) has vasorelaxant activity. Thereafter, the mechanisms involved in producing the vasorelaxation were investigated. The plants were subjected to hot solvent extraction in a sequential manner (72 h each) with n-hexane, ethyl acetate and methanol using a Soxhlet apparatus. The methanolic extract was subjected to bioassay-guided fractionation in order to isolate pure compounds and determine their vasorelaxant activity. The vascular effects of the crude methanolic extracts, sub-fractions, and pure compounds were studied on the rat aorta *in vitro* using myography techniques. In this study, hibiscus acid has been isolated as one of the main organic acids of *Hibiscus sabdariffa*. Parallel studies were also carried out with garcinia acid, which is a diastereoisomer of hibiscus acid and is commercially available. Hibiscus acid produced a concentration-dependent relaxation of the aorta pre-contracted with either phenylephrine (3  $\mu$ M) or KCl (60 mM), irrespective of the presence or absence of the endothelium. When the tissue was pre-contracted with phenylephrine, the concentration required to produce 50% relaxation ( $IC_{50}$ ), was  $0.09 \pm 0.01$  mg/ml. Moreover, garcinia acid was found to have an almost identical vasorelaxant effect. When the aorta was pre-contracted with the  $Ca^{2+}$  channel activator Bay K8644 (1,4-dihydro-2,6-dimethyl-5-nitro-4-(2-[trifluoromethyl] phenyl) pyridine-3-carboxylic

acid methyl ester or FPL 64176 (2,5-dimethyl-4-[2-(phenylmethyl) benzoyl]-1H-pyrrole-3-carboxylic acid methyl ester), both hibiscus and garcinia acid were able to produce almost complete relaxation. Hibiscus acid had no effect on the phasic contraction induced by phenylephrine in  $\text{Ca}^{2+}$ -free physiological solution; but it did affect the component of the contraction that is due to  $\text{Ca}^{2+}$  influx. Previous studies have showed that the crude extracts of *H. sabdariffa* have negative inotropic activity and relaxant effects on the tracheal tissues. Therefore, it was plausible to determine whether hibiscus acid has similar effects. Both hibiscus and garcinia acid, at a concentration of 0.6 mg/ml almost completely relaxed the electrically evoked contraction of the rat atria. Furthermore, both organic acids produced a concentration-dependent relaxation of the rat trachea, pre-contracted with either carbachol (1  $\mu\text{M}$ ) or KCl (60 mM). The vasorelaxant action of both compounds appears to be through inhibition of extracellular calcium influx, most likely by inhibition of voltage-dependent  $\text{Ca}^{2+}$  channels. There may be a slight modulatory role of the endothelium in the action of these substances; but the endothelium is not essential for the vasorelaxant response.

With regard to the activity of *Polygonum salicifolium*, the crude methanolic extract of this plant produced a concentration-dependent relaxation of the aorta pre-contracted with phenylephrine. The  $\text{IC}_{50}$  was  $0.04 \pm 0.007$  mg/ml and the extract caused complete relaxation of the aorta. The vasorelaxant activity of the crude extract was completely inhibited upon removal of the endothelium. Also, the crude extract was unable to relax the aorta when it was pre-contracted with KCl (60 mM).

In conclusion, the diastereomers, hibiscus acid and garcinia acid were demonstrated to cause vasorelaxation in a similar manner. This thesis also reported for the first time the vasorelaxant activity of the medicinal plant *Polygonum salicifolium*, and the vasorelaxant action of this plant appears to be mediated through an endothelium-dependent mechanism.

## List of Contents

<b>Declaration.....</b>	<b>I</b>
<b>Acknowledgements.....</b>	<b>III</b>
<b>Abstract.....</b>	<b>IV</b>
<b>List of Contents .....</b>	<b>VII</b>
<b>List of Figures.....</b>	<b>XI</b>
<b>List of Tables .....</b>	<b>XVI</b>
<b>List of Spectra.....</b>	<b>XVIII</b>
<b>List of Publications and Presentations .....</b>	<b>XXIV</b>
<b>List of Abbreviations .....</b>	<b>XXV</b>
<b>1      Introduction.....</b>	<b>1</b>
1.1 <i>Hibiscus sabdariffa</i> (Malvaceae).....	2
1.1.1 <i>Chemical composition of H. sabdariffa</i> .....	4
1.1.2 <i>Pharmacological activity</i> .....	12
1.1.3 <i>Toxicity of H. sabdariffa</i> .....	30
1.2 <i>Polygonum salicifolium</i> (Polygonaceae) .....	31
1.3      Smooth muscle and cardiac muscle physiology .....	36
1.3.1 <i>Smooth muscle cell contraction</i> .....	36
1.3.2 <i>Smooth muscle cell relaxation</i> .....	40
1.3.3 <i>Cardiac excitation-contraction coupling</i> .....	43
1.4      Project aims .....	46
<b>2      Materials and Methods.....</b>	<b>47</b>
2.1      Solvents .....	47

2.2	Apparatus, reagents, and chemicals.....	47
2.3	Equipment.....	48
2.4	Plant Material .....	49
2.4.1	<i>Extraction method</i> .....	49
2.5	Separation techniques .....	49
2.5.1	<i>Thin layer chromatography</i> .....	49
2.5.2	<i>Preparative thin layer chromatography</i> .....	50
2.5.3	<i>Gel permeation chromatography</i> .....	52
2.5.4	<i>Vacuum liquid chromatography</i> .....	52
2.5.5	<i>Silica gel column chromatography</i> .....	53
2.6	Spectroscopic examination .....	56
2.6.1	<i>Nuclear magnetic resonance spectroscopy</i> .....	56
2.6.2	<i>Liquid chromatography-Mass spectrometry (LC-MS)</i> .....	57
<b>3</b>	<b>Phytochemical and pharmacological studies of <i>H. sabdariffa</i></b> .....	<b>58</b>
3.1	Introduction .....	58
3.2	Materials and Methods .....	59
3.2.1	<i>Fractionation of <i>H. sabdariffa</i> crude extracts</i> .....	59
3.2.2	<i>Drugs, solvents and chemicals</i> .....	62
3.2.3	<i>Aorta preparation and contractile studies</i> .....	62
3.2.4	<i>Effect of PE and KCl on the rat aorta</i> .....	63
3.2.5	<i>Effects of the crude, and sub-fractions from the methanolic extract of <i>H. sabdariffa</i> on the rat aorta</i> .....	63
3.3	Statistical analysis .....	65
3.4	Results .....	65
3.4.1	<i>Phytochemical Results</i> .....	65
3.4.2	<i>Vasorelaxant effects of the methanolic extract of <i>H. sabdariffa</i></i> .....	76
3.5	Discussion.....	84

## **4 Phytochemical and pharmacological studies of hibiscus acid..... 87**

4.1	Introduction .....	87
4.2	Materials and Methods .....	91
4.2.1	<i>X-ray crystallography</i> .....	91
4.2.2	<i>Drugs, solvents and chemicals</i> .....	96
4.2.3	<i>Aorta and tracheal tissue preparation and contractile studies</i> .....	96
4.2.4	<i>Effects of hibiscus acid and garcinia acid on the rat aorta</i> .....	97
4.2.5	<i>Role of L-type voltage-dependent calcium channels on hibiscus acid and garcinia acid-induced relaxation</i> .....	98
4.2.6	<i>Effect of hibiscus acid and garcinia acid on the release of intracellular <math>Ca^{2+}</math></i> .....	98
4.2.7	<i>Effect of hibiscus acid and garcinia acid on the influx of extracellular <math>Ca^{2+}</math></i> .....	99
4.2.8	<i>Effect of blocking potassium channels on the relaxant activity of hibiscus acid and garcinia acid</i> .....	99
4.2.9	<i>Effect of hibiscus acid and garcinia acid on the rat left atria</i> .....	100
4.2.10	<i>Concentration-response curves to carbachol and KCl on the rat trachea</i> .....	101
4.2.11	<i>Effects of hibiscus acid and garcinia acid on the rat trachea</i> .....	101
4.3	Results .....	102
4.3.1	<i>Phytochemical results</i> .....	102
4.3.2	<i>Vasorelaxant effects of hibiscus and garcinia acids</i> .....	140
4.4	Discussion.....	177

## **5 Phytochemical and pharmacological studies of *P. salicifolium*..... 188**

5.1	Introduction .....	188
5.2	Materials and Methods .....	189
5.2.1	<i>Fractionation of the crude extracts of <i>P. salicifolium</i></i> .....	189
5.2.2	<i>Drugs, solvents and chemicals</i> .....	190
5.2.3	<i>Effects of the crude methanolic extract of <i>P. salicifolium</i> on the rat aorta</i> .....	190
5.3	Results .....	191

5.3.1	<i>Phytochemical results</i> .....	191
5.3.2	<i>Vasorelaxant effects of the methanolic extract of <i>H. sabdariffa</i></i> .....	230
5.4	Discussion.....	236
<b>6</b>	<b>General discussion</b> .....	<b>239</b>
6.1	Recommendations for future work .....	243
6.2	Conclusion.....	244
<b>7</b>	<b>References</b> .....	<b>245</b>

## List of Figures

<b>Figure 1.1: (A) The growing plant of <i>H. sabdariffa</i>, stems, leaves, and calyces. (B) The dried calyces of <i>H. sabdariffa</i>.....</b>	<b>3</b>
<b>Figure 1.2: Aerial parts of <i>P. salicifolium</i>. .....</b>	<b>32</b>
<b>Figure 1.3: Mechanisms regulating smooth muscle contraction. .....</b>	<b>39</b>
<b>Figure 1.4: Mechanisms controlling smooth muscle relaxation.....</b>	<b>42</b>
<b>Figure 1.5: Schematic diagram of excitation-contraction coupling in a cardiomyocyte.....</b>	<b>45</b>
<b>Figure 2.1: Soxhlet apparatus. .....</b>	<b>51</b>
<b>Figure 2.2: Photograph showing the gel permeation column (GPC) for chromatographic separation of the methanol extract of calyces of <i>H. sabdariffa</i>. .....</b>	<b>54</b>
<b>Figure 3.1: Thin layer chromatography (TLC) of the (A) n-hexane, (B) ethyl acetate (EtOAc), and (C) methanol (MeOH) crude extracts.....</b>	<b>61</b>
<b>Figure 3.2: The organ bath set up. .....</b>	<b>64</b>
<b>Figure 3.3: Structure of (A) <math>\beta</math>-sitosterol, and (B) stigmasterol. .....</b>	<b>74</b>
<b>Figure 3.4: Concentration-response curve to phenylephrine (PE) on the rat aorta. .....</b>	<b>78</b>
<b>Figure 3.5: Concentration-response curve to potassium chloride (KCl) on the rat aorta.....</b>	<b>79</b>
<b>Figure 3.6: Relaxant effect of the crude methanolic extract of <i>H. sabdariffa</i> (HSM) on the rat aorta pre-contracted with PE. ....</b>	<b>80</b>
<b>Figure 3.7: Relaxant effect of the crude methanolic extract of <i>H. sabdariffa</i> (HSM) on the rat aorta pre-contracted with KCl.....</b>	<b>81</b>

<b>Figure 3.8: Relaxant effect of the sub-fractions (HS-F) of the crude methanolic extract of <i>H. sabdariffa</i> on the rat aorta pre-contracted with PE.....</b>	<b>82</b>
<b>Figure 3.9: Relaxant effect of the sub-fractions (HS-F) of the crude methanolic extract of <i>H. sabdariffa</i> on the rat aorta pre-contracted with PE.....</b>	<b>83</b>
<b>Figure 4.1: Chemical structure of garcinia acid.....</b>	<b>92</b>
<b>Figure 4.2: Chemical structure of hibiscus acid dimethyl ester.....</b>	<b>103</b>
<b>Figure 4.3: The molecular structures of the two independent molecules comprising the asymmetric unit of hibiscus acid dimethyl ester.....</b>	<b>111</b>
<b>Figure 4.4: A section of the extended structure of hibiscus acid dimethyl ester showing the hydrogen bond contacts along the (a) axis. ....</b>	<b>111</b>
<b>Figure 4.5: Chemical structure of hibiscus acid.....</b>	<b>112</b>
<b>Figure 4.6: The molecular structure of hibiscus acid, with the atom labelling.</b>	<b>122</b>
<b>Figure 4.7: Hydrogen bond contacts in hibiscus acid. ....</b>	<b>122</b>
<b>Figure 4.8: The crystal packing of hibiscus acid, viewed along the (a) axis. ....</b>	<b>123</b>
<b>Figure 4.9: Chemical structure of hibiscus acid-6-methyl ester. ....</b>	<b>124</b>
<b>Figure 4.10: Chemical structure of quercetin.....</b>	<b>132</b>
<b>Figure 4.11: Effect of carbachol on rat aorta pre-contracted with PE. ....</b>	<b>142</b>
<b>Figure 4.12: Relaxant effect of hibiscus acid (HA) on rat aorta pre-contracted with PE. ....</b>	<b>143</b>
<b>Figure 4.13: Relaxant effect of hibiscus acid (HA) on rat aorta pre-contracted with PE. ....</b>	<b>144</b>
<b>Figure 4.14: Relaxant effect of hibiscus acid (HA) on rat aorta pre-contracted with PE in absence or presence of L-NAME. ....</b>	<b>145</b>

<b>Figure 4.15: Relaxant effect of garcinia acid (GA) on rat aorta pre-contracted with PE.....</b>	<b>147</b>
<b>Figure 4.16: Relaxant effect of garcinia acid (GA) on rat aorta pre-contracted with PE.....</b>	<b>148</b>
<b>Figure 4.17: Relaxant effect of garcinia acid (GA) on rat aorta pre-contracted with PE in absence or presence of L-NAME.....</b>	<b>149</b>
<b>Figure 4.18: Relaxant effect of hibiscus acid (HA) on rat aorta pre-contracted with KCl.....</b>	<b>151</b>
<b>Figure 4.19: Relaxant effect of hibiscus acid (HA) on rat aorta pre-contracted with KCl.....</b>	<b>152</b>
<b>Figure 4.20: Relaxant effect of garcinia acid (GA) on rat aorta pre-contracted with KCl.....</b>	<b>153</b>
<b>Figure 4.21: Relaxant effect of garcinia acid (GA) on rat aorta pre-contracted with KCl.....</b>	<b>154</b>
<b>Figure 4.22: Relaxant effect of hibiscus acid (HA) and garcinia acid (GA), on rat aorta pre-contracted with an L-type calcium channel activator.....</b>	<b>156</b>
<b>Figure 4.23: Effect of hibiscus acid (HA) and garcinia acid (GA) on the phasic component of contraction induced by PE (3 <math>\mu</math>M) in rat aorta.....</b>	<b>158</b>
<b>Figure 4.24: Relaxant effect of hibiscus (HA) and garcinia acid (GA) on the sustained component of the PE-induced contraction.....</b>	<b>159</b>
<b>Figure 4.25: The effect of potassium channel blockade on the relaxation induced by hibiscus acid (HA) on PE pre-contracted rat aorta.....</b>	<b>161</b>
<b>Figure 4.26: The effect of selective calcium activated potassium channel blockade on relaxation induced by hibiscus acid (HA) on PE pre-contracted rat aorta.</b>	<b>162</b>

<b>Figure 4.27: The effect of potassium channel blockade on relaxation induced by garcinia acid (GA) on PE pre-contracted rat aorta.....</b>	<b>163</b>
<b>Figure 4.28: The effect of selective calcium activated potassium channel blockade on relaxation induced by garcinia acid (GA) on PE pre-contracted rat aorta.</b>	<b>164</b>
<b>Figure 4.29: Effect of hibiscus acid (HA) on the electrically stimulated rat left atrium.....</b>	<b>166</b>
<b>Figure 4.30: Effect of garcinia acid (GA) on the electrically stimulated rat left atrium.....</b>	<b>167</b>
<b>Figure 4.31: Summary figure showing % inhibitory effect of (A) hibiscus acid (HA) and (B) garcinia acid (GA) on the electrically stimulated rat left atrium.</b>	<b>168</b>
<b>Figure 4.32: Concentration-response curve to carbachol on the rat trachea...</b>	<b>170</b>
<b>Figure 4.33: Concentration-response curve to KCl on the rat trachea.....</b>	<b>171</b>
<b>Figure 4.34: Relaxant effect of hibiscus acid (HA) and garcinia acid (GA) on rat trachea pre-contracted with carbachol .....</b>	<b>172</b>
<b>Figure 4.35: Relaxant effect of hibiscus acid (HA) and garcinia acid (GA) on rat trachea pre-contracted with carbachol .....</b>	<b>173</b>
<b>Figure 4.36: Relaxant effect of hibiscus acid and garcinia acid on rat trachea pre-contracted with KCl.....</b>	<b>175</b>
<b>Figure 4.37: Relaxant effect of hibiscus acid (HA) and garcinia acid (GA) on rat trachea pre-contracted with KCl.....</b>	<b>176</b>
<b>Figure 5.1: Chemical structure of 2',4'-dimethoxy-6'-hydroxychalcone.....</b>	<b>194</b>
<b>Figure 5.2: Chemical structure of 2',5'-dimethoxy-4',6'-dihydroxychalcone..</b>	<b>203</b>
<b>Figure 5.3: Chemical structure of 5,7-dimethoxyflavanone.....</b>	<b>212</b>

<b>Figure 5.4: Chemical structure of 5,8-dimethoxy-7-hydroxyflavanone.....</b>	<b>221</b>
<b>Figure 5.5: Relaxant effect of the crude methanolic extract of <i>P. salicifolium</i> (PSM) on the endothelium-intact rat aorta pre-contracted with PE (3 <math>\mu</math>M)....</b>	<b>232</b>
<b>Figure 5.6: Relaxant effect of the crude methanolic extract of <i>P. salicifolium</i> (PSM) on the endothelium-intact rat aorta pre-contracted with PE (3 <math>\mu</math>M)....</b>	<b>233</b>
<b>Figure 5.7: Effect of the crude methanolic extract of <i>P. salicifolium</i> (PSM) on the endothelium-denuded rat aorta pre-contracted with PE. ....</b>	<b>234</b>
<b>Figure 5.8: Effect of the crude methanolic extract of <i>P. salicifolium</i> (PSM) on the rat aorta pre-contracted with KCl.....</b>	<b>235</b>

## List of Tables

<b>Table 1.1: Selection of phytochemicals previously identified in <i>H. sabdariffa</i> .....</b>	<b>5</b>
<b>Table 1.2: Hypolipidemic effect of <i>H. sabdariffa</i> (clinical studies overview).....</b>	<b>17</b>
<b>Table 1.3: Hypolipidemic effect of <i>H. sabdariffa</i> (animal studies overview) .....</b>	<b>19</b>
<b>Table 1.4: Antihypertensive effect of <i>H. sabdariffa</i> (clinical studies overview)..</b>	<b>26</b>
<b>Table 1.5: Antihypertensive effect of <i>H. sabdariffa</i> (animal studies overview) ..</b>	<b>29</b>
<b>Table 1.6: Selection of phytochemicals previously isolated from <i>P. salicifolium</i></b>	<b>33</b>
<b>Table 2.1: Mobile phase systems used for vacuum liquid chromatography.....</b>	<b>55</b>
<b>Table 2.2: Mobile phase systems used for siliga gel chromatography .....</b>	<b>55</b>
<b>Table 4.1: Experimental details for hibiscus acid .....</b>	<b>93</b>
<b>Table 4.2: Experimental details for hibiscus acid dimethyl ester .....</b>	<b>94</b>
<b>Table 4.3: <math>^1\text{H}</math> (500MHz), <math>^{13}\text{C}</math> (100MHz), and HSQC data of hibiscus acid dimethyl ester in Acetone-<math>d_6</math>.....</b>	<b>108</b>
<b>Table 4.4: Hydrogen-bond geometry (<math>\text{\AA}</math>, <math>^\circ</math>) for hibiscus acid dimethyl- ester..</b>	<b>110</b>
<b>Table 4.5: <math>^1\text{H}</math> (500MHz), <math>^{13}\text{C}</math> (100MHz), COSY, HMBC and HSQC data of hibiscus acid in Acetone-<math>d_6</math> and DMSO-<math>d_6</math>.....</b>	<b>119</b>
<b>Table 4.6: Hydrogen-bond geometry (<math>\text{\AA}</math>, <math>^\circ</math>) for hibiscus acid .....</b>	<b>121</b>
<b>Table 4.7: <math>^1\text{H}</math> (500MHz), <math>^{13}\text{C}</math> (100MHz), and HSQC data of hibiscus acid-6-methyl ester in Acetone-<math>d_6</math>.....</b>	<b>131</b>
<b>Table 4.8: <math>^1\text{H}</math> (400MHz) and <math>^{13}\text{C}</math> (100MHz) and HMBC data of quercetin (3', 4', 3, 5, 7-pentahydroxyflavone) in Acetone-<math>d_6</math>.....</b>	<b>139</b>
<b>Table 5.1: NMR data for 2',4'-dimethoxy-6'-hydroxychalcone in Chloroform-<math>d</math> .....</b>	<b>202</b>

<b>Table 5.2: NMR data for 2',5'-dimethoxy-4',6'-dihydroxychalcone in chloroform-<i>d</i></b> .....	<b>211</b>
<b>Table 5.3: NMR data for 5,7-dimethoxyflavanone in chloroform-<i>d</i></b> .....	<b>220</b>
<b>Table 5.4: NMR data for 5,8-dimethoxy-7-hydroxyflavanone in chloroform-<i>d</i></b> .....	<b>229</b>

## List of Spectra

<b>Spectrum 3.1: <math>^1\text{H}</math> NMR spectrum (400 MHz) of the hexane crude extract of <i>H. sabdariffa</i> in Chloroform-<math>d</math>.....</b>	<b>68</b>
<b>Spectrum 3.2: <math>^1\text{H}</math> NMR spectrum (400 MHz) of the ethyl acetate crude extract of <i>H. sabdariffa</i> in DMSO-<math>d_6</math>.....</b>	<b>68</b>
<b>Spectrum 3.3: <math>^1\text{H}</math> NMR spectrum (400 MHz) of the crude methanolic extract of <i>H. sabdariffa</i> in DMSO-<math>d_6</math>.....</b>	<b>69</b>
<b>Spectrum 3.4: <math>^1\text{H}</math> NMR spectrum (400 MHz) of the sub-fraction F1 (HS-F1) of crude methanolic extract of <i>H. sabdariffa</i> in DMSO-<math>d_6</math>.....</b>	<b>69</b>
<b>Spectrum 3.5 : <math>^1\text{H}</math> NMR spectrum (400 MHz) of the sub-fraction F2 (HS-F2) of crude methanolic extract of <i>H. sabdariffa</i> in DMSO-<math>d_6</math>.....</b>	<b>70</b>
<b>Spectrum 3.6: <math>^1\text{H}</math> NMR spectrum (400 MHz) of the sub-fraction F3 (HS-F3) of crude methanolic extract of <i>H. sabdariffa</i> in DMSO-<math>d_6</math>.....</b>	<b>70</b>
<b>Spectrum 3.7: <math>^1\text{H}</math> NMR spectrum (400 MHz) of the sub-fraction F4 (HS-F4) of crude methanolic extract of <i>H. sabdariffa</i> in DMSO-<math>d_6</math>.....</b>	<b>71</b>
<b>Spectrum 3.8: <math>^1\text{H}</math> NMR spectrum (400 MHz) of the sub-fraction F5 (HS-F5) of crude methanolic extract of <i>H. sabdariffa</i> in DMSO-<math>d_6</math>.....</b>	<b>71</b>
<b>Spectrum 3.9: <math>^1\text{H}</math> NMR spectrum (400 MHz) of the VLC sub-fraction 2 of crude methanolic extract of <i>H. sabdariffa</i> (HS VLC2) in Acetone-<math>d_6</math>. .....</b>	<b>72</b>
<b>Spectrum 3.10: <math>^1\text{H}</math> NMR spectrum (400 MHz) of the VLC sub-fraction 3 (HS VLC3) of crude methanolic extract of <i>H. sabdariffa</i> in Acetone-<math>d_6</math>.....</b>	<b>72</b>
<b>Spectrum 3.11: <math>^1\text{H}</math> NMR spectrum (400 MHz) of the VLC sub-fraction 4 (HS VLC4) of crude methanolic extract of <i>H. sabdariffa</i> in Acetone-<math>d_6</math>.....</b>	<b>73</b>

<b>Spectrum 3.12: <math>^1\text{H}</math> NMR spectrum (400 MHz) of the VLC sub-fraction 5 (HS VLC5) of the crude methanolic extract of <i>H. sabdariffa</i> in Acetone-<math>d_6</math>.....</b>	73
<b>Spectrum 3.13: <math>^1\text{H}</math> NMR spectrum (400 MHz) of <math>\beta</math>-sitosterol and stigmasterol in Chloroform-<math>d</math>.....</b>	75
<b>Spectrum 4.1: Molecular ion peak [M-H]<math>^-</math> spectrum of hibiscus acid dimethyl ester.....</b>	<b>105</b>
<b>Spectrum 4.2: <math>^1\text{H}</math> NMR spectrum (400 MHz) of hibiscus acid dimethyl ester in Acetone-<math>d_6</math> .....</b>	<b>105</b>
<b>Spectrum 4.3: <math>^{13}\text{C}</math> (100 MHz) NMR spectrum of hibiscus acid dimethyl ester in Acetone-<math>d_6</math> .....</b>	<b>106</b>
<b>Spectrum 4.4: Cosy NMR spectrum (400 MHz) of hibiscus acid dimethyl ester in Acetone-<math>d_6</math> .....</b>	<b>106</b>
<b>Spectrum 4.5: HSQC (400 MHz, Acetone-<math>d_6</math>) spectrum of hibiscus acid dimethyl ester.....</b>	<b>107</b>
<b>Spectrum 4.6: HMBC (400 MHz, Acetone-<math>d_6</math>) spectrum of hibiscus acid dimethyl ester.....</b>	<b>107</b>
<b>Spectrum 4.7: Molecular ion peak [M-H]<math>^-</math> spectrum of hibiscus acid.....</b>	<b>115</b>
<b>Spectrum 4.8: <math>^1\text{H}</math> NMR spectrum (400 MHz) of hibiscus acid in Acetone-<math>d_6</math>. .</b>	<b>116</b>
<b>Spectrum 4.9: <math>^{13}\text{C}</math> (100 MHz) NMR spectrum of hibiscus acid in Acetone-<math>d_6</math>. 116</b>	
<b>Spectrum 4.10: Cosy NMR (400 MHz) spectrum of hibiscus acid in Acetone-<math>d_6</math>.</b>	
.....	117
<b>Spectrum 4.11: HSQC (400 MHz, Acetone-<math>d_6</math>) spectrum of hibiscus acid. ....</b>	<b>117</b>
<b>Spectrum 4.12: HMBC (400 MHz, Acetone-<math>d_6</math>) spectrum of hibiscus acid. ....</b>	<b>118</b>

<b>Spectrum 4.13: Molecular ion peak [M-H]<sup>-</sup> spectrum of the hibiscus acid-6-methyl ester.....</b>	<b>127</b>
<b>Spectrum 4.14: <sup>1</sup>H NMR spectrum (400 MHz) of the hibiscus acid-6-methyl ester in Acetone-<i>d</i><sub>6</sub>.....</b>	<b>128</b>
<b>Spectrum 4.15: <sup>13</sup>C NMR (100 MHz) spectrum of the hibiscus acid-6-methyl ester in Acetone-<i>d</i><sub>6</sub>.....</b>	<b>128</b>
<b>Spectrum 4.16: COSY NMR (400 MHz) spectrum of hibiscus acid-6-methyl ester in Acetone-<i>d</i><sub>6</sub>.....</b>	<b>129</b>
<b>Spectrum 4.17: HSQC (400 MHz, Acetone-<i>d</i><sub>6</sub>) spectrum of hibiscus acid-6-methyl ester.....</b>	<b>129</b>
<b>Spectrum 4.18: HMBC (400 MHz, Acetone-<i>d</i><sub>6</sub>) spectrum of hibiscus acid-6-methyl ester.....</b>	<b>130</b>
<b>Spectrum 4.19: Molecular ion peak [M-H]<sup>-</sup> spectrum of quercetin .....</b>	<b>135</b>
<b>Spectrum 4.20: <sup>1</sup>H NMR spectrum (400 MHz) of the quercetin in Acetone-<i>d</i><sub>6</sub>.136</b>	
<b>Spectrum 4.21: <sup>13</sup>C NMR (100 MHz) spectrum of the quercetin in Acetone-<i>d</i><sub>6</sub>.</b>	
.....	<b>136</b>
<b>Spectrum 4.22: COSY NMR spectrum (400 MHz, Acetone-<i>d</i><sub>6</sub>) of quercetin... 137</b>	
<b>Spectrum 4.23: HSQC (400 MHz, Acetone-<i>d</i><sub>6</sub>) spectrum of quercetin. .... 137</b>	
<b>Spectrum 4.24: (A) Full and (B) selected expansion of HMBC spectrum (400 MHz) of quercetin in Acetone-<i>d</i><sub>6</sub>. .... 138</b>	
<b>Spectrum 5.1: <sup>1</sup>H NMR spectrum (400 MHz) of (A) the crude methanolic extract of <i>P. salicifolium</i> and (B) Fraction 2 from the VLC of crude methanolic extract of <i>P. salicifolium</i> (VLC F 2) in DMSO-<i>d</i><sub>6</sub>. .... 192</b>	

<b>Spectrum 5.2: <math>^1\text{H}</math> NMR spectrum (400 MHz) of (A) sub-fraction (PSM-F9) of crude methanolic extract of <i>P. salicifolium</i> in Acetone-<math>d_6</math>, and (B) sub-fraction 11 (PSM-F11) of crude methanolic extract of <i>P. salicifolium</i> in DMSO-<math>d_6</math>.</b>	193
<b>Spectrum 5.3: Molecular ion peak [M-H]<math>^+</math> spectrum of 2',4'-dimethoxy-6'-hydroxychalcone.....</b>	195
<b>Spectrum 5.4: (A) Full and (B) selected expansion of <math>^1\text{H}</math> NMR spectrum (400 MHz) of 2',4'-dimethoxy-6'-hydroxychalcone in Chloroform-<math>d</math>.</b>	197
<b>Spectrum 5.5: (A) Full and (B) selected expansion of COSY spectrum (400 MHz) of 2',4'-dimethoxy-6'-hydroxychalcone in Chloroform-<math>d</math>.</b>	198
<b>Spectrum 5.6: (A) Full and (B) selected expansion of <math>^{13}\text{C}</math> NMR spectrum (100 MHz) of 2',4'-dimethoxy-6'-hydroxychalcone in Chloroform-<math>d</math>.</b>	199
<b>Spectrum 5.7: (A) Full and (B) selected expansion of HMBC spectrum (400 MHz) of 2',4'-dimethoxy-6'-hydroxychalcone in Chloroform-<math>d</math>.</b>	200
<b>Spectrum 5.8: (A) Full and (B) selected expansion of HSQC spectrum (400 MHz) of 2',4'-dimethoxy-6'-hydroxychalcone in Chloroform-<math>d</math>.</b>	201
<b>Spectrum 5.9: Molecular ion peak [M-H]<math>^+</math> spectrum of 2',5'-dimethoxy-4',6'-dihydroxychalcone.</b>	204
<b>Spectrum 5.10: (A) Full <math>^1\text{H}</math> NMR spectrum (500 MHz) of 2',5'-dimethoxy-4',6'-dihydroxychalcone with (B) selected expansion of the aromatic region in Chloroform-<math>d</math>.</b>	206
<b>Spectrum 5.11: (A) Full and (B) selected expansion of COSY spectrum (500 MHz) of 2',5'-dimethoxy-4',6'-dihydroxychalcone in Chloroform-<math>d</math>.</b>	207

<b>Spectrum 5.12: (A) Full and (B) selected expansion of DEPTq 135 <math>^{13}\text{C}</math> NMR spectrum (100 MHz) of 2',5'-dimethoxy-4',6'-dihydroxychalcone in Chloroform-<i>d</i>.</b>	208
<b>Spectrum 5.13: (A) Full and (B) selected expansion of HMBC spectrum (500 MHz) of 2',5'-dimethoxy-4',6'-dihydroxychalcone in Chloroform-<i>d</i>.</b>	209
<b>Spectrum 5.14: (A) Full and (B) selected expansion of HSQC spectrum (500 MHz) of 2',5'-dimethoxy-4',6'-dihydroxychalcone in Chloroform-<i>d</i>.</b>	210
<b>Spectrum 5.15: Molecular ion peak [M-H]<math>^+</math> spectrum of 5,7-dimethoxyflavan-one.</b>	213
<b>Spectrum 5.16: (A) Full with (B) selected expansion of <math>^1\text{H}</math> NMR spectrum (400 MHz) of 5,7-dimethoxyflavanone in Chloroform-<i>d</i>.</b>	215
<b>Spectrum 5.17: (A) Full and (B) selected expansion of COSY spectrum (400 MHz) of 5,7-dimethoxyflavanone in Chloroform-<i>d</i>.</b>	216
<b>Spectrum 5.18: (A) Full and (B) selected expansion of DEPTq 135 <math>^{13}\text{C}</math> NMR spectrum (100 MHz) of 5,7-dimethoxyflavanone in Chloroform-<i>d</i>.</b>	217
<b>Spectrum 5.19: (A) Full and (B) selected expansion of HMBC spectrum (400 MHz) of 5,7-dimethoxyflavanone in Chloroform-<i>d</i>.</b>	218
<b>Spectrum 5.20: (A) Full and (B) selected expansion of HSQC spectrum (400 MHz) of 5,7-dimethoxyflavanone in Chloroform-<i>d</i>.</b>	219
<b>Spectrum 5.21: Molecular ion peak [M-H]<math>^+</math> spectrum of 5,8-dimethoxy-7-hydroxyflavanone.</b>	222
<b>Spectrum 5.22: (A) Full <math>^1\text{H}</math> NMR spectrum (400 MHz) of 5,8-dimethoxy-7-hydroxyflavanone and (B) selected expansion of the two methoxy region in Chloroform-<i>d</i>.</b>	224

<b>Spectrum 5.23: (A) Full with (B) Selected expansion of COSY spectrum (400 MHz) of 5,8-dimethoxy-7-hydroxyflavanone in Chloroform-<i>d</i>.</b>	225
<b>Spectrum 5.24: (A) Full DEPTq 135 <math>^{13}\text{C}</math> NMR spectrum (100 MHz) of 5,8-dimethoxy-7-hydroxyflavanone with selected expansion of the ring-B in Chloroform-<i>d</i>.</b>	226
<b>Spectrum 5.25: (A) Full HMBC spectrum (400 MHz) and (B) selected expansion of the methoxy peaks of 5,8-dimethoxy-7-hydroxyflavanone in Chloroform-<i>d</i>.</b>	227
<b>Spectrum 5.26: (A) Full and (B) selected expansion of HSQC spectrum (400 MHz) of 5,8-dimethoxy-7-hydroxyflavanone in Chloroform-<i>d</i>.</b>	228

## List of Publications and Presentations

Some of the work contained in this thesis has been the subject of, or is related to the following publications or presentations:

Zheoat, A.M., Gray, A.I., Igoli, J.O., Kennedy, A.R., & Ferro, V.A. 2017. Crystal structures of hibiscus acid and hibiscus acid dimethyl ester isolated from *Hibiscus sabdariffa* (Malvaceae). *Acta Crystallographica Section E: Crystallographic Communications*, 73, 1368-1371.

Zheoat, A.M., Gray, A.I., Igoli, J.O., Ferro, V.A., & Drummond, R.M., 2018. Hibiscus acid from *Hibiscus sabdariffa* (Malvaceae) has a vasorelaxant effect on the rat aorta. *Fitoterapia* 134 (2019) 5-13.

### Conference proceedings

Ahmed M Zheoat, Robert M Drummond., Valerie A Ferro., 2018. Mechanism of the vasorelaxant effect of hibiscus acid from *Hibiscus sabdariffa* on the rat aorta. Trends in Natural Product Research-PSE Young Scientists' Meeting 2018 Advances in Phytochemical Analysis (PSE-YSM), Liverpool John Moores University, UK.

Ahmed M Zheoat, Robert M Drummond., Valerie A Ferro., 2018. *In vitro* relaxant and negative inotropic effects of hibiscus acid on the rat trachea and heart atria. International Pharmaceutical Federation (FIP) World Congress 2018, Glasgow, Scotland.

## List of Abbreviations

AC	Adenylyl cyclase
<sup>13</sup> C	<sup>13</sup> Carbon
cAMP	Cyclic adenosine monophosphate
CAT	Catalase
CC	Column chromatography
IC <sub>50</sub>	Concentration required to produce 50% of the maximum inhibitory effect
cGMP	Cyclic guanosine monophosphate
COSY	<sup>1</sup> H- <sup>1</sup> H Correlation spectroscopy
DAG	Diacylglycerol
DNA	Deoxyribonucleic acid
EDRFs	Endothelial-derived relaxing factors
GPC	Gel permeation chromatography
GPCRs	G-protein coupled receptors
GSH	Glutathione
GST	Glutathione-S- transferase
GC	guanylate cyclase
HDL	High density lipoprotein
HMBC	Heteronuclear multiple bond correlation
HMG-CoA reductase	3-hydroxy-3-methyl-glutaryl-CoA reductase
HPLC	High pressure liquid chromatography
HSQC	Heteronuclear single quantum coherence
HepG <sub>2</sub>	Human liver carcinoma cells
H <sub>2</sub> O <sub>2</sub>	Hydrogen peroxide
IP <sub>3</sub>	Inositol-1, 4, 5 triphosphate
LC	Liquid chromatography
LP	Lipid peroxidation
LDL	Low density lipoprotein
MDA	Malondialdehyde
MS	Mass spectroscopy
LD <sub>50</sub>	Median lethal dose
MLC	Myosin light chain

MLCK	Myosin light chain kinase
MLCP	Myosin light chain phosphatase
NCX	Sodium/calcium exchanger
NHE	Sodium/proton exchanger
NO	Nitric oxide
NMR	Nuclear magnetic resonance
PLC $\beta$	Phospholipase C $\beta$
PIP <sub>2</sub>	Phosphatidylinositol (4,5) bisphosphate
PKA	Protein kinase A
PKC	Protein kinase C
PKG	Protein kinase G
$^1\text{H}$	Proton
ROS	Reactive oxygen species
R <sub>f</sub>	Retardation factor
RYRs	Ryanodine receptors
SERCA	Sarco-endoplasmic reticulum calcium ATPase
SOD	Superoxide dismutase
t-BHP	Tertiary butyl hydroperoxide
TLC	Thin layer chromatography
TOF	Time of Flight
TC	Total cholesterol
TG	Triglycerides
VDCCs	Voltage-dependent calcium channels
VLC	Vacuum liquid chromatography
VLDL	Very low density lipoprotein

# ***Chapter 1***

## **1 Introduction**

Medicinal plants have been used for the alleviation of many diseases since early human history as reviewed by Savithramma *et al.* (2011). Traditional medicines utilise a wide range of medicinal plant species (Compean and Ynalvez, 2014), and these plants are rich sources of naturally occurring bioactive compounds (Savithramma *et al.*, 2011). In fact, natural products or their derivatives form the basis of many of the currently available drugs, for example salicin (which is the historical origin of aspirin), from willow tree bark, *Salix alba*, digoxin from *Digitalis lanata*, morphine from opium (*Papaver somniferum*), and the anticancer drug paclitaxel derived from the Pacific yew tree, *Taxus brevifolia* (Mathur and Hoskins, 2017).

The popularity of herbal medicine consumption for the prevention and treatment of many ailments is ascribed to the general belief that these traditional medicinal plants are safer, have fewer side effects and are more readily accessible than synthetic medicines (Savithramma *et al.*, 2011). However, researchers are struggling to document the scientific benefits of these plants as medicines. This is because of various difficulties encountered, such as limited quantities of naturally available plants and inadequate measurements of the plant bioactivities as different compounds are contained in one plant. These compounds need to be separated and purified to correlate a specific biological activity to a particular compound and to avoid the interactions that may occur as a result of compound mixtures. In addition, these compounds are

often chemically unstable and are difficult to formulate due to their poor pharmaceutical properties (McChesney *et al.*, 2007).

Phytochemical studies of medicinal plants have displayed high concentrations of common compounds, including alkaloids, tannins, flavonoids, glycosides and saponins, whilst, at the same time, revealing diverse biological activities (Compean and Ynalvez, 2014). Therefore, phytochemicals isolated from traditional medicinal plants may lead to discovery of novel drugs (Amor *et al.*, 2009). This thesis will investigate compounds isolated from the plants *Hibiscus sabdariffa* (*H. sabdariffa*) and *Polygonum salicifolium* (*P. salicifolium*), which have been and are still used in traditional medicine (Calis *et al.*, 1999, Hussein and Mohamed, 2013, Hussein *et al.*, 2017).

## **1.1 *Hibiscus sabdariffa* (Malvaceae)**

*Hibiscus sabdariffa* (*H. sabdariffa*) Linn is a species of hibiscus from the Malvaceae family. This plant, which is an annual, perennial herb or subshrub, is broadly cultivated in Africa, Asia and other areas to make jams, as well as beverages (Bolade *et al.*, 2009). The calyces of *H. sabdariffa* are traditionally used worldwide as a herbal tea or cold drink, and this has the common name ‘Karkade’ or ‘Zoborodo’ in Egypt and Sudan; ‘Red sorrel’ or ‘Roselle’ in English; ‘Jamaica’ or ‘Aqua de Jamaica’ in Mexico; ‘Gongura’ in Hindi and ‘Pulicha Keerai’ in Tamil (Ali *et al.*, 2005, Kuriyan *et al.*, 2010).

The plant is characterised by red, smooth, and cylindrical stalks about 2.4 metres in length. The leaves are typically green with reddish veins and are simple except for the

lower leaves, which are divided into three, five or sometimes seven deep lobes, each around 7.5-12.5 cm long (Da-Costa-Rocha *et al.*, 2014). The flowers are white or yellow with a maroon basal spot. The cup-shaped calyces (**Figure 1.1**) are typically bright red in colour, and 3-3.5 cm wide for the mature calyx, which consists of large sepals and the epicalyx (a collar). The seed capsules turn brown and split open on drying or maturation.

In traditional medicine, extracts of *H. sabdariffa* are commonly used for their hypotensive and diuretic effects and to lower body temperature, blood viscosity, and to relieve coughs and sore throats as reviewed by Da-Costa-Rocha *et al.* (2014). Leaves of the plant are used as an emollient in the treatment of wounds and sores. In India, seed decoctions are prescribed to relieve dysuria and digestion problems, whilst in Iran, hibiscus sour tea is used widely in the treatment of hypertension as reviewed by Ali *et al.* (2005) and Da-Costa-Rocha *et al.* (2014).

**A**



**B**



**Figure 1.1:** (A) The growing plant of *H. sabdariffa*, stems, leaves, and calyces. (B) The dried calyces of *H. sabdariffa*.

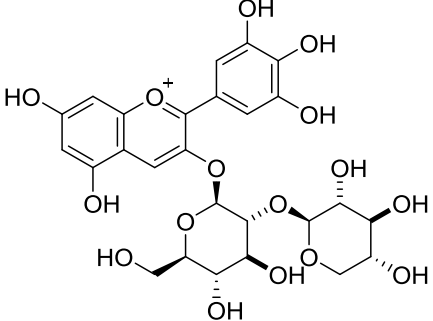
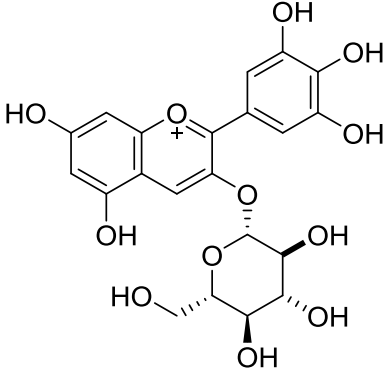
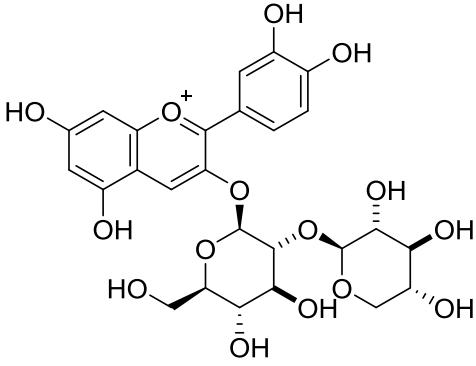
### **1.1.1 Chemical composition of *H. sabdariffa***

Different chromatographic techniques including, thin layer chromatography (TLC), solid phase extraction-capillary electrophoresis-mass spectroscopy (time-of-flight/ion trap), liquid chromatography/quadrupole-time-of-flight mass spectrometry (LC-Q-TOF-MS), have been used to identify the chemical constituents of *H. sabdariffa* (Salah *et al.*, 2002, Segura-Carretero *et al.*, 2008). The main compounds detected in *H. sabdariffa* have been organic acids, mainly hibiscus, citric and malic acids (Ali *et al.*, 2005). In addition, delphinidin and cyanidin-based anthocyanins, which are a group of flavonoid derivatives, such as delphinidin-3-sambubioside (hibiscin or hiviscin) and cyanidin-3-sambubioside (gossypcyanin), have been identified as the major anthocyanins present in *H. sabdariffa* extracts (Alarcón-Alonso *et al.*, 2012, Herranz-Lopez *et al.*, 2012). Various polyphenols such as quercetin, luteolin, myricetin-3-arabinogalactoside, myricetin-3-glucose, luteolin-7-glucoside, and protocatechuic acid have also been identified (Salah *et al.*, 2002, Segura-Carretero *et al.*, 2008, Beltran-Debon *et al.*, 2010, Peng *et al.*, 2011, Wang *et al.*, 2014, Sindi *et al.*, 2014, Herranz-Lopez *et al.*, 2012). **Table 1.1**, shows a selection of the phytochemicals that have been reported to be present in *H. sabdariffa*.

**Table 1.1: Selection of phytochemicals previously identified in *H. sabdariffa***

Compounds	Structure	Reference
<i>Organic acids</i>		
Hibiscus acid		
Hibiscus acid-6-methyl ester		(Herranz-Lopez <i>et al.</i> , 2012)
Hydroxycitric acid		
Citric acid		(Wong <i>et al.</i> , 2002)

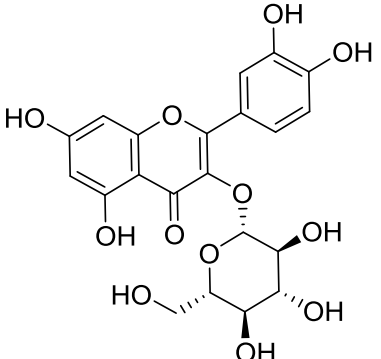
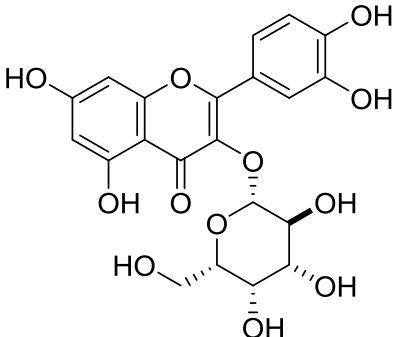
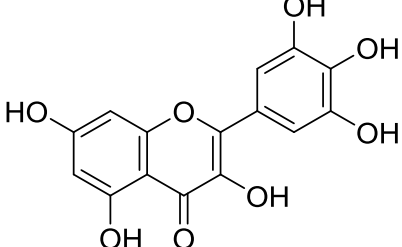
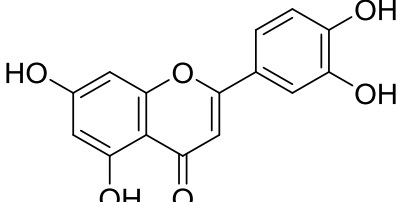
**Table 1.1 (continued): Selection of phytochemicals previously identified in *H. sabdariffa***

Compounds	Structure	Reference
<b><i>Anthocyanins</i></b>		
Delphinidin-3-O-sambuboside (hibiscin)		(Sindi <i>et al.</i> , 2014)
Delphinidin-3-O-glucoside		(Sindi <i>et al.</i> , 2014, Segura-Carretero <i>et al.</i> , 2008)
Cyanidin-3-O-sambubioside (gossypiccyanin)		(Sindi <i>et al.</i> , 2014)

**Table 1.1 (continued): Selection of phytochemicals previously identified in *H. sabdariffa***

Compounds	Structure	Reference
Cyanidin-3-O-glucoside (chrysanthemin)		(Sindi <i>et al.</i> , 2014)
<b>Flavonoids</b>		
Hibiscetin		
Gossypetin		
Quercetin		(Herranz-Lopez <i>et al.</i> , 2012)

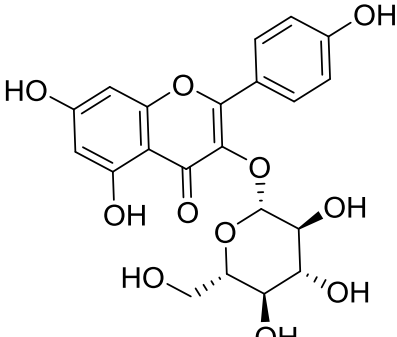
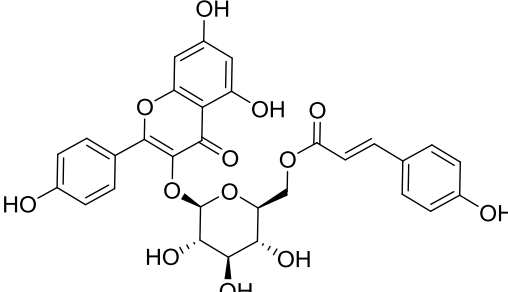
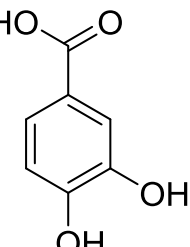
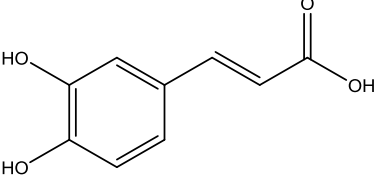
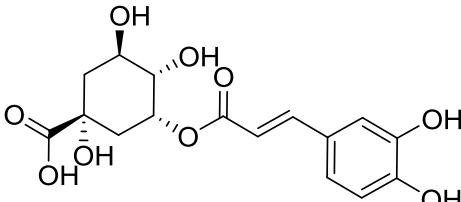
**Table 1.1 (continued): Selection of phytochemicals previously identified in *H. sabdariffa***

Compounds	Structure	Reference
Isoquercetin		(Salah <i>et al.</i> , 2002, Wang <i>et al.</i> , 2014)
Hyperoside		(Salah <i>et al.</i> , 2002)
Myricetin		(Beltran-Debon <i>et al.</i> , 2010, Herranz-Lopez <i>et al.</i> , 2012)
Luteolin		(Salah <i>et al.</i> , 2002)

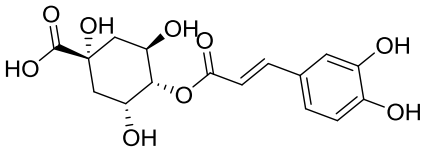
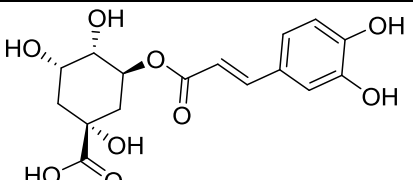
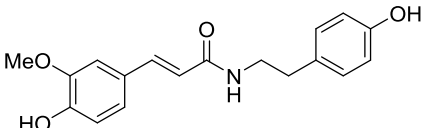
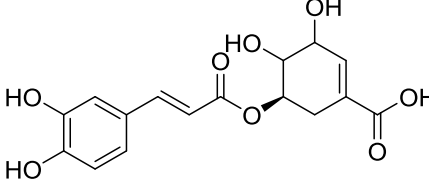
**Table 1.1 (continued): Selection of phytochemicals previously identified in *H. sabdariffa***

Compounds	Structure	Reference
Quercetin-3-O-rutinoside (rutin)		
Quercetin-3-O-sambubioside		
Kaempferol-3-O-rutinoside		(Beltran-Debon <i>et al.</i> , 2010, Herranz-Lopez <i>et al.</i> , 2012)
Kaempferol-3-O-sambubioside (leucoside)		

**Table 1.1 (continued): Selection of phytochemicals previously identified in *H. sabdariffa***

Compounds	Structure	Reference
Kaempferol-3-O-glucoside		(Peng et al., 2011)
Tiliroside		
<i>Other polyphenols</i>		
Protocatechuic acid		Peng et al., 2011, Ramírez-Rodrigues et al., 2011)
Caffeic acid		(Beltran-Debon et al., 2010, Herranz-Lopez et al., 2012)
3-O-caffeooyl quinic acid		

**Table 1.1 (continued): Selection of phytochemicals previously identified in *H. sabdariffa***

Compounds	Structure	Reference
4-O-caffeooyl quinic acid		(Beltran-Debon <i>et al.</i> , 2010, Herranz-Lopez <i>et al.</i> , 2012)
5-O-caffeooyl quinic acid		
N-feruloyltyramide		
5-O-caffeooylshikimic acid,		

## **1.1.2 Pharmacological activity**

### **1.1.2.1 Antioxidant activity**

Under normal physiological conditions, there is a critical balance in the generation of oxygen free radicals and antioxidant defense systems used by organisms to deactivate and protect themselves against free radical toxicity. Oxidative stress can develop from the overproduction of reactive oxygen species (ROS) and the deterioration of the endogenous antioxidant defence mechanisms, which can cause damage to proteins, lipid and deoxyribonucleic acid (DNA) with deleterious consequences (Halliwell, 1996, Ramakrishna and Jailkhani, 2007). Antioxidants are very important for cells, because of their role as free radical ‘scavengers’, and for their preservation of normal cell signalling pathways (Bafana *et al.*, 2011). As reviewed by Da-Costa-Rocha *et al.* (2014), several studies have shown that extracts of *H. sabdariffa* have a potent antioxidant effect. This activity of this plant is due to its strong scavenging effect on ROS that was linked to the presence of polyphenols and protocatechuic acid.

#### **1.1.2.1.1 Clinical studies**

To clinically assess the antioxidant properties and health benefits of *H. sabdariffa*, a randomised, two-way, cross-over study was undertaken with eight male and female subjects. The trial showed that the oral administration of a single daily dose (10 g/200 ml) of a water extract led to positive effects on the total antioxidant potential in plasma and urine after 24 hours. The consumption of an aqueous extract significantly decreased the malondialdehyde (MDA) level, which is a biomarker for oxidative stress.

Furthermore, a significantly increased urinary hippuric acid excretion within 24 h after the extract consumption indicates a high biotransformation of the ingested *H. sabdariffa* polyphenols (Frank *et al.*, 2012).

#### **1.1.2.1.2 *In vitro* and *in vivo* studies**

In recent years, the antioxidant activities of *H. sabdariffa* have been reported in different *in vitro* and *in vivo* studies. The antioxidant activity of the extracts of *H. sabdariffa* has been investigated using a variety of cell lines, including rat primary hepatocytes (Tseng *et al.*, 1997), mouse macrophages RAW264.7 and J774A.1 (Chang *et al.*, 2006, Kao *et al.*, 2009), Human liver carcinoma cells (HepG2) (Yang *et al.*, 2009), and through *in vivo* experiments in rat models (Da-Costa-Rocha *et al.*, 2014). Both alcoholic and aqueous extracts of *H. sabdariffa* have been widely studied as antioxidants. Researchers have found that both the alcoholic and aqueous extracts of *H. sabdariffa* have the potential to scavenge free radicals, inhibit xanthine oxidase, protect against oxidative damage induced by tert-butyl hydroperoxide (*t*-BHP), reduce lipid peroxidation (LP) (Tseng *et al.*, 1997), inhibit copper induced-low density lipoprotein (LDL) oxidation, and induce macrophage apoptosis (Chang *et al.*, 2006). For example, the pre-treatment of rats for 6 days with 200 mg/ml of 80% ethanolic extract of *H. sabdariffa* protects against the sodium arsenite (10 mg/ml)-induced depletion of hepatic glutathione (GSH), 86% improvement, and increases the levels of hepatic antioxidant enzymes, including SOD by ~350%, catalase (CAT) by ~800%, glutathione-s-transferase (GST) by ~37%. The extract also reduces the content of thiobarbituric acid reactive substances induced by pro-oxidants (Usoh *et al.*, 2005).

It is known that the *ex vivo* culture of hematopoietic stem cells promotes excessive ROS production. The antioxidant potential of *H. sabdariffa* was examined on these stem cells. An aqueous extract of *H. sabdariffa* was added at varying concentrations (0–1000 ng/mL) for 24 hours to the freshly isolated murine bone marrow cell cultures. The extract showed protective activity against hydrogen peroxide ( $\text{H}_2\text{O}_2$ ) produced by hematopoietic stem cells. In addition, the intracellular antioxidant capacity and the survivability of these cells was improved by the addition of the extract. As the SOD activity was increased by  $2.2 \pm 0.2$  U/min/mg and the levels of GSH was increased by  $4 \pm 0.2$  nmol/g in presence of the hibiscus extract. In addition, the viability of these cells significantly increased by ~122% (Abdul Hamid *et al.*, 2014).

A variety of studies have also been conducted on animal models to investigate the antioxidant properties of *H. sabdariffa* extracts. For instance, alloxan has been used as a diabetogenic agent to induce diabetes. It selectively induces pancreatic  $\beta$ -cell death, resulting in an insulin-dependent diabetes mellitus, with characteristics similar to type 1 diabetes (Zhou *et al.*, 2017). In alloxan-treated rats, the ethanol extract of *H. sabdariffa* exhibited a strong free radical scavenging activity (Farombi and Ige, 2007). The ethanol extract at 200 mg/kg attenuated the alloxan-induced decrease in the activities of superoxide dismutase (SOD), catalase (CAT) and the level of GSH by 36%, 44%, and 64% in the liver and by 20%, 43%, and 85% in the kidney of rats (Farombi and Ige, 2007). A more recent study investigated the protective effect of the aqueous extract of the calyces, against red blood cell (RBC) membrane oxidative stress in streptozotocin-

induced diabetic rats. Streptozotocin is used to induce type 1 diabetes mellitus, because it selectively destroys pancreatic beta cells. Normally, the protein and lipid status of the RBC membrane is found to deteriorate in streptozotocin-treated rats (Mohamed *et al.*, 2013). Administration of the aqueous extract of *H. sabdariffa* was found to improve the oxidative status of these rats. This amelioration followed a significant increase in red blood cell membrane SOD levels, which is an important enzyme in preserving the integrity of the cell membrane through the reduction of free radicals (Mohamed *et al.*, 2013).

Most of these studies proposed a positive correlation between the polyphenolic contents of *H. sabdariffa*, specifically anthocyanin compounds and protocatechuic acid, and the strong antioxidant bioactivities of these extracts (Tseng *et al.*, 1996, Wang *et al.*, 2000, Lin *et al.*, 2003, Ali *et al.*, 2003, Ajiboye *et al.*, 2011). The aqueous extract gave the highest yield of individual anthocyanins and polyphenols and exhibited higher free radical scavenging activity than the methanol extract; in comparison, ethyl acetate and hexane extracts showed negative antioxidant capacity and no anthocyanin content (Sindi *et al.*, 2014).

### **1.1.2.2 Hypolipidemic activity**

#### **1.1.2.2.1 Clinical studies**

Recently, researchers have shown an increased interest in investigating the health benefits and antihyperlipidemic effects of *H. sabdariffa* flowers and calyces on healthy and unhealthy volunteers by conducting clinical trials. (**Table 1.2** summarises these studies)

(Lin *et al.*, 2007, Mozaffari-Khosravi *et al.*, 2009a, Gurrola-Diaz *et al.*, 2010, Mohagheghi *et al.*, 2011). Lin *et al.* (2007) reported that a consumption of two oral capsules containing a flower extract (500 mg) of *H. sabdariffa* for one month resulted in a significant lowering of the serum cholesterol level by 8.3% to 14.4%.

A randomised controlled trial was conducted by Mozaffari-Khosravi *et al.* (2009a) on 53 patients having type II diabetes mellitus for more than 5 years, and not taking antihyperlipidemic medicines. The researchers showed that a daily oral administration of 2 grams of hibiscus tea to these patients for one month has a significant effect on blood lipid profile. As they reported that the levels of total cholesterol (TC), LDL, and triglyceride (TG) in the hibiscus tea treated patients, were decreased by 7.6%, 8.0%, and 14.9%, respectively. Whereas, the level of HDL was increased by 16.7% (Mozaffari-Khosravi *et al.*, 2009a). The blood lipid profile lowering effect of a microencapsulated powder of hibiscus calyces (100 mg kg<sup>-1</sup>) was also reported by Gurrola-Diaz *et al.* (2010), when it was consumed by patients with metabolic syndrome for 30 days. As the levels of glucose, TC, and LDL were reduced from 105±16 to 95±24 mg/dl, 199±40 to 179±21 mg/dl, and 130±34 to 104±20 mg/dl, respectively. In fact, increase in HDL and decrease in LDL and TC have clinical relevance because it has been postulated as an adjunctive therapy to prevent and treat of cardiovascular diseases and management of metabolic syndrome (Gurrola-Diaz *et al.*, 2010).

**Table 1.2: Hypolipidemic effect of *H. sabdariffa* (clinical studies overview)**

Experimental conditions	sample size	Extract	Dosing	Duration (day)	Significantly improved lipid profile markers	Reference
Hyperlipidemia	14	Aq, HS Flower	3g/day	28	TC	(Lin <i>et al.</i> , 2007)
Hyperlipidemia	14	Aq, HS Flower	6g/day	28	TC	(Lin <i>et al.</i> , 2007)
Diabetes	27	Aq, HS Calyx	4g/day	30	TC, TG, LDL & HDL	(Mozaffari-Khosravi <i>et al.</i> , 2009a)
Hyperlipidemia	28	Aq, HS Leaf	1g/day	90	LDL & TG	(Kuriyan <i>et al.</i> , 2010)
Metabolic syndrome	18	Al, HS Calyx	100 mg/day	30	TC, LDL & HDL	(Gurrola-Diaz <i>et al.</i> , 2010)
None	26	Al, HS Calyx	100 mg/day	30	TG & HDL	(Gurrola-Diaz <i>et al.</i> , 2010)
Hyperlipidemia	42	Al, HS Calyx	30 mg/day	15	HDL	(Mohagheghi <i>et al.</i> , 2011)
Obesity	19	Aq, HS Flower	450mg/day	84	FFA	(Chang <i>et al.</i> , 2014)

**HS**=*H. sabdariffa*, **C**=cholesterol, **LDL**=low density lipoprotein-cholesterol, **TC**=total cholesterol, **TG**= triglyceride, **HDL**=high density

lipoprotein-cholesterol, **Aq**=Aqueous, **Al**=Alcohol, & **FFA**=free fatty acid.

### **1.1.2.2.2 *In vitro* and *in vivo* studies**

Previous studies have shown that extracts from different parts of *H. sabdariffa*, including the calyces, leaves and seeds, possess antihyperlipidemic activity (as detailed in **Table 1.3**). This could protect the cardiovascular system from deleterious effects, mainly from atherosclerosis, which is caused by a decline in the level of the cardio protective high density lipoprotein (HDL), as well as high blood levels of TG, LDL, very low density lipoprotein (VLDL), and cholesterol (Chen *et al.*, 2003, Chen *et al.*, 2004, Carvajal-Zarrabal *et al.*, 2005, Yang *et al.*, 2009, Kuriyan *et al.*, 2010, Gosain *et al.*, 2010, Hirunpanich *et al.*, 2006, Peng *et al.*, 2011, Mohd-Esa *et al.*, 2010).

The hypolipidemic and hepatic fat lowering effect of a hibiscus extract has also been reported by Yang *et al.* (2009). They showed that a polyphenolic extract from *H. sabdariffa* has a hypolipidemic effect, which was proposed to work via inhibiting the expression of fatty acid synthase and 3-hydroxy-3-methyl-glutaryl-CoA reductase (HMG-CoA reductase) (Yang *et al.*, 2009).

**Table 1.3: Hypolipidemic effect of *H. sabdariffa* (animal studies overview)**

Experimental conditions	Sample size	Extract	Dosing	Duration (days)	Significantly improved lipid profile markers	Reference
Hyperlipidaemia	6 rats	N/A, HS Calyx	5% & 10% (w/w) (at the expense of starch within the high fat-diet)	63	TC & TG	(El-Saadany <i>et al.</i> , 1991)
Hyperlipidaemia	6 rabbits	Aq, HS N/A	0.5% & 1% (w/w)	70	TC, LDL, & TG	(Chen <i>et al.</i> , 2003)
Hyperlipidaemia	6 rats	Aq, HS Flower	1&2 g/kg/day	84	TC & LDL	(Chen <i>et al.</i> , 2004)
None	6 rats	Aq, HS Petal	1 mg/kg/day	28	LDL	(Olatunji <i>et al.</i> , 2005)
None	6 rats	Aq, HS Petal	1.5 mg/kg/day	28	TC & LDL	(Olatunji <i>et al.</i> , 2005)
Hyperlipidaemia	N/A rats	Al, HS Calyx	5g/100g diet	28	TC, LDL, & TG	(Carvajal-Zarrabal <i>et al.</i> , 2005)
Hyperlipidaemia	N/A rats	Al, HS Calyx	10g/100g diet, & 15g/100g diet	28	LDL & TG	(Carvajal-Zarrabal <i>et al.</i> , 2005)
Hyperlipidaemia	6 rats	Aq, HS Calyx	250 mg/kg/day	42	TC & LDL	(Hirunpanich <i>et al.</i> , 2006)

HS=*H. sabdariffa*, LDL=low density lipoprotein, TC=total cholesterol, TG=triglyceride, HDL=high density lipoprotein, Aq=Aqueous,

Al=Alcohol.

**Table 1.3 (continued): Hypolipidemic effect of *H. sabdariffa* (animal studies overview)**

Experimental conditions	sample size	Extract	Dose mg/kg/day	Duration (day)	Significantly improved lipid profile markers	Reference
Hyperlipidaemia	6 rats	Aq, HS Calyx	500	42	TC & LDL	(Hirunpanich <i>et al.</i> , 2006)
Hyperlipidaemia	6 rats	Aq, HS Calyx	1000	42	TC & LDL	(Hirunpanich <i>et al.</i> , 2006)
Diabetes	5 rats	Al, HS Flower	100 & 200	28	TC	(Farombi and Ige, 2007)
Hyperlipidemia	6 rats	Al, HS Calyx or Leaf	500	30	TC, LDL, TG & HDL	(Ochani and D'Mello, 2009)
Diabetes	5 rats	Al, HS Flower	100 & 200	56	TC, LDL, & TG	(Lee <i>et al.</i> , 2009)
Hyperlipidemia	6 rats	Al, HS Leaf	200 & 300	28	TC, LDL, & TG	(Gosain <i>et al.</i> , 2010)
Hyperlipidemia	8 rats	Al, HS Calyx	100 & 200	63	TC & TG	(Peng <i>et al.</i> , 2011)
Hyperlipidemia, diabetes	8 rats	Al, HS Calyx	100 & 200	63	TC, & TG	(Peng <i>et al.</i> , 2011)

HS=*H. sabdariffa*, LDL=low density lipoprotein, TC=total cholesterol, TG=triglyceride, HDL=high density lipoprotein, Aq=Aqueous,

Al=Alcohol.

### **1.1.2.3 Antihypertensive activity**

#### **1.1.2.3.1 Clinical studies**

The matured dried calyces are widely used to prepare hot and cold beverages in many countries throughout the world, including the United States, Mexico, West Africa, Iran, Arabia, and South Asia (Da-Costa-Rocha *et al.*, 2014). Previous studies have reported the traditional medical consumption, specifically the calyces, as a remedy for hypertension, hyperlipidaemia, obesity, and cardiovascular diseases (Ali *et al.*, 2005, Hopkins *et al.*, 2013, Da-Costa-Rocha *et al.*, 2014). In these studies, a decoction or infusion is obtained from the calyces and flowers; sometimes the leaves, have been used safely and effectively in the treatment of these diseases as well (Hopkins *et al.*, 2013).

The antihypertensive activity of *H. sabdariffa* has been studied clinically in patients with high blood pressure, with complete tolerability and without any adverse effects (**Table 1.4** summarises these studies). These studies have shown that regular daily consumption of hibiscus tea caused a clinically significant reduction of approximately 10% in both systolic blood pressure (SBP) and diastolic blood pressure (DBP) (Faraji and Tarkhani, 1999, Herrera-Arellano *et al.*, 2004, Herrera-Arellano *et al.*, 2007, McKay *et al.*, 2009, Mozaffari-Khosravi *et al.*, 2009b, Mozaffari-Khosravi *et al.*, 2013). The magnitude of the effect of hibiscus tea was similar to that obtained with the angiotensin converting enzyme inhibitors captopril or lisinopril (Herrera-Arellano *et al.*, 2004, Herrera-Arellano *et al.*, 2007). For instance, a study was conducted with 54 patients of both sexes, who all suffered moderate essential hypertension (SBP 160-180 mmHg and/or

DBP 100-114 mmHg). Thirty-one patients were randomly selected as subjects for *H. sabdariffa* tea consumption, while the other 23 patients were assigned as a control group consuming ordinary tea. After 2 weeks of treatment with a daily dose of the tea (two spoonfuls of blended hibiscus brewed in a glass of boiled water for 20-30 min.), both SBP and DBP significantly decreased by approximately 10%. At the end of the 2 weeks treatment, the difference of blood pressure between the control and experimental groups are significant (with P<0.00001) for SBP and P<0.00002 for DBP (Faraji and Tarkhani, 1999).

In another clinical trial involving 75 diagnosed hypertensive male and female patients (30-80 years old) was conducted to test the antihypertensive activity of *H. sabdariffa*. Subjects were randomly allocated into experimental group of 39 patients and treated with hibiscus calyx infusion (10 g in 500 ml of boiled water). For comparison, another 36 patients were treated with a daily dose of 50 mg captopril (Herrera-Arellano *et al.*, 2004). The hibiscus infusion dose was taken orally daily for 4 weeks, which reduced the SDP and DBP by  $15.32 \pm 4.8$  and  $11.29 \pm 5$  mmHg, respectively (Herrera-Arellano *et al.*, 2004). The researchers reported that the antihypertensive activity of hibiscus infusion was not significantly different from that produced by captopril in the control group (Herrera-Arellano *et al.*, 2004). These results were confirmed by Herrera-Arellano *et al.* (2007), who conducted another randomised controlled, double-blind clinical trial, which was carried out on 193 patients diagnosed with stage I and stage II hypertension. From this sample, 100 patients were allocated to the experimental group and treated with hibiscus tea (standardised to 250 mg anthocyanins) as a daily dose for 4 weeks, whilst the other

group of 93 patients (control) were treated with 10 mg lisinopril. After 4 weeks of treatment, the *H. sabdariffa* treated group showed a reduction in their SBP and DBP of approximately 12%. While, the 10 mg daily dose of lisinopril reduced SBP and DBP by approximately 15%. The results also showed 100% tolerability for hibiscus treatment compared to 98.81% for the lisinopril treatment (Herrera-Arellano *et al.*, 2007).

A placebo-controlled clinical trial was conducted on pre-hypertensive and mildly-hypertensive patients, with SBP between 120 and 150 mmHg, and with a DBP of 95 mmHg or less (McKay *et al.*, 2009). In this study, smaller quantities of hibiscus tea was used in comparison with the previous clinical trials. Patients were asked to drink 720 ml of hibiscus tea (1.25 g of *H. sabdariffa* brewed in 240 ml boiled water), and after 6 weeks of treatment, a significant reduction (approximately 5%) in the SBP, DBP, and mean arterial pressure (MAP) was observed. Whereas the placebo beverage (artificial hibiscus flavour concentrate) did not affect these variables (McKay *et al.*, 2009).

The effect of hibiscus tea has also tested on type II diabetic patients who were also diagnosed with mild hypertension (Mozaffari-Khosravi *et al.*, 2009b). In a random controlled, double-blind trial, 53 diabetic patients of both sexes participated, and they had SBP<160 mmHg and DBP<100 mmHg (mild hypertension). Patients were asked to intake hibiscus tea, which was prepared by pouring a 2 g sachet of hibiscus tea into 240 ml of boiled water, twice daily for 30 days. The control group of participants were asked to consume black tea. At the end of the study, the SBP of the hibiscus treated patients had decreased significantly from  $134.4 \pm 11.8$  to  $112.7 \pm 5.7$  mmHg and the mean pulse

pressure (MPP) decreased from  $52.2 \pm 12.2$  to  $34.5 \pm 9.3$  mmHg. However, there was no significant difference in the DBP (Mozaffari-Khosravi *et al.*, 2009b). A similar findings were reported by Mozaffari-Khosravi *et al.* (2013), who conducted another trial on 100 patients with mild hypertension and type II diabetes mellitus. Patients were served with hibiscus tea infusions (3 g teabag in 150 ml hot water to be taken at once). The researchers reported that the three times daily consumption of this dose for 4 weeks, effectively reduced the SBP from  $123.1 \pm 15.5$  to  $116.8 \pm 16.3$  mmHg, and DBP from  $79.4 \pm 11.1$  to  $74.5 \pm 9.3$  mmHg (Mozaffari-Khosravi *et al.*, 2013).

The antihypertensive activity of *H. sabdariffa* was compared to a diuretic in a clinical study carried out on 80 patients diagnosed with hypertension. Participants were randomly allocated into one of three groups: a group treated with a diuretic (hydrochlorothiazide); a group were treated with a daily dose ( $150 \text{ mg kg}^{-1}$ ) of *H. sabdariffa* aqueous extract (20 g/L) for 4 weeks; or a group that was provided with a placebo (control) group (Nwachukwu *et al.*, 2015). At the end of the study, the SBP and DBP were significantly reduced by  $17.08 \pm 5.12$  and  $11.12 \pm 3.12$  mmHg respectively, in the hibiscus treated group. Whereas, the reduction in the SBP and DBP were  $12.9 \pm 4.31$  and  $9.50 \pm 2.06$  mmHg respectively, in the hydrochlorothiazide treated group. The researchers concluded that treatment of mildly and moderately hypertensive patients with *H. sabdariffa* calyces, is more effective than treatment with hydrochlorothiazide. They also noted that the electrolyte imbalance that can occur with diuretic treatment was not an issue in patients treated with the hibiscus extract (Nwachukwu *et al.*, 2015).

To assess the overall therapeutic potential of *H. sabdariffa* as an antihypertensive herb, most of the above randomised clinical trials have been included in a meta-analysis. The search included PUBMED, Cochrane Library, Scopus, and EMBASE databases (up to July 2014) to identify randomised clinical trials investigating the efficacy of *H. sabdariffa* supplementation on SBP and DBP values. This meta-analysis showed a significant effect of *H. sabdariffa* in lowering both SBP and DBP. Furthermore, the findings from the meta-analysis favoured the use of this natural, safe, and inexpensive hibiscus supplement in patients with essential hypertension (Serban *et al.*, 2015).

**Table 1.4: Antihypertensive effect of *H. sabdariffa* (clinical studies overview)**

Experimental condition	Extract	Participants	Number of doses/day	Duration (day)	Mean reduction in SBP/DBP (mmHg)	Within group p-values	Reference
Stage-II hypertension	Aq HS Leaf	31	1	12	17.6/ 10.9	S	(Faraji and Tarkhani, 1999)
Pre and Stage-I hypertension	Aq HS calyx	39	1	28	14.2/ 11.2	S	(Herrera-Arellano <i>et al.</i> , 2004)
Stage-I, and Stage-II hypertension	Aq HS calyx	100	1	28	17.1/ 11.9	S	(Herrera-Arellano <i>et al.</i> , 2007)
Mild hypertension, Diabetes II	Aq HS calyx	27	2	30	21.7/ 1.2	S/NS	(Mozaffari-Khosravi <i>et al.</i> , 2009b)
Hypertension	Aq HS calyx	35	3	42	7.2/ 3.1	S	(McKay <i>et al.</i> , 2009)
Mild Hypertension, Diabetes II	Aq HS calyx	100	3	30	7/ 4.5	S	(Mozaffari-Khosravi <i>et al.</i> , 2013)

**HS**=*H. sabdariffa*, **SBP**=systolic blood pressure, **DBP**=diastolic blood pressure, **Aq**=aqueous, **S**=significant, **NS**=not significant.

### **1.1.2.3.2 In vivo studies**

There have been a number of *in vivo* studies, detailed in **Table 1.5**, which have also supported the use of *H. sabdariffa* as a hypotensive agent. For example, researchers have showed that intravenous administration of an aqueous hibiscus extract (25-100 mg) caused a dose-dependent reduction in the blood pressure in anaesthetised cats (Ali *et al.*, 1991). Aqueous extracts of the calyces and petals have been shown to reduce blood pressure and heart rate in rats at doses between 1 and 1000 mg kg<sup>-1</sup>day<sup>-1</sup>, which was without any adverse effect (Onyenekwe *et al.*, 1999, Odigie *et al.*, 2003, Mojiminiyi *et al.*, 2007, Inuwa *et al.*, 2012). An extract from hibiscus calyces decreased the MAP in a dose-dependent manner, and this was not affected by sectioning the vagal nerve, but was attenuated by atropine (Adegunloye *et al.*, 1996). The researchers concluded that the antihypertensive effect of the extract is not mediated through inhibition of the sympathetic nervous system. However, it could be due to mechanisms similar to that of acetylcholine as well as through direct vasorelaxation (Adegunloye *et al.*, 1996).

The activity of hibiscus was also investigated in 2K-1C (2-Kidney, 1-Clip) renovascular hypertensive rats, where treatment with orally administered water extract of hibiscus petals (250 mg kg<sup>-1</sup>day<sup>-1</sup>) for 8 weeks considerably lowered the SBP, DBP, MAP, and the heart rate (HR). In addition, it also attenuated the cardiac hypertrophy produced as a result of clamping the renal vessels (Odigie *et al.*, 2003). In another study, salt and N $\omega$ -nitro-L-arginine methyl ester hydrochloride (L-NAME), a nitric oxide synthase (NOS) inhibitor were used to produce hypertension in rats (Mojiminiyi *et al.*, 2007). An aqueous extract of hibiscus calyces was

administered intravenously ( $1\text{-}125 \text{ mg kg}^{-1}$ ) to these salt-induced and L-NAME-induced hypertensive rats, as well as to normotensive rats (Mojiminiyi *et al.*, 2007). The extract lowered blood pressure and heart rate in a dose-dependent manner in these hypertensive rats. In addition, it lowered blood pressure in normotensive rats; but the fall in blood pressure was significantly larger in the hypertensive group (Mojiminiyi *et al.*, 2007). Chronic administration of the extract to spontaneously hypertensive rats lowered SBP and DBP (Inuwa *et al.*, 2012, Abubakar *et al.*, 2015), and enhanced myocardial capillarisation, as evidenced by an increase in the ventricular myocardial capillary surface area and length density, as well as reducing the myocardial mass (Inuwa *et al.*, 2012). The effect of a methanolic extract obtained from *H. sabdariffa* leaves was also investigated in salt-induced hypertensive rats (Balogun *et al.*, 2016). Long-term daily administration of the extract at 200 and 400  $\text{mg kg}^{-1}$  body weight to these hypertensive rats, lowered the SBP, DBP, and MAP in a dose-dependent manner (Balogun *et al.*, 2016).

**Table 1.5: Antihypertensive effect of *H. sabdariffa* (animal studies overview)**

Experimental condition	Extract	Dose (mg/kg/day)	Duration (days)	SBP & DBP	Reference
Normotensive 5 rats	Aq HS Calyx	500 & 1000	21	Reduced	(Onyenekwe et al., 1999)
Spontaneous hypertensive 5 rats	Aq HS Calyx	500 & 1000	21	Reduced	(Onyenekwe et al., 1999)
2-kidney,1-clip renovascular hypertensive 6 rats	Aq HS Petals	250	56	Reduced	(Odigie et al., 2003)
Normotensive 6 rats	Aq HS Calyx	1,5,25 & 125	1	Reduced	(Mojiminiyi et al., 2007)
Salt-induced and L-NAME induced hypertensive 6 rats	Aq HS Calyx	1,5,25 & 125	1	Reduced	(Mojiminiyi et al., 2007)
Spontaneous hypertensive 6 rats	Aq HS Calyx	10%,15% & 20%	70	Reduced	(Inuwa et al., 2012)
Spontaneous hypertensive 5 rats	Aq HS Calyx	250 & 500	28	Reduced	(Abubakar et al., 2015)
Spontaneous hypertensive 5 rats	Al HS Leaf	200 & 400	28	Reduced	(Balogun et al., 2016)

**HS**=*H. sabdariffa*, **Aq**=aqueous, **Al**=alcohol, **SBP**=systolic blood pressure, and

**DBP**=diastolic blood pressure.

### **1.1.3 Toxicity of *H. sabdariffa***

It has been shown that a high intake of *H. sabdariffa* is generally non-toxic (Onyenekwe *et al.*, 1999, Sireeratawong *et al.*, 2013). The intraperitoneal administration of up to 5000 mg/kg body weight into rats caused no deaths, suggesting a median lethal dose (LD<sub>50</sub>) of aqueous extract of hibiscus to be more than 5000 mg/kg (Onyenekwe *et al.*, 1999). Furthermore, the administration of an alcoholic extract of calyces or seeds in a dose  $\geq$  5000 mg/kg, was not toxic to adult mice or rats (Sireeratawong *et al.*, 2013, Da-Costa-Rocha *et al.*, 2014). Oral administration of an *H. sabdariffa* extract at doses of 50, 100 and 200 mg/kg body weight for 270 days did not cause chronic toxicity in rats (Sireeratawong *et al.*, 2013).

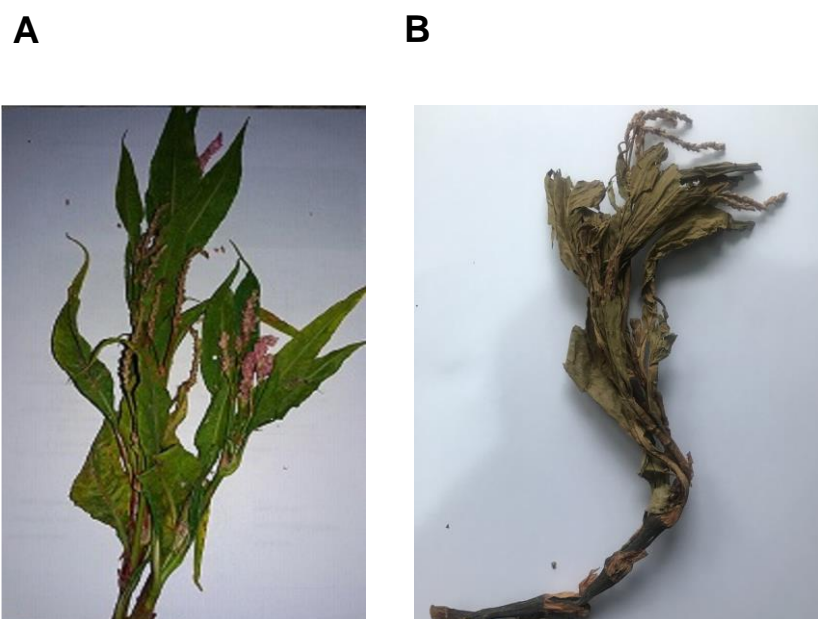
## 1.2 *Polygonum salicifolium* (Polygonaceae)

*Polygonum salicifolium* Brouss.ex Wild (*P. salicifolium*) (**Figure 1.2**), is an annual aquatic plant belongs to the family Polygonaceae. The synonyms for this species include *Persicaria salicifolia*, and it is commonly known as knotweed or swamp willow weed. The plant is a herb about one metre in height while the stems possess hairy rooting nodes. The plant is also characterised by simple, smooth, hairless and alternate leaves and slender raceme inflorescences with white or pink flowers. Traditionally, various plants in this family have been used as foods or medicinally for the treatment of renal disease, particularly to remove kidney stones and as diuretic. In addition it has been used to treat diarrhoea, gout, and diabetes (Kawasaki *et al.*, 1986, Calis *et al.*, 1999, Hussein and Mohamed, 2013).

It is well known that the plants of this genus produce a variety of compounds including flavonoids, in addition to other constituents, including triterpenoids, anthraquinones, coumarins, and phenylpropanoids (Lopez *et al.*, 2006).

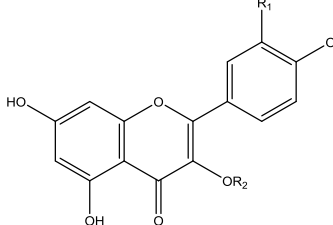
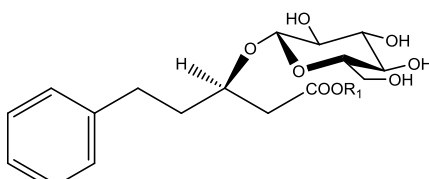
The plant, *P. salicifolium* has been shown to have potent antioxidant and free radical scavenging activities (Calis *et al.*, 1999, Hussein and Mohamed, 2013), and studies with *P. salicifolium* indicated that flavonoid glycosides (Calis *et al.*, 1999), and flavonol glycosides (Hussein and Mohamed, 2013), are predominant in the aerial parts of this plant.. **Table 1.6** summarises the phytochemicals present in *P. salicifolium*. López *et al.* (2006) studied the plant *P. ferrugineum* for its chemical constituents, and reported that different compounds including chalcones, homoisoflavanone, and dihydrochalcone were isolated from the leaves of this plant.

More recently, researchers have reported that the compounds isolated from the seeds of another close species (*Persicaria lapathifolia*), have antimicrobial and antifungal activities, and they identified these compounds as chalcones, particularly flavokawain B, pinostrobin, and pashanone (Hailemariam *et al.*, 2018). In a recent review, researchers reported the traditional use of the leaves of the plant species, *P. hydropiper* in Pakistan to combat hypertension (Ahmad *et al.*, 2018). Actually, local people living in rural areas of Iraq use *P. salicifolium* as a source of food and as a preventive treatment for diabetes and hypertension. In fact, not much information has been documented in the scientific literature about *P. salicifolium*, and no previous studies have investigated the potential effect of this plant.

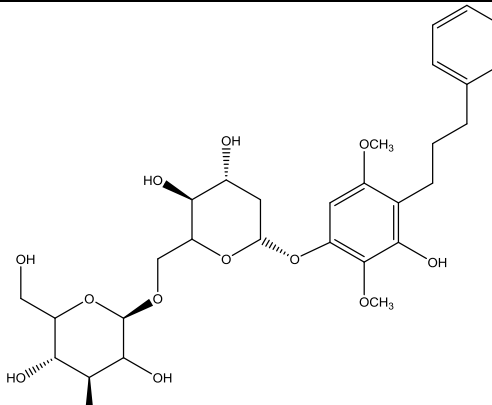
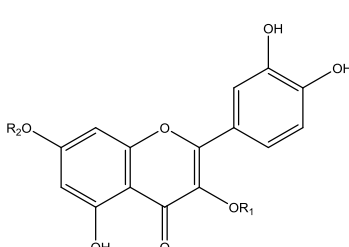


**Figure 1.2: Aerial parts of *P. salicifolium*. (A)** Freshly harvested aerial parts. **(B)** Dried stem with leaves and flowers.

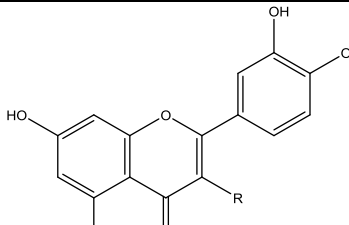
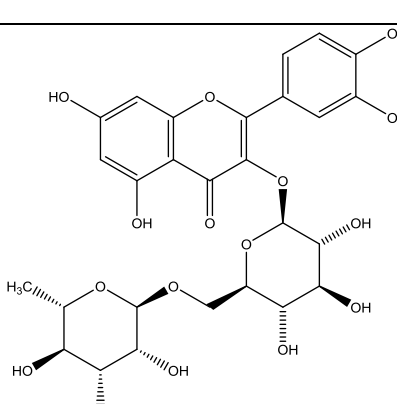
**Table 1.6: Selection of phytochemicals previously isolated from *P. salicifolium***

Compound	Parts of the plant	Reference
 <b>R<sub>1</sub>=H, R<sub>2</sub>=β-D-glucopyranose</b> Kaempferol-3-O-β-D-glucopyranoside (astragalin)		
<b>R<sub>1</sub>=H, R<sub>2</sub>=β-D-galactopyranose</b> Kaempferol-3-O-β-D-galactopyranoside		
<b>R<sub>1</sub>=OH, R<sub>2</sub>=β-D-glucopyranose</b> Quercetin-3-O-β-D-glucopyranoside (isoquercitrin)		
<b>R<sub>1</sub>=OH, R<sub>2</sub>=β-D-galactopyranose</b> Quercetin-3-O-β-D-galactopyranoside (hyperoside)		
<b>R<sub>1</sub>=OH, R<sub>2</sub>=β-D-(2''-O-galloyl)-glucopyranose</b> Quercetin-3-O-(2'-O-galloyl) - β-D-glucuronopyranoside	Aerial	(Calis <i>et al.</i> , 1999)
<b>R<sub>1</sub>=OH, R<sub>2</sub>=β-D-glucuronopyranose</b> Quercetin-3-O-β-D-glucuronopyranoside		
 <b>R=H</b> (3R)-O-[β-D- glucopyranosyl- oxy-5- phenyl valeric acid		
<b>R=C<sub>4</sub>H<sub>9</sub></b> (3R)-O-[β-D- glucopyranosyl- oxy-5- phenyl valeric acid n-butyl ester		

**Table 1.6 (continued): Selection of phytochemicals previously isolated from *P. salicifolium***

Compound	Parts of the plant	Reference
 4'-[ $\beta$ -D-glucopyranosyl-(1-6)-glucopyranosyl]oxy-2'-hydroxy-3'-6'-dimethoxydihydrochalcone (Salicifolioside A)	Aerial	(Calis <i>et al.</i> , 1999)
 <b>R<sub>1</sub>=R<sub>2</sub></b> =glucopyranose (Quercetin-3, 7- di-O-glucopyranoside)	Aerial	(Hussein and Mohamed, 2013)

**Table 1.6 (continued): Selection of phytochemicals previously isolated from *P. salicifolium***

Compound	Parts of the plant	Reference
 <b>R=H</b> (Luteolin)		
<b>R=OH</b> (Quercetin)  <b>R=O- α-L- Rhamnopyranose</b> (Quercetin-3-O-α-L- Rhamnopyranoside, quercitrin)	Aerial	(El-Anwar <i>et al.</i> , 2016)
 Quercetin-3-O- α-L- rhamnosyl (1''''- 6'') β-D-glucoside (Rutin)		

## **1.3 Smooth muscle and cardiac muscle physiology**

### **1.3.1 Smooth muscle cell contraction**

Smooth muscle cells are found in the walls of the hollow organs in the body, specifically blood vessels, airways, the uterus, the gastrointestinal tract, and the bladder, among others. These cells play a vital role in regulating the function of these organs (Bárány, 1996). A defect in the activities of these organs can result in the development of various significant diseases, for example abnormalities of blood vessel contractility contributes to hypertension, pulmonary hypertension, and coronary artery spasm. Similarly, bronchospasms and asthma are attributed to the abnormal functioning of airway smooth muscle.

Vascular smooth muscle cells which form the medial layer of blood vessels are differentiated cells functioning mainly for contraction. They contain a diverse range of different proteins, ion channels and signalling molecules that help them contract (Owens, 1995). As shown in **Figure 1.3**, pharmacomechanical and electromechanical coupling mechanisms are the main pathways for the regulation of smooth muscle contraction and the free intracellular calcium concentration plays a central role in the regulation of the contractile response (Somlyo and Somlyo, 1968, Somlyo and Somlyo, 1994, Gerthoffer and Larsen, 2000). Pharmacomechanical coupling involves the stimulation of G-protein coupled receptors (GPCRs) by many agonists, including circulating neurotransmitters, endothelial-derived vasoconstrictors, and peptides. A number of excitatory agonists, such as noradrenaline, angiotensin II, and endothelin-1, can initiate contraction in vascular smooth muscle cells by activating a phosphatidylinositol signalling cascade, which is mediated via G<sub>αq</sub> (Kuriyama *et al.*,

1998, Wynne *et al.*, 2009). This pathway involves the activation of the membrane-bound enzyme, phospholipase C $\beta$  (PLC $\beta$ ), which promotes the hydrolysis of phosphatidylinositol (4,5) bisphosphate (PIP<sub>2</sub>), and the generation of the second messengers, inositol-1, 4, 5 triphosphate (IP<sub>3</sub>) and diacylglycerol (DAG) (Berridge *et al.*, 1984, Downes and Michell, 1982). IP<sub>3</sub> triggers the release of intracellular Ca<sup>2+</sup> from sarcoplasmic reticulum (SR), thereby raising intracellular Ca<sup>2+</sup> to the levels required for the initiation of contraction (Somlyo *et al.*, 1988). Depolarisation of the cell membrane will activate the voltage-dependent calcium channels (VDCCs), which allows Ca<sup>2+</sup> influx (as evidenced by the generation of a measurable Ca<sup>2+</sup> current). This substantially increases intracellular Ca<sup>2+</sup> and triggers contraction (Droogmans *et al.*, 1977, Fleischmann *et al.*, 1994, McDonald *et al.*, 1994). Ultimately, both intracellular and extracellular Ca<sup>2+</sup> sources contribute to the contraction of smooth muscle cells (Karaki *et al.*, 1997).

Once intracellular Ca<sup>2+</sup> is increased, a Ca<sup>2+</sup>-calmodulin complex is formed through the binding of four Ca<sup>2+</sup> ions to each calmodulin, which acts as a transducer (Kamm and Stull, 1985). This activated regulatory complex is essential for the activation of the enzyme myosin light chain kinase (MLCK), which is primarily responsible for the phosphorylation of the regulatory myosin light chain (MLC<sub>20</sub>) subunit (Hartshorne, 1987). Phosphorylation of MLC<sub>20</sub> facilitates the actin activation of the myosin Mg<sup>2+</sup>-ATPase, which in turn enables binding of the myosin globular head with the actin thin filament. This initiates cross-bridge cycling, and results in a contraction (Hartshorne, 1987).

In addition, agonists can also increase the  $\text{Ca}^{2+}$  sensitivity of the contractile proteins, which is proposed to be controlled by DAG/PKC/CPI-17. In this regard, activation of PKC will phosphorylate and activate a specific MLCP inhibitor (CPI-17). Once phosphorylated, CPI-17 binds to, and inactivates MLCP, which blocks the reversal of myosin phosphorylation and sustains the contraction of the smooth muscle cells (Woodsome *et al.*, 2006).

There is another signal transduction pathway that has a role in the regulation of smooth muscle contraction; this is the RhoA/Rho kinase pathway (Hirata *et al.*, 1992, Amano *et al.*, 2010). RhoA is a small, GTP binding protein that has GTPase activity, which interacts with the GPCRs through the G-protein  $\alpha$  subunit, and is activated whenever a vasoconstrictor ligand binds to its receptor, and this activation is facilitated via guanine nucleotide exchange factors (RhoGEF) (Amano *et al.*, 1996, Webb, 2003, Amano *et al.*, 2010). Rho A is activated when it switches from the Rho-GDP bound state to the Rho-GTP bound state, activating a serine/threonine kinase known as Rho kinase (RhoK). RhoK, in turn, phosphorylates the myosin binding subunit (MYPT1) of the enzyme MLCP, rendering it inactive. The inactivation of MLCP indirectly facilitates the phosphorylation of MLC<sub>20</sub>, increasing the  $\text{Ca}^{2+}$  sensitivity of the actomyosin system, and producing a sustained contraction (Bishop and Alan, 2000, Seko *et al.*, 2003). Furthermore, the RhoA/Rho kinase signalling pathway also increase  $\text{Ca}^{2+}$  sensitisation by activating CPI-17 (Uehata *et al.*, 1997, Koyama *et al.*, 2000).

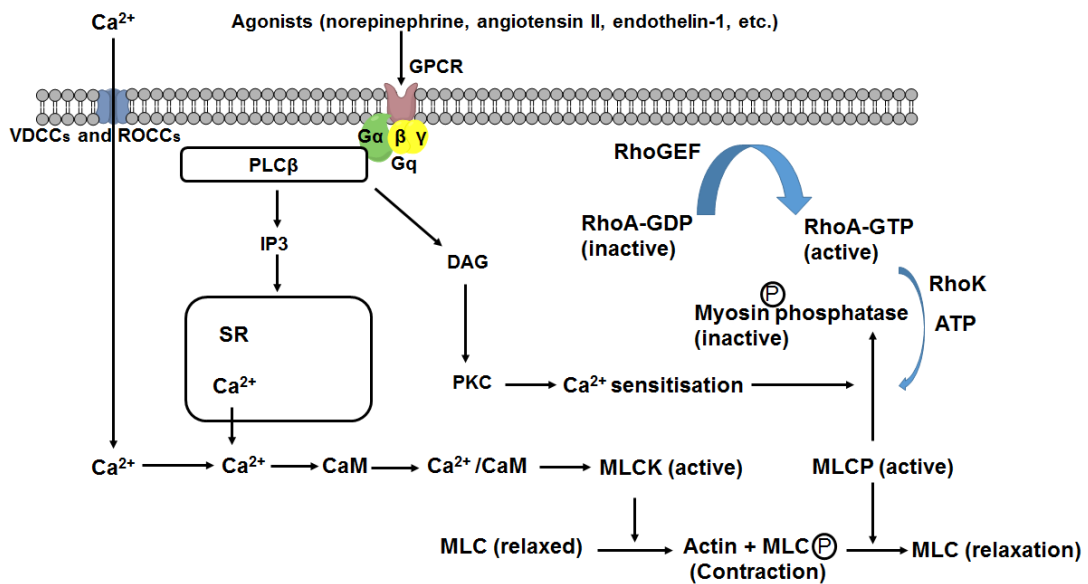


**Figure 1.3: Mechanisms regulating smooth muscle contraction.** Various excitatory agonists bind to G-protein coupled receptors (GPCR) to produce two second messengers, inositol triphosphate (IP<sub>3</sub>) and diacylglycerol (DAG). On the sarcoplasmic reticulum (SR) resides the IP<sub>3</sub> receptor (IP<sub>3</sub>R), which the IP<sub>3</sub> binds to, causing the release of SR  $\text{Ca}^{2+}$ , which then activates the  $\text{Ca}^{2+}$ -calmodulin (CaM)-dependent myosin light chain kinase (MLCK). Upon activation of MLCK, myosin light chain (MLC) is phosphorylated, leading to contraction of the smooth muscle cell. DAG activates protein kinase C (PKC). Agonists can also activate the RhoA/Rho kinase (RhoK) pathway. Both activated PKC and increased RhoK activity lead to inhibition of myosin light chain phosphatase (MLCP), and an increase in  $\text{Ca}^{2+}$  sensitisation of the contractile proteins. PLC $\beta$  (phospholipase C $\beta$ ), RhoGEF (guanine nucleotide exchange factor), VDCC (voltage dependent calcium channel), ROCC (receptor operated calcium channel) (Webb, 2003).

### 1.3.2 Smooth muscle cell relaxation

Relaxation of smooth muscle cells can occur through the termination of a contraction either by withdrawal of the contractile stimuli, or by stimulation of signalling pathways that promote relaxation (**Figure 1.4**). All these responses culminate in the dephosphorylation of MLC (Morgan, 1990, Somlyo *et al.*, 1999). When the free cytoplasmic  $\text{Ca}^{2+}$  concentration falls below the level that activates calmodulin, MLCK inhibition will occur; and active MLCP will dephosphorylate MLC, and thus relaxing the smooth muscle (Barron *et al.*, 1980, Lanerolle and Paul, 1991).

Binding of different agonists, such as  $\beta_2$ -agonists, adenosine, and prostacyclin to their receptors, which are coupled to Gs-protein, causes activation of the cyclic adenosine monophosphate (cAMP)-dependent signal transduction pathway (Stiles *et al.*, 1984, Knox and Tattersfield, 1995, Delmotte *et al.*, 2010). This cascade involves the activation of the enzyme adenylyl cyclase (AC), which catalyses the formation of the second messenger, cAMP, from ATP. The increased levels of intracellular cAMP activates cAMP-dependent protein kinase (PKA), which phosphorylates MLCK, thereby inactivating it (Stiles *et al.*, 1984, Bülbring and Tomita, 1987, Murray, 1990). Endothelial-derived relaxing factors (EDRFs) can provide an additional mechanism for the relaxation of the smooth muscle cells. It is well known that endothelial-derived nitric oxide (NO) exerts its activity on smooth muscle cells through the activation of the enzyme guanylate cyclase (GC) (Ignarro *et al.*, 1987, Palmer *et al.*, 1987, Moncada *et al.*, 1988, Denninger and Marletta, 1999, Triggle, 2012). The stimulation of this enzyme leads to an increase in the production of the second messenger cyclic guanosine-monophosphate (cGMP), which in turn activates protein

kinase G (PKG) (Moncada *et al.*, 1988, Denninger and Marletta, 1999, Carvajal *et al.*, 2000, Delmotte *et al.*, 2010). Once activated, PKG phosphorylates several ion pumps, ion channels, and enzymes that are involved in either the re-sequestration of free intracellular  $\text{Ca}^{2+}$  into intracellular storage sites, or efflux from the cell (Robertson *et al.*, 1993, Yamakage *et al.*, 1996, Zhou *et al.*, 1996, Quignard *et al.*, 1997, Mikawa *et al.*, 1998, Tanaka *et al.*, 1998). For example, the activation of the SR  $\text{Ca}^{2+}$ /ATPase pump will promote the re-uptake of  $\text{Ca}^{2+}$  from the cytoplasm into its intracellular storage site (Yoshida *et al.*, 1991). In comparison, the activation of the  $\text{Ca}^{2+}$ /ATPase pump and the  $\text{Na}^+/\text{Ca}^{2+}$  exchanger at the cell membrane level will remove  $\text{Ca}^{2+}$  from the cell to the extracellular space (Furukawa *et al.*, 1988).

The NO-cGMP-PKG pathway is also involved in the activation of potassium channels (Bolotina *et al.*, 1994, Archer *et al.*, 1994, Yamakage *et al.*, 1996, Mikawa *et al.*, 1998, Tanaka *et al.*, 1998, Stankevičius *et al.*, 2011). Once activated, these channels allow the efflux of potassium ions, which hyperpolarises the cell membrane; this will inhibit opening of VDCCs, thereby preventing  $\text{Ca}^{2+}$  influx via that route. Furthermore, it has been reported that VDCCS are also controlled by the NO-cGMP-PKG pathway, and that PKG directly inhibits the activated VDCCs (Tewari and Simard, 1997, Carabelli *et al.*, 2002, Carvajal *et al.*, 2000). There is also evidence that PKG can increase the activity of MLCP, thereby promoting relaxation (Bonnevier and Arner, 2004).

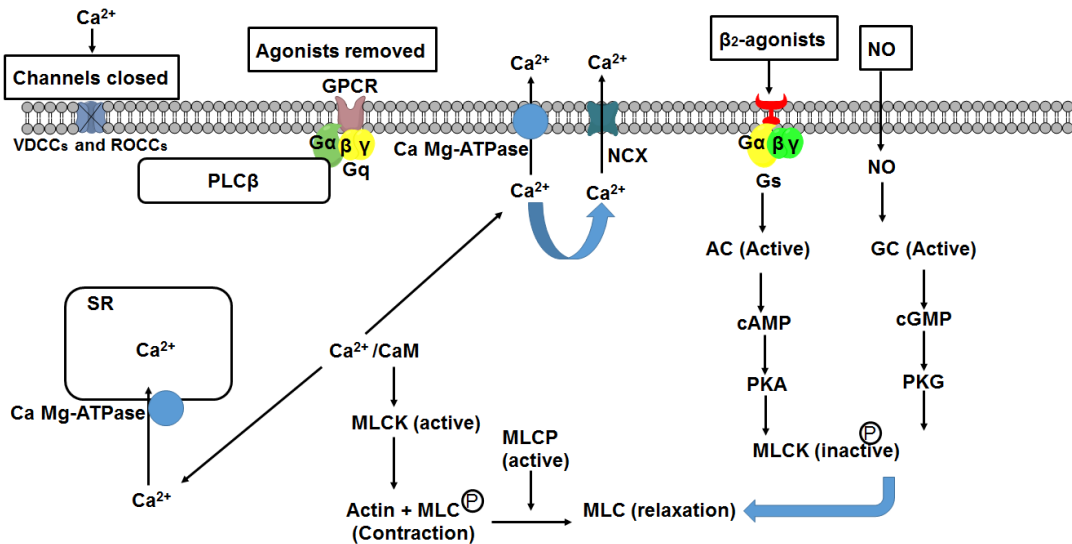


**Figure 1.4: Mechanisms controlling smooth muscle relaxation.** The process of relaxation requires the removal of the stimulatory agonist, causing the inhibition of  $\text{Ca}^{2+}$  influx through voltage-dependent (VDCC) and receptor-operated (ROCC)  $\text{Ca}^{2+}$  channels along with the removal of intracellular  $\text{Ca}^{2+}$  via the activation of  $\text{Ca}^{2+}$ -ATPase pumps and  $\text{Na}^{+}/\text{Ca}^{2+}$  exchanger.  $\beta_2$ -agonist binding to G-protein coupled receptor (GPCRs) stimulates adenylyl cyclase (AC) that catalyses the formation of cyclic adenosine monophosphate (cAMP), which activates protein kinase A (PKA). Nitric oxide (NO) causes relaxation via stimulation of guanylyl cyclase (GC), which catalyses the formation of cyclic guanosine monophosphate (cGMP) that activates protein kinase G (PKG). PKA and PKG induce the phosphorylation of specific proteins, leading to smooth muscle relaxation. PLC $\beta$  (phospholipase C $\beta$ ), CaM (calmodulin), SR (sarcoplasmic reticulum),  $\text{Na}^{+}/\text{Ca}^{2+}$  exchanger (NCX), MLC (myosin light chain), MLCK (myosin light chain kinase), MLCP (myosin light chain phosphatase) (Webb, 2003).

### **1.3.3 Cardiac excitation-contraction coupling**

Cardiomyocytes are the cardiac muscle cells found in the heart. They represent the largest mass of the heart and are responsible for its contractility, generating the force required to eject the blood. Cardiac excitation-contraction coupling is the resulting event of the electrical excitation of the myocyte sarcolemma, which increases the cytoplasmic  $\text{Ca}^{2+}$  concentration and activates the contractile myofilaments to produce the cardiac contraction force (Bers and Perez-Reyes, 1999, Kobirumaki-Shimozawa *et al.*, 2014).

In cardiomyocytes, the VDCCs and ryanodine receptor (RyRs) are the main ion channels that contribute to the rise in intracellular  $\text{Ca}^{2+}$  (**Figure 1.5**). The contraction-relaxation cycle of cardiomyocytes is initiated by depolarisation of the sarcolemma produced by the action potential, which activates L-type VDCCs thereby allowing  $\text{Ca}^{2+}$  entry (Bers and Perez-Reyes, 1999). After entering the cytoplasm through the sarcolemmal membrane,  $\text{Ca}^{2+}$  will trigger the release of  $\text{Ca}^{2+}$  from the SR via the activation of the RyRs in a process termed calcium-induced calcium release (Fabiato, 1983, Cheng *et al.*, 1993).

In cardiac muscle cells, the troponin I represents the inhibitory protein that prevents actin-myosin cross-bridges from forming (Solaro and Rarick, 1998). The elevation of the intracellular  $\text{Ca}^{2+}$  results in  $\text{Ca}^{2+}$  binding to troponin C; this changes the proximity of troponin I to actin, increasing the distance between troponin I and actin,

allowing myosin to interact with actin, thereby forming the cross-bridge (Tao *et al.*, 1990, Solaro and Rarick, 1998).

The sympathetic nervous system increases the force of a contraction of the heart (positive inotropic effect), through the activation of  $\beta_1$ -adrenergic receptors (Brown, 1990). These receptors are abundant in the heart, and they are coupled to AC. Catecholamines stimulate these receptors to activate the stimulatory GTP-binding protein (Gs), which activates the enzyme AC, thereby elevating cAMP. This, in turn, activates PKA, which can phosphorylate L-type calcium channels thereby enhancing the inward  $\text{Ca}^{2+}$  current, and ultimately increasing the contraction of the cardiomyocytes (Vaughan-Jones, 1986, Brown, 1990, Bers, 2002).

In the heart, the  $\text{Ca}^{2+}$  release is terminated (depletion of store, inhibition of RyRs ), which leads to a fall in intracellular  $\text{Ca}^{2+}$  through activity of the sarco-endoplasmic reticulum calcium ATPase (SERCA), sarcolemmal  $\text{Na}^+-\text{Ca}^{2+}$ exchange (NCX), and sarcolemmal  $\text{Ca}^{2+}$ -ATPase (Vaughan-Jones, 1986, Bers, 2002, Eisner *et al.*, 2017).

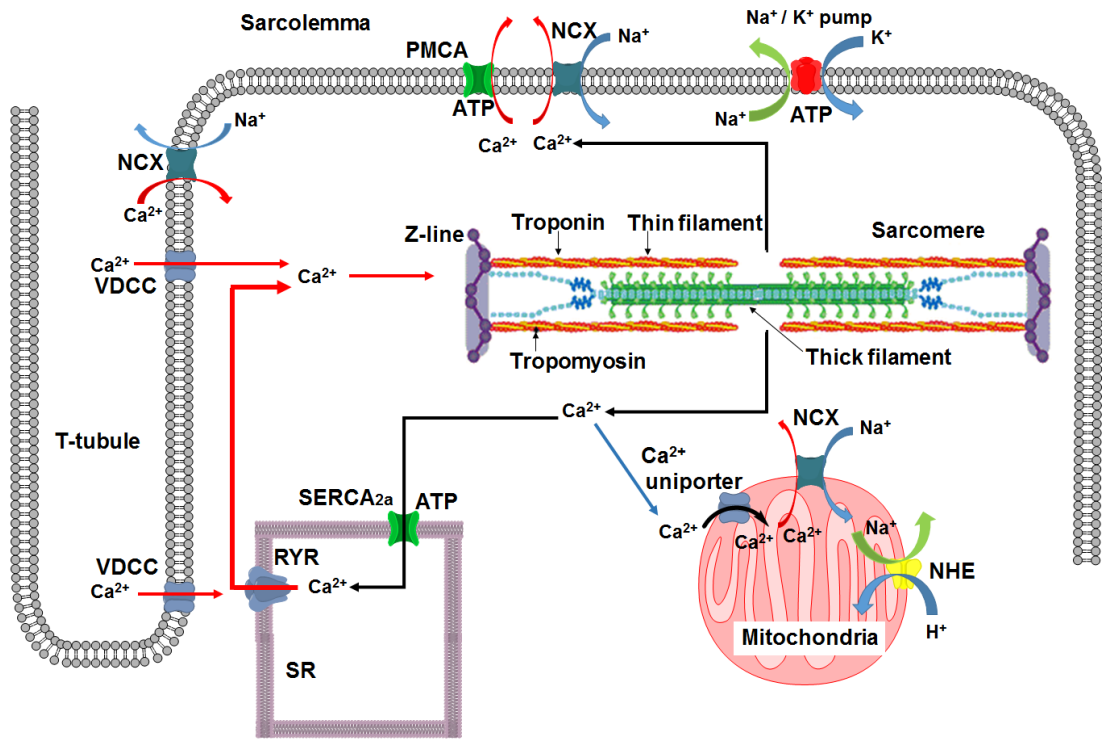


**Figure 1.5: Schematic diagram of excitation-contraction coupling in a cardiomyocyte.** Excitation of the sarcolemma by an action potential leads to the activation of voltage-dependent  $\text{Ca}^{2+}$  channels (VDCCs) and  $\text{Ca}^{2+}$  release from the sarcoplasmic reticulum (SR). The resulting elevation of cytosolic  $\text{Ca}^{2+}$  serves to activate the contractile apparatus, producing a contraction. Removal of  $\text{Ca}^{2+}$  from the cytosol by various  $\text{Ca}^{2+}$ -ATPases in the SR and sarcolemma, and  $\text{Na}^{+}/\text{Ca}^{2+}$  exchange at sarcolemma, causes relaxation.  $\text{Na}^{+}/\text{Ca}^{2+}$  exchanger (NCX), SERCA (sarco-endoplasmic reticulum  $\text{Ca}^{2+}$  ATPase), plasma membrane  $\text{Ca}^{2+}$ -ATPase (PMCA),  $\text{Na}^{+}/\text{H}^{+}$  exchanger (NHE) (Kobirumaki-Shimozawa *et al.*, 2014).

## **1.4 Project aims**

This study attempted to determine the constituent(s) is (are) responsible for the vasorelaxant property of *H. sabdariffa* (Malvaceae) that are not well known at the present time. The first step was sequential extraction of dried, powdered calyces of *H. sabdariffa* with solvents of increasing polarity using a Soxhlet apparatus. A preliminary bioactivity-led fractionation process was carried out to examine the vasorelaxant activity of the crude extract and the sub-fractions obtained from the crude methanolic extract on isolated rat aorta, using *in vitro* myography techniques. Further purification of the identified compounds was carried out using different chromatographic techniques such as TLC, gel permeation chromatography (GPC), column chromatography (CC), vacuum liquid chromatography (VLC), and preparative TLC (PTLC). That was followed by structure elucidation of the isolates using Nuclear Magnetic Resonance (NMR) and Mass spectroscopy. X-ray crystallography was also used to confirm the structure and the absolute configuration of isolated crystallised compounds

Thereafter, the activities of the pure compounds on isolated rat aorta, left atria, and trachea were carried out, using these myography techniques. Subsequent studies were carried out to determine the mechanism of action for the vasorelaxant activity of the pure compounds on the rat aorta.

The present work also aimed to carry out a phytochemical investigation on the plant *P. salicifolium* (Polygonaceae), with the aim of determining whether this plant has vasorelaxant activity.

# ***Chapter 2***

## **2 Materials and Methods**

### **2.1 Solvents**

The following solvents were used

n-Hexane HPLC grade, VWR chemicals (Lutterworth, UK)
Dimethyl sulfoxide Sigma-Aldrich (Irvine, UK)
Ethyl acetate HPLC grade, VWR chemicals (Lutterworth, UK)
Methanol HPLC grade, VWR chemicals (Lutterworth, UK)
Deuterated (99.9%) solvents: Chloroform- <i>d</i> , DMSO- <i>d</i> <sub>6</sub> , and Acetone- <i>d</i> <sub>6</sub> , Sigma-Aldrich (Irvine, UK)

### **2.2 Apparatus, reagents, and chemicals**

<i>p</i> -anisaldehyde (FSA laboratory, UK)
(±)-Bay K8644 Sigma-Aldrich (Gillingham, UK)
Carbamylcholine chloride Sigma-Aldrich (Gillingham, UK)
Calcium chloride Sigma-Aldrich (Gillingham, UK)
Column grade silica gel (Silica gel 60, mesh size 20-200 µm), Merck (Darmstadt, Germany)
FPL 64176 Tocris (Abingdon, UK)
(+)-Garcinia acid Sigma-Aldrich (Gillingham, UK)
Glacial Acetic acid HPLC grade, VWR chemicals (Lutterworth, UK)
Glucose VWR chemicals (Lutterworth, UK)
(4-(2-hydroxyethyl)-1-piperazineethanesulfonic acid) (HEPES) VWR chemicals (Lutterworth, UK)
Iberiotoxin Tocris (Abingdon, UK)
Lipophilic Sephadex LH-20, GE Healthcare (Little Chalfont, UK)
Magnesium chloride Sigma-Aldrich (Gillingham, UK)

N $\omega$ -nitro-L-arginine methyl ester hydrochloride Sigma-Aldrich (Gillingham, UK)
Potassium chloride VWR chemicals (Lutterworth, UK)
R-(-)-phenylephrine hydrochloride Sigma-Aldrich (Gillingham, UK)
Silica gel 60 RP-18 F254s plates, Merck (KGaA, Germany)
Sodium chloride VWR chemicals (Lutterworth, UK)
Sulfuric acid, VWR chemicals (Lutterworth, UK)
Tetraethylammonium chloride Sigma-Aldrich (Gillingham, UK)
TLC grade silica gel 60H, Merck (Darmstadt, Germany)
TLC pre-coated aluminium sheets (20 x 20 cm). Silica gel PF254, Merck (Darmstadt, Germany)

## 2.3 Equipment

Avance DRX500 MHz NMR, Bruker (Coventry, UK)
Decon Sonicator, Decon laboratories (Hove, UK)
Edwards Freeze Dryer, Edwards (Crawley, UK)
Force displacement transducer (Grass FT03, Astro-Med, Slough, UK)
IKA® Grinder (IKA® Werke GmbH & Co. KG, Staufen im Breisgau, Germany)
JEOL Eclipse 400 NMR spectrometer, JEOL (Pleasanton, USA)
Mettler Balance (Toledo, UK)
NMR tubes (5mm x 178 mm), Sigma-Aldrich (Poole, UK)
Orbitrap HR-ESI mass spectrometer, Thermo Fisher (Hemel Hempstead, UK)
Rotary evaporator, Büchi (Flawil, Switzerland)
Safety Cabinet (Walker, Glossop, UK)
Soxhlet extractor, Electro thermal (Staffordshire, UK)
UV- lamps 254nm and 364nm UVGL-58, UVP (Chicago, USA)

## **2.4 Plant Material**

*H. sabdariffa* (Malvaceae), was provided by Prof. John Igoli (University of Agriculture PMB 2373 Makurdi, Nigeria). It was collected from Makurdi in Benue State, Nigeria and identified at the Herbarium of the National Institute for Pharmaceutical Research and Development (Abuja, Nigeria) by Dr Jemilat Ibrahim, where a voucher specimen number NIPRD/H/6972 was deposited. The plant *P. salicifolium* Brouss ex Wild was collected from the banks of River Tigris in Southern Iraq in April 2015, and identified at the College of Science, University of Diyala by Assist. Prof. Dr Khazal Dh. Wadi Al-Jibouri.

### **2.4.1 Extraction method**

The dried plant materials were ground to a fine powder using an IKA<sup>®</sup> grinder. The ground plant materials were loaded into a small thimble and extracted with n-hexane, ethyl acetate (EtOAc), and methanol (MeOH) (72 h each) using a Soxhlet apparatus (**Figure 2.1**). The solvents were removed at 40°C using a rotary evaporator, and the extracts were then subjected to further investigation.

## **2.5 Separation techniques**

### **2.5.1 Thin layer chromatography**

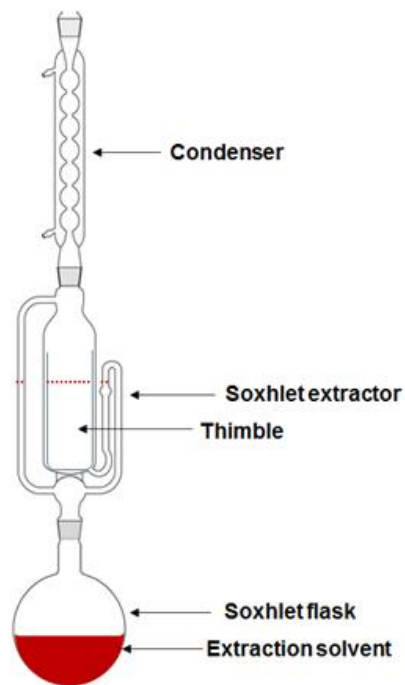
Thin layer chromatography (TLC) is a simple and fast method used to analyse and separate a mixture of compounds from crude extracts into individual components. Plant crude extracts, sub-fractions, or pure compounds were dissolved in a suitable solvent (determined by trials and errors), and spotted on TLC plates (normal or reverse phase), about 1 cm above the lower edge of the pre-coated aluminium plates

using a capillary tube. Solvent systems used included: *n*-hexane/ EtOAc; *n*-hexane/EtOAc/MeOH; EtOAc/MeOH; and EtOAc/MeOH/ formic acid. They were added to the TLC tank as the mobile phase, depending on the nature of the fractions, and left for a while to saturate the environment of the tank, with the aid of a filter paper placed inside the tank. Ascending development was achieved by placing the spotted TLC plates in a tank and removing them before the solvent reached the top of the plate. The plates were immediately air-dried after marking the solvent front with a pencil line.

The TLC plates were examined under short ( $\lambda=254$  nm) and long ( $\lambda=366$  nm) wave ultraviolet light (UV), then visualised by spraying the plate with *p*-anisaldehyde-sulphuric acid spray (0.5 ml anisaldehyde, 10 ml glacial acetic acid, 85 ml methanol, and 5 ml sulphuric acid) and heated at 110 °C using a heat gun until the spots appeared.

### **2.5.2 Preparative thin layer chromatography**

This technique was used for separation and purification of compounds from the fractions containing simple mixtures obtained from the column chromatography. A small scale separation was carried out on TLC sheets to determine the best solvent system needed to achieve optimum separation. Then, separation of greater amounts of the compounds were performed on larger TLC plates (20×20 cm). The samples were dissolved in a minimum volume of an appropriate solvent and were then applied 2 cm from the bottom as a thin band across the entire width of the plate using a capillary tube.

**A****B**

**Figure 2.1: Soxhlet apparatus.** (A) Assembly of the apparatus (B) Photograph of the Soxhlet apparatus used for the extraction of the fine powdered dried calyces of *H. sabdariffa*.

The plates were developed as above (**Methods Section 2.5.1**), and observed under UV light (sometimes sprayed at one side with *p*-anisaldehyde-sulphuric acid spray if they were invisible). The bands of interest were cut into strips along with the absorbent, then the strips attributed to each separate component were cut into small pieces. Compounds were recovered from the silica gel by eluting the recovered stationary phase with 100% EtOAc, a mixture of EtOAc /MeOH (50:50%), and finally with 100% MeOH for maximum recovery from the silica gel. After filtration and evaporation, the obtained components were analysed by NMR spectroscopy.

### **2.5.3 Gel permeation chromatography**

This method was used to separate compounds based on the difference in their molecular size. A wet slurry was prepared by adding methanol to 30 g of Sephadex® LH20 and packed into a glass column 45 cm high and 2 cm in diameter. The methanol extract (2 g) was dissolved in about 2 ml methanol and then loaded onto the top of the column. The columns were eluted with methanol and fractions (5 ml each) were collected in vials (**Figure 2.2**). This method was also used for the purification of some fractions.

### **2.5.4 Vacuum liquid chromatography**

A glass funnel column was dry-packed with TLC grade silica gel 60H (300g) under vacuum (via a water vacuum pump) to compress the silica gel to a uniform layer. The methanol extract (10 g) was dissolved and mixed with a small quantity of silica gel 60H and allowed to dry. The dry slurry was loaded onto the column, spread to a uniform layer on the silica bed and covered with a filter paper. The column was eluted

with approximately 400 ml of different solvents and solvent ratios (**Table 2.1**), and the fractions were collected. Fractions were evaporated and examined by TLC.

### 2.5.5 Silica gel column chromatography

This technique was applied to fractionate polar and non-polar components. A wet slurry of silica gel was prepared by adding 50 g of silica gel 60H (mesh size 0.063-0.200 mm) to hexane and then packed into a glass column 55×3 cm plugged with cotton wool. The hexane or ethyl acetate extracts were dissolved in hexane or ethyl acetate, respectively, and adsorbed on a small quantity of silica gel 60H. The dry sample slurry was then loaded onto the column and covered by a protective layer of silica gel 60H. The elution was carried out gradient-wise using mixtures of polar and non-polar solvents (**Table 2.2**). Fractions were analysed by TLC and combined according to the band similarity and evaporated to dryness.

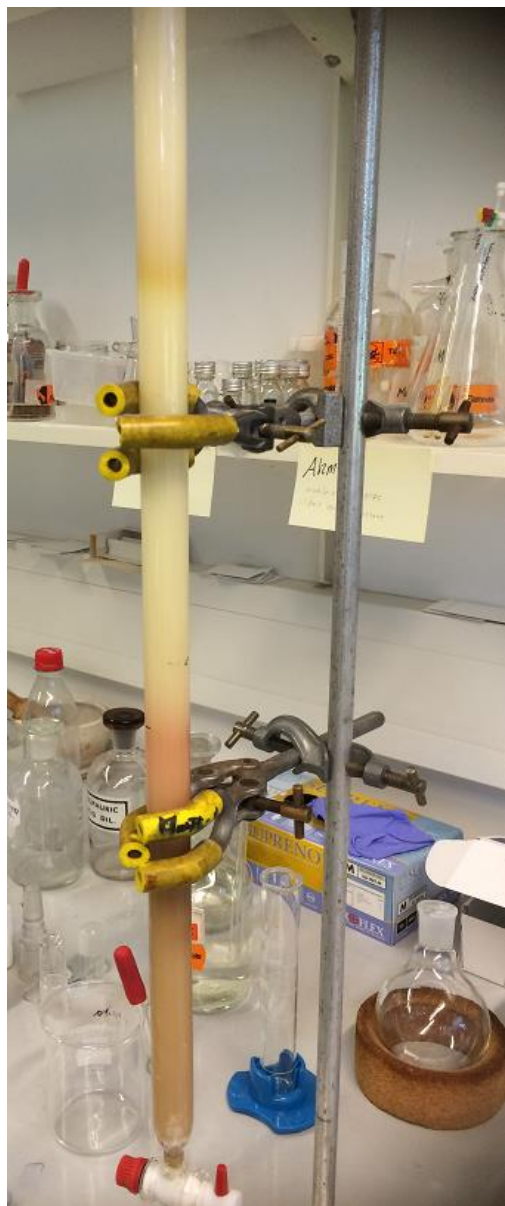


**Figure 2.2: Photograph showing the gel permeation column (GPC) for chromatographic separation of the methanol extract of calyces of *H. sabdariffa*.**

**Table 2.1: Mobile phase systems used for vacuum liquid chromatography**

Hexane %	Ethyl acetate %	Methanol %
100	0	0
70	30	0
50	50	0
40	60	0
20	80	0
10	90	0
30	70	0
0	100	0
0	90	10
0	80	20
0	70	30

**Table 2.2: Mobile phase systems used for silica gel chromatography**

Hexane extract mobile phase	Ethyl acetate extract mobile phase
Hexane: Ethyl acetate 100:0	Hexane: Ethyl acetate 90:10
Hexane: Ethyl acetate 90:10	Hexane: Ethyl acetate 80:20
Hexane: Ethyl acetate 80:20	Hexane: Ethyl acetate 70:30
Hexane: Ethyl acetate 70:30	Hexane: Ethyl acetate 60:40
Hexane: Ethyl acetate 60:40	Hexane: Ethyl acetate 50:50
Hexane: Ethyl acetate 50:50	Hexane: Ethyl acetate 40:60
Hexane: Ethyl acetate 40:60	Hexane: Ethyl acetate 30:70
Hexane: Ethyl acetate 30:70	Hexane: Ethyl acetate 20:80
Hexane: Ethyl acetate 20:80	Hexane: Ethyl acetate 10:90
Hexane: Ethyl acetate 10:90	Hexane: Ethyl acetate 0:100
Hexane: Ethyl acetate 0:100	Ethyl acetate: Methanol 90:10
Ethyl acetate: Methanol 90:10	

## **2.6 Spectroscopic examination**

### **2.6.1 Nuclear magnetic resonance spectroscopy**

Samples (5-50 mg) were dissolved in about 0.65 ml of an appropriate deuterated solvent, mostly deuterated chloroform ( $\text{CDCl}_3$ ), or deuterated dimethyl sulfoxide ( $\text{DMSO}-d_6$ ), or acetone- $d_6$ , depending on the solubility of the compound and the extent of resolution obtained. NMR experiments including one-dimensional (1D) proton  $^1\text{H}$ , carbon  $^{13}\text{C}$ , distortionless enhancement of polarization transfer (DEPTq135), and two-dimensional (2D) experiments were run using a JEOL (JNM LA400) 400 MHz and a Bruker Avance DRX-500 (500MHz) spectrophotometer. The spectral data obtained for the samples were processed via MestReNova software 11.0.2 (Mestrelab Research, A Coruña, Spain), and ChemBioDraw Ultra, Version 15 (PerkinElmer, Yokohama, Japan), was used to draw the compound structures.

#### **2.6.1.1 1D NMR**

This technique, specifically  $^1\text{H}$  and  $^{13}\text{C}$  NMR, is the primary technique used for structure identification of compounds. Both  $^1\text{H}$  and  $^{13}\text{C}$  spectra provided information about the types of protons and carbon atoms in the compounds.

#### **2.6.1.2 2D NMR**

Correlation spectroscopy (COSY), Heteronuclear single quantum correlation (HSQC), Heteronuclear multiple bond connectivity (HMBC), are examples of the most useful 2D NMR techniques.

COSY experiments were performed by plotting the  $^1\text{H}$  chemical shifts on both frequency (horizontal and vertical) axes, and the connectivity of protons can be shown by the  $^1\text{H}$ - $^1\text{H}$  COSY contour plot along the diagonal of the square.

HSQC was used to identify the correlation between protons and carbons atoms in samples through direct one bond ( $^1J$ ) coupling between them. HMBC provided the correlation between the chemical shift of the protons in the samples and the heteronucleus  $^{13}\text{C}$  through long range bond  $^2J$  and  $^3J$  coupling interaction between the nuclei (long-range H-X-C-C-C correlations).

### **2.6.2 Liquid chromatography-Mass spectrometry (LC-MS)**

This technique is used to separate and identify the elemental composition of a sample. About 1 mg of each sample was dissolved in 1 ml methanol and 10  $\mu\text{L}$  of the solution was then injected along with an infusion of 0.1% (v/v) formic acid in water (solution A) and 0.1% (v/v) formic acid in acetonitrile (solution B) at a flow rate of 300  $\mu\text{L}/\text{min}$ . A gradient method was used for elution of the mobile phase starting with 10% (v/v) solution B in solution A to reach 100% of solution B then reduced again to 10% (v/v) solution B. Positive ion and negative ion mode electrospray (ESI) experiments were carried out on a Dionex ultimate 5000 LC-Exactive Orbitrap mass spectrometer.

# ***Chapter 3***

## **3 Phytochemical and pharmacological studies of *H. sabdariffa***

### **3.1 Introduction**

The red calyces of *H. sabdariffa* (Malvaceae), have been used in many countries throughout the world for their health benefits, particularly as a treatment for hypertension (Ali *et al.*, 2005, Hopkins *et al.*, 2013, Da-Costa-Rocha *et al.*, 2014).

The antihypertensive activity of *H. sabdariffa* has also been studied clinically in patients with high blood pressure (Faraji and Tarkhani, 1999, Herrera-Arellano *et al.*, 2004, Herrera-Arellano *et al.*, 2007, McKay *et al.*, 2009, Mozaffari-Khosravi *et al.*, 2009b, Mozaffari-Khosravi *et al.*, 2013).

A number of *in vivo* studies have also shown the blood pressure reducing activity of *H. sabdariffa* calyces in hypertensive animals (Onyenekwe *et al.*, 1999, Odigie *et al.*, 2003, Mojiminiyi *et al.*, 2007, Abubakar *et al.*, 2015). For example, in salt-induced hypertensive rats, the aqueous extract of the calyces lowered both systolic and diastolic blood pressure by 6 and 7 mmHg, respectively (Abubakar *et al.*, 2015). There have also been a number of *in vitro* studies examining the vasorelaxant effects of the crude extracts of *H. sabdariffa*. Both aqueous and alcohol extracts of hibiscus calyces produced vasorelaxation of the rat aorta pre-contracted with either an adrenoceptor agonist or by depolarization (Ali *et al.*, 1991, Obiefuna *et al.*, 1994, Adegunloye *et al.*, 1996, Ajay *et al.*, 2007, Sarr *et al.*, 2009).

Phytochemical studies on the extracts (alcoholic or aqueous) of hibiscus calyces have shown that they contain a number of organic acids (hydroxycitric and hibiscus), flavonoids (quercetin, hibiscetin, and gossypetin), and anthocyanins (hibiscin) (Da-Costa-Rocha *et al.*, 2014). However, the compounds which are responsible for the antihypertensive activity of *H. sabdariffa* are still unclear. Therefore, in an attempt to identify the constituents responsible for this vasorelaxant activity, investigation of the vasorelaxant effect of the crude extracts of *H. sabdariffa* on the rat aorta was carried out. Thereafter, a preliminary bioactivity-led fractionation process was carried out to examine the vasorelaxant activity of the sub-fractions obtained from the crude methanolic extract using myography techniques.

## 3.2 Materials and Methods

### 3.2.1 Fractionation of *H. sabdariffa* crude extracts

Ground material of the calyces of *H. sabdariffa* (75 g) was extracted with hexane, ethyl acetate and then methanol (500 ml each) using a Soxhlet apparatus. The extracts were dried at 40 °C using a rotary evaporator. The crude hexane, ethyl acetate, and methanol extracts were fractionated by different chromatographic techniques. A silica gel CC was used to fractionate the hexane extract starting with a mobile phase of 10% (v/v) ethyl acetate in hexane until 100% (v/v) ethyl acetate. Fractions were collected (vials 1 to 89; 5 ml each) and then left in a fume cupboard to evaporate. Similarly, the ethyl acetate crude extract was fractionated by CC, eluted with a stepwise mobile phase of 10% (v/v) ethyl acetate in hexane until 100% (v/v) ethyl

acetate then 10% (v/v) methanol in ethyl acetate and the fractions were collected (vials 1 to 60; 5 ml each) and left in a fume cupboard to evaporate.

The methanol extract was fractionated using GPC with a Sephadex LH-20 column, and eluted with methanol as the mobile phase. Fractions (vials 1 to 40; 5 ml each) were collected and left to evaporate in the fume cupboard. Preliminary assessment was achieved by visualisation of these fractions on TLC plates and fractions of similar profiles were pooled together (**Figure 3.1**). All in all, 5 sub-fractions were obtained (HS-F1, HS-F2, HS-F3, HS-F4, and HS-F5).

The methanol extract was also subjected to VLC (**Methods Section 2.5.4** ). 22 fractions; 300 ml each were obtained and evaporated using rotary evaporator. Analysis of these fractions using  $^1\text{H}$  NMR and collection of similar fractions yields 5 sub-fractions; HS VLC1 (vials 1-4), HS VLC2 (vials 5-9), HS VLC3 (vials 10-14), HS VLC4 (vials 15-19), and HS VLC5 (vials 20-22). The composition of these samples was investigated by NMR spectroscopy to characterise and elucidate the compounds of interest.

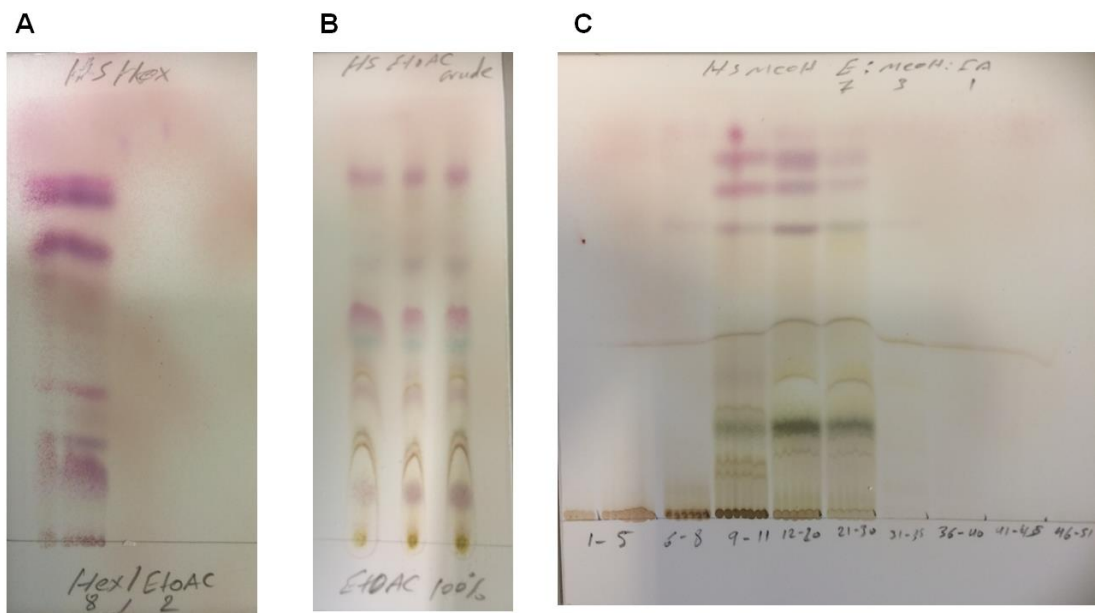


**Figure 3.1: Thin layer chromatography (TLC) of the (A) n-hexane, (B) ethyl acetate (EtOAc), and (C) methanol (MeOH) crude extracts.** A 20:80% EtOAc/n-hexane was used as a mobile phase for the hexane crude extract, and 100% EtOAc as a mobile phase for the ethyl acetate crude extract, whereas, for the methanol crude extract a mobile phase mixture of 70:30% EtOAc/ MeOH was used. The bands were visible after spraying with *p*-anisaldehyde-sulphuric acid.

### **3.2.2 Drugs, solvents and chemicals**

R-(-)-phenylephrine hydrochloride was purchased from Sigma-Aldrich (Gillingham, UK). All other reagents and salts used were from either VWR Chemicals (Lutterworth, UK), or Sigma-Aldrich. The crude methanolic extract of *H. sabdariffa* was prepared as 20 mg/ml stock solution dissolved in physiological salt solution (PSS). The PSS had the following composition (in mM): NaCl 150, KCl 5.4, glucose 10, (4-(2-hydroxyethyl)-1-piperazineethanesulfonic acid) (HEPES) 10, MgCl<sub>2</sub> 1.2, and CaCl<sub>2</sub> 1.8, adjusted to pH 7.4 with NaOH. Sub-fractions were also dissolved in PSS. KCl was dissolved in deionised water to prepare a stock solution of 2 M concentration, which was used without subsequent dilutions. A stock solution of phenylephrine (PE) (100 mM) was prepared in PSS, and subsequent dilutions were carried out using PSS.

### **3.2.3 Aorta preparation and contractile studies**

In-house bred male and female Sprague-Dawley rats (200-250 g) were sacrificed by cervical dislocation according to Schedule 1 of the Animals (Scientific Procedures) Act 1986. The thoracic and abdominal sections of the aorta were subsequently removed and placed in cold PSS. Under a dissecting microscope (Nikon SMZ645), the aorta was cleaned of any adhering fat and loose connective tissue. The aorta was then cut into 4-5 mm long rings. Then, these tissue rings were mounted on intraluminal parallel wires; one of which was fixed and the other attached to a Grass FT03C force displacement transducer. The organ bath (1 ml in volume) was filled with PSS and maintained at 37°C whilst being aerated with air. A resting tension of 1 g was applied to the tissue and a 1 h equilibration period was allowed, with regular

reintroduction of fresh PSS and re-adjustment of the 1 g resting tension. The contractile response was acquired through a PowerLab 4/30 data acquisition system and recorded by Chart (v5.2) software (ADInstruments, Ltd., Oxfordshire, UK) (**Figure 3.2**). Before commencing any experimental protocol the tissue was challenged repeatedly with 40 mM KCl until the contractile responses were reproducible.

### **3.2.4 Effect of PE and KCl on the rat aorta**

PE (1 nM-30 µM) was applied to the rat aorta in a cumulative manner in order to obtain a concentration response curve and to calculate the EC<sub>50</sub> and the E<sub>max</sub> for PE, which were then used to produce pre-contraction of the aorta in subsequent studies. The same protocol of application was repeated for KCl (5-80 mM) for the same purpose.

### **3.2.5 Effects of the crude, and sub-fractions from the methanolic extract of *H. sabdariffa* on the rat aorta**

A preliminary *in vitro* screen was carried out by examining the vasorelaxant effect of the crude methanol extract of *H. sabdariffa* (0.001-1 mg/ml), when added to the aorta pre-contracted with either PE (3 µM) or KCl (60 mM). In order to find out which compounds were responsible for this activity, a further preliminary bioactivity-led fractionation process was carried out to examine the vasorelaxant activity of the sub-fractions obtained from the crude methanolic extract using myography techniques.

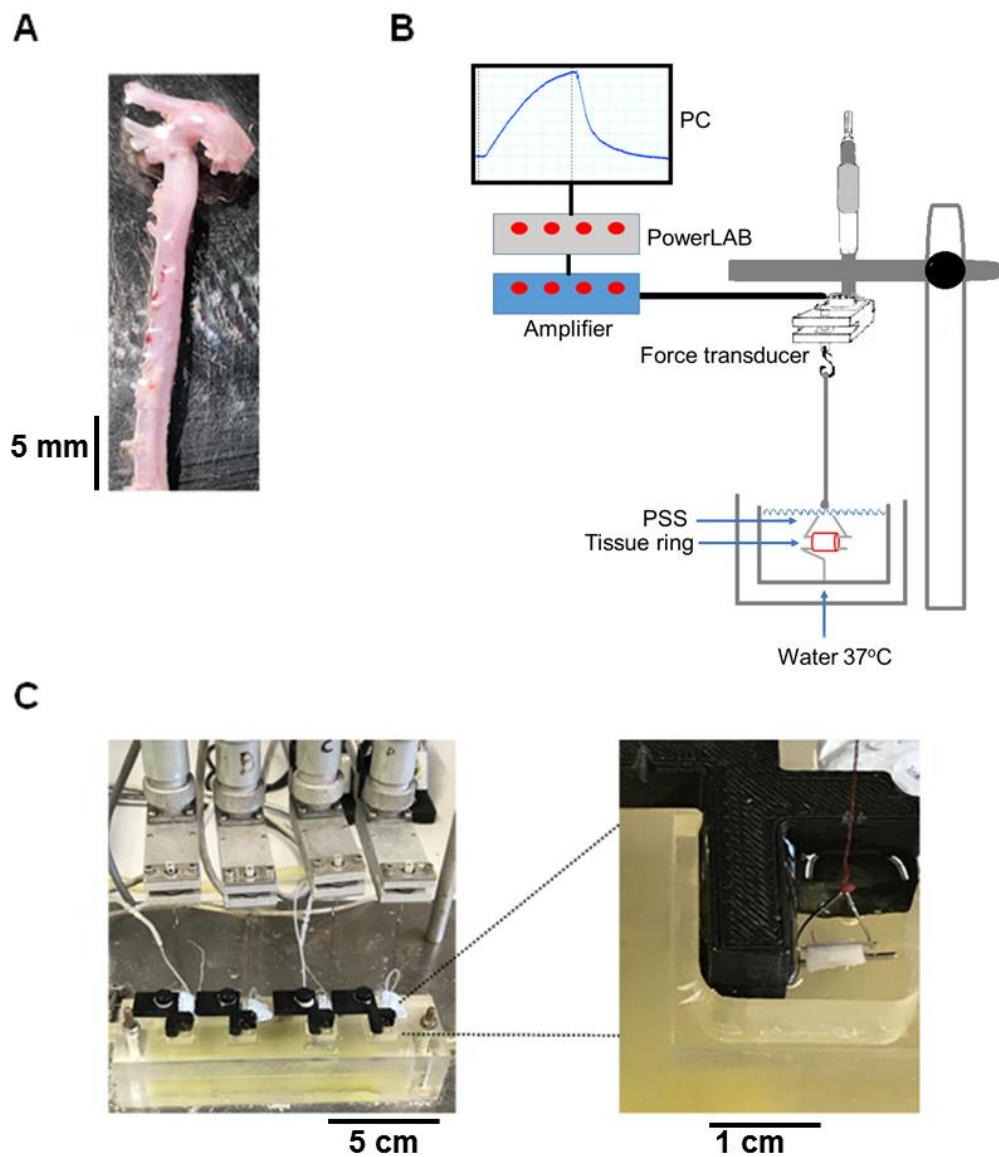


**Figure 3.2: The organ bath set up.** (A) Photograph of the rat aorta after preparation for the myograph studies. (B) Schematic diagram showing the organ bath with the PowerLab data acquisition system. (C) Photograph of the actual organ bath set up and expanded photograph of the mounted aortic ring. The aortic ring is mounted in physiological salt solution (PSS), and attached to a Grass FT03C force displacement transducer. Air was continuously bubbled into the organ bath through a crimped syringe needle.

### **3.3 Statistical analysis**

For the contractile responses, the data were expressed as a percentage of the maximum contraction to either agonist or KCl. The relaxant effect is expressed as the measured tension following the addition of the extracts divided by the steady state tension produced by the contractile stimulus being used,  $\times 100$ . Nonlinear regression analysis (GraphPad Prism version 7, San Diego, CA, USA) was used for fitting the log concentration-response curve and determination of the  $IC_{50}$  (concentration required to produce 50% of the maximum inhibitory effect) and  $I_{max}$  (the maximum inhibitory effect). One tissue that was pre-contracted always served as a control. All data are presented as mean  $\pm$  standard error of the mean (s.e.m.). The number of observations are expressed in the format of  $n=N/n$  where  $N$  is the number of tissues and  $n$  is the number of animals. One-way ANOVA with Tukey's multiple comparisons test was used to compare the treatments with control groups, and Student's two-tailed unpaired  $t$ -test was applied for statistical comparison of  $IC_{50}$  of different groups.  $P<0.05$  was considered to be statistically significant.

## **3.4 Results**

### **3.4.1 Phytochemical Results**

#### **3.4.1.1 Soxhlet extraction and yield**

The extraction of *H. sabdariffa* calyces (75 g powder) was carried out by hot solvent extraction using a Soxhlet apparatus. The yields obtained with the different solvents were as follows: hexane (1.66 g; 2.2% yield); ethyl acetate (1.69 g; 2.2% yield); and methanol (20 g; 26.6% yield). These extracts were subjected to further processing and investigations.

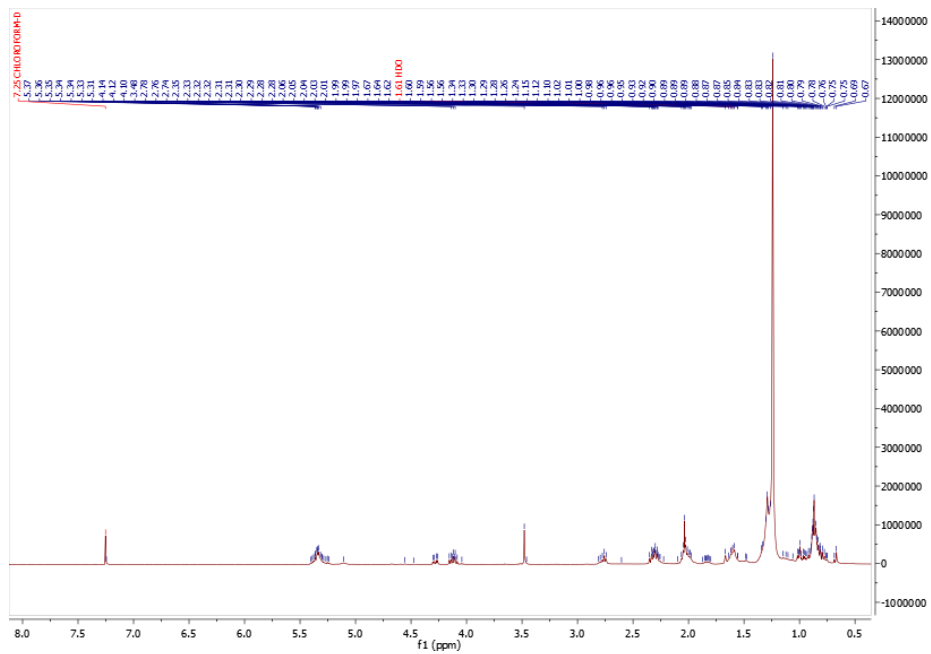
### **3.4.1.2 Fractionation of *H. sabdariffa* crude extracts**

The  $^1\text{H}$  NMR of the hexane extract showed signals suggesting the presence of fats and steroids (**Spectrum 3.1**). Analysis of the  $^1\text{H}$  NMR of the ethyl acetate extract showed the presence of a mixture of fats, steroids, and organic acids (**Spectrum 3.2**).

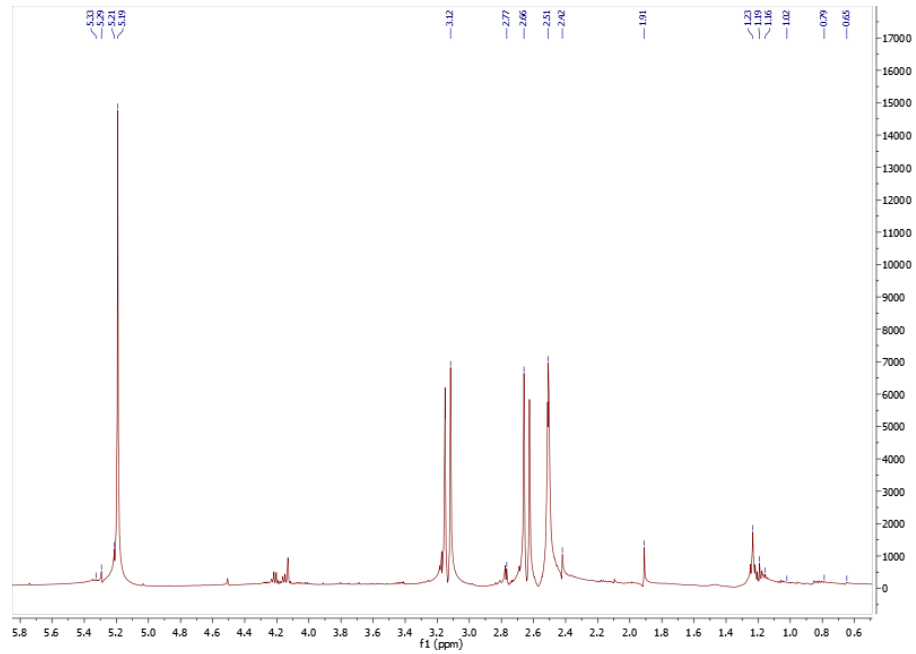
Analysis of the  $^1\text{H}$  NMR spectra of the methanol extract and sub-fractions obtained using GPC showed the presence of organic acids and sugars as the major compounds, and the polyphenolic compounds appeared to be minor (**Spectrum 3.3**). As, sub-fraction HS-F1 (vials 1-14, 6% yield) was identified as a mixture of sugars (**Spectrum 3.4**), while sub-fraction HS-F2 (vials 15-21, 25% yield) was identified as a mixture of organic acids and the ester forms of these organic acids (**Spectrum 3.5**). The compounds in sub-fraction HS-F3 (vials 22-29, 29% yield) were identified as a mixture of organic acids mainly, hibiscus acid and its derivatives as the major constituents; in addition to the polyphenolic compounds that appear as the minor constituents (**Spectrum 3.6**). NMR analysis of the sub-fraction HS-F4 (vials 30-34, 12% yield) showed that hibiscus acid was the major compound, and hibiscus acid-6-methyl ester was a minor compound (**Spectrum 3.7**), whereas HS-F5 (vials 35-40, 6% yield) was identified as hibiscus acid (**Spectrum 3.8**).

Analysis of the  $^1\text{H}$  NMR spectra of the sub-fractions obtained from the VLC of the methanol extract showed the presence of hibiscus acid derivatives and fats. As, sub-fraction HS VLC1, was identified as mixtures of fats and sterols. Other sub-fractions HS VLC2, HS VLC3, HS VLC4, and HS VLC5 were identified as different mixtures

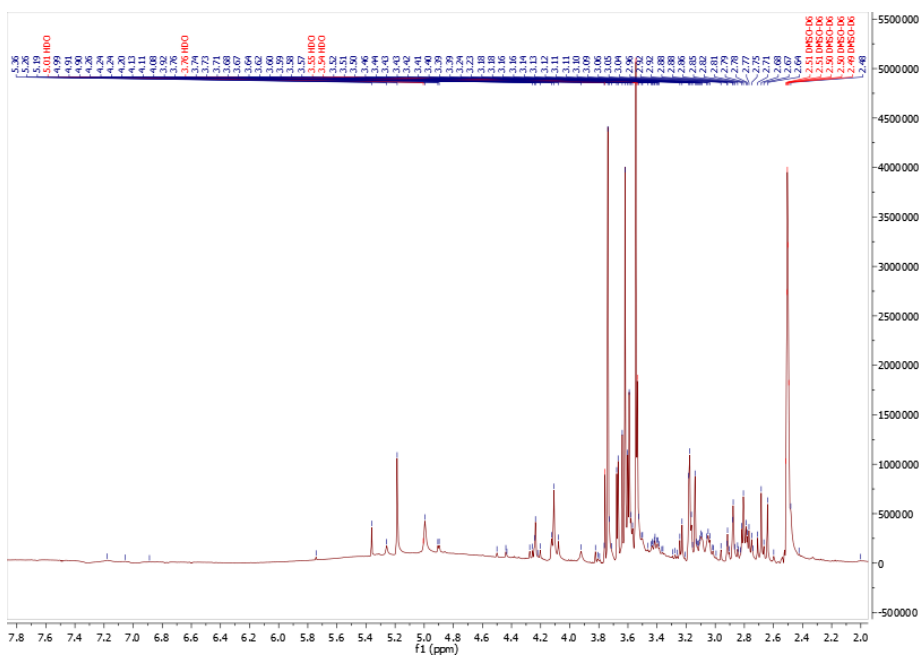
of hibiscus acid derivatives such as hibiscus acid-6-methyl ester and hibiscus acid dimethyl ester (**Spectrum 3.9**, **Spectrum 3.10**, **Spectrum 3.11**, and **Spectrum 3.12**).



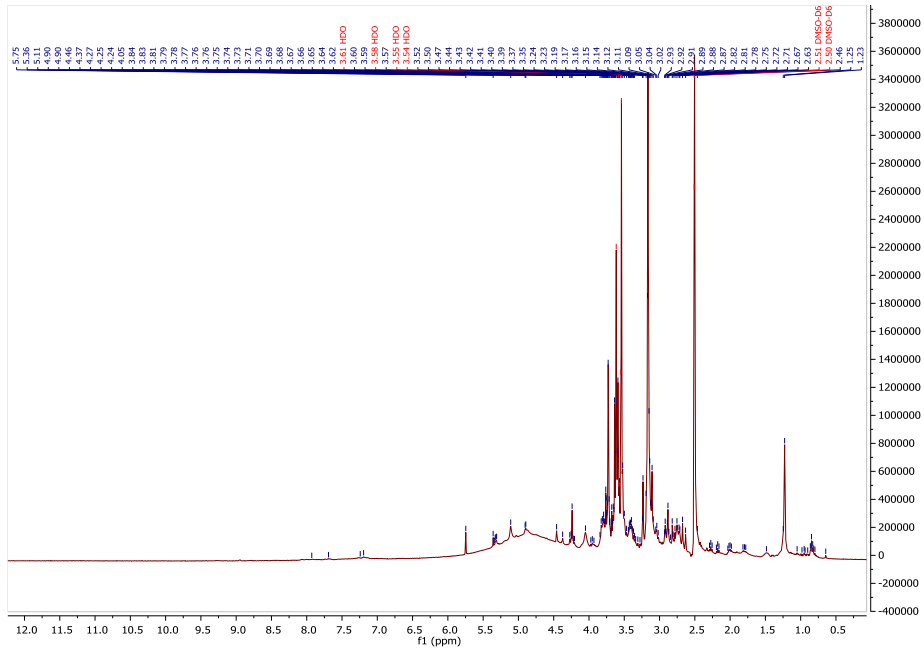
**Spectrum 3.1:**  $^1\text{H}$  NMR spectrum (400 MHz) of the hexane crude extract of *H. sabdariffa* in Chloroform-*d*.



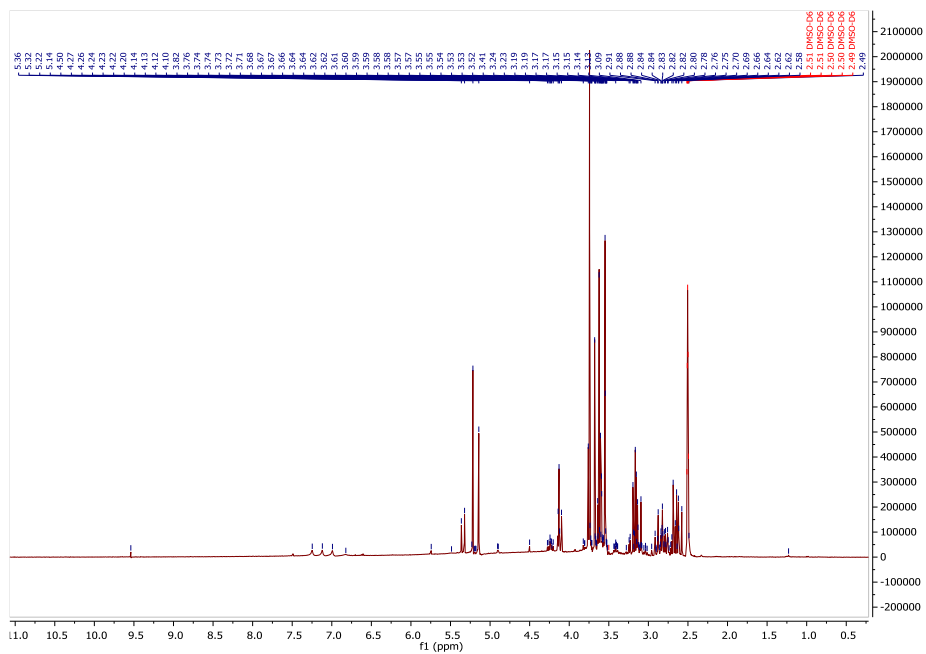
**Spectrum 3.2:  $^1\text{H}$  NMR spectrum (400 MHz) of the ethyl acetate crude extract of *H. sabdariffa* in  $\text{DMSO}-d_6$ .**



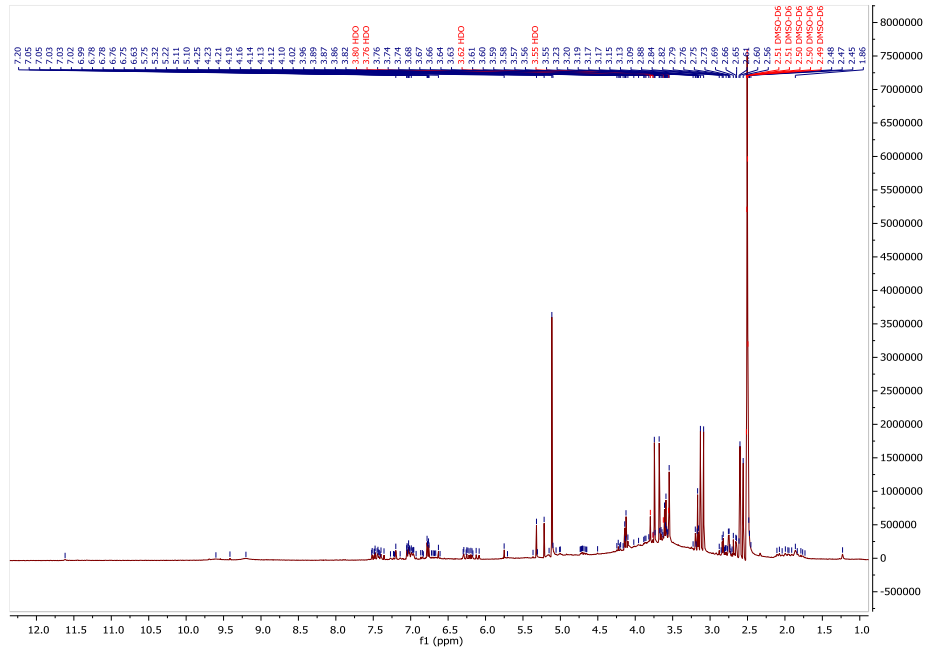
**Spectrum 3.3:**  $^1\text{H}$  NMR spectrum (400 MHz) of the crude methanolic extract of *H. sabdariffa* in DMSO-*d*6.



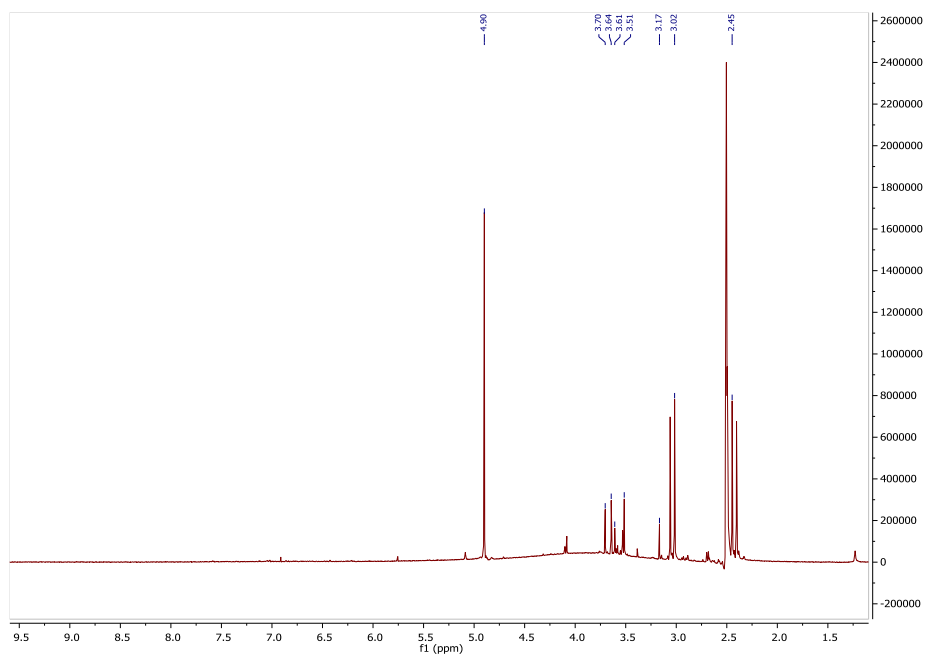
**Spectrum 3.4:**  $^1\text{H}$  NMR spectrum (400 MHz) of the sub-fraction F1 (HS-F1) of the crude methanolic extract of *H. sabdariffa* in DMSO-*d*6.



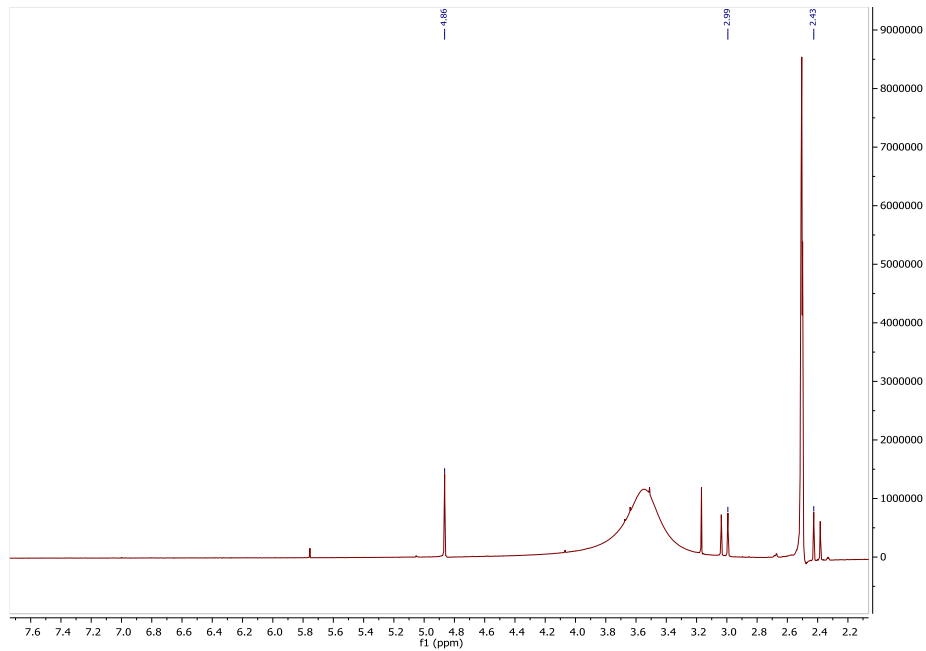
**Spectrum 3.5 :  $^1\text{H}$  NMR spectrum (400 MHz) of the sub-fraction F2 (HS-F2) of crude methanolic extract of *H. sabdariffa* in  $\text{DMSO}-d_6$ .**



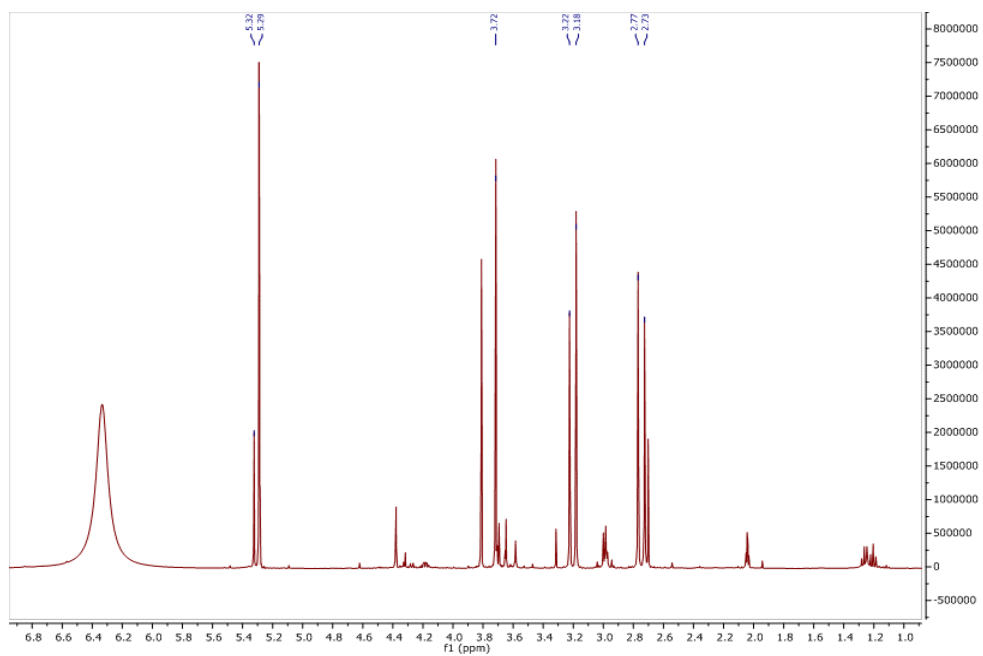
**Spectrum 3.6:  $^1\text{H}$  NMR spectrum (400 MHz) of the sub-fraction F3 (HS-F3) of crude methanolic extract of *H. sabdariffa* in  $\text{DMSO}-d_6$ .**



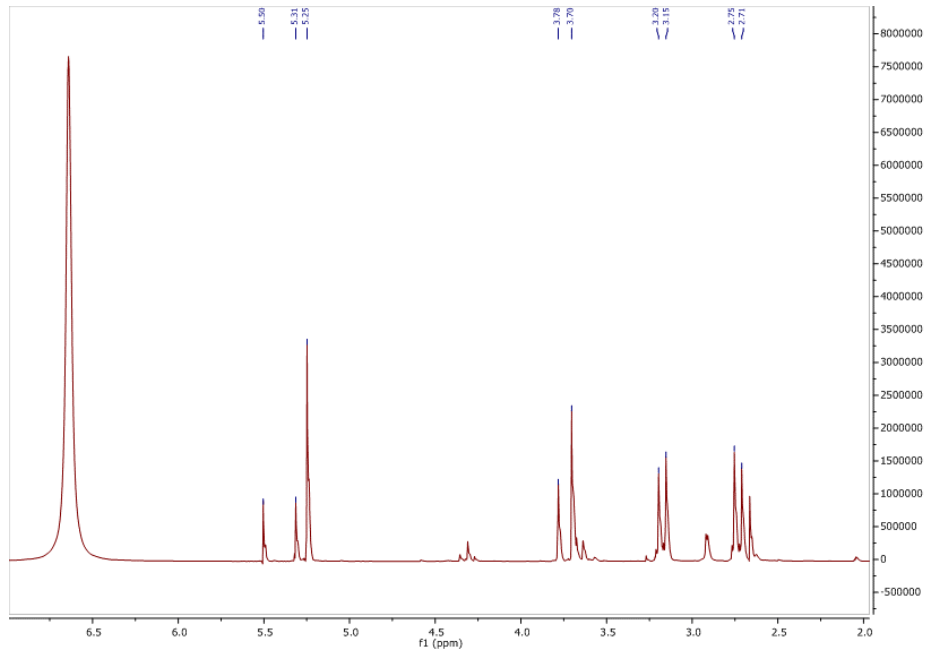
**Spectrum 3.7:** <sup>1</sup>H NMR spectrum (400 MHz) of the sub-fraction F4 (HS-F4) of crude methanolic extract of *H. sabdariffa* in DMSO-*d*<sub>6</sub>.



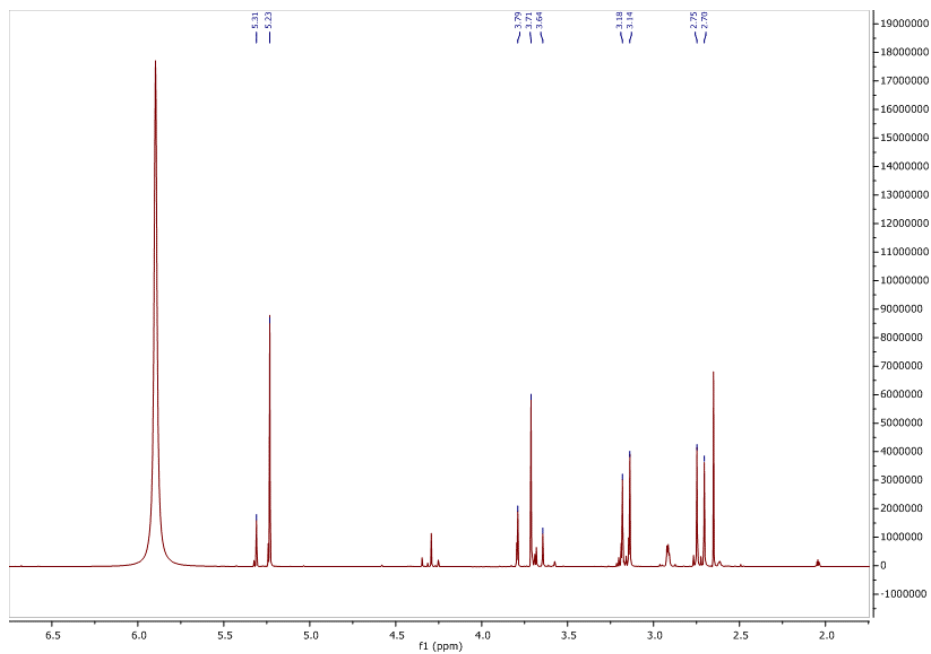
**Spectrum 3.8:** <sup>1</sup>H NMR spectrum (400 MHz) of the sub-fraction F5 (HS-F5) of crude methanolic extract of *H. sabdariffa* in DMSO-*d*<sub>6</sub>.



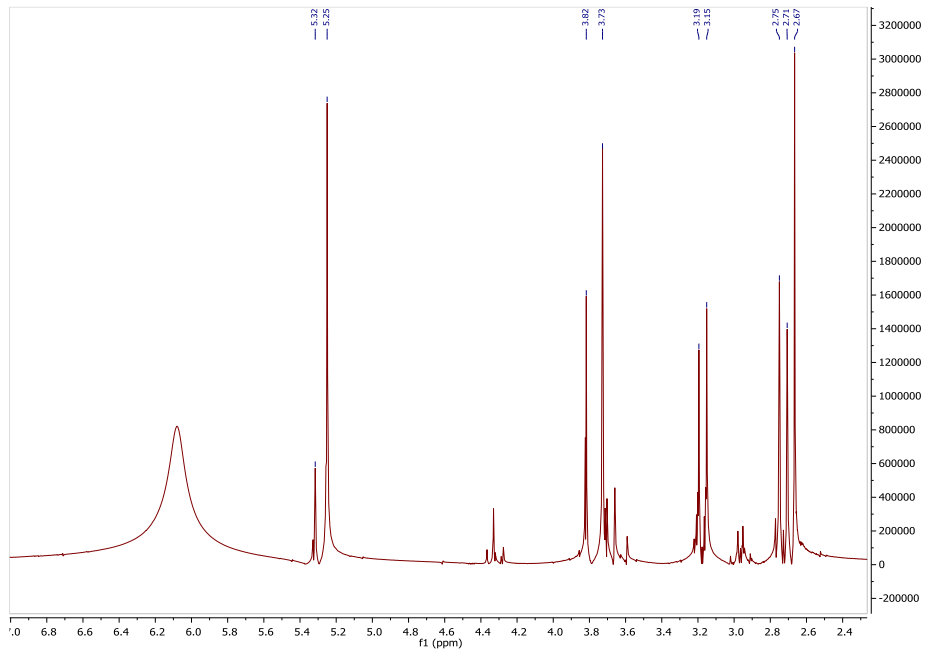
**Spectrum 3.9:**  $^1\text{H}$  NMR spectrum (400 MHz) of the VLC sub-fraction 2 of crude methanolic extract of *H. sabdariffa* (HS VLC2) in Acetone- $d_6$ .



**Spectrum 3.10:**  $^1\text{H}$  NMR spectrum (400 MHz) of the VLC sub-fraction 3 (HS VLC3) of crude methanolic extract of *H. sabdariffa* in Acetone- $d_6$ .



**Spectrum 3.11:**  $^1\text{H}$  NMR spectrum (400 MHz) of the VLC sub-fraction 4 (HS VLC4) of crude methanolic extract of *H. sabdariffa* in Acetone- $d_6$ .



**Spectrum 3.12:**  $^1\text{H}$  NMR spectrum (400 MHz) of the VLC sub-fraction 5 (HS VLC5) of the crude methanolic extract of *H. sabdariffa* in Acetone- $d_6$ .

### 3.4.1.3 Characterisation of $\beta$ -sitosterol and stigmasterol as a mixture from the ethyl acetate extract of *H. sabdariffa*.

Two compounds (**Figure 3.3**) were isolated from the ethyl acetate extract using silica gel CC. On the TLC plates, they appeared as a purple spot after treatment with *p*-anisaldehyde-sulphuric acid reagent and heating. The  $^1\text{H}$  NMR spectrum (**Spectrum 3.13**) showed a doublet at  $\delta_{\text{H}}$  5.29 characteristic of the existence of the signal for olefinic proton H-6. Two signals at  $\delta_{\text{H}}$  5.08 and 4.96 were assigned to the olefinic protons H-20 and H-21 of stigmasterol. A signal at  $\delta_{\text{H}}$  3.48 (1H) was assigned to the oxymethine proton H-3 of sitosterol and stigmasterol. The spectrum also showed two single peaks at  $\delta_{\text{H}}$  0.94 and 0.72 attributable to Me-19 and Me-18, respectively; and 0.74 (3H, s) (Me-28) and four doublets at  $\delta_{\text{H}}$  0.93 (Me-21), 0.9 (Me-26), 0.78 (Me-29) and 0.76 (Me-27).

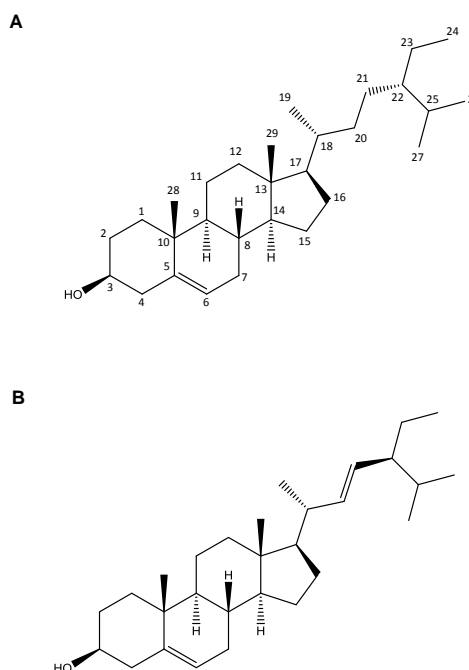
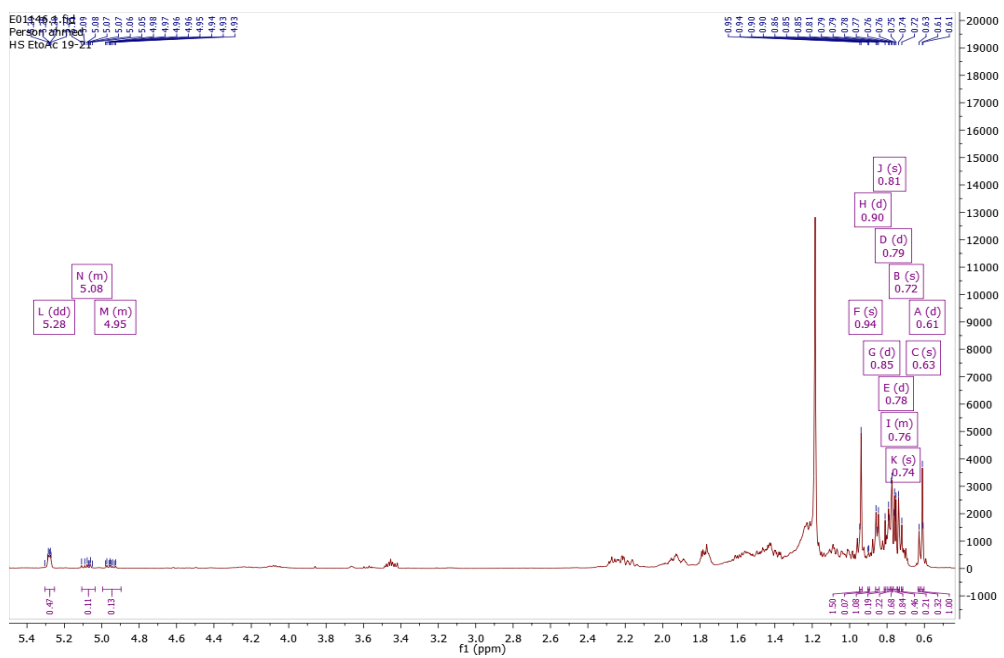


**Figure 3.3: Structure of (A)  $\beta$ -sitosterol, and (B) stigmasterol.**



**Spectrum 3.13:**  $^1\text{H}$  NMR spectrum (400 MHz) of  $\beta$ -sitosterol and stigmasterol in Chloroform-*d*.

### **3.4.2 Vasorelaxant effects of the methanolic extract of *H. sabdariffa***

#### **3.4.2.1 Determining the sensitivity of the rat aorta to PE and KCl**

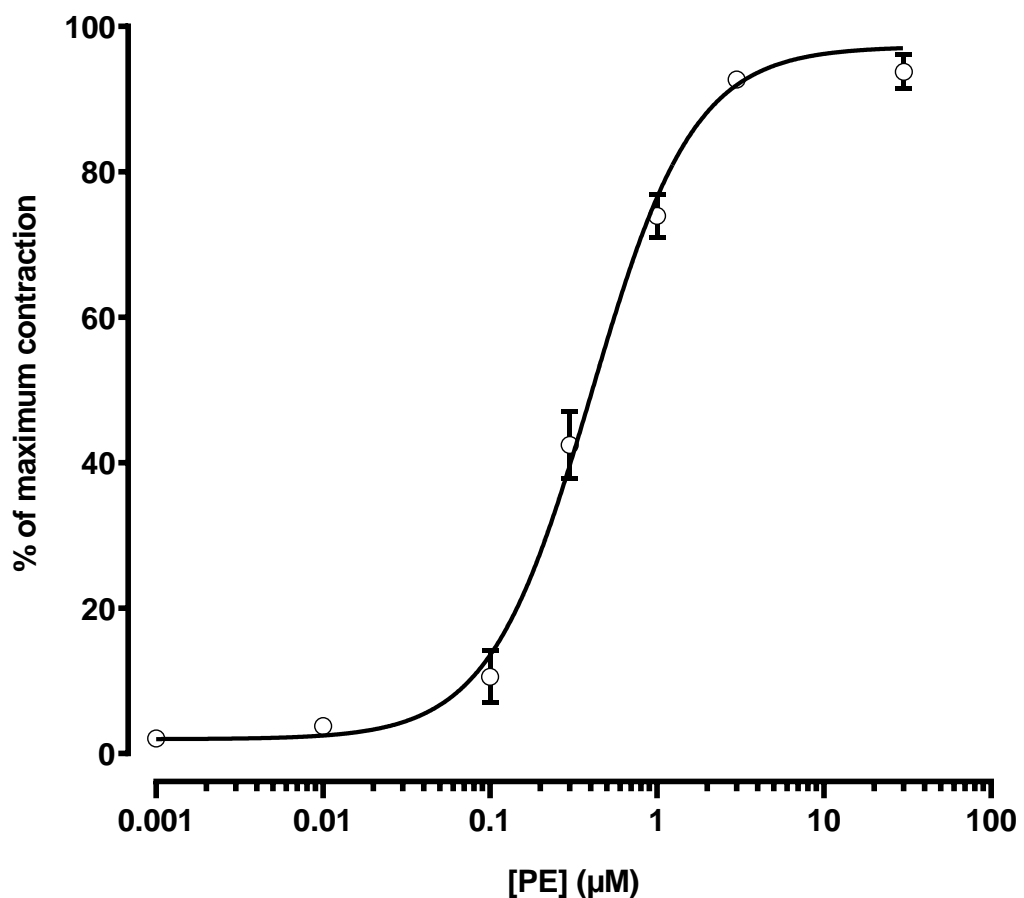
A concentration-dependent contraction was produced upon application of PE to the aorta (**Figure 3.4**), with a maximum response of  $0.94 \pm 0.08$  g at  $10 \mu\text{M}$  PE and an  $\text{EC}_{50}$  of  $0.4 \pm 0.03 \mu\text{M}$  ( $n=8/3$ ). A concentration-dependent contraction was also produced when using KCl, and a response of  $0.73 \pm 0.04$  g was achieved with  $80 \text{ mM}$  KCl (**Figure 3.5**). The  $\text{EC}_{50}$  for KCl was  $38.3 \pm 1.07 \text{ mM}$  ( $n=12/3$ ).

#### **3.4.2.2 The relaxant effect of the crude/sub-fractions obtained from the methanolic extract of *H. sabdariffa* on the rat aorta**

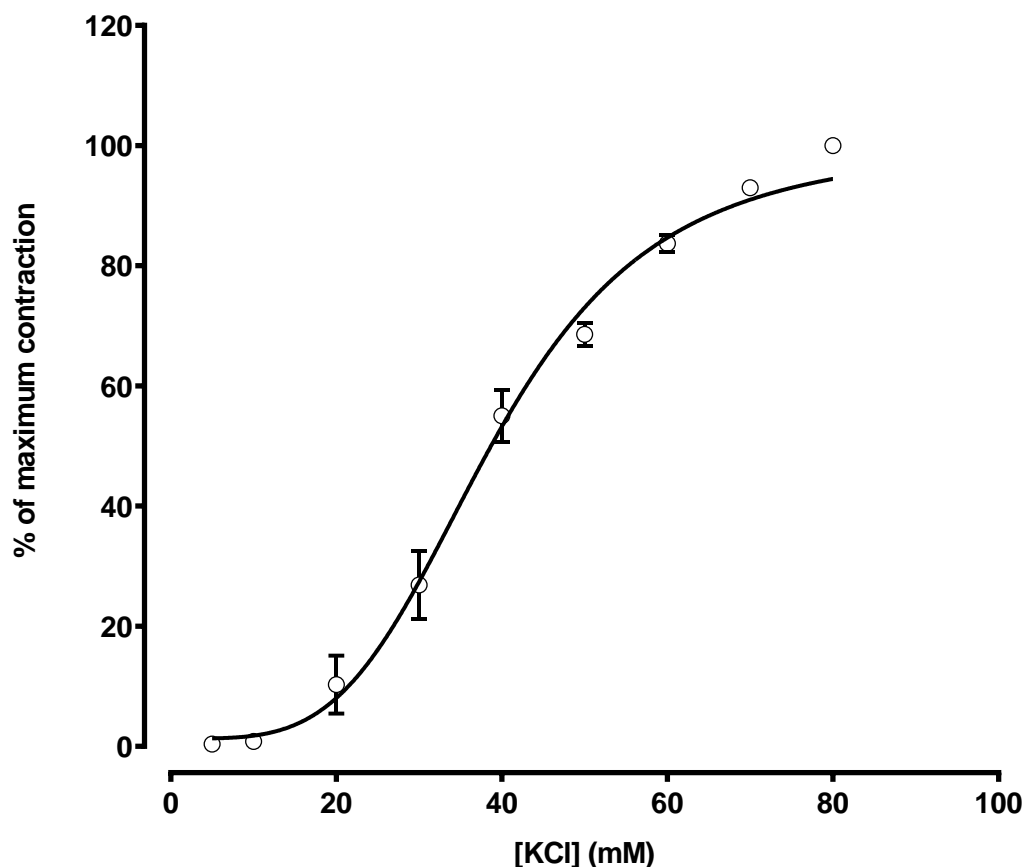
A preliminary *in vitro* pharmacological screen showed that the crude methanolic extract of *H. sabdariffa* produced a concentration-dependent relaxation of endothelium-intact aorta pre-contracted with PE ( $3 \mu\text{M}$ ). The highest concentration of the crude extract tested (1 mg/ml) relaxed the tissue by  $76 \pm 4\%$  ( $n=12/4$ ) with an  $\text{IC}_{50}$  of  $0.33 \pm 0.05 \text{ mg/ml}$  (**Figure 3.6**). The crude extract also produced a concentration-dependent relaxation of the aorta when it was pre-contracted with KCl ( $60 \text{ mM}$ ). At a concentration of 1 mg/ml, the crude extract produced relaxation of  $33 \pm 2\%$  when it was applied to the aorta pre-contracted with KCl. The relaxation was increased to  $68 \pm 2\%$  ( $n=16/4$ ) with an  $\text{IC}_{50}$  of  $1.37 \pm 0.04 \text{ mg/ml}$  when 2 mg/ml of the crude extract was applied (**Figure 3.7**).

Further investigation was carried out on the sub-fractions. Sub-fraction HS-F1 (1 mg/ml) had only a slight vasorelaxant effect on the PE induced contraction of the aorta (**Figure 3.8A**), and application of the sub-fraction HS-F2 to these pre-

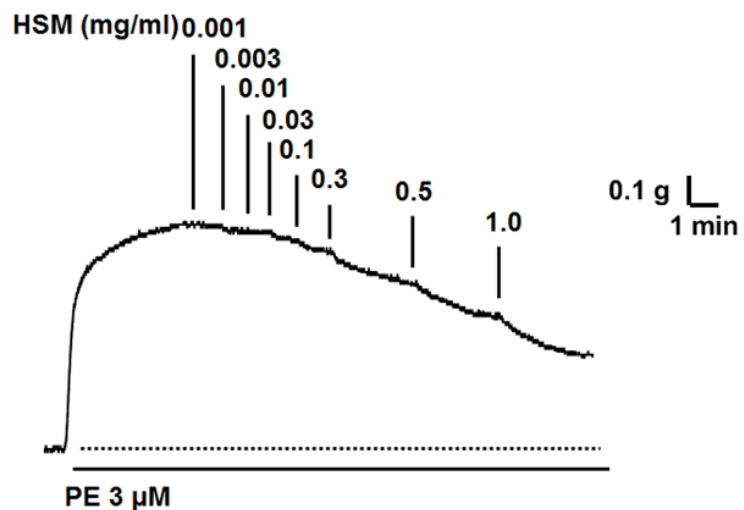
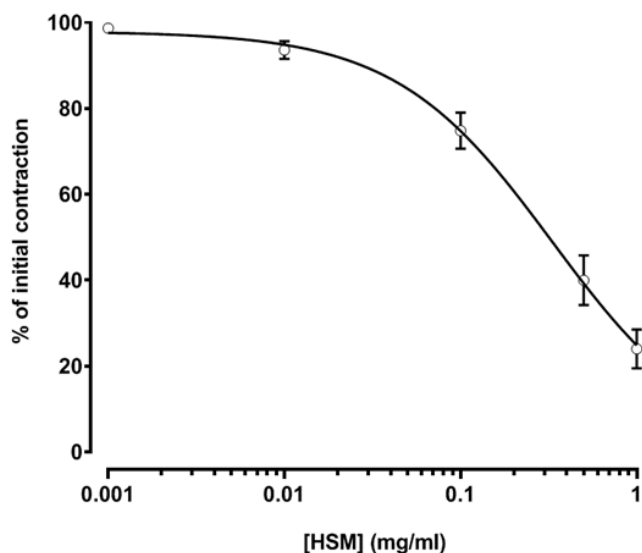
contracted aortic rings, produced a partial relaxation (**Figure 3.8B**). Whereas HS-F3 caused complete relaxation when applied at a concentration of 1 mg/ml (**Figure 3.9A**). Furthermore, the fractions HS-F4 (**Figure 3.9B**) and similarly HS-F5 (**Figure 3.9C**) produced almost complete relaxation at the highest concentration examined (1 mg/ml). Phytochemical analysis of these sub-fractions indicated that the main constituents of HS-F2, HS-F3, and HS-F4 were hibiscus acid and its derivatives. Whereas, HS-F5 was predominantly hibiscus acid. Thus, these findings suggest that hibiscus acid has a significant role in the vasorelaxant activity of *H. sabdariffa*.



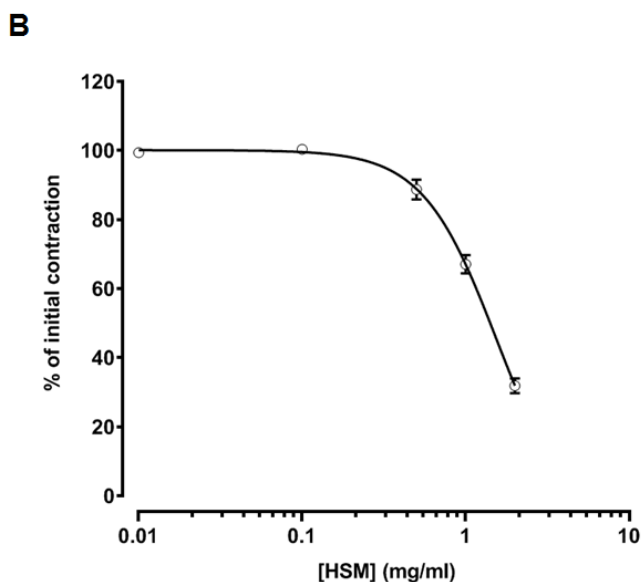
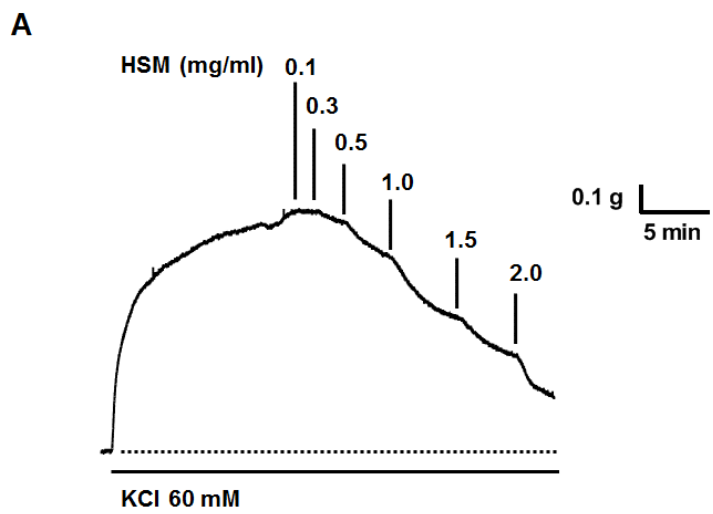
**Figure 3.4: Concentration-response curve to phenylephrine (PE) on the rat aorta.** PE was added cumulatively in concentrations 1 nM to 30  $\mu$ M. The responses are expressed as a percentage of the maximum contraction produced by PE and the data is fitted by a four-parameter concentration-response curve. Each data point is shown as mean  $\pm$  s.e.m,  $n=8/3$ .



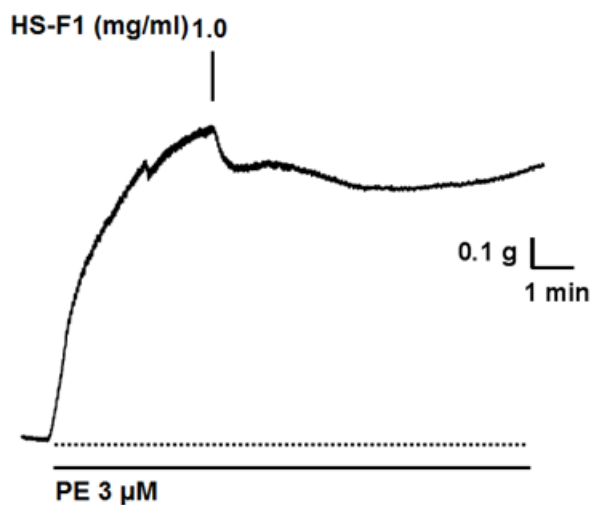
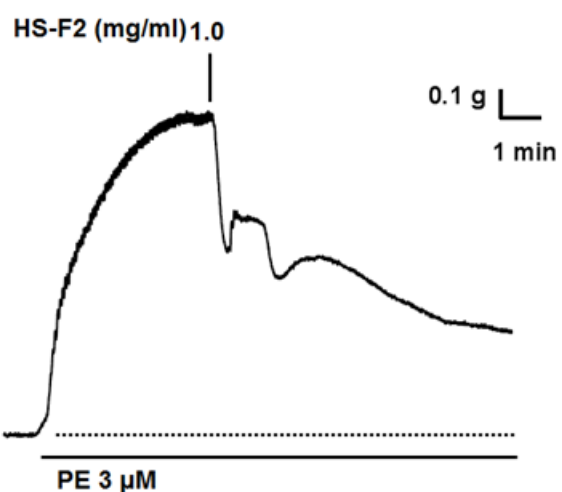
**Figure 3.5: Concentration-response curve to potassium chloride (KCl) on the rat aorta.** KCl was added cumulatively in concentrations 5 mM to 80 mM. The responses are expressed as a percentage of the maximum contraction produced by KCl and the data is fitted by a four-parameter concentration-response curve. Each data point is shown as mean  $\pm$  s.e.m., n=12/3.

**A****B**

**Figure 3.6: Relaxant effect of the crude methanolic extract of *H. sabdariffa* (HSM) on the rat aorta pre-contracted with PE.** (A) Representative recordings showing the relaxant effect of HSM on the PE ( $3 \mu\text{M}$ ) pre-contracted aorta. (B) Summary figure showing the relaxant effect of HSM in concentrations (0.001-1 mg/ml) on the PE pre-contracted aorta. The relaxant effect is expressed as a percentage of the initial contraction. Data represent mean  $\pm$  s.e.m. ( $n=12/4$ ).



**Figure 3.7: Relaxant effect of the crude methanolic extract of *H. sabdariffa* (HSM) on the rat aorta pre-contracted with KCl.** (A) Representative recordings showing the relaxant effect of HSM on the KCl (60 mM) pre-contracted aorta. (B) Summary figure showing the relaxant effect of HSM in concentrations (0.01-2 mg/ml) on the KCl pre-contracted aorta. The relaxant effect is expressed as a percentage of the initial contraction. Data represent mean  $\pm$  s.e.m. (n=16/4).

**A****B**

**Figure 3.8: Relaxant effect of the sub-fractions (HS-F) of the crude methanolic extract of *H. sabdariffa* on the rat aorta pre-contracted with PE.** Representative recordings of the effect of (A) HS-F1, and (B) HS-F2 on the aorta pre-contracted with PE (3  $\mu$ M).

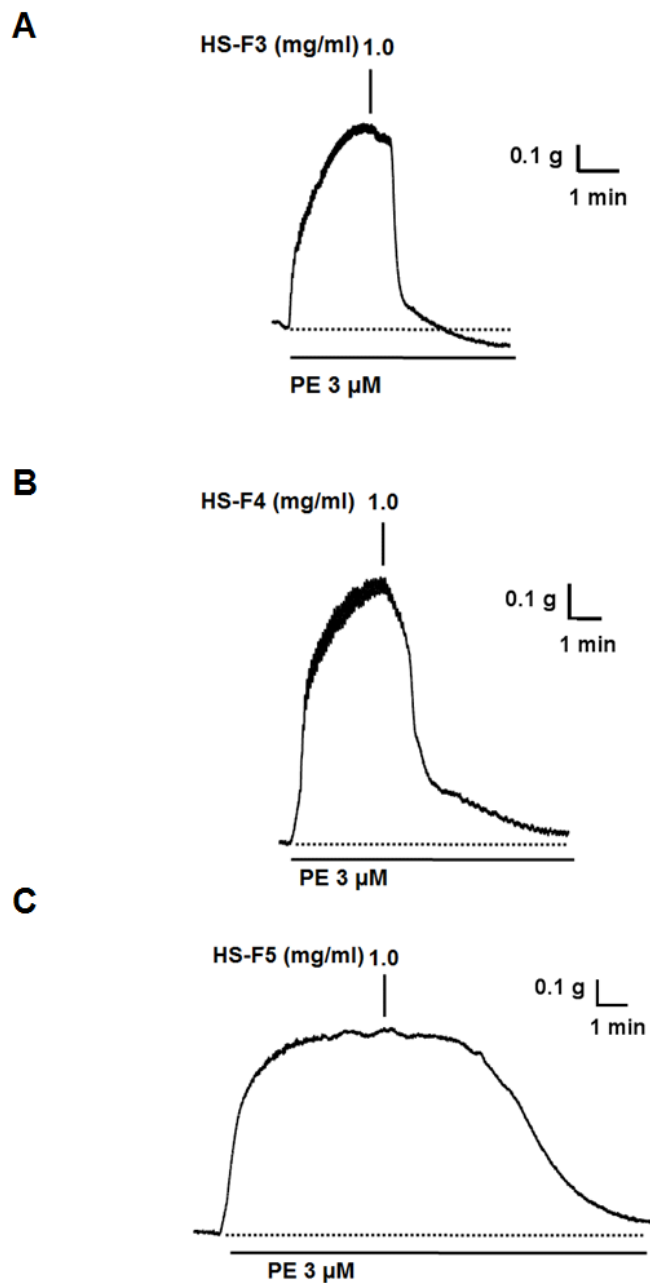


**Figure 3.9: Relaxant effect of the sub-fractions (HS-F) of the crude methanolic extract of *H. sabdariffa* on the rat aorta pre-contracted with PE. Representative recordings of the effect of (A) HS-F3, (B) HS-F4, and (C) HS-F5 on the aorta pre-contracted with PE (3  $\mu$ M).**

### **3.5 Discussion**

This chapter set out with the aim to investigate whether the crude methanolic extract of *H. sabdariffa* has vasorelaxant activity, then to determine which constituent(s) is (are) responsible for this vasorelaxant activity. Therefore, extraction, fractionation and bioactivity-led fractionation processes were carried out to examine the vasorelaxant activity of this plant, as well as the sub-fractions that were obtained from the crude methanolic extract of *H. sabdariffa*.

To achieve this goal, extraction of the calyces was carried out sequentially with solvents of different polarities, starting with the least polar, hexane, then ethyl acetate, and finally the most polar solvent, methanol. NMR was used to elucidate and confirm the structure of the isolated compounds; this technique can also be used for quantification of these compounds. No compounds were separated from the fractionation of *H. sabdariffa* hexane extract and the  $^1\text{H}$  NMR spectrum of this crude extract displayed signals that indicated the existence of the mixture of fats, showing that extraction with hexane is good in defatting the material. The  $^1\text{H}$  NMR spectrum of the sample prepared by dissolving the ethyl acetate crude extract in deuterated DMSO revealed the presence of hibiscus acid in addition to sterols and fats. Fractionation of the ethyl acetate crude extract using silica gel CC led to the isolation of steroidal compounds, which were a mixture of  $\beta$ -sitosterol and stigmasterol.

For extraction of the polar constituents from the hibiscus calyces, methanol was used as the solvent. The  $^1\text{H}$  NMR spectrum of the methanol crude extract revealed that the

majority of compounds were aliphatic in nature, with the presence of aromatic compounds as minor constituents.

There is considerable evidence in the literature that *H. sabdariffa* has an antihypertensive effect and this is further supported by a number of *in vitro* studies demonstrating a vasorelaxant effect of the crude extract of this plant (Ali *et al.*, 1991, Obiefuna *et al.*, 1994, Owolabi *et al.*, 1995, Adegunloye *et al.*, 1996, Ajay *et al.*, 2007, Sarr *et al.*, 2009, Micucci *et al.*, 2015). This study has confirmed the vasorelaxant activity of the crude methanolic extract of *H. sabdariffa* calyces on the rat aorta, and it was found to be significantly more potent in its relaxant effect when the tissue was pre-contracted with PE, than when compared to pre-contraction with KCl. This finding is also similar to what has been reported previously by Ajay *et al.* (2007), who showed that the crude extract at a concentration of 1 mg/ml, could produce ~30% relaxation when the aorta was pre-contracted with KCl, and ~80% relaxation when the tissue was pre-contracted with PE. However, in this study, the crude methanolic extract of *H. sabdariffa* (2 mg/ml) was capable of producing ~70% relaxation when the aorta was pre-contracted with KCl.

Proton ( $^1\text{H}$ ) spectra of the sub-fractions obtained from the GPC and the VLC led to the identification of hibiscus acid or its derivatives as the major constituents. These were characterised after observing that, peaks between,  $\delta_{\text{H}}$  2.6 to 2.8,  $\delta_{\text{H}}$  3.12 to 3.2,  $\delta_{\text{H}}$  3.5 to 3.83, and from  $\delta_{\text{H}}$  4.9 to 5.4 had identical nature with different sizes. Whereas,  $^{13}\text{C}$  NMR showed that the fractions obtained from *H. sabdariffa* contained

both ester and carboxylic groups together, indicating that most of the compounds present are either organic acids or ester containing compounds.

In this study, preliminary bioactivity-guided fractionation of the crude methanolic extract has found that the isolated sub-fractions enriched with hibiscus acid and its derivatives had the greatest vasorelaxant effect on the pre-contracted aorta. These results provide the justification for further work to isolate and purify the compounds in order to examine their effect on the aorta.

Polyphenolic compounds were also isolated from the methanolic extract of the calyces of *H. sabdariffa* as minor mixtures. This is in agreement with Herranz-Lopez *et al.* (2012), who identified the presence of many polyphenolic compounds in the calyces of *H. sabdariffa*.

# ***Chapter 4***

## **4 Phytochemical and pharmacological studies of hibiscus acid**

### **4.1 Introduction**

Researchers have extensively studied the effect of the crude extracts of *H. sabdariffa* in order to understand the mechanisms underlying the vasorelaxant effect of the plant. For instance, Ali *et al.* (1991) investigated the relaxant effect of an aqueous extract of *H. sabdariffa* on isolated rabbit aortic strip. The extract was found to produce relaxation when applied on the aorta, which was pre-contracted with noradrenaline. This vasorelaxant activity was not affected by pre-addition of the anticholinergic (atropine),  $\beta$ -blocker (propranolol), or antihistamine (ranitidine). As the relaxant effect of the extract was not antagonised by different receptor blockers, the researchers suggested that the extract exerts its activity through a direct effect on the smooth muscle cells (Ali *et al.*, 1991).

Obiefuna *et al.* (1994) investigated the relaxant effect of an aqueous extract of *H. sabdariffa* petals on isolated rat aorta. When the endothelium-intact aorta was pre-contracted with noradrenaline, the extract caused almost complete relaxation ( $91 \pm 4$ ) of the contraction when applied at a concentration of  $1.7 \text{ mg ml}^{-1}$ , with an  $IC_{50}$  of  $0.53 \pm 0.06 \text{ mg/ml}$ . The relaxant effect was significantly reduced by ~70% upon removal of the endothelium. The relaxation was found to be due to both endothelium-dependent and endothelium-independent mechanisms (Obiefuna *et al.*, 1994).

The endothelium-dependent mechanism of action for *H. sabdariffa* was also reported by others (Ajay *et al.*, 2007, Sarr *et al.*, 2009). The relaxant effect of a crude methanolic extract of hibiscus calyces on PE pre-contracted aorta, isolated from hypertensive rats was shown by Ajay *et al.* (2007). They found that the relaxation was partially attenuated by the removal of the endothelium, or by pre-incubation with the endothelial NOS inhibitor (L-NAME). In addition, pre-incubation of the aorta with the competitive muscarinic antagonist (atropine) or the cGMP inhibitor (methylene blue) also caused a partial decrease in the relaxant effect of the crude extract. The relaxant effect of different alcoholic extracts of hibiscus calyces on the pre-contracted rat aorta was also studied by Sarr *et al.* (2009). They extracted the calyces of *H. sabdariffa* with different solvents, namely methanol, butanol, and ethyl acetate. Phytochemical analysis of these fractions revealed the presence of anthocyanins in the butanolic fraction. The crude extract and these different alcoholic fractions showed relaxant activity when they were applied to rat aorta pre-contracted with noradrenaline, and the butanolic extract displayed greater potency than the crude extract (Sarr *et al.*, 2009). Furthermore, either removal of the endothelium or treatment with L-NAME significantly reduced (by ~60%) the vasorelaxation produced by the crude extract. Therefore, it was suggested that the extract produced its vasorelaxant activity via an endothelium-dependent mechanism, which could be due to the activation of endothelium derived NO/cGMP-relaxant pathway by polyphenolic compounds (Ajay *et al.*, 2007, Sarr *et al.*, 2009). The inhibition of  $\text{Ca}^{2+}$  influx was also postulated as an endothelium-independent mechanism of action for the vasorelaxant activity of *H. sabdariffa* (Owolabi *et al.*, 1995).

The crude aqueous extract of hibiscus caused attenuation of the contraction following the cumulative addition of  $\text{Ca}^{2+}$ , in aorta which had previously been incubated in  $\text{Ca}^{2+}$  free PSS and stimulated with noradrenaline. However, the relaxant effect of the extract (0.6 mg/ml) was not significant when the tissue was pre-contracted with KCl (Owolabi *et al.*, 1995). Furthermore, when the aorta was incubated in  $\text{Ca}^{2+}$  free PSS, the crude extract significantly decreased the phasic contraction induced by noradrenaline. So, it was proposed that the relaxant activity of the extract seems to occur through the inhibition of  $\text{Ca}^{2+}$  influx, and by the inhibition of  $\text{Ca}^{2+}$  release from intracellular stores (Owolabi *et al.*, 1995). Further support for the idea that *H. sabdariffa* causes blockade of the VDCCs was reported by Ajay *et al.* (2007). They showed the ability of the crude methanolic extract to relax the KCl pre-contracted rat aorta. Similarly, Micucci *et al.* (2015) reported that the aqueous extract causes almost complete relaxation when applied to isolated guinea pig aorta that were pre-contracted with KCl, with an  $\text{IC}_{50}$  of 6.6 mg  $\text{ml}^{-1}$ .

The cardiovascular effects of *H. sabdariffa*, were also examined on the left and right atria from the guinea pig (Micucci *et al.*, 2015). It was reported that at a concentration of 1 mg  $\text{ml}^{-1}$ , the crude extract exerts negative inotropic activity when applied on the electrically stimulated left atria (~75% inhibition) (Micucci *et al.*, 2015). The negative inotropic effects of the crude extract have also been reported by Lim *et al.* (2017), moreover they also reported negative chronotropic, and positive lusitropic (increased the velocity of relaxation) effects of hibiscus extract. The polyphenols from *H. sabdariffa*, consisting of flavonoids and phenolic acids, had a direct effect on the cardiac contractility in the Langendorff perfused rat heart model. At

concentrations between 125 and 500 µg ml<sup>-1</sup> a negative inotropic effect was observed through lowering the left ventricular-developed pressure (LVEDP), and there was a reduction in heart rate, indicating negative chronotropic activity. The calyx extract also produced a positive lusitropic effect and improved coronary blood flow by having a vasorelaxant effect on the coronary arteries. The mechanism of action for these activities were not fully understood (Lim *et al.*, 2017)

The inhibitory activity of *H. sabdariffa* on non-vascular smooth muscle cells was previously investigated by Salah *et al.* (2002). The methanolic extract of the dried hibiscus flowers reduced the intestinal transit time in rats when administered intraperitoneally. The crude extract relaxed the phasic contraction of the electrically stimulated ileal strips in a concentration-dependent manner (Salah *et al.*, 2002).

Contractions of guinea-pig trachea induced by acetylcholine, histamine, and serotonin were also relaxed by the application of the aqueous extract of hibiscus; which was not reduced by pre-addition of propranolol (Ali *et al.*, 1991). Furthermore, the aqueous extract of hibiscus also produced a concentration-dependent relaxation, reaching ~30% (relaxation) when it was applied to isolated guinea pig ileal strips, which were pre-contracted with KCl. Thus, the inhibitory effect on non-vascular smooth muscle was 3 times less than that exhibited on vascular smooth muscle, evidencing its selectively (Micucci *et al.*, 2015).

In Chapter 3, fractionation of the crude methanolic extract of *H. sabdariffa* has led to the isolation of 5 sub-fractions, and the first two of these sub-fractions (HS-F1 and

HS-F2) produced partial relaxation when applied to the PE pre-contracted aorta. Whereas, the other sub-fractions (HS-F3, HS-F4, and HS-F5) had a complete relaxant effect. Phytochemical studies showed that these three sub-fractions are enriched with hibiscus acid and its derivatives (ester forms of hibiscus acid). However, one of these sub-fractions was almost entirely hibiscus acid.

The aim of this current chapter was to determine whether hibiscus acid has vasorelaxant activity, thereafter, subsequent studies were carried out to determine the mechanism of action for the vasorelaxant activity of this compound on the aorta. Hibiscus acid is not available commercially; however, it is a chiral compound and its diastereomer garcinia acid is available commercially. Therefore, parallel studies were carried out with garcinia acid from (*Garcinia cambogia*) (**Figure 4.1**) in order to determine if it had similar vasorelaxant effects.

The fact that previous studies have shown that the crude extract of *H. sabdariffa* has a relaxant effect when applied to the pre-contracted trachea, in addition to a negative inotropic effect, prompted further examination to determine whether hibiscus and garcinia acid have similar effects on the trachea and atria.

## 4.2 Materials and Methods

### 4.2.1 X-ray crystallography

Experimental: Single-crystal data were measured at 123(2) K with an Oxford Diffraction Gemini S instrument and monochromated Cu radiation. The structures

were refined to convergence on  $F^2$  and against all independent reflections by full-matrix least squares using SHELXL programs (Sheldrick, 2015).

#### 4.2.1.1 Refinement

Crystal data, data collection and structure refinement details are summarised in **Table 4.1** and **Table 4.2**. For all structures, C-bound H atoms were placed in their expected geometrical positions and treated as riding, with C–H=0.95–0.99 Å and U<sub>iso</sub>(H)=1.5U eq(C) for methyl C atoms and 1.2U eq(C) for the other H atoms.

The absolute configuration was determined for the molecules in hibiscus acid for arbitrarily named atoms [C2(R),C1(S), Flack parameter 0.00] and both arbitrarily named equivalent atoms in hibiscus acid dimethyl ester [C3(R),C4(S) (molecule A) and C11(R),C12(S) (molecule B), Flack parameter 0.08] (Parsons *et al.*, 2013).

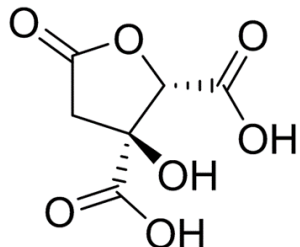


**Figure 4.1:** Chemical structure of garcinia acid

**Table 4.1: Experimental details for hibiscus acid**

Crystal data	
Chemical formula	C <sub>6</sub> H <sub>6</sub> O <sub>7</sub> ·C <sub>2</sub> H <sub>6</sub> OS
M <sub>r</sub>	268.24
Crystal system, space group	Monoclinic, P2 <sub>1</sub>
Temperature (K)	123
a, b, c (Å)	5.4258 (2), 8.9491 (3), 11.4365 (3)
β (°)	94.092 (3)
V (Å <sup>3</sup> )	553.90 (3)
Z	2
Radiation type	Cu Kα
μ (mm <sup>-1</sup> )	2.94
Crystal size (mm)	0.30 × 0.15 × 0.05
Data collection	
Diffractometer	Oxford Diffraction Gemini S CCD
Absorption correction	Multi-scan ( <i>CrysAlis PRO</i> ; Oxford Diffraction, 2010)
T <sub>min</sub> , T <sub>max</sub>	0.554, 1.000
No. of measured, independent and observed [I > 2σ(I)] reflections	4397, 1854, 1640
R <sub>int</sub>	0.054
(sin θ/λ) <sub>max</sub> (Å <sup>-1</sup> )	0.619
Refinement	
R[F <sup>2</sup> > 2σ(F <sup>2</sup> )], wR(F <sup>2</sup> ), S	0.047, 0.113, 1.05
No. of reflections	1854
No. of parameters	169
No. of restraints	4
H-atom treatment	H atoms treated by a mixture of independent and constrained refinement
Δρ <sub>max</sub> , Δρ <sub>min</sub> (e Å <sup>-3</sup> )	0.44, -0.25

**Table 4.1 (continued): Experimental details for hibiscus acid**

Absolute structure	Flack $x$ determined using 698 quotients $[(I^+) - (I^-)]/[(I^+) + (I^-)]$
Absolute structure parameter	0.00 (4)

**Table 4.2: Experimental details for hibiscus acid dimethyl ester**

Crystal data	
Chemical formula	C <sub>8</sub> H <sub>10</sub> O <sub>7</sub>
$M_r$	218.16
Crystal system, space group	Monoclinic, P2 <sub>1</sub>
Temperature (K)	123
$a, b, c$ (Å)	9.3057 (6), 7.6934 (6), 13.4012 (11)
$\beta$ (°)	96.243 (7)
$V$ (Å <sup>3</sup> )	953.74 (12)
$Z$	4
Radiation type	Cu $K\alpha$
$\mu$ (mm <sup>-1</sup> )	1.20
Crystal size (mm)	0.30 × 0.20 × 0.04
Data collection	
Diffractometer	Oxford Diffraction Gemini S CCD
Absorption correction	Multi-scan ( <i>CrysAlis PRO</i> ; Oxford Diffraction, 2010)
$T_{\min}, T_{\max}$	0.747, 1.000
No. of measured, independent and observed [ $I > 2\sigma(I)$ ] reflections	8046, 3506, 2976
$R_{\text{int}}$	0.036
$(\sin \theta/\lambda)_{\max}$ (Å <sup>-1</sup> )	0.622
Refinement	
$R[F^2 > 2\sigma(F^2)], wR(F^2), S$	0.044, 0.121, 1.10
No. of reflections	3506

**Table 4.2 (continued): Experimental details for hibiscus acid dimethyl ester**

No. of parameters	281
No. of restraints	3
H-atom treatment	H atoms treated by a mixture of independent and constrained refinement
$\Delta\rho_{\max}$ , $\Delta\rho_{\min}$ ( $e \text{ \AA}^{-3}$ )	0.23, -0.22
Absolute structure	Flack $x$ determined using 1098 quotients $[(I^+) - (I^-)]/[(I^+) + (I^-)]$
Absolute structure parameter	0.08

#### **4.2.2 Drugs, solvents and chemicals**

Hibiscus acid was extracted and purified from dried *H. sabdariffa* calyces (See **Section 4.2.1**). (+)-Garcinia acid, ( $\pm$ )-Bay K8644, tetraethylammonium chloride, carbamylcholine chloride, and N $\omega$ -nitro-L-arginine methyl ester hydrochloride were all purchased from Sigma-Aldrich (Gillingham, UK). FPL 64176 and iberiotoxin were obtained from Tocris (Abingdon, UK). All other reagents and salts used were from either VWR Chemicals (Lutterworth, UK), or Sigma-Aldrich. Hibiscus acid and garcinia acid were prepared as 20 mg/ml stock solutions dissolved in PSS. Stock solutions of carbamylcholine chloride (carbachol), tetraethylammonium chloride (TEA), N $\omega$ -nitro-L-arginine methyl ester hydrochloride (L-NAME) and PE (all 100 mM) were prepared using PSS. FPL 64176 (2,5-dimethyl-4-[2-(phenyl methyl) benzoyl]-1H-pyrrole-3-carboxylic acid methyl ester) and Bay K8644 (1,4-dihydro-2,6-dimethyl-5-nitro-4-(2-[trifluoromethyl] phenyl) pyridine-3-carboxylic acid methyl ester) were dissolved in dimethyl sulfoxide (DMSO) as 10 mM stock solutions, and subsequent dilutions were made using PSS. In the case of Bay K8644 and FPL 64176, the same dilutions of DMSO were used in the vehicle control experiments.

#### **4.2.3 Aorta and tracheal tissue preparation and contractile studies**

The thoracic and abdominal aortic rings were prepared as described in **Section 3.2.3**. For studies involving tracheal tissue, in-house bred male and female Sprague-Dawley rats (200-250 g) were sacrificed by an intraperitoneal overdose (100 mg/kg) of the anaesthetic pentobarbitone and lidocaine (Pentoject), according to Schedule 1 of the Animals (Scientific Procedures) Act 1986. The trachea were subsequently removed

and placed in cold PSS. Under a dissecting microscope (Nikon SMZ645), the trachea were cleaned of any adhering fat and loose connective tissue. The trachea were then cut into 4-5 mm long rings. The rings were mounted on intraluminal parallel wires; one of which was fixed and the other attached to a Grass FT03C force displacement transducer. The organ bath (1 ml in volume) was filled with PSS and maintained at 37°C whilst being aerated with air and a resting tension of 1 g was applied to the tissue and a 1 h equilibration period was allowed.

#### **4.2.4 Effects of hibiscus acid and garcinia acid on the rat aorta**

In order to investigate vasorelaxant activity, the aorta was pre-contracted with either PE (3  $\mu$ M) or KCl (60 mM). Once the contractions were stable, 0.001-1 mg/ml hibiscus or garcinia acid was added in a cumulative manner to the tissues pre-contracted with PE, and 0.01-2 mg/ml hibiscus or garcinia acid was used in the tissues pre-contracted with KCl. Following these experiments, the tissues were washed of all agents with fresh bath solution. Allowing a 30-60 min recovery time, the experiment was then repeated following the same protocol in order to test the reproducibility of the effects of hibiscus or garcinia acid.

The majority of the experiments were carried out on endothelium-intact tissues. This was confirmed by a relaxation of more than 70% in response to carbachol (10  $\mu$ M) when the aorta was pre-contracted with PE. The influence of the endothelium on the relaxant response of either hibiscus or garcinia acid was examined, and this was established by removing the endothelium. The endothelium was removed by gently rubbing the luminal surface of the aortic ring with a sanded down wooden cocktail

stick. Successful denudation was confirmed by the lack of relaxation (<10%) to carbachol.

Another set of experiments was performed in the presence of the nitric oxide synthase (NOS) inhibitor, L-NAME. The aortic preparations were treated with 300 µM L-NAME, 20 min before induction of PE contraction. The inhibitory effect of L-NAME was confirmed by <10% relaxation in response to carbachol.

#### **4.2.5 Role of L-type voltage-dependent calcium channels on hibiscus acid and garcinia acid-induced relaxation**

To establish whether hibiscus acid and garcinia acid produce their relaxation by inhibiting L-type VDCCs, their effect on the contractions produced by FPL 64176, a benzopyrrole-type agonist of L-type VDCCs (Zheng *et al.*, 1991) or Bay K8644 (Thomas *et al.*, 1985) was examined. The tissue was initially depolarised with 20 mM KCl for 5 min, to activate VDCCs and produce a sub-maximal contractile response. Thereafter, FPL 64176 (30 µM) or Bay K8644 (0.1 µM) was added in order to produce further activation of VDCCs (Zheng *et al.*, 1991, Roy *et al.*, 1995). Once the contractile response had stabilised, either hibiscus acid or garcinia acid, was applied in concentrations of 0.5-1 mg/ml.

#### **4.2.6 Effect of hibiscus acid and garcinia acid on the release of intracellular Ca<sup>2+</sup>**

A component of the contractile response to PE involves Ca<sup>2+</sup> release from the SR, which produces a phasic contractile response (Nishimura *et al.*, 1991). To examine

the effect of hibiscus acid and garcinia acid on SR  $\text{Ca}^{2+}$  release a control contractile response to PE in regular PSS was initially obtained. After a 1 h recovery period, the tissue was exposed to a  $\text{Ca}^{2+}$  free PSS containing 1 mM ethylene glycol-bis ( $\beta$ -aminoethyl ether)-N,N,N',N'-tetraacetic acid (EGTA) for 15 min. During this period, either vehicle, hibiscus acid or garcinia acid was applied and the tissue was subsequently re-challenged with PE.

#### **4.2.7 Effect of hibiscus acid and garcinia acid on the influx of extracellular $\text{Ca}^{2+}$**

Another component of the contractile response to PE involves  $\text{Ca}^{2+}$  influx from the extracellular space, which produces the sustained (tonic) phase of the contractile response (Nishimura *et al.*, 1991). To examine the effect of hibiscus acid and garcinia acid on the tonic phase of contraction, the tissue was exposed to a  $\text{Ca}^{2+}$  free PSS containing 1 mM EGTA for 15 min; the tissue was then challenged with PE (3  $\mu\text{M}$ ) for 5 min to produce the phasic contractile response. After that, 1.8 mM  $\text{Ca}^{2+}$  was reintroduced to the organ bath (giving a free calcium concentration of 0.8 mM, as determined by the MAXC computer program for calculating free  $\text{Ca}^{2+}$  concentrations) (Bers *et al.*, 2010), which produced a tonic contraction. Hibiscus acid or garcinia acid (0.5 mg/ml) was then applied during the tonic phase of the contraction.

#### **4.2.8 Effect of blocking potassium channels on the relaxant activity of hibiscus acid and garcinia acid.**

To establish whether the relaxation to hibiscus or garcinia acid involves the activation of  $\text{K}^+$  channels, their involvement was examined in the presence of the non-selective

$K^+$  channel blocker TEA (Khodakhah *et al.*, 1997). The aorta was challenged with PE (3  $\mu$ M) alone, and 0.001-1 mg/ml hibiscus acid or garcinia acid was then added as described above (**Section 4.2.4**). After washout and a 1 h recovery period, the aorta was preincubated with 6 mM TEA for 20 min prior to pre-contraction with PE. Once the contractile response had stabilised, hibiscus acid or garcinia acid was applied to the tissue in a cumulative manner. The above protocol was also repeated for the selective  $K^+$  channel blocker iberiotoxin, Ibtx (100 nM), in a separate series of experiments.

#### **4.2.9 Effect of hibiscus acid and garcinia acid on the rat left atria**

In-house bred adult male and female Sprague-Dawley rats (200-250 g), were humanely sacrificed by cervical dislocation according to Schedule 1 of the Animals (Scientific Procedures) Act 1986. The heart was subsequently removed, and quickly immersed in cold PSS. Thereafter the heart was transferred to a dissecting dish and both the right and left atria were separated from the ventricles with the aid of a dissecting microscope (Nikon SMZ645). An organ bath (10 ml in volume) was filled with PSS and maintained at 37°C whilst being aerated with oxygen. The atria were mounted using silk thread; one end was fixed to a stainless steel gas bubbler and the other end was connected to a force displacement transducer (Grass FT03, Astro-Med, Slough, UK). The atrial contractile response detected by the isometric transducer, was amplified through a PowerLab 4/30 data acquisition system, before being stored and displayed on a personal computer running Chart (v5.2) software (ADInstruments, Ltd, Oxfordshire, UK). A resting tension of 0.7 g was applied to the atrial tissues and a 1 h equilibration period was allowed before challenging the tissue

with either hibiscus acid or garcinia acid. The atria were stimulated using a Grass S88 stimulator, at a frequency of 0.1 Hz, with a pulse amplitude of 12-13 V and a duration of 0.6 ms. The stimulus was delivered by two platinum electrodes that were positioned either side of the atria. Once the electrically stimulated contractile response had stabilised, either hibiscus acid or garcinia acid, was applied in a cumulative manner at concentrations of 0.1-0.6 mg/ml.

#### **4.2.10 Concentration-response curves to carbachol and KCl on the rat trachea**

Carbachol (1 nM-30  $\mu$ M) was applied to the rat trachea in a cumulative manner in order to obtain a concentration-response curve and to determine the EC<sub>50</sub> and the E<sub>max</sub> for carbachol, which was then used to produce pre-contraction of the trachea. To obtain a concentration-response curve and to determine the EC<sub>50</sub> and the E<sub>max</sub> for KCl on the rat trachea, KCl was applied cumulatively in concentrations ranging from (5-70 Mm). Afterwards, the tissues were washed regularly with fresh PSS and a recovery period of 20 min was allowed, and the experiment was then repeated to test the reproducibility of results.

#### **4.2.11 Effects of hibiscus acid and garcinia acid on the rat trachea**

To determine the effect of hibiscus and garcinia acids, the tracheal tissues were pre-contracted with either carbachol (1  $\mu$ M) or KCl (60 mM). Once the contraction was stable, 0.01-0.5 mg/ml hibiscus or garcinia acid was added cumulatively to the carbachol pre-contracted tissues and 0.01-1 mg/ml to the KCl pre-contracted tissues.

## 4.3 Results

### 4.3.1 Phytochemical results

#### 4.3.1.1 Characterisation of hibiscus acid dimethyl ester

Hibiscus acid dimethyl ester [systematic name: (2S, 3R) - dimethyl, 3- hydroxy-5-oxo-2, 3, 4, 5-tetrahydrofuran-2, 3-dicarboxylic acid] was isolated from the sub-fraction 2 obtained from the methanol extract (HS VLC2) using Sephadex LH-20 column (**Methods Section 2.5.3**). The molecular formula was deduced from its HRMS (**Spectrum 4.1**) as  $C_8H_{10}O_7$  from the molecular ion peak  $[M-H]^-$  at  $m/z$  217.0000 (Calc 217.035). The compound was identified from its 1D and 2D NMR data ((Boll *et al.*, 1969), and confirmed by its X-ray crystallographic structure (**Figure 4.2**).

#### NMR data analysis

The  $^1H$  NMR spectrum (500MHz, Acetone-*d*) showed proton signals between  $\delta_H$  2.77 and 5.35 ppm (**Spectrum 4.2**). The signal at  $\delta_H$  5.35 ppm (1H, s) was assigned to the proton coupled to the secondary carbon ( $\gamma$ -C), two doublet signals were attributed to two protons coupled to the secondary carbon ( $\alpha$ -C), one signal at  $\delta_H$  2.77 ppm (1H, d,  $J=17.31$  Hz,) and the other signal at  $\delta_H$  3.23 ppm (1H, d,  $J=17.28$  Hz). The two strong singlets at  $\delta_H$  3.76 (3H, s) and  $\delta_H$  3.87 (3H, s) ppm were attributed to the protons of the two methoxy groups.

The  $^{13}C$  spectrum (**Spectrum 4.3**) indicated the presence of eight signals corresponding to each of the carbon atoms comprising of the three carbonyl, one methylene, two oxygen bearing carbons and two methoxy carbons. The peak at  $\delta_C$

$\delta_{\text{C}}$  171.9 ppm was ascribed to the lactone carbonyl while the other signals at  $\delta_{\text{C}}$  166.0 ppm and  $\delta_{\text{C}}$  170.8 ppm for the carboxylic acids attached to the secondary ( $\gamma$ -C at  $\delta_{\text{C}}$  82.26 ppm) and the tertiary carbon ( $\beta$ -C at  $\delta_{\text{C}}$  77.67 ppm), respectively. The oxomethylene carbon ( $\alpha$ -C) was assigned  $\delta_{\text{C}}$  40.8 ppm. The peak at  $\delta_{\text{C}}$  51.7 ppm and  $\delta_{\text{C}}$  52.8 ppm was ascribed to the methoxy carbons.

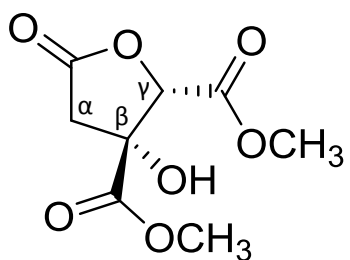
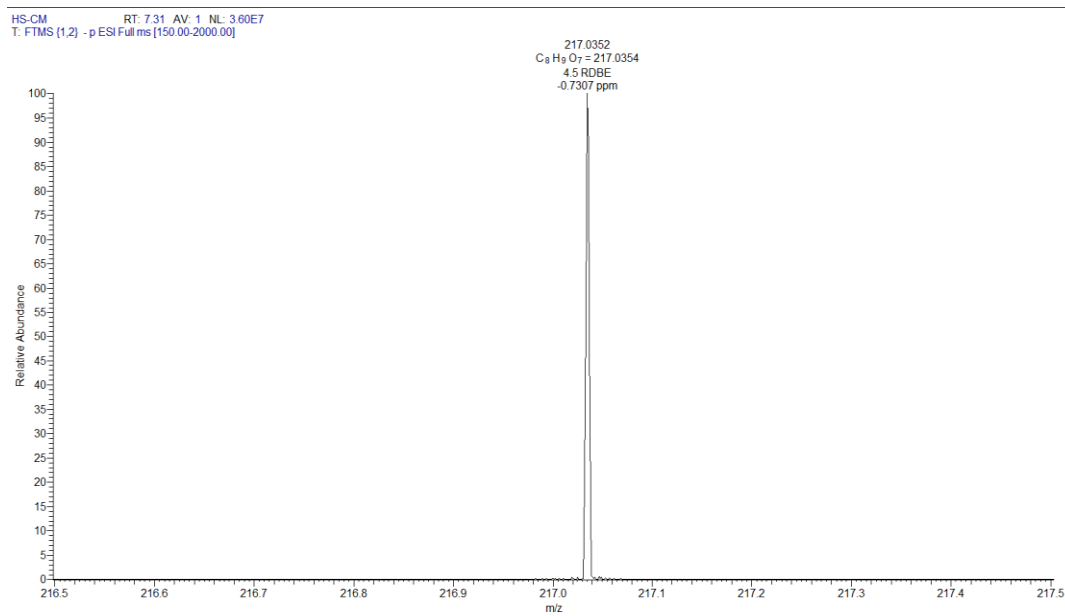


**Figure 4.2: Chemical structure of hibiscus acid dimethyl ester.**

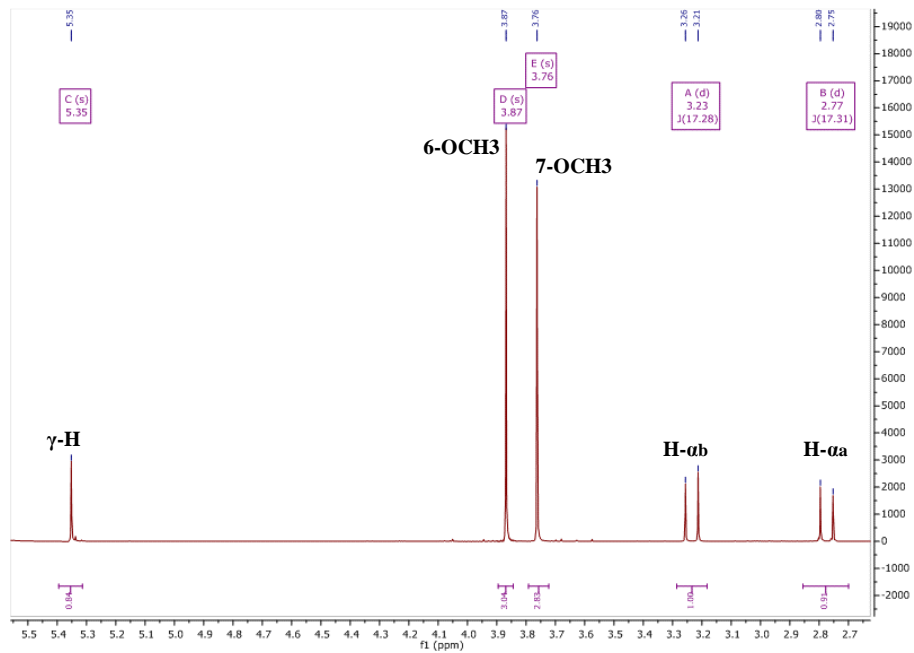
Using 2D NMR (COSY, HSQC and HMBC) the structure was deduced as follows: the proton (H- $\alpha$ a) doublet signals at  $\delta_H$  2.77 ppm shows a correlation with the proton (H- $\alpha$ b) doublet signal at  $\delta_H$  3.23 ppm in the COSY correlation spectrum (**Spectrum 4.4**).

The HSQC spectrum (**Spectrum 4.5**) showed direct correlations of the two protons at  $\delta_H$  2.77 ppm and  $\delta_H$  3.23 ppm to the carbon at  $\delta_C$  40.8 ppm ( $\alpha$ -C). While the proton at  $\delta_H$  5.35 ppm was directly correlated to the carbon  $\delta_C$  82.26 ppm ( $\gamma$ -C). The proton at  $\delta_H$  3.76 ppm was directly correlated to the carbon  $\delta_C$  51.7 ppm, while the proton at  $\delta_H$  3.87 ppm was directly correlated to the carbon  $\delta_C$  52.8 ppm.

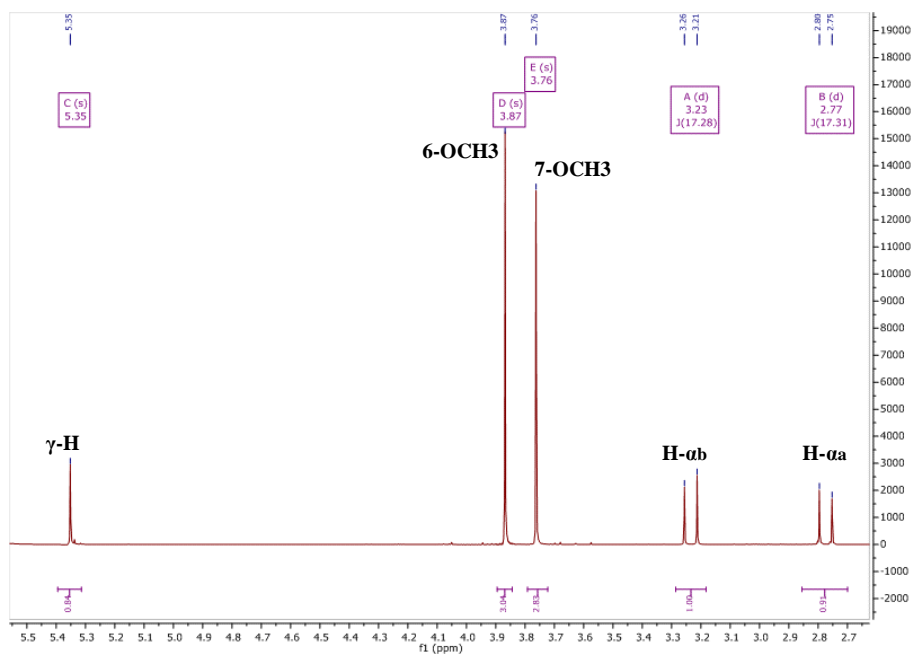
The chemical shifts were further confirmed by long range ( $^2J$  and  $^3J$ ) correlations  $^1H$ - $^{13}C$  in the HMBC spectrum of hibiscus acid dimethyl ester (**Spectrum 4.6**). The protons at  $\delta_H$  2.77 and 3.23 ppm showed  $^2J$  correlations with the carbon at  $\delta_C$  77.7 whereas  $^3J$  correlation was observed with the carbon at  $\delta_C$  82.3 ppm. The proton at  $\delta_H$  5.31 showed  $^2J$  correlations with the carbon at  $\delta_C$  77.7. Also the same proton and the ones at 2.77, and 3.23 ppm showed  $^3J$  correlations to the carbonyl carbon at  $\delta_C$  170.8 ppm ( $\beta$ -CO). The two methylene protons at  $\delta_H$  2.77 ppm and 3.23 ppm showed  $^2J$  correlation to the carbonyl carbon at  $\delta_C$  171.9. The protons at  $\delta_H$  3.76 and 3.87 ppm showed correlations with the carbonyls at  $\delta_C$  166 and 170.8 ppm, respectively, that confirmed the assignment of carbon signal at  $\delta_C$  171.9 as the lactone carbonyl (**Table 4.3**).



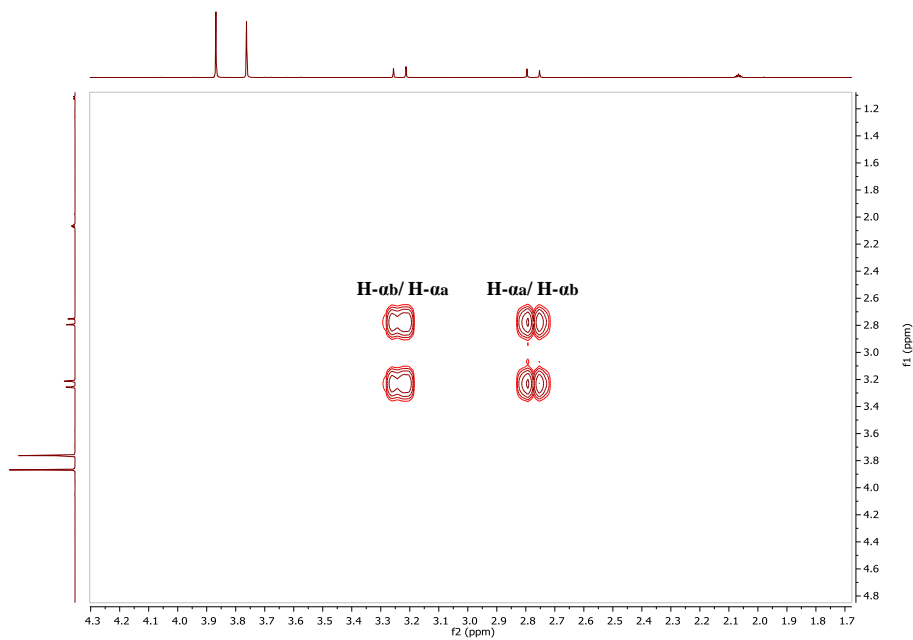
**Spectrum 4.1:** Molecular ion peak  $[M-H]^-$  spectrum of hibiscus acid dimethyl ester.



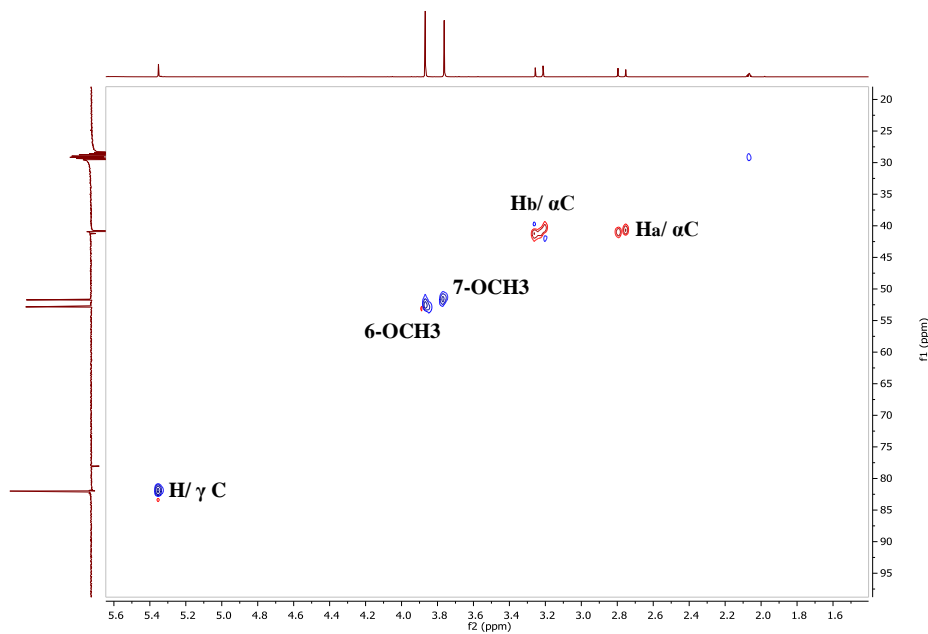
**Spectrum 4.2:**  $^1H$  NMR spectrum (400 MHz) of hibiscus acid dimethyl ester in Acetone-*d*<sub>6</sub>.



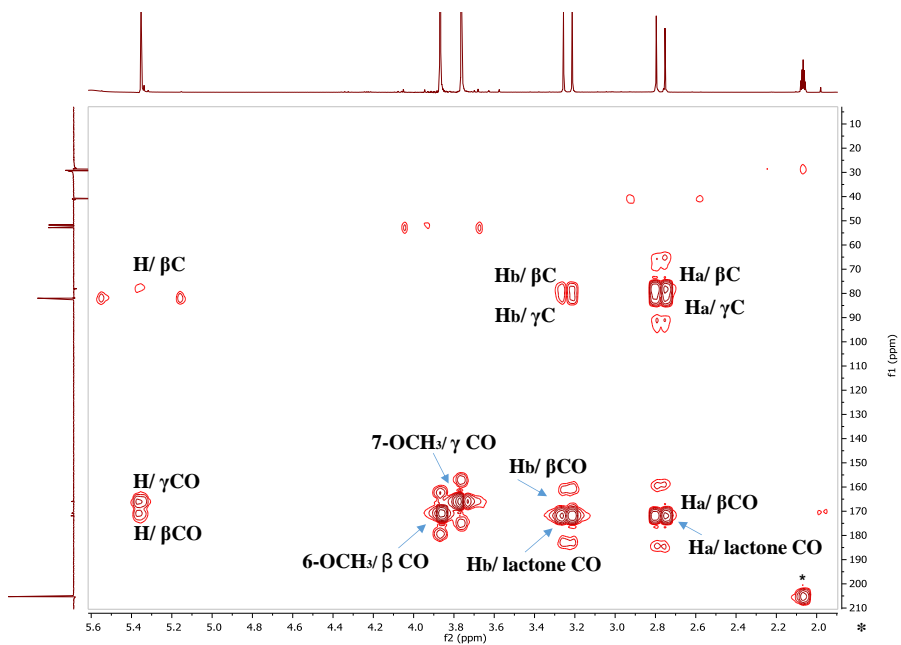
**Spectrum 4.3:**  $^{13}\text{C}$  (100 MHz) NMR spectrum of hibiscus acid dimethyl ester in Acetone- $d_6$ .



**Spectrum 4.4:** Cosy NMR spectrum (400 MHz) of hibiscus acid dimethyl ester in Acetone- $d_6$ .



**Spectrum 4.5: HSQC (400 MHz, Acetone-*d*<sub>6</sub>) spectrum of hibiscus acid dimethyl ester.**



**Spectrum 4.6: HMBC (400 MHz, Acetone-*d*<sub>6</sub>) spectrum of hibiscus acid dimethyl ester.**

**Table 4.3:  $^1\text{H}$  (500MHz),  $^{13}\text{C}$  (100MHz), and HSQC data of hibiscus acid dimethyl ester in Acetone- $d_6$**

Position	$\delta_{\text{H}}$ (mult, $J$ (Hz))	$\delta_{\text{C}}$ (mult)
	5.35 (1H, s)	82.26
$\alpha$ (Hb)	3.23 (1H, d, 17.31)	40.8
$\alpha$ (Ha)	2.77 (1H, d, 17.28)	40.8
6-OCH <sub>3</sub>	3.87 (3H, s)	52.84
7-OCH <sub>3</sub>	3.76 (3H, s)	51.76

#### **4.3.1.1.1 X-ray crystallographic description**

Hibiscus acid dimethyl ester was crystallised and characterised by single crystal diffraction (**Figure 4.3** and **Figure 4.4**). The structure of this compound contained two crystallographically independent molecules (*A* and *B*) ( $Z'=2$ ), whose molecular geometries differ only by small deviations in torsion angles, for example, C3—C5—O5—C6 in *A* is 175.1 (4) $^{\circ}$ , whilst the equivalent angle in *B* (C11—C13—O12—C—14) is 180.0 (4) $^{\circ}$ . As with hibiscus acid, the five-membered ring adopts envelope conformations, with the OH-bearing C atoms lying out of the plane of the other four atoms, here by 0.505 (5) and 0.530 (5) Å for molecules *A* and *B*, respectively.

##### **4.3.1.1.1.1 Supramolecular feature**

Both independent molecules in the structure of hibiscus acid dimethyl ester donate single hydrogen bonds through their OH groups, but only one molecule (*A*) acts as a hydrogen-bond acceptor (O3—H $\cdots$ O4i and O10—H $\cdots$ O2ii; **Table 4.4**). That a total of four carbonyl O atoms do not act as acceptors is probably related to the low ratio of classic hydrogen-bond donors to acceptors in this compound. In hibiscus acid dimethyl ester the hydrogen bonding combines to give a four-molecule-wide one-dimensional ribbon of linked molecules that propagates parallel to the *a* axis (**Figure 4.4**).

**Table 4.4: Hydrogen-bond geometry ( $\text{\AA}$ ,  $^\circ$ ) for hibiscus acid dimethyl-ester**

$D-\text{H}\cdots A$	$D-\text{H}$	$\text{H}\cdots A$	$D\cdots A$	$D-\text{H}\cdots A$
O3—H1H…O4 <sup>i</sup>	0.88 (1)	2.36 (5)	2.951 (4)	125 (4)
O10—H2H…O2 <sup>ii</sup>	0.88 (1)	2.03 (3)	2.802 (4)	147 (5)

Symmetry codes: (i)  $-x + 1, y + \frac{1}{2}, -z + 1$ ; (ii)  $x + 1, y, z$ .

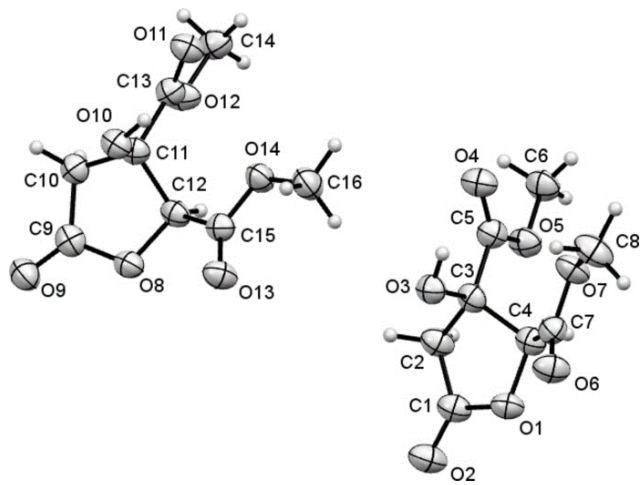


**Figure 4.3:** The molecular structures of the two independent molecules comprising the asymmetric unit of hibiscus acid dimethyl ester.

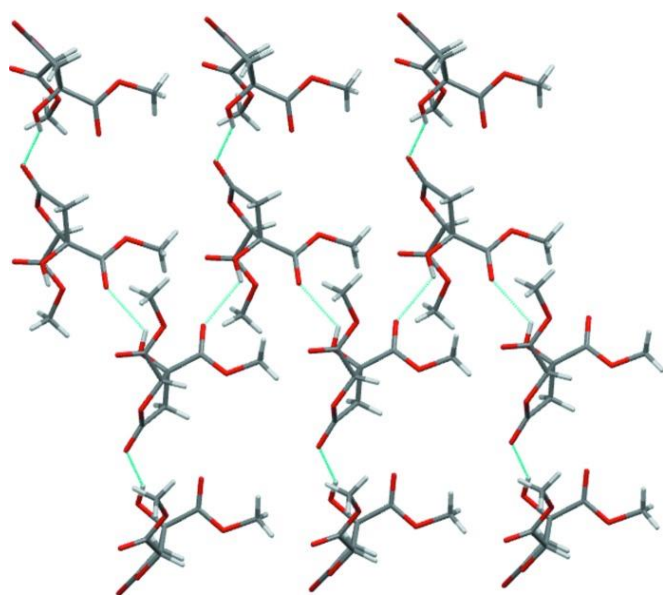


**Figure 4.4:** A section of the extended structure of hibiscus acid dimethyl ester showing the hydrogen bond contacts along the (*a*) axis.

#### 4.3.1.2 Characterisation of hibiscus acid

Hibiscus acid was isolated and further purified from the methanol extract using a Sephadex LH-20 column. On TLC, using 60% methanol in ethyl acetate as the mobile phase, hibiscus acid appeared as a yellow spot with an  $R_f$  value of 0.8 after visualisation with *p*-anisaldehyde-sulphuric acid reagent. The HRMS data (**Spectrum 4.7**) showed a molecular ion peak  $[M-H]^-$  at  $m/z$  189.00 (Calc 189.00) which suggested a molecular formula of  $C_6H_6O_7$  for this compound. The compound was identified from its 1D and 2D NMR data (Boll *et al.*, 1969), and confirmed by its X-ray crystallographic structure (**Figure 4.5**).

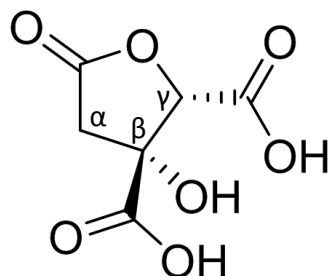


**Figure 4.5:** Chemical structure of hibiscus acid.

## NMR data analysis

The  $^1\text{H}$  and  $^{13}\text{C}$  NMR spectrum for this compound were identical to those of hibiscus acid dimethyl ester except for the absence of the peaks of the two methoxy groups. The  $^1\text{H}$  NMR spectrum (500 MHz, Acetone-*d*) showed proton signals clearly appeared as two doublet and one singlet peaks. The signal at  $\delta_{\text{H}}$  5.31 ppm (1H, s) was attributed to the proton carried on the secondary oxymethine carbon ( $\gamma$ -C), whereas the two doublet signals were assigned to the two protons of the methylene carbon ( $\alpha$ -C), one signal at  $\delta_{\text{H}}$  2.77 ppm (1H, d,  $J=17.2$  Hz,) and the other signal at  $\delta_{\text{H}}$  3.23 ppm (1H, d,  $J=17.2$  Hz) (**Spectrum 4.8**).

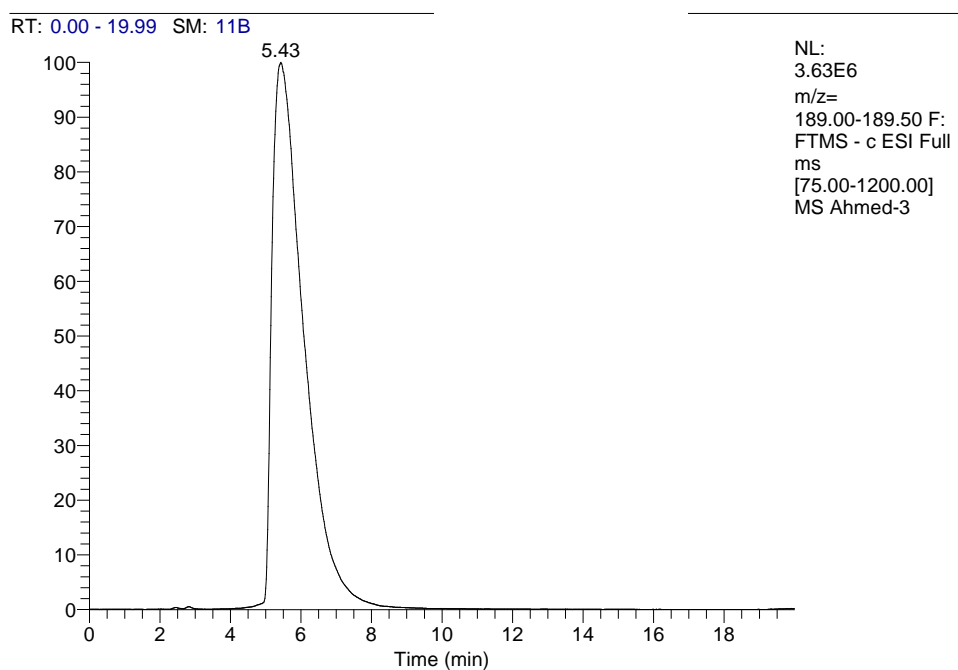
The  $^{13}\text{C}$  spectrum (**Spectrum 4.9**) displayed six signals and confirmed the presence of three carbonyls, one methylene and two oxygen bearing carbons. The peak at  $\delta_{\text{C}}$  172.4 ppm was ascribed to the lactone carbonyl while the other signals at  $\delta_{\text{C}}$  166.53 ppm and  $\delta_{\text{C}}$  171.90 ppm for the two acidic carbonyls attached to the secondary ( $\gamma$ -C at  $\delta_{\text{C}}$  82.26 ppm) and the tertiary carbon ( $\beta$ -C at  $\delta_{\text{C}}$  77.67 ppm), respectively. The oxomethylene carbon ( $\alpha$ -C) was assigned  $\delta_{\text{C}}$  41.31 ppm.

Using 2D NMR (COSY, HSQC and HMBC) the structure was identified as follows: the proton ( $\text{H-}\alpha\alpha$ ) doublet signals at  $\delta_{\text{C}}$  2.77 ppm shows a correlation with the proton ( $\text{H-}\alpha\beta$ ) doublet signal at  $\delta_{\text{H}}$  3.23 ppm in the COSY correlation spectrum (**Spectrum 4.10**).

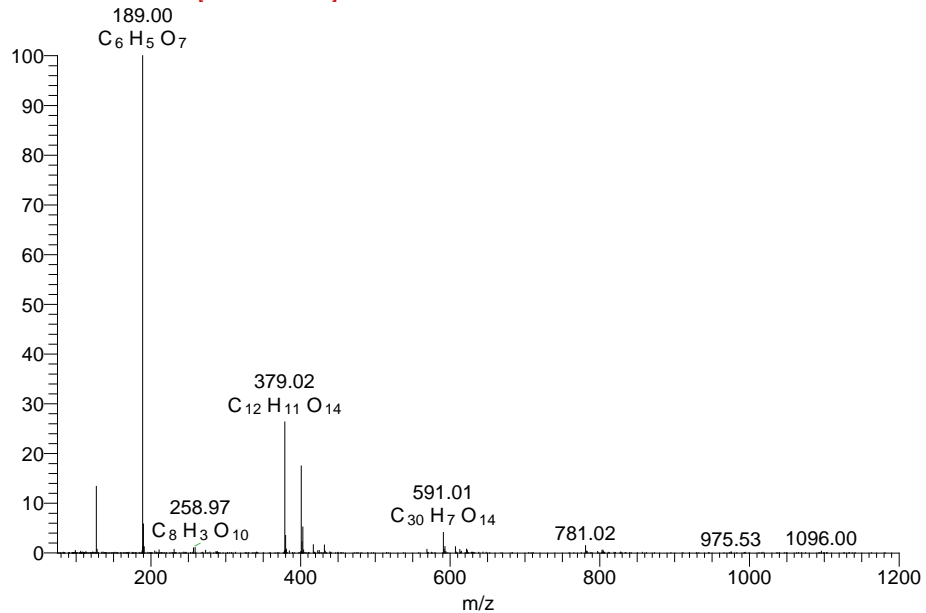
The HSQC spectrum (**Spectrum 4.11**) shows direct correlations of the two protons at  $\delta_{\text{H}}$  2.77 ppm and  $\delta_{\text{H}}$  3.23 ppm to the carbon at  $\delta_{\text{C}}$  41.31 ppm ( $\alpha$ -C).

While the proton at  $\delta_H$  5.31 ppm was directly correlated to the carbon  $\delta_C$  82.26 ppm ( $\gamma$ -C).

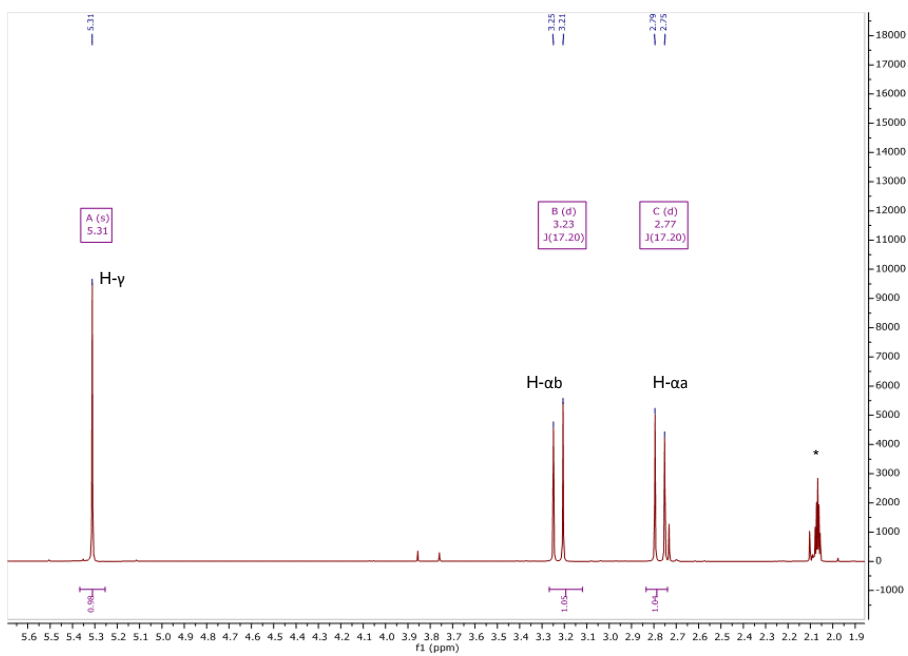
The chemical shifts were further confirmed by long range ( $^2J$  and  $^3J$ ) correlations  $^1H$ - $^{13}C$  in the HMBC spectrum of hibiscus acid (**Spectrum 4.12**). The methylene protons at  $\delta_H$  2.77 and 3.23 ppm showed  $^2J$  and  $^3J$  correlations with the carbons at  $\delta_C$  77.7 and 82.3 ppm, respectively. While the proton at  $\delta_H$  5.31 showed  $^2J$  correlations with the tertiary carbon at  $\delta_C$  77.7. The correlations ( $^2J$ ) of the proton at  $\delta_H$  5.31 with the carbonyl carbon at  $\delta_C$  166.53 ppm and  $^3J$  correlations with the carbonyl carbon at  $\delta_C$  171.90 ppm confirmed the assignment of the signal at  $\delta_C$  172.4 ppm as the lactone carbonyl. The two methylene protons at  $\delta_H$  2.77 ppm and 3.23 ppm showed  $^2J$  and  $^3J$  correlations to the lactone carbonyl carbon at  $\delta_C$  172.4 ppm and the acidic carbonyl carbon at  $\delta_C$  171.90 ppm, respectively (**Table 4.5**).



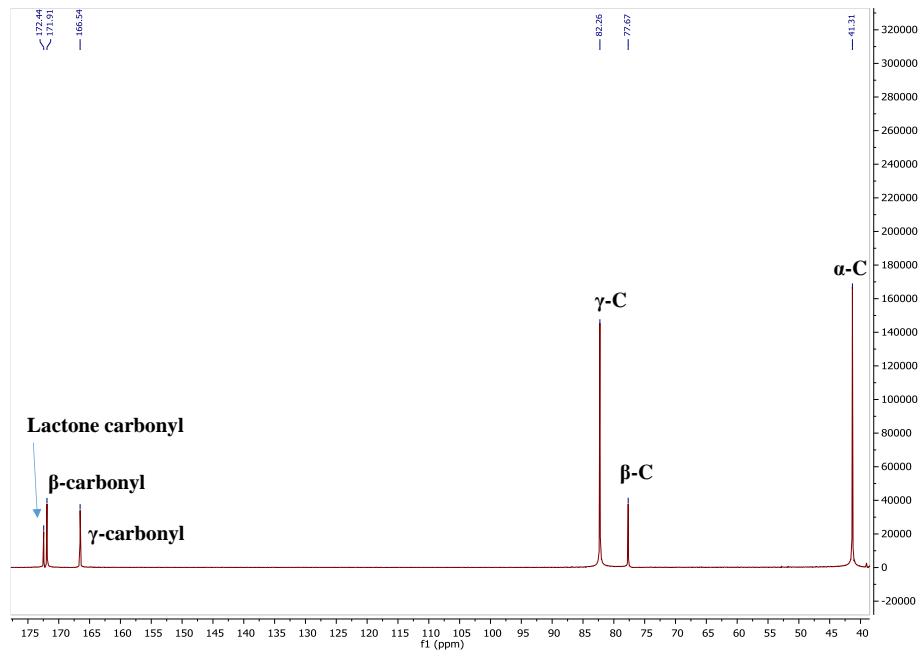
Ahmed-3 #417 RT: 5.42 AV: 1 NL: 3.35E6  
F: FTMS - c ESI Full ms [75.00-1200.00]



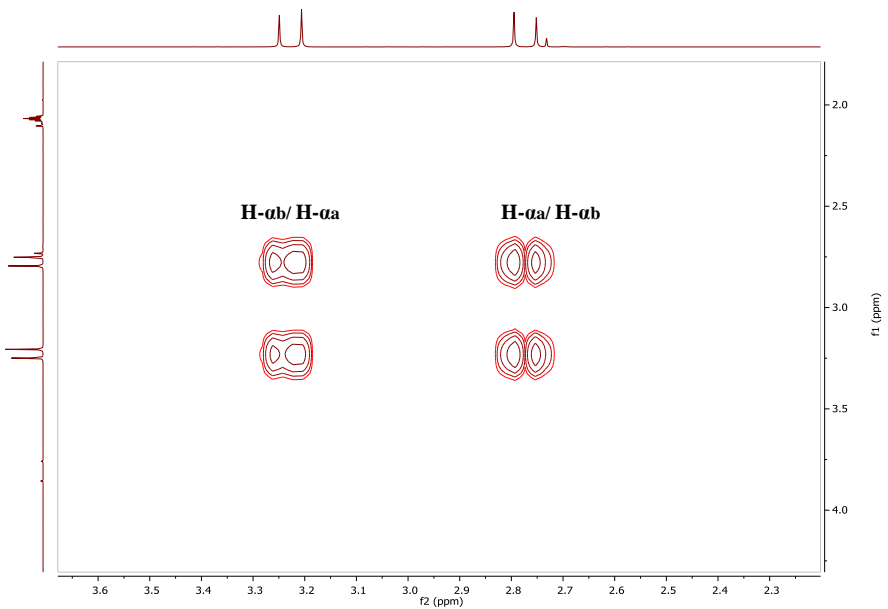
**Spectrum 4.7: Molecular ion peak  $[M-H]^-$  spectrum of hibiscus acid.**



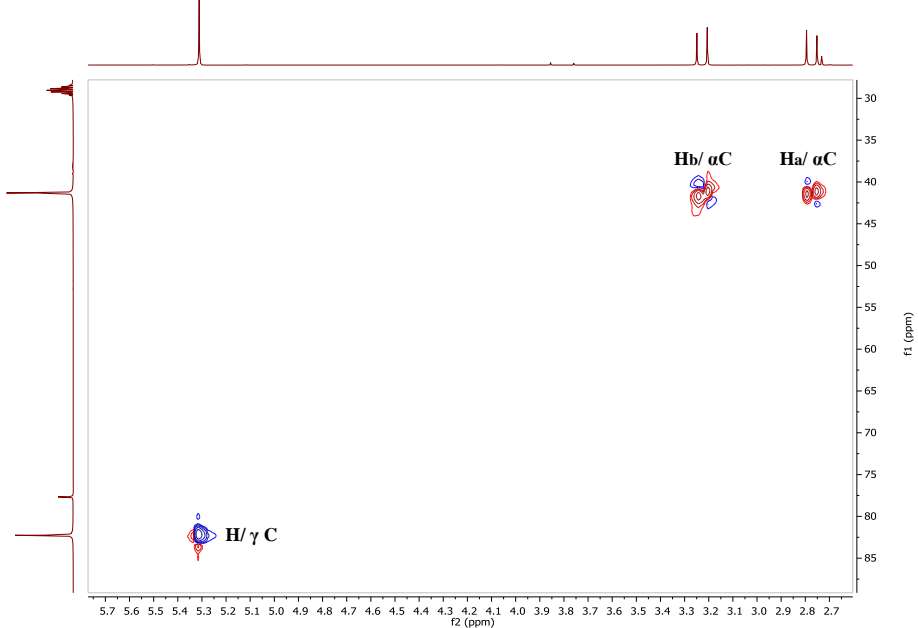
**Spectrum 4.8:**  $^1\text{H}$  NMR spectrum (400 MHz) of hibiscus acid in Acetone- $d_6$ .



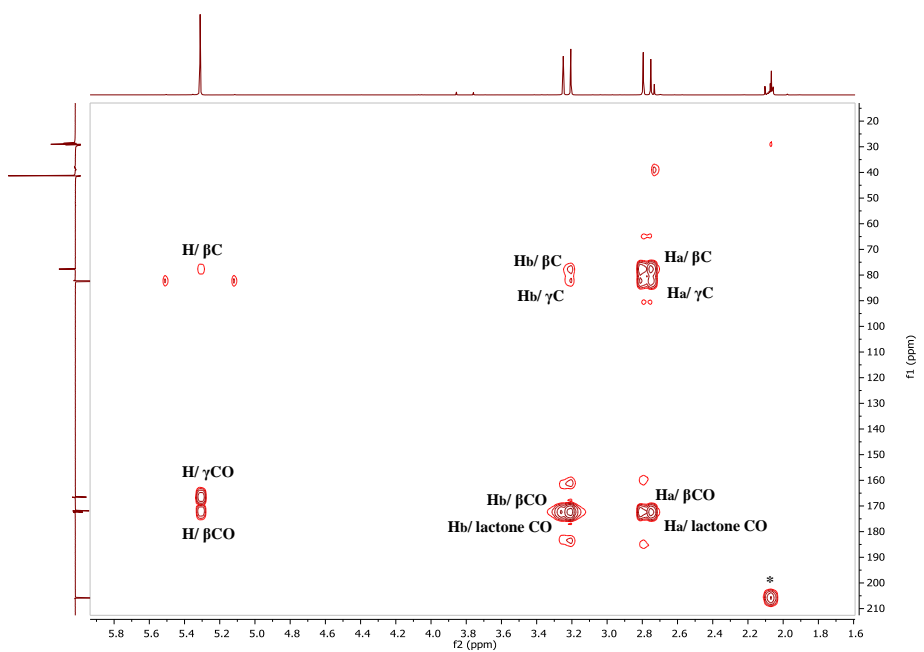
**Spectrum 4.9:**  $^{13}\text{C}$  (100 MHz) NMR spectrum of hibiscus acid in Acetone- $d_6$ .



**Spectrum 4.10:** Cosy NMR (400 MHz) spectrum of hibiscus acid in Acetone-*d*<sub>6</sub>.



**Spectrum 4.11:** HSQC (400 MHz, Acetone-*d*<sub>6</sub>) spectrum of hibiscus acid.



**Spectrum 4.12: HMBC (400 MHz, Acetone-*d*<sub>6</sub>) spectrum of hibiscus acid.**

**Table 4.5:  $^1\text{H}$  (500MHz),  $^{13}\text{C}$  (100MHz), COSY, HMBC and HSQC data of hibiscus acid in Acetone- $d_6$  and DMSO- $d_6$**

	Acetone- $d_6$		DMSO- $d_6$	
Position	$\delta_{\text{H}}$ (mult, $J$ (Hz))	$\delta_{\text{C}}$ (mult)	$\delta_{\text{H}}$ (mult, $J$ (Hz))	$\delta_{\text{C}}$ (mult)
	5.31 (1H, s)	82.26	4.90 (1H, s)	82.34
$\alpha$ (H-b)	3.23 (1H, d, 17.2)	41.31	3.04 (1H, d, 17.4)	41.88
$\alpha$ (H-a)	2.77 (1H, d, 17.2)	41.31	2.43 (1H, d, 17.4)	41.88

#### 4.3.1.2.1 X-ray crystallographic description

The crystal structures of the 1:1 DMSO solvate of hibiscus acid, are shown in **Figure 4.6**, **Figure 4.7** and **Figure 4.8**. The presence of the heavy S atom allows the absolute configuration to be assigned as (S, R) as shown in **Figure 4.6**. The COOH groups lie in equatorial positions on their rings and the absolute configuration of this compound is confirmed by the Flack parameter values (Parsons *et al.*, 2013), for arbitrarily named atoms in hibiscus acid [C2(R), C1(S), 0.00 (4)] (**Table 4.6**). The five-membered ring of hibiscus acid adopts an envelope conformation, with the OH-bearing C2 atom 0.582 (6) Å out of the plane defined by the other four atoms.

#### 4.3.1.2.1.1 Supramolecular features

Despite containing two carboxylic acid functionalities, the structure of hibiscus acid does not feature the classic  $R_2^2$  (8) carboxylic acid dimer motif. Instead, each of the three potential hydrogen-bond donors of the acid molecule form interactions with a total of three separate neighbouring molecules (**Figure 4.7**). The H atom of the carboxylic acid group (O3—H) adjacent to the ether forms a bifurcated hydrogen bond that is accepted by the ROH and C=O functions (*i.e.* O<sup>4i</sup> and O<sup>6i</sup>) of one neighbour, whilst the other two donors, the second carboxylic acid (O5—H) and the hydroxy group (O4—H), form hydrogen bonds with atoms O<sup>8ii</sup> and O<sup>8</sup> of DMSO solvent molecules, respectively (**Table 4.6**). These interactions combine to give a 2D hydrogen-bonded layered structure, with DMSO and acid layers alternating along the *c*-cell direction (**Figure 4.8**).

**Table 4.6: Hydrogen-bond geometry ( $\text{\AA}$ ,  $^\circ$ ) for hibiscus acid**

$D-\text{H}\cdots A$	$D-\text{H}$	$\text{H}\cdots A$	$D\cdots A$	$D-\text{H}\cdots A$
O3—H1H…O4 <sup>i</sup>	0.87 (2)	2.42 (4)	2.996 (4)	124 (3)
O3—H1H…O6 <sup>i</sup>	0.87 (2)	1.98 (3)	2.805 (4)	158 (4)
O4—H3H…O8	0.87 (2)	1.87 (3)	2.714 (5)	160 (7)
O5—H2H…O8 <sup>ii</sup>	0.89 (2)	1.73 (2)	2.603 (4)	167 (5)

Symmetry codes: (i)  $-x + 2, y - \frac{1}{2}, -z + 1$ ; (ii)  $-x + 1, y - \frac{1}{2}, -z + 1$

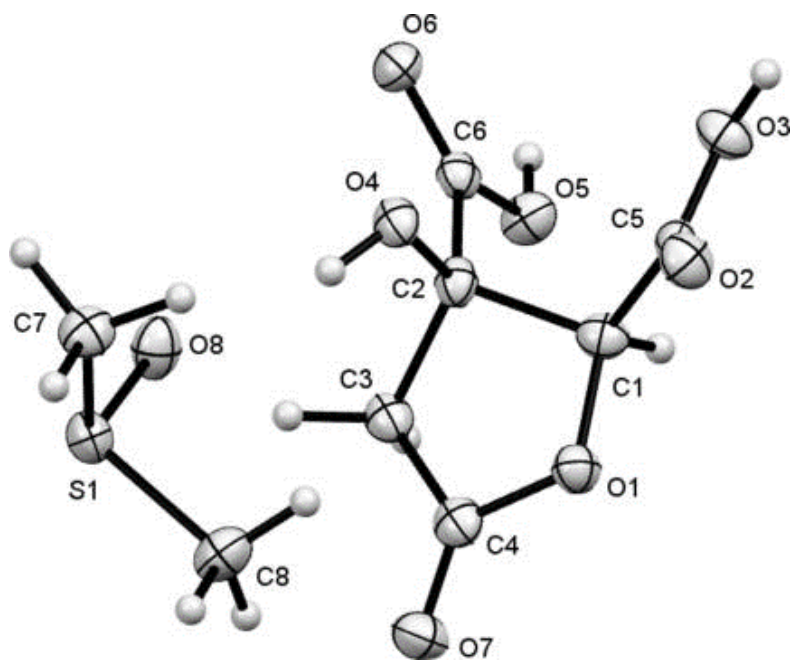


**Figure 4.6:** The molecular structure of hibiscus acid, with the atom labelling.

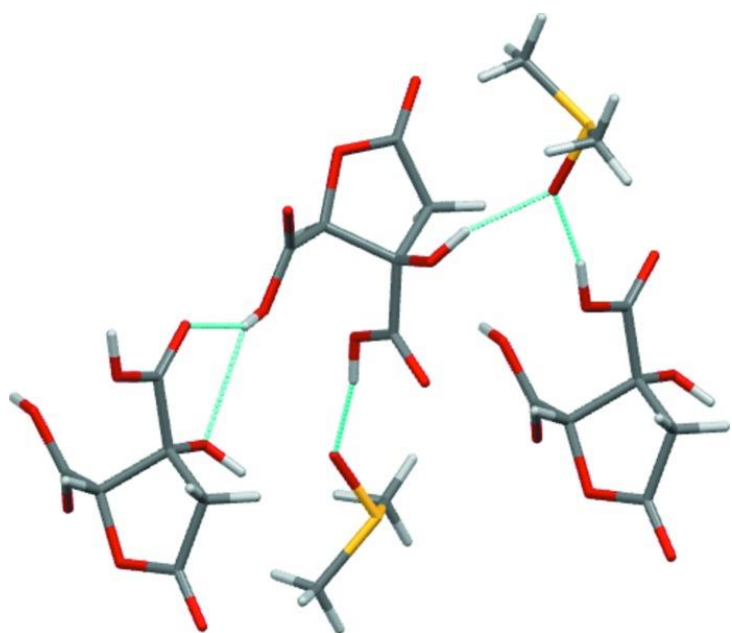


**Figure 4.7:** Hydrogen bond contacts in hibiscus acid.

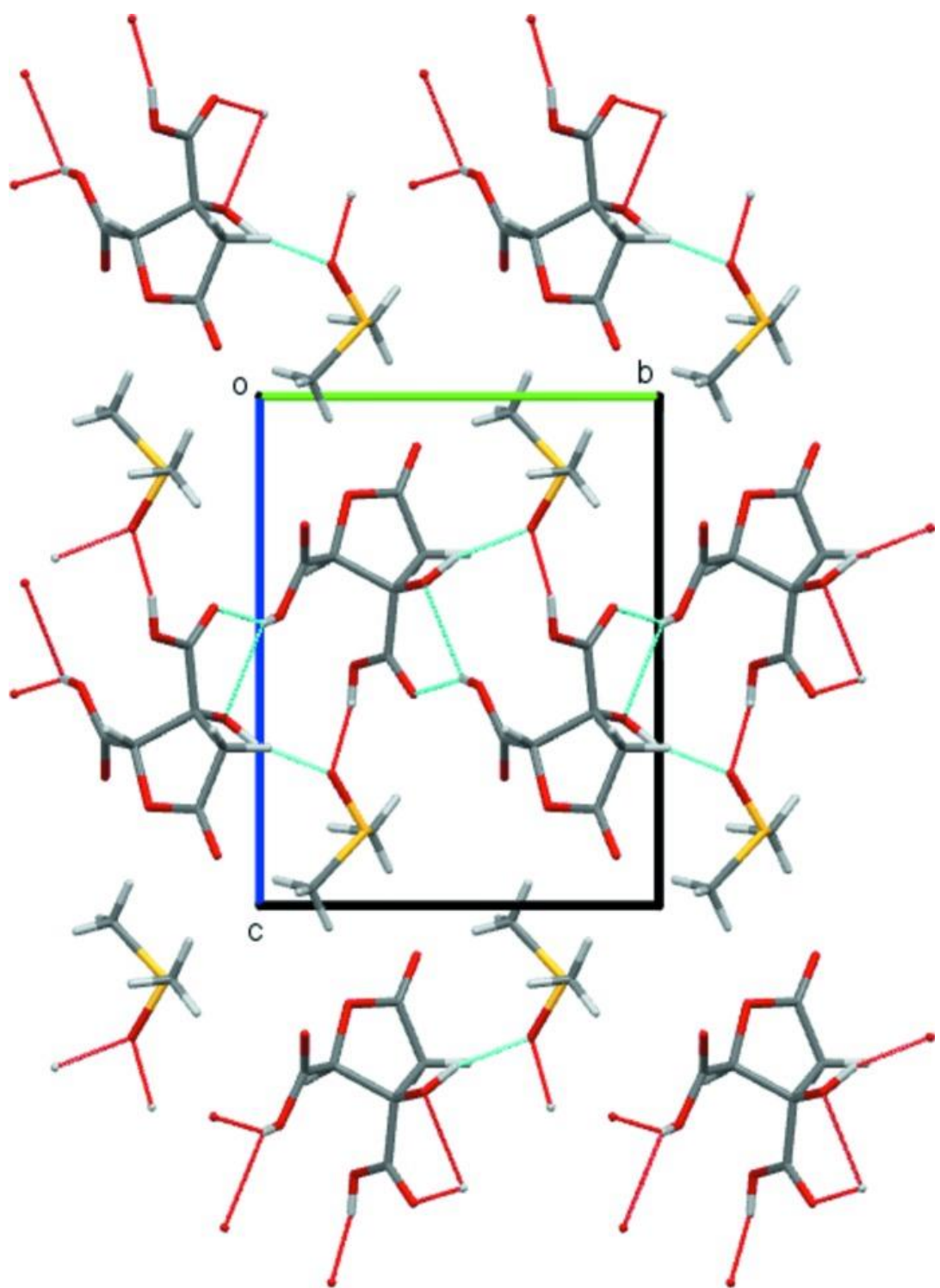


**Figure 4.8:** The crystal packing of hibiscus acid, viewed along the (*a*) axis.

#### 4.3.1.3 Characterisation of hibiscus acid-6-methyl ester

Hibiscus acid-6-methyl ester [systematic name: (2S, 3R) - 6-methyl, 3- hydroxy-5-oxo-2, 3, 4, 5-tetrahydrofuran-2, 3-dicarboxylic acid] was isolated from the sub-fraction 4 obtained from the methanol extract (HS VLC4) using Sephadex LH-20. The molecular formula was deduced from its HRMS (**Spectrum 4.13**) as C<sub>7</sub>H<sub>8</sub>O<sub>7</sub> from the molecular ion peak [M-H]<sup>-</sup> at *m/z* 203.0000 (Calc 203.02). The compound was identified from its 1D and 2D NMR data (**Figure 4.9**).

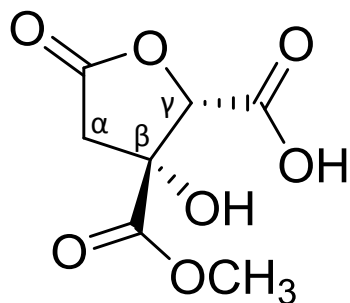


**Figure 4.9:** Chemical structure of hibiscus acid-6-methyl ester.

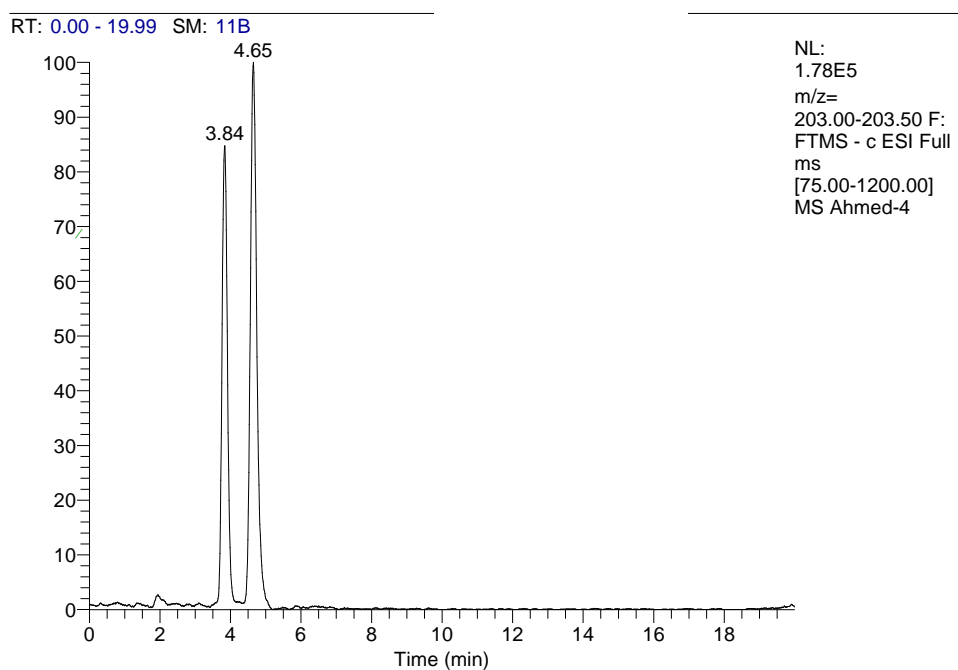
## NMR data analysis

The  $^1\text{H}$  NMR spectrum (500MHz, Acetone- $d_6$ ) exhibited proton signals between  $\delta_{\text{H}}$  2.75 and 5.29 ppm (**Spectrum 4.14**). The signal at  $\delta_{\text{H}}$  5.29 ppm (1H, s) was assigned to the oxymethine proton coupled to the secondary carbon ( $\gamma$ -C), two doublet signals were attributed to two ketomethylene protons coupled to the secondary carbon ( $\alpha$ -C), one signal at  $\delta_{\text{H}}$  2.75 ppm (1H, d,  $J=17.2$  Hz) and the other signal at  $\delta_{\text{H}}$  3.21 ppm (1H, d,  $J=17.3$  Hz). The strong single peak at  $\delta_{\text{H}}$  3.82 ppm was attributed to the three protons of the methoxy group.

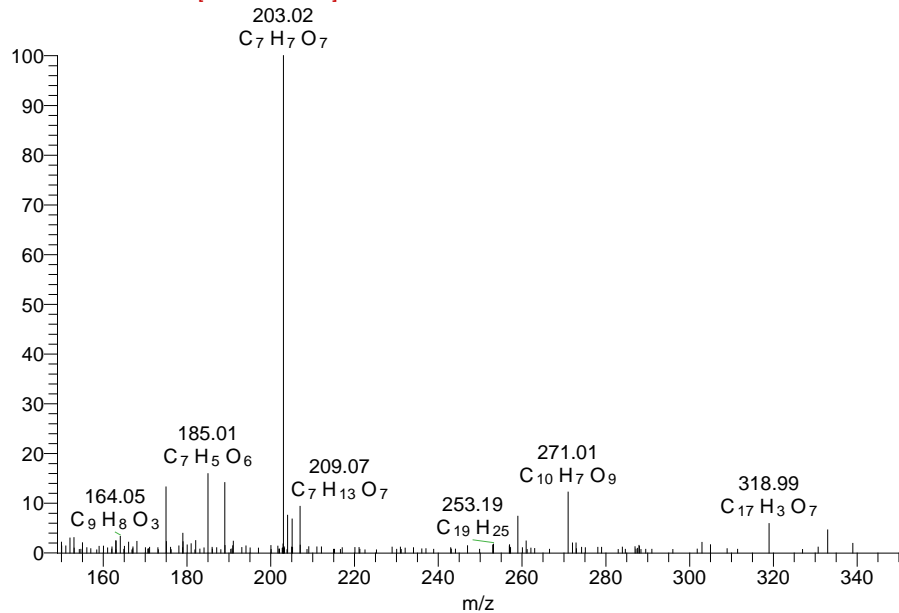
The  $^{13}\text{C}$  spectrum (**Spectrum 4.15**) indicated the presence of 7 variable signals corresponding to each carbon atom comprising of three carbonyl, one methylene, two oxygen bearing carbons and one methoxy carbon. The peak at  $\delta_{\text{C}}$  172.42 ppm accounted for the lactone carbonyl and the peak at  $\delta_{\text{C}}$  166.39 ppm accounted for the acidic carbonyl attached to the secondary carbon ( $\gamma$  CO), while the signal at  $\delta_{\text{C}}$  171.17 corresponded to the ester carbonyl carbon attached to the tertiary carbon ( $\beta$  CO). The carbonyl carbons attached to the secondary carbon atom at  $\delta_{\text{C}}$  82.08 ppm and the tertiary carbon atom at  $\delta_{\text{C}}$  78.11 ppm are assigned  $\delta_{\text{C}}$  166.39 ppm ( $\gamma$  CO) and  $\delta_{\text{C}}$  171.17 ( $\beta$  CO) ppm, respectively. The ketomethylene carbon was assigned at  $\delta_{\text{C}}$  41.46 ppm ( $\alpha$  C). The peak at  $\delta_{\text{C}}$  52.96 ppm was ascribed to the methoxy carbons. Using 2D NMR, COSY correlation spectrum shows a correlation between the proton (H- $\alpha$ a) doublet signals at  $\delta_{\text{H}}$  2.75 ppm and the proton (H- $\alpha$ b) doublet signals at  $\delta_{\text{H}}$  3.21 ppm (**Spectrum 4.16**).

The  $^1\text{H}$ - $^{13}\text{C}$  experiment in the HSQC spectrum (**Spectrum 4.17**) shows that the methylene carbon at  $\delta_{\text{C}}$  41.46 ppm ( $\alpha$  C) carried the two protons at  $\delta_{\text{H}}$  2.75 ppm and  $\delta_{\text{H}}$  3.21 ppm. While the proton at  $\delta_{\text{H}}$  5.29 ppm was directly correlated to the carbon  $\delta_{\text{C}}$  82.08 ppm ( $\gamma$  C). The methyl protons at  $\delta_{\text{H}}$  3.83 ppm was directly correlated to the methoxy carbon at  $\delta_{\text{C}}$  52.96 ppm.

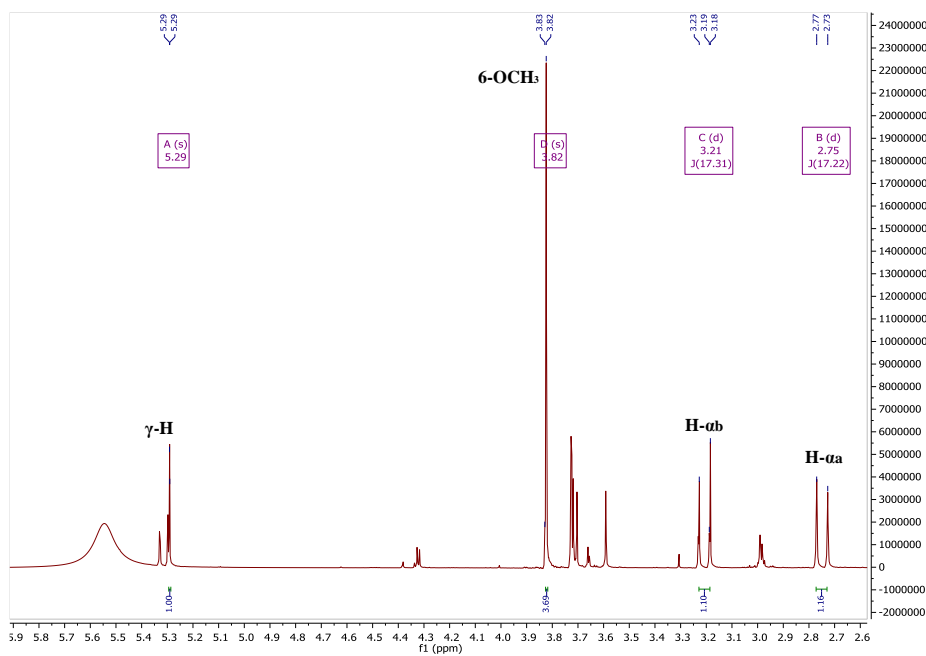
The structure of this compound was further elucidated by long range ( $^2J$  and  $^3J$ ) correlations  $^1\text{H}$ - $^{13}\text{C}$  in the HMBC spectrum (**Spectrum 4.18**). The protons at  $\delta_{\text{H}}$  2.75 and 3.21 ppm showed  $^2J$  and  $^3J$  correlations with the carbons at  $\delta_{\text{C}}$  78.11 and 82.08 ppm, respectively. While the proton at  $\delta_{\text{H}}$  5.29 showed  $^2J$  correlations with the carbon at  $\delta_{\text{C}}$  78.11 and carbonyl carbon at  $\delta_{\text{C}}$  166.39. Also the same proton and the ones at 2.75, and 3.21 ppm showed  $^3J$  correlations to the carbonyl carbon at  $\delta_{\text{C}}$  171.17 ppm ( $\beta$ -CO). The two methylene protons at  $\delta_{\text{H}}$  2.75 ppm and 3.21 ppm showed  $^2J$  correlation to the lactone carbonyl carbon at  $\delta_{\text{C}}$  172.42. The protons at  $\delta_{\text{H}}$  3.82 ppm showed  $^3J$  correlations with the ester carbonyl at  $\delta_{\text{C}}$  171.17 ppm (**Table 4.7**).



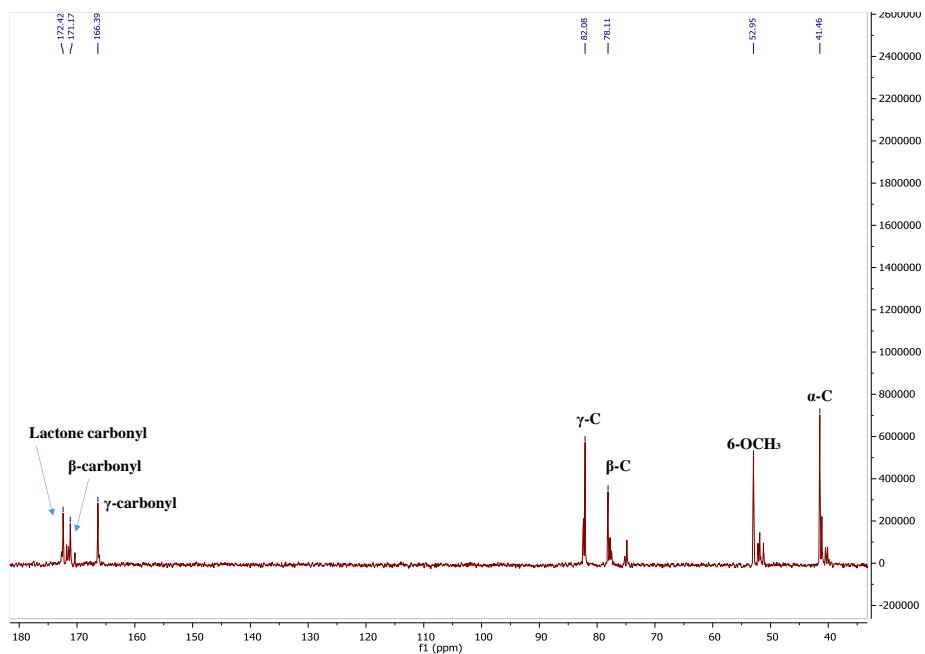
Ahmed-4 #359 RT: 4.66 AV: 1 NL: 2.00E5  
F: FTMS - c ESI Full ms [75.00-1200.00]



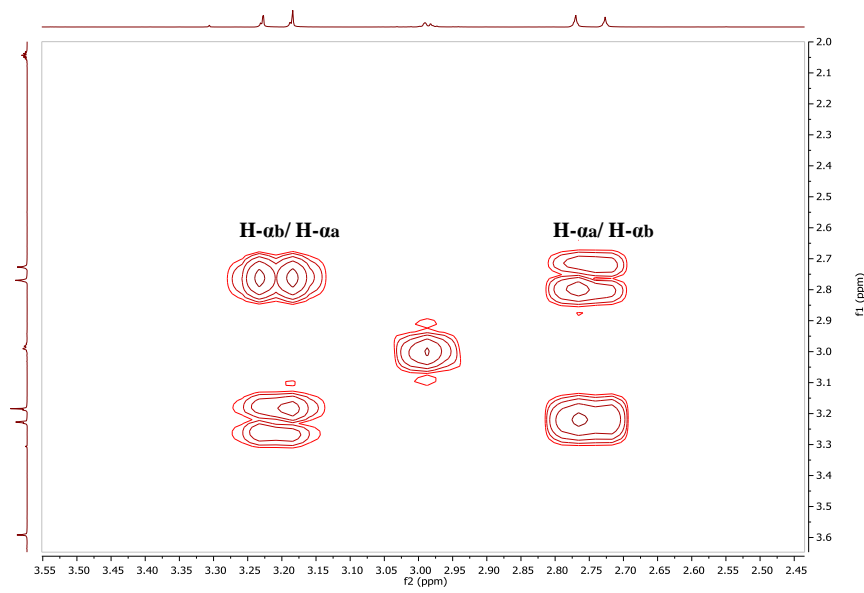
**Spectrum 4.13:** Molecular ion peak  $[M-H]^-$  spectrum of the hibiscus acid-6-methyl ester.



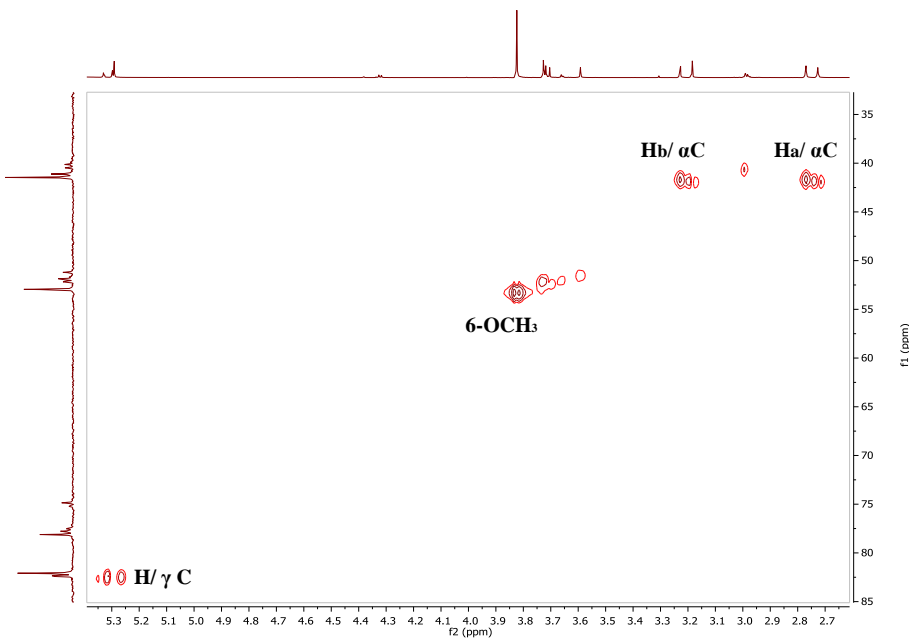
**Spectrum 4.14:**  $^1\text{H}$  NMR spectrum (400 MHz) of the hibiscus acid-6-methyl ester in Acetone- $d_6$ .



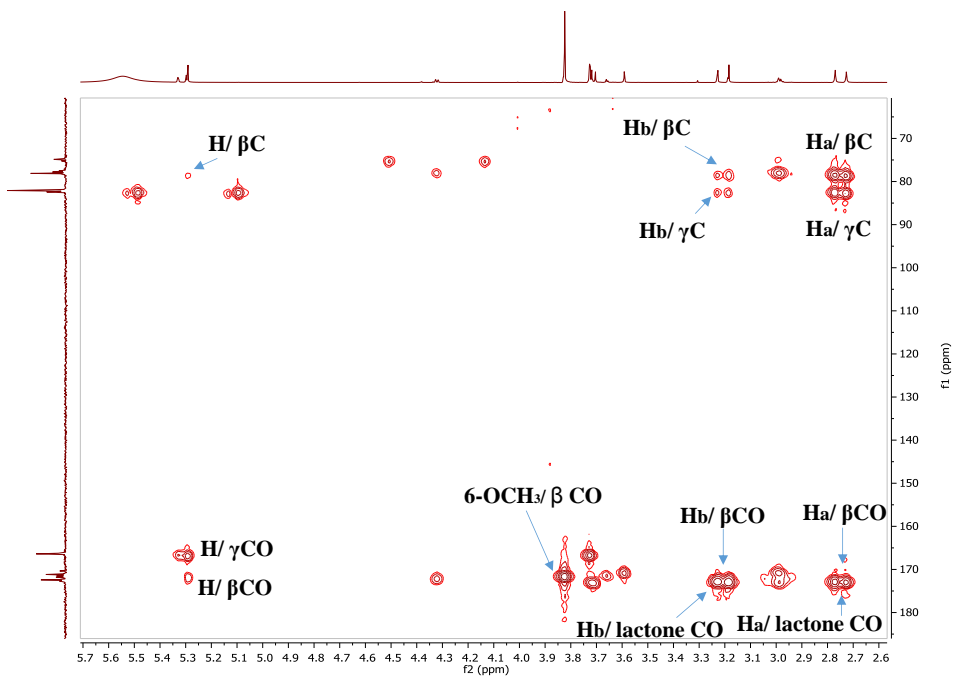
**Spectrum 4.15:**  $^{13}\text{C}$  NMR (100 MHz) spectrum of the hibiscus acid-6-methyl ester in Acetone- $d_6$ .



**Spectrum 4.16:** COSY NMR (400 MHz) spectrum of hibiscus acid-6-methyl ester in Acetone-*d*<sub>6</sub>.



**Spectrum 4.17:** HSQC (400 MHz, Acetone-*d*<sub>6</sub>) spectrum of hibiscus acid-6-methyl ester.



**Spectrum 4.18: HMBC (400 MHz, Acetone-*d*<sub>6</sub>) spectrum of hibiscus acid-6-methyl ester.**

**Table 4.7:  $^1\text{H}$  (500MHz),  $^{13}\text{C}$  (100MHz), and HSQC data of hibiscus acid-6-methyl ester in Acetone- $d_6$**

Position	$\delta_{\text{H}}$ (mult, $J$ (Hz))	$\delta_{\text{C}}$ (mult)
	5.29 (1H, s)	82.08
$\alpha$ (H-b)	3.21 (1H, d, 17.3)	41.46
$\alpha$ (H-a)	2.75 (1H, d, 17.2)	41.46.
6-OCH <sub>3</sub>	3.82 (3H,s)	52.96

#### 4.3.1.4 Characterisation of 3', 4', 3, 5, 7-pentahydroxyflavone (quercetin)

The compound (**Figure 4.10**) was isolated from the methanol extract using a Sephadex column. After spraying with *p*-anisaldehyde-sulphuric acid reagent and heating, a yellow spot appeared with  $R_f$  value of 0.33 using hexane/EtOAc/MeOH (6:3:1) as the mobile phase on TLC. The HRMS data (**Spectrum 4.19**) showed a molecular ion  $[M-H]^-$  at  $m/z$  301.0000 (Calc 301.03) which indicated that the molecular formula of this compound was  $C_{15}H_{10}O_7$ .

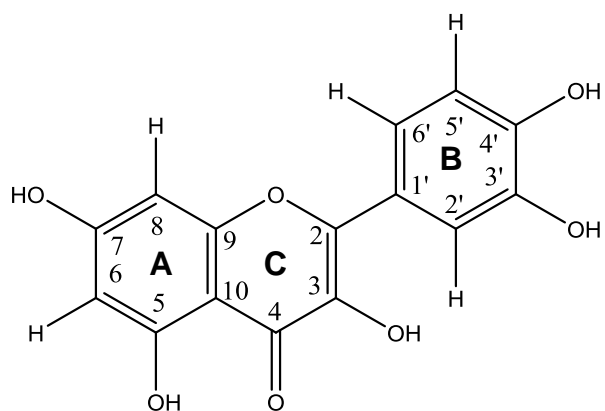


**Figure 4.10:** Chemical structure of quercetin.

### NMR data analysis

The  $^1\text{H}$  NMR (**Spectrum 4.20**) showed a downfield singlet at  $\delta_{\text{H}}$  12.15 attributed to a H-bonded phenolic hydroxyl proton usually found at position-5 of flavonoids. The protons at  $\delta_{\text{H}}$  6.26 (1H, d,  $J=2.08$  Hz) and 6.52 (1H, d,  $J=2.08$  Hz) accounted for the flavone A-ring as H-6 and H-8 protons, respectively, while the set of aromatic protons belonging to the ABX spin system (H-5', H-6' and H-2') of ring B appeared at 6.99 (1H, d,  $J=8.5$  Hz) and 7.69 (1H, dd,  $J=8.5, 2.18$  Hz), and  $\delta_{\text{H}}$  7.82 (1H, d,  $J=2.17$  Hz).

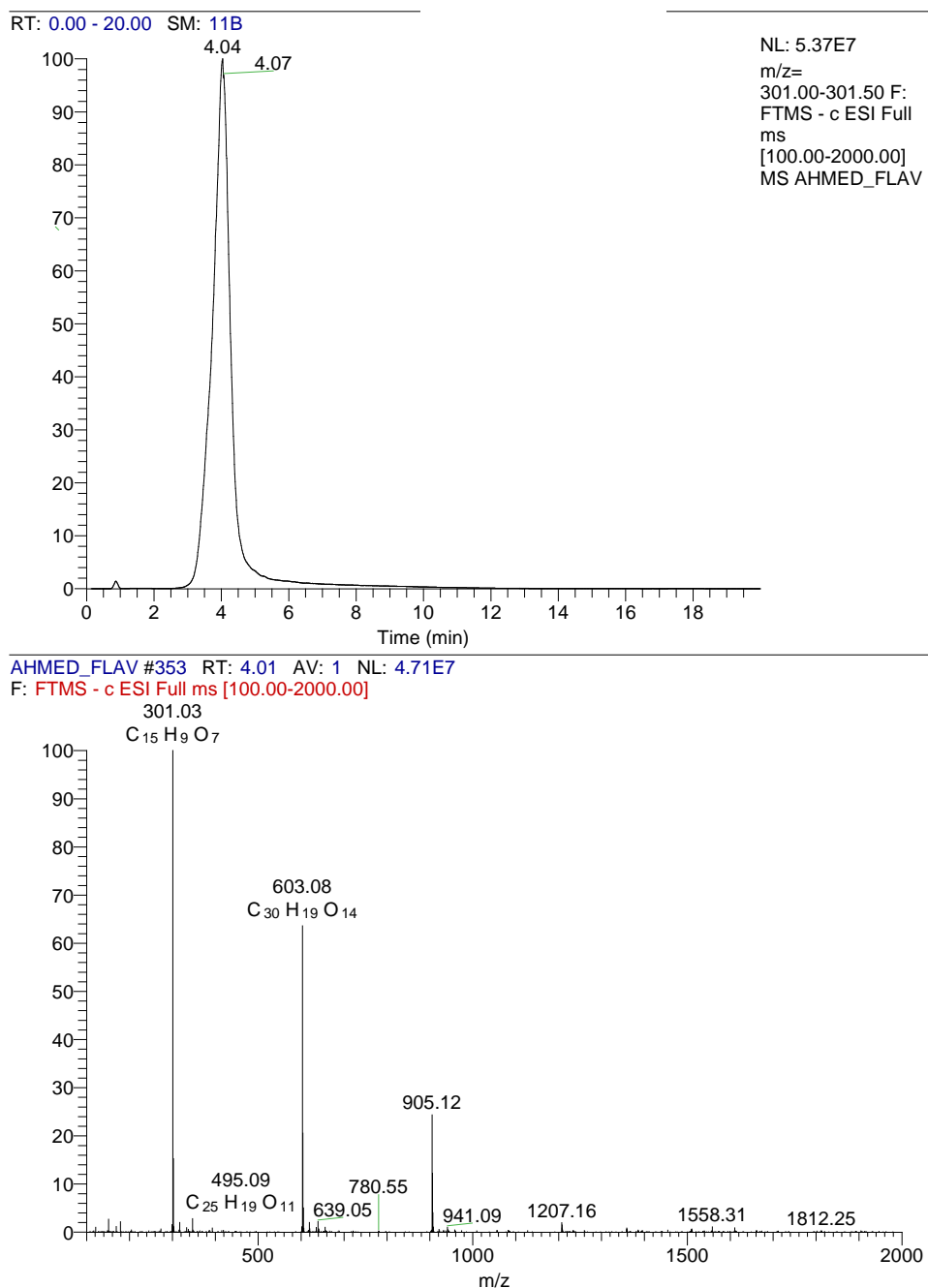
The  $^{13}\text{C}$  NMR (**Spectrum 4.21**) indicated the presence of 15 carbon atoms including a carbonyl at  $\delta_{\text{C}}$  175.66 (C-4) and five aromatic CH at  $\delta_{\text{C}}$  98.26, 93.55, 114.87, 115.33 and 120.86 ppm (C-6, C-8, C-2 $^\circ$ , C-5 $^\circ$  and C-6 $^\circ$ , respectively). Seven phenolic carbons were observed at  $\delta_{\text{C}}$  147.45, 135.87, 161.41, 164.07, 156.88, 144.87, and 146.06 ppm (C-2, C-3, C-5, C-7, C-9, C-3 $^\circ$  and C-4 $^\circ$ ) and two quaternary carbons at  $\delta_{\text{C}}$  103.23, and 122.86 ppm (C-10 and C-1 $^\circ$ ).

Using 2D NMR (COSY, HSQC and HMBC) the compound was elucidated as follows: the doublet signal for the proton at  $\delta_{\text{H}}$  6.26 (1H, d,  $J=2.08$  Hz) shows a correlation with the doublet signal at  $\delta_{\text{H}}$  6.52 (1H, d,  $J=2.08$  Hz) in the COSY correlation (**Spectrum 4.22**). In the ring B, the proton signal at  $\delta_{\text{H}}$  7.69 (1H, dd,  $J=8.5, 2.18$  Hz) showed a correlation with the signal at  $\delta_{\text{H}}$  6.99 (1H, d,  $J=8.5$  Hz) and  $\delta_{\text{H}}$  7.82 (1H, d,  $J=2.17$  Hz).

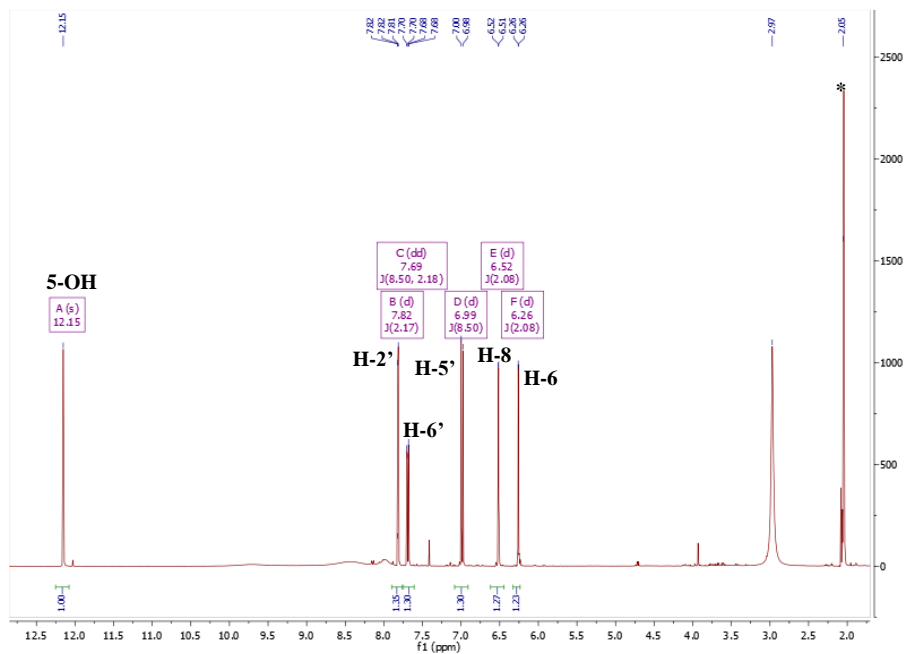
The HSQC spectrum showed a direct correlation of the two protons at  $\delta_H$  6.26 and 6.52 ppm to the carbons at  $\delta_C$  98.55 (C-6) and 93.55 (C-8), respectively. Also, the three protons at  $\delta_H$  7.82, 6.99, 7.69, are directly correlated to the B-ring carbons at  $\delta_C$  114.87, 115.33 and 120.86 ppm, respectively (**Spectrum 4.23**).

HMBC of the compound (**Spectrum 4.24**) was confirmed as follows: the A ring protons at  $\delta_H$  6.26 (H-6) and 6.52 (H-8) displayed  $^3J$  correlation to the carbons at  $\delta_C$  93.55 (C-8) and  $\delta_C$  98.55 (C-6), respectively. These protons also showed  $^3J$  and  $^2J$  correlation to the same quaternary carbon at  $\delta_C$  103.23 (C-10) and carbon at  $\delta_C$  164.1(C-7), respectively. The proton at  $\delta_H$  6.52 (H-8) displayed a  $^2J$  coupling to the carbon at  $\delta_C$  156.8 (C-9), whereas the proton at  $\delta_H$  6.26 (H-6) displayed a  $^2J$  correlation to the carbon at  $\delta_C$  161.41 (C-5). The B ring proton at  $\delta_H$  6.99 (H- $5^\gamma$ ) showed  $^3J$  correlation to the quaternary carbons at  $\delta_C$  144.93 (C- $3^\gamma$ ) and  $\delta_C$  122.86 (C- $1^\gamma$ ). It also displayed  $^2J$  correlation to the oxygen-bearing quaternary carbon at  $\delta_C$  146.06 (C- $4^\gamma$ ). The protons at  $\delta_H$  7.82 (H- $2^\gamma$ ) and 7.69 (H- $6^\gamma$ ) correlated via  $^3J$  coupling to C-2 of C ring. In addition the H- $6^\gamma$  showed  $^2J$  and  $^3J$  coupling to C- $5^\gamma$ , C- $4^\gamma$  and C- $2^\gamma$ . While the H- $2^\gamma$  displayed  $^2J$  and  $^3J$  correlation to C- $3^\gamma$  and C- $6^\gamma$ , respectively.

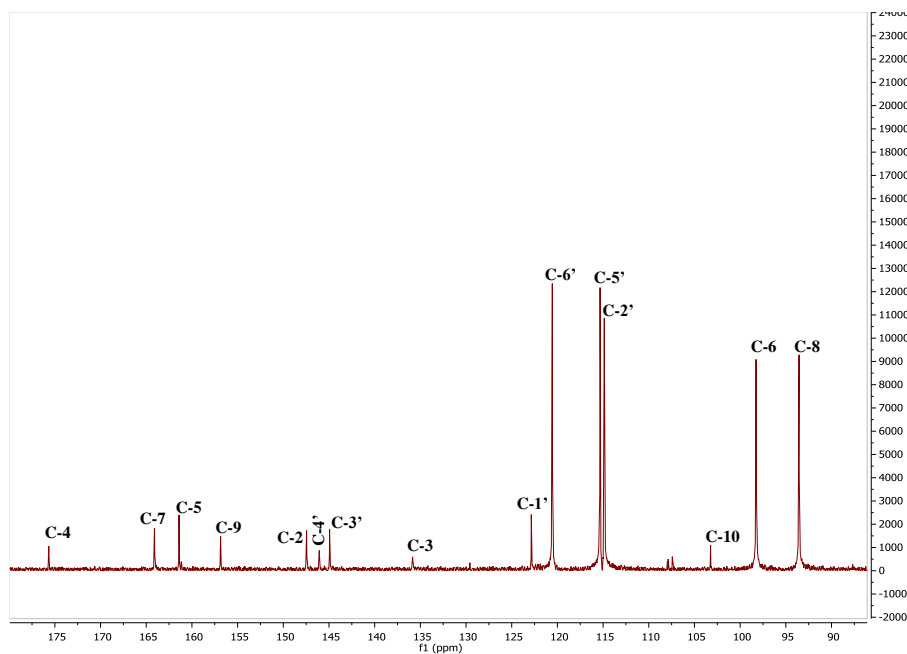
Couplings between the singlet at  $\delta_H$  12.15 of -OH in C-5 and its neighbouring carbons were also detected, including a  $^3J$  correlation to C-6 at  $\delta_C$  98.2, C-10 at  $\delta_C$  103.1, and a  $^2J$  correlation to C-5 (161.4 ppm) (**Table 4.8**).



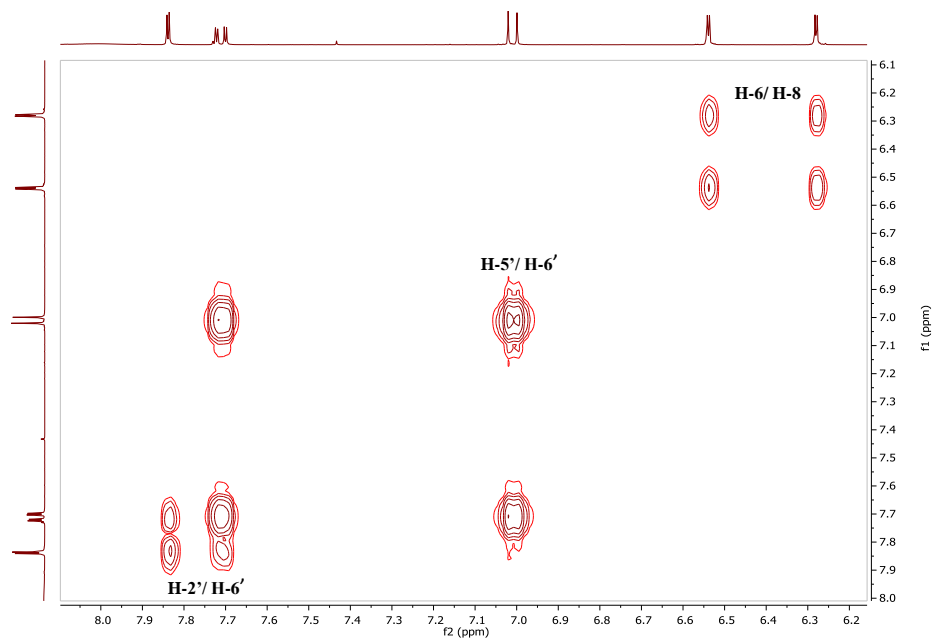
**Spectrum 4.19: Molecular ion peak [M-H]<sup>-</sup> spectrum of quercetin**



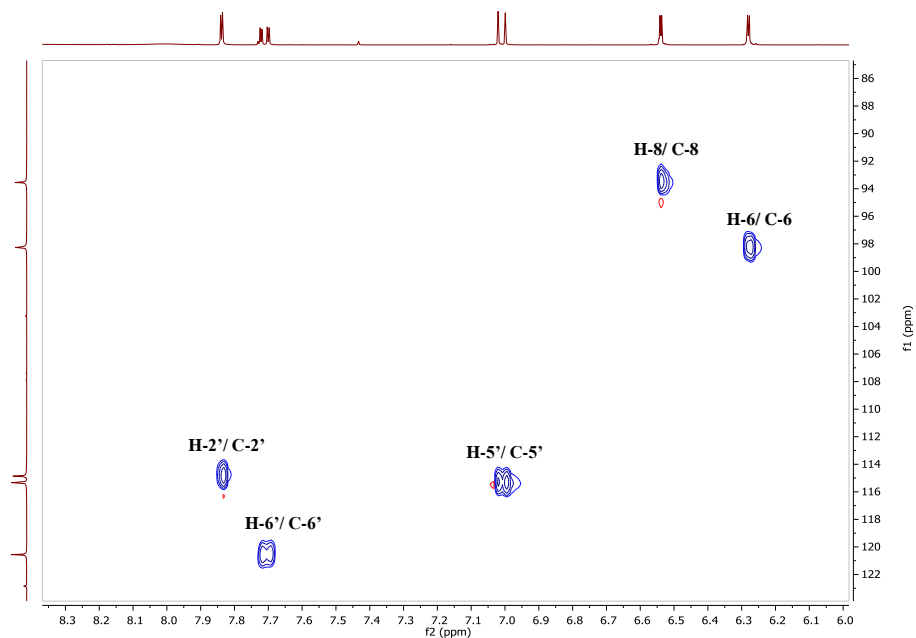
**Spectrum 4.20:**  $^1\text{H}$  NMR spectrum (400 MHz) of the quercetin in Acetone- $d_6$ .



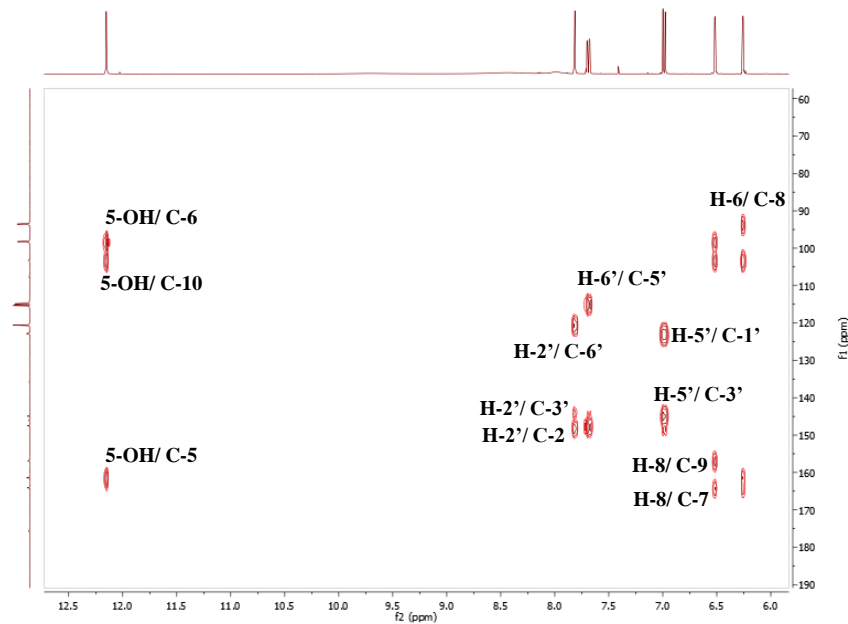
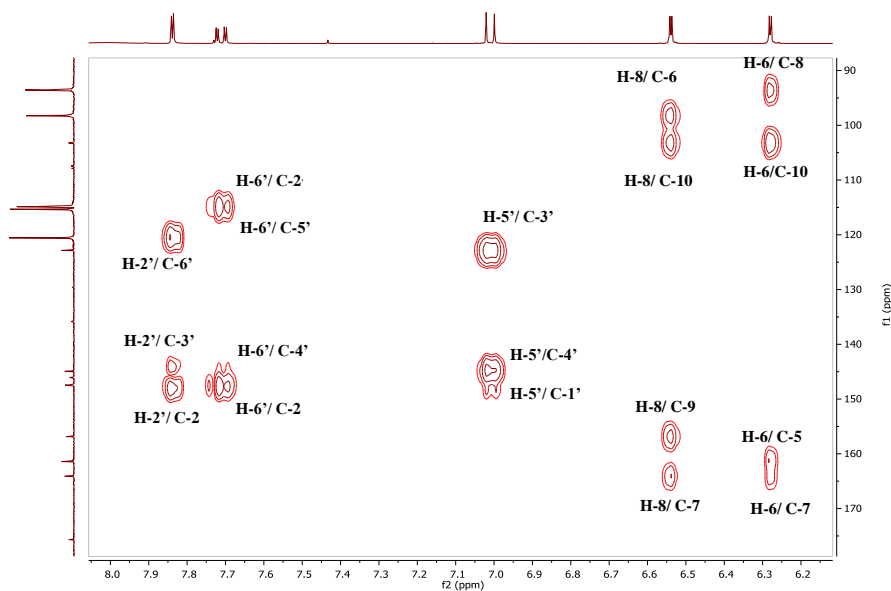
**Spectrum 4.21:**  $^{13}\text{C}$  NMR (100 MHz) spectrum of the quercetin in Acetone- $d_6$ .



**Spectrum 4.22: COSY NMR spectrum (400 MHz, Acetone- $d_6$ ) of quercetin.**



**Spectrum 4.23: HSQC (400 MHz, Acetone- $d_6$ ) spectrum of quercetin.**

**A****B**

**Spectrum 4.24: (A) Full and (B) selected expansion of HMBC spectrum (400 MHz) of quercetin in Acetone-*d*<sub>6</sub>.**

**Table 4.8:  $^1\text{H}$  (400MHz) and  $^{13}\text{C}$  (100MHz) and HMBC data of quercetin ( $3^\circ, 4^\circ, 3, 5, 7$ -pentahydroxyflavone) in Acetone- $d_6$**

Position	$\delta_{\text{H}}$ (mult, $J$ (Hz))	$\delta_{\text{C}}$ (mult)	HMBC correlations
1	-	-	-
2	-	147.45	-
3	-	135.87	-
4	-	175.66	-
5	-	161.41	-
6	6.26 (1H, d, 2.08 Hz)	98.26	C-5, C-7, C-8, C-10
7	-	164.1	-
8	6.52 (1H, d, 2.08 Hz)	93.55	C-9, C-7, C-6, C-10
9	-	156.86	-
10	-	103.23	-
$1^\circ$	-	122.86	-
$5^\circ$	6.99 (1H, d, 8.5 Hz)	115.33	C-3 $^\circ$ , C-1 $^\circ$ , C-4 $^\circ$
$2^\circ$	7.82 (1H, d, 2.1 Hz)	114.87	C-2, C-3 $^\circ$ , C-6 $^\circ$
$6^\circ$	7.69 (1H, dd, 8.5, 2.1 Hz)	120..86	C-2, C-5 $^\circ$ , C-2 $^\circ$ , C-4 $^\circ$

## **4.3.2 Vasorelaxant effects of hibiscus and garcinia acids**

### **4.3.2.1 Determining the viability of the endothelium in the rat aorta**

In the intact aorta, the muscarinic agonist, carbachol produced relaxation of the PE-pre-contracted aorta, and this relaxation was almost complete. However, the relaxant activity of the carbachol was either completely diminished or reduced by ~90%, upon either removal of the endothelium or treatment of the aorta with L-NAME (**Figure 4.11**).

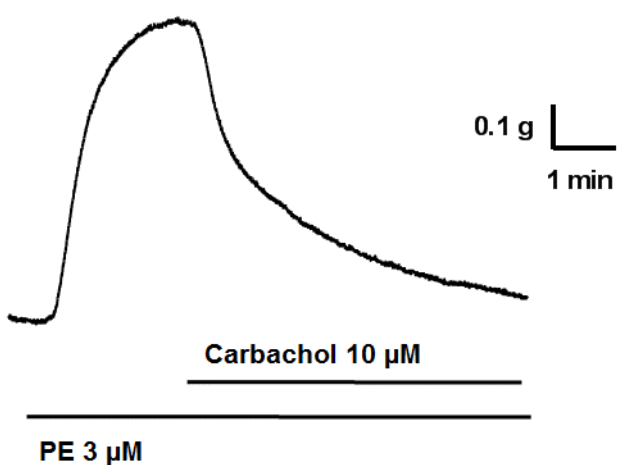
### **4.3.2.2 Effect of hibiscus acid and garcinia acid on the rat aorta**

Hibiscus acid caused a concentration-dependent relaxation of the aorta contracted with PE. The  $IC_{50}$  for hibiscus acid was  $0.09 \pm 0.01$  mg/ml (**Figure 4.12A** and **Figure 4.13**) in the endothelium-intact aorta and the highest concentration tested (1 mg/ml) almost completely relaxed the tissue ( $96 \pm 2\%$  relaxation) ( $n=18/6$ ). The relaxation was maintained for as long as hibiscus acid was present, and the tissue showed complete recovery in the response to PE after washing it out and allowing approximately 60 min for recovery, thus, the tissue was reproducible to carry out more than one experiment (see **Figure 4.14A**). The time control for these experiments showed a slight relaxation ( $15 \pm 4\%$ ) in the PE-induced contraction, over the time course of the experiment. When the endothelium was removed, the calculated magnitudes of the contraction produced by PE increased by 27% ( $n=34/8$ ) compared to that induced in intact aorta. The relaxant effect of hibiscus acid was also examined on endothelium-denuded aorta, where the magnitude of the relaxation was similar ( $89 \pm 3\%$ ) ( $n=9/6$ ); but there was a 2-fold shift to the right with regard to the sensitivity to hibiscus acid, yielding an  $IC_{50} 0.19 \pm 0.02$  mg/ml ( $P<0.001$ ),

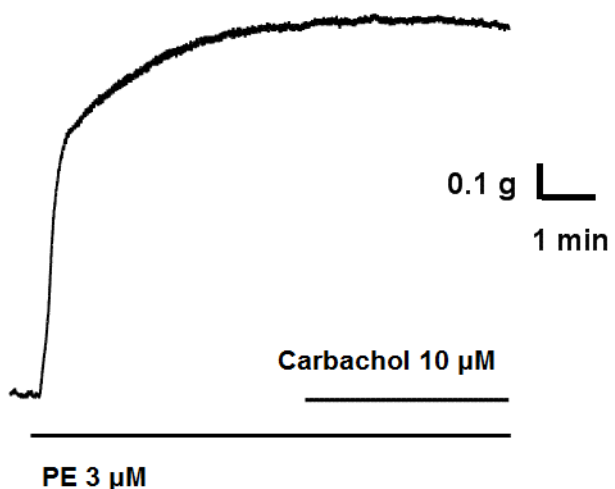
compared to when the endothelium was intact (**Figure 4.12B** and **Figure 4.13**). It was also evident that the lowest concentration of hibiscus acid tested (0.001 mg/ml) had no relaxant effect in denuded aorta, whereas it caused  $10 \pm 2\%$  relaxation in the intact aorta.

In tissues that had been denuded of endothelium, which served as a time control, there was a slight increase in the PE-induced contraction of  $5 \pm 9\%$  over the course of the experiment (**Figure 4.12C**). Pre-incubation of the aorta with L-NAME (300  $\mu\text{M}$ ) increased the magnitude of PE (3  $\mu\text{M}$ ) contraction by 45% ( $n=20/6$ ) when compared to that produced in absence of L-NAME (**Figure 4.14**). The  $IC_{50}$  for hibiscus acid induced relaxation of the PE pre-contracted aorta slightly increased from  $0.05 \pm 0.01$  mg/ml under control conditions to  $0.13 \pm 0.01$  mg/ml in the presence of L-NAME. However, this increase in the  $IC_{50}$  was not significant ( $P>0.05$ ). Also, the magnitude of the relaxation was not affected by L-NAME, as hibiscus acid at 1 mg/ml produced almost complete relaxation irrespective of the presence or absence of L-NAME, being  $97 \pm 1\%$  and  $95 \pm 2\%$ , respectively;  $n=10/6$  (**Figure 4.14**).

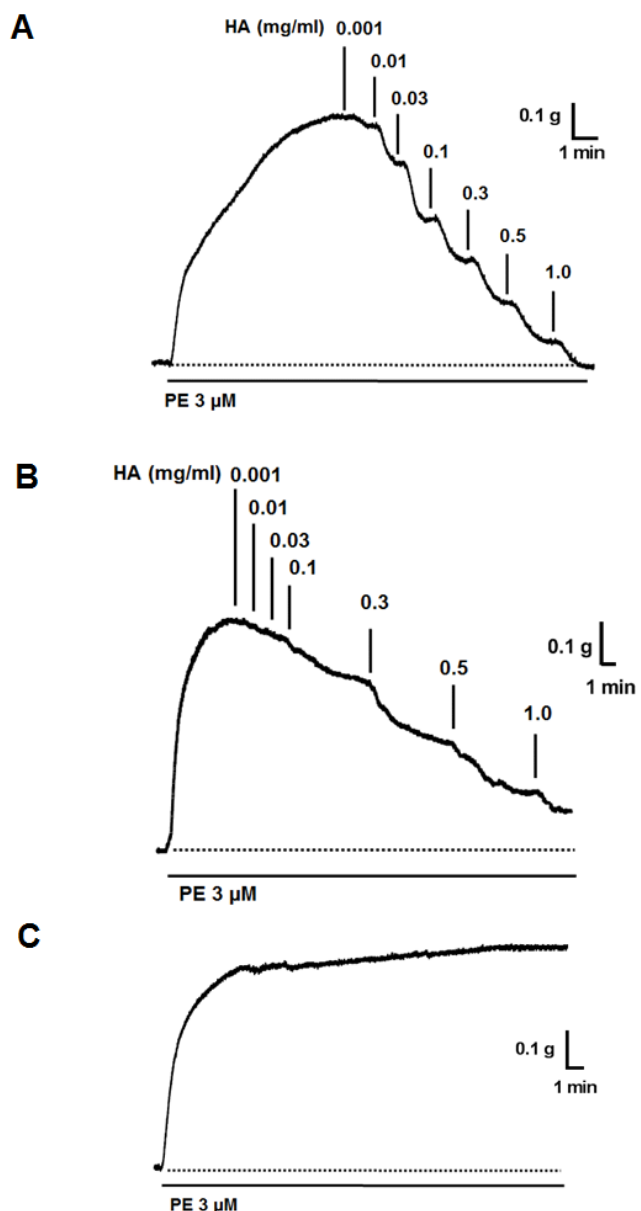
**A**



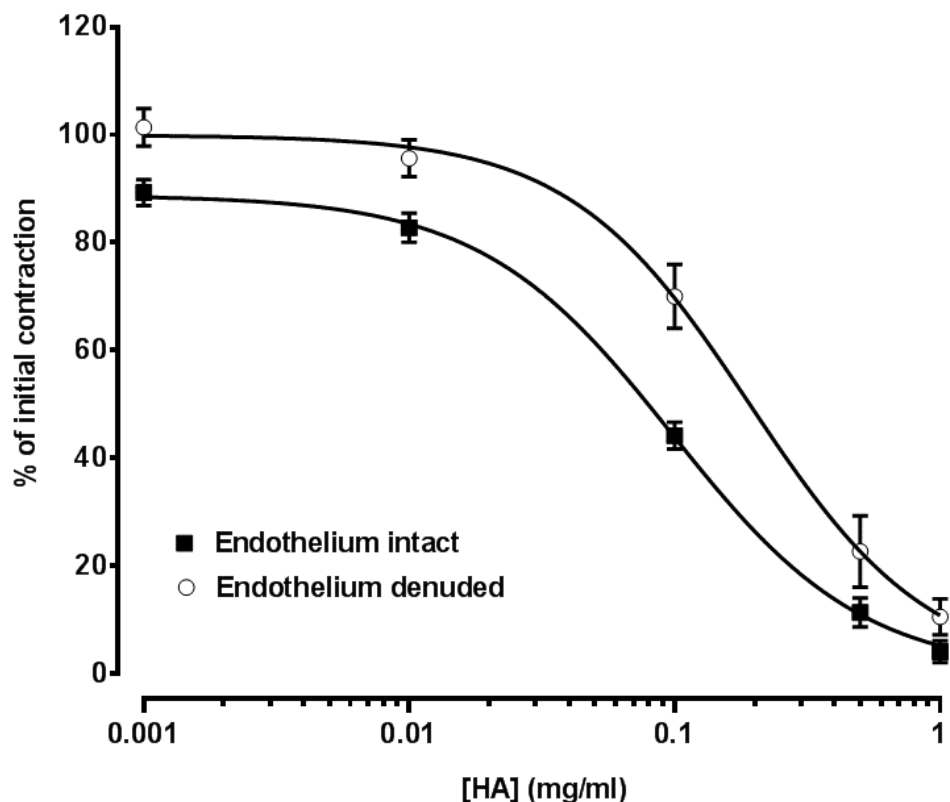
**B**



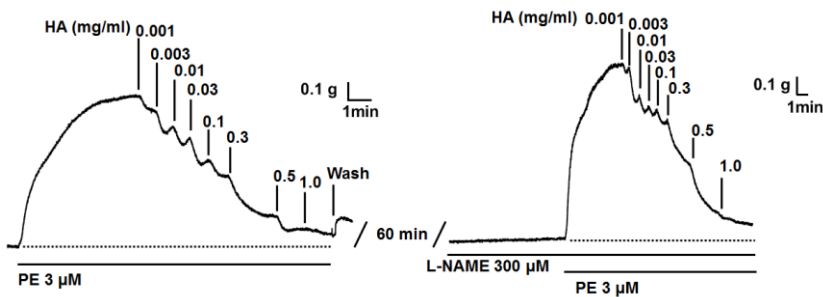
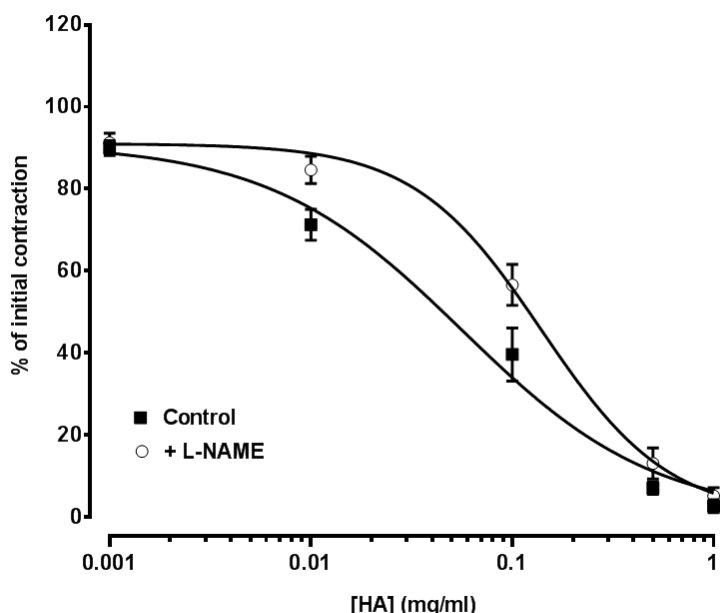
**Figure 4.11: Effect of carbachol on rat aorta pre-contracted with PE.** (A) Representative recordings confirming the presence of the endothelium and relaxation to carbachol. (B) Representative recordings confirming the absence of the endothelium.



**Figure 4.12: Relaxant effect of hibiscus acid (HA) on rat aorta pre-contracted with PE.** Representative recordings of the effect of HA on the (A) endothelium-intact and (B) endothelium-denuded aorta pre-contracted with PE (3  $\mu$ M). (C) Representative recording of the time control, showing that there was no decline in the contractile response by the end of the experiment.



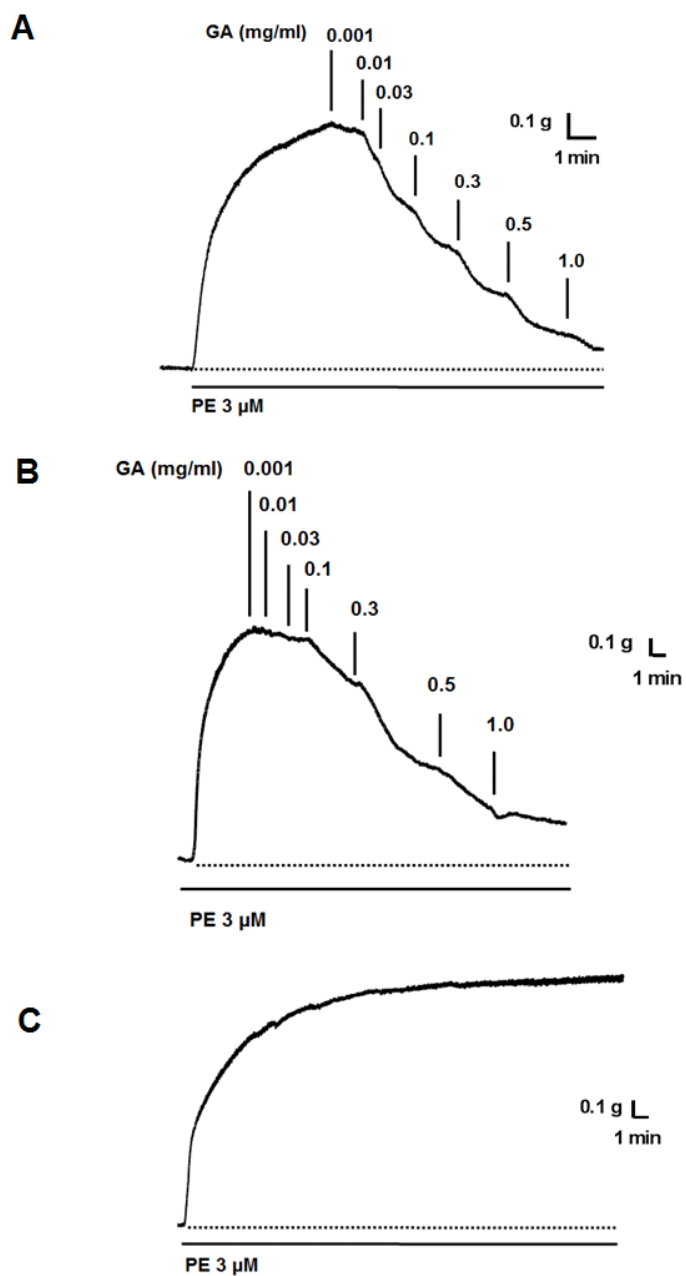
**Figure 4.13: Relaxant effect of hibiscus acid (HA) on rat aorta pre-contracted with PE.** Relaxant effect of HA against PE ( $3 \mu\text{M}$ ) induced contractions of endothelium-intact (square) and endothelium-denuded (circle) aortic rings. The relaxant effect is expressed as a percentage of the initial contraction. Values represent mean  $\pm$  s.e.m. ( $n=18/6$  for the intact aortic rings and  $n=9/6$  for the denuded rings).

**A****B**

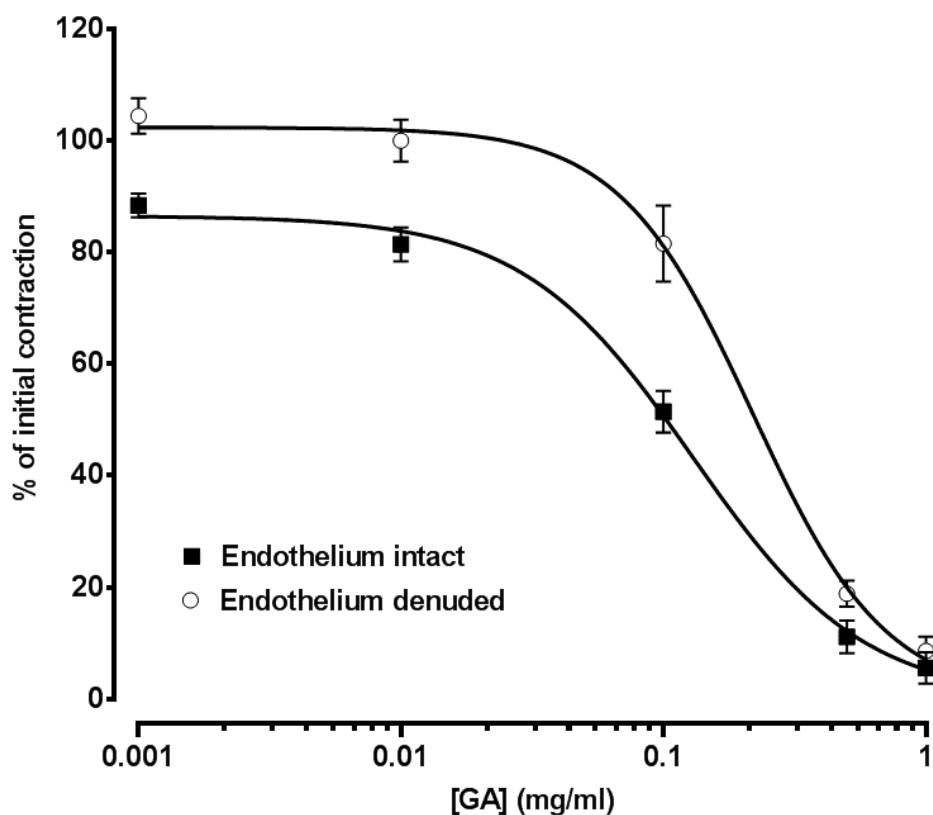
**Figure 4.14: Relaxant effect of hibiscus acid (HA) on rat aorta pre-contracted with PE in absence or presence of L-NAME.** (A) Representative recordings of the whole experiment performed on the same tissue showing the effect of HA on the endothelium-intact aorta pre-contracted with PE (3  $\mu$ M) in absence, then in presence of L-NAME (300  $\mu$ M). (B) Summary figure illustrating the effect of HA on the PE pre-contracted intact aorta in presence (circle) or absence (square) of L-NAME. HA was added cumulatively in concentrations 0.001-1 mg/ml. The relaxation is expressed as a percentage of the initial contraction. Values represent mean  $\pm$  s.e.m. (n=10/6).

Garcinia acid was found to have a similar effect to that of hibiscus acid, showing almost complete relaxation in both endothelium-intact and denuded aorta. The maximum relaxation to garcinia acid was similar irrespective of whether the endothelium was intact ( $94 \pm 2\%$ ) or denuded ( $92 \pm 2\%$ ). However, the  $IC_{50}$  value for garcinia acid was significantly lower in the endothelium-intact aorta, being  $0.12 \pm 0.01$  mg/ml ( $n=18/6$ ) compared to the endothelium-denuded preparations, being  $0.2 \pm 0.02$  mg/ml ( $n=9/6$ ;  $P<0.001$ ) (**Figure 4.15** and **Figure 4.16**).

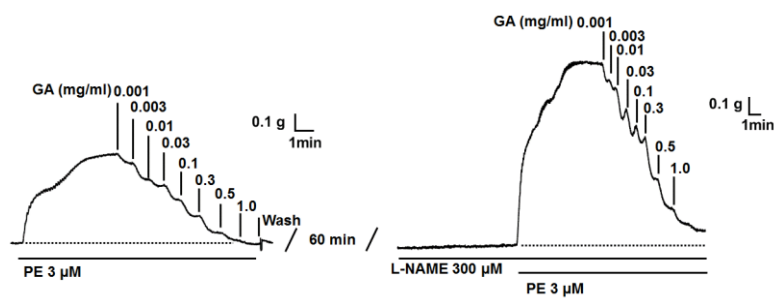
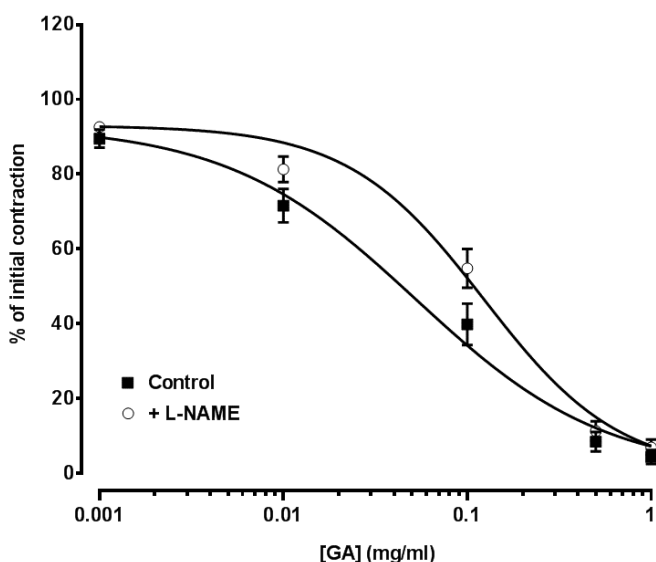
The effect of L-NAME was also examined on the relaxant effect of garcinia acid in the intact aorta. There was a slight, but not significant increase in the  $IC_{50}$  for the garcinia acid induced relaxation of the PE pre-contraction, being increased from  $0.05 \pm 0.01$  mg/ml under control to  $0.12 \pm 0.01$  mg/ml in the presence of L-NAME ( $P>0.05$ ). Also, the magnitude of the relaxation was not affected by L-NAME, and at the concentration 1 mg/ml, almost complete relaxation was produced irrespective of the presence or absence of L-NAME, being  $96 \pm 2\%$  and  $94 \pm 2\%$ , respectively;  $n=10/6$  (**Figure 4.17**). By comparing the  $IC_{50}$  and the maximum relaxant activities of both hibiscus and garcinia acids, it is obvious that there is no significant ( $P>0.05$ ) difference between the diastereomers to relax the PE-induced contraction.



**Figure 4.15: Relaxant effect of garcinia acid (GA) on rat aorta pre-contracted with PE.** Representative recordings of the effect of GA on the (A) endothelium-intact and (B) endothelium-denuded aorta pre-contracted with PE (3  $\mu$ M). (C) Representative recordings of the time control, showing that there was no decline in the contractile response by the end of the experiment.



**Figure 4.16: Relaxant effect of garcinia acid (GA) on rat aorta pre-contracted with PE.** Relaxant effect of GA on PE (3  $\mu$ M) pre-contracted endothelium-intact (square) and endothelium-denuded (circle) aortic rings. The relaxant effect is expressed as a percentage of the initial contraction. Values represent mean  $\pm$  s.e.m. (n=18/6 for the intact aortic rings and n=9/6 for the denuded rings).

**A****B**

**Figure 4.17: Relaxant effect of garcinia acid (GA) on rat aorta pre-contracted with PE in absence or presence of L-NAME.** (A) Representative recordings of the whole experiment (performed on the same tissue) showing the effect of GA on the endothelium-intact aorta pre-contracted with PE (3  $\mu\text{M}$ ) in absence, then in presence of the L-NAME (300  $\mu\text{M}$ ). (B) Summary figure illustrating the effect of HA on the PE pre-contracted aorta in the presence (circle) or absence (square) of L-NAME. GA was added cumulatively in concentrations 0.001-1 mg/ml. The relaxant effect is expressed as a percentage of the initial contraction. Values represent mean  $\pm$  s.e.m. ( $n=10/6$ ).

When the aorta was pre-contacted with KCl (60 mM), hibiscus acid also produced a concentration-dependent relaxation. The  $IC_{50}$  was  $0.57 \pm 0.06$  mg/ml; n=12/6 and the highest concentration of hibiscus acid examined (2 mg/ml) produced a relaxation of  $77 \pm 5\%$  (**Figure 4.18A** and **Figure 4.19**). When the endothelium was removed, there was no change in the sensitivity of the aorta to hibiscus acid ( $IC_{50}$   $0.66 \pm 0.1$  mg/ml; n=6/4) or the magnitude of the relaxation obtained at the highest concentration examined ( $72 \pm 6\%$ ) (**Figure 4.18B** and **Figure 4.19**).

Similarly, garcinia acid also relaxed the aorta pre-contracted with KCl (**Figure 4.20** and **Figure 4.21**). As with hibiscus acid, there was no significant effect of removing the endothelium on the  $IC_{50}$  ( $0.38 \pm 0.06$  mg/ml; n=13/6 for intact and  $0.45 \pm 0.08$  mg/ml; n=10/4 for denuded), or the magnitude of the relaxation produced by garcinia acid at the highest concentration tested ( $77 \pm 5\%$  and  $72 \pm 5\%$ , respectively). Over the course of these experiments, the time control showed a  $20 \pm 4\%$  increase in the contractile response to KCl in the endothelium-intact preparation and a  $22 \pm 3\%$  increase in the endothelium-denuded preparation (**Figure 4.20C**). Also, no significant difference between hibiscus acid and garcinia acid was noted in their ability to relax the KCl pre-contracted tissue. A comparison of the  $IC_{50}$  values indicated that either hibiscus or garcinia acid was significantly more potent ( $P<0.01$ ) in relaxing the contraction of the aorta, which had been pre-contracted with PE compared with KCl.

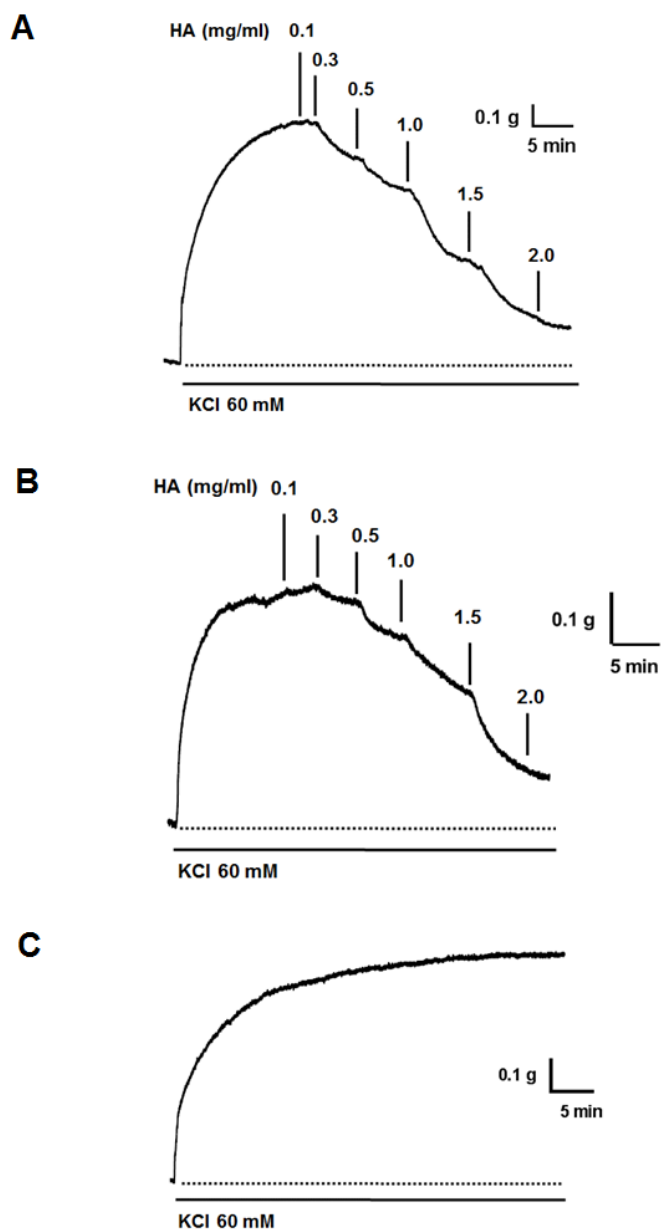


**Figure 4.18: Relaxant effect of hibiscus acid (HA) on rat aorta pre-contracted with KCl.** Representative recording of the effect of HA on the (A) endothelium-intact and (B) endothelium-denuded aorta pre-contracted with KCl (60 mM). (C) Representative recordings of the time control, showing there was no contractile decline by the end of the experiment.

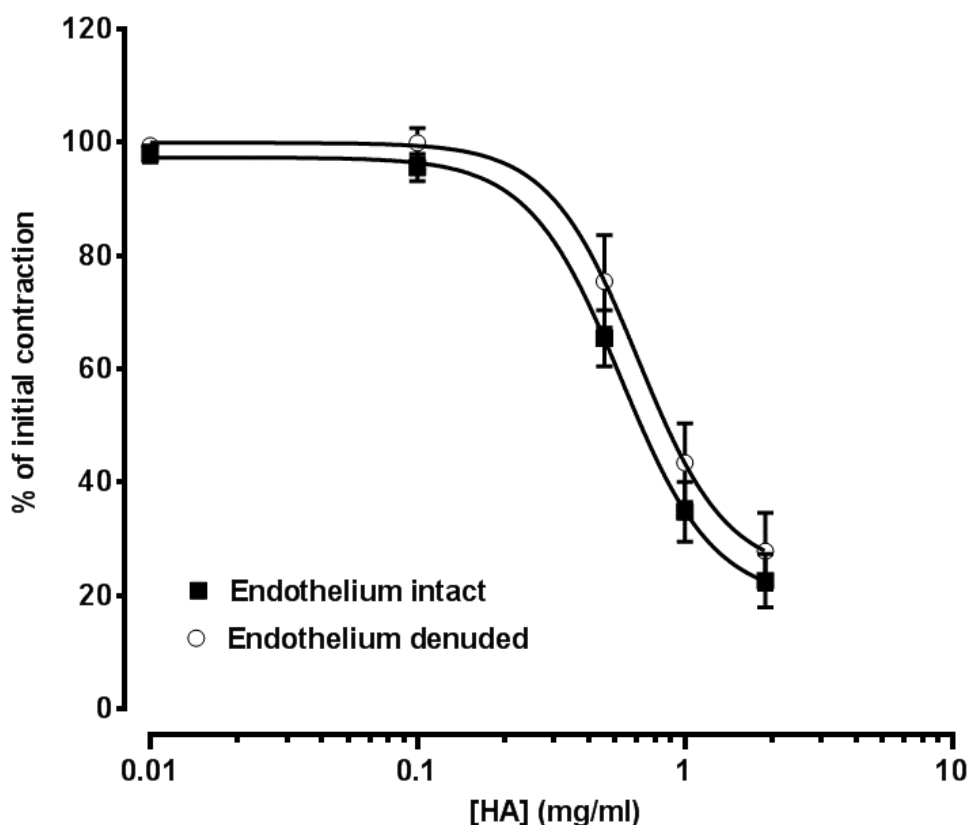


**Figure 4.19: Relaxant effect of hibiscus acid (HA) on rat aorta pre-contracted with KCl.** Relaxant effect of HA against KCl (60 mM) induced contractions of endothelium-intact (square) and endothelium-denuded (circle) aortic rings. The relaxant effect is expressed as a percentage of the initial contraction. Values represent mean  $\pm$  s.e.m. (12/6 for the intact aortic rings and n=6/4 for the denuded rings).

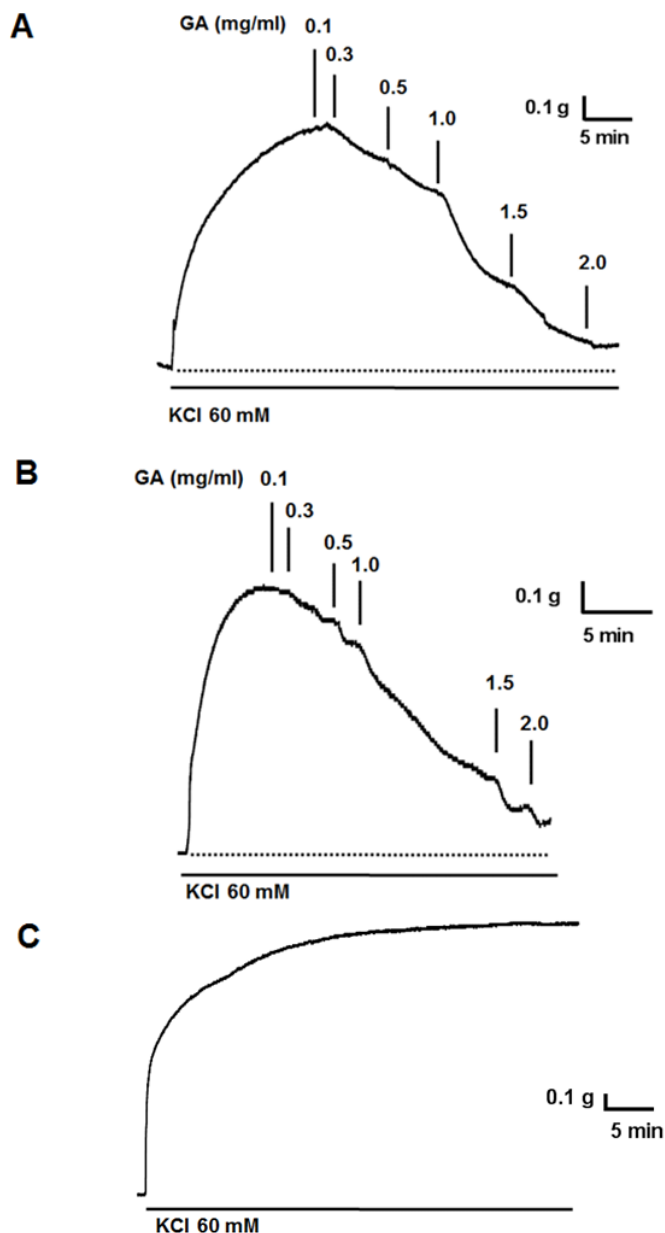


**Figure 4.20: Relaxant effect of garcinia acid (GA) on rat aorta pre-contracted with KCl.** Representative recording of the effect of GA on the (A) endothelium-intact and (B) endothelium-denuded aorta pre-contracted with KCl (60 mM). (C) Representative recordings of the time control, showing there was no contractile decline by the end of the experiment.

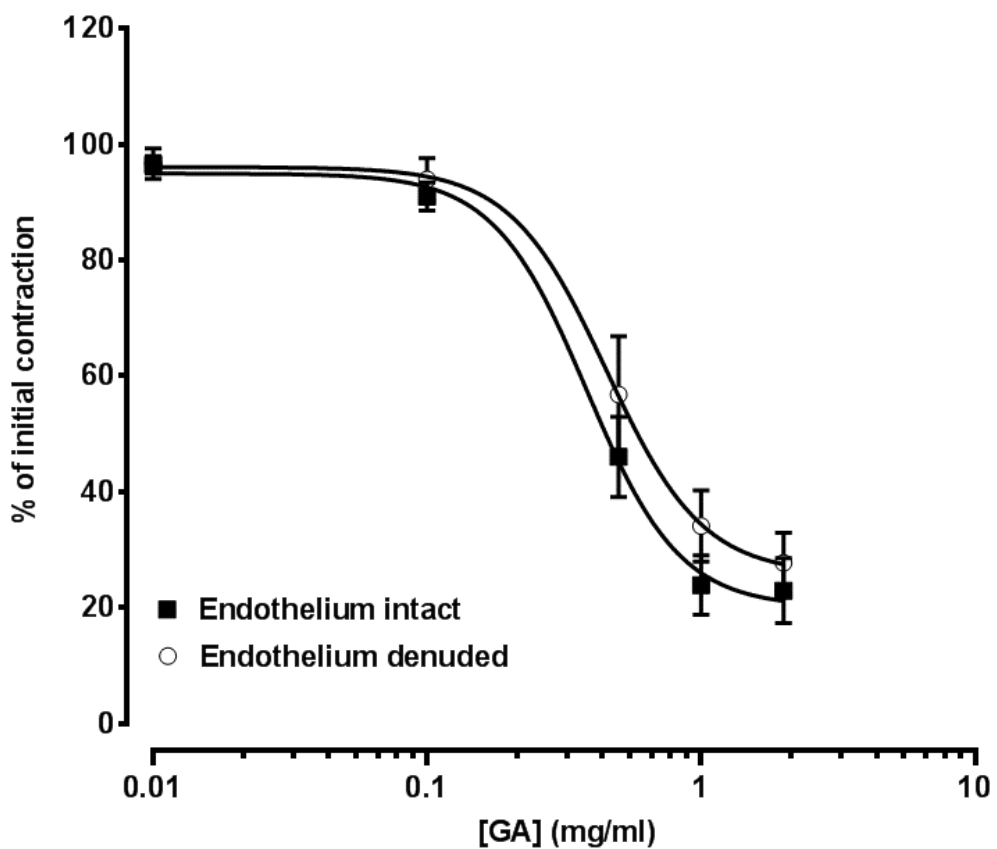


**Figure 4.21: Relaxant effect of garcinia acid (GA) on rat aorta pre-contracted with KCl.** Relaxant effect of GA against KCl (60 mM) pre-contracted endothelium-intact (square) and endothelium-denuded (circle) rat aortic rings. The relaxant effect is expressed as a percentage of the initial contraction. Values represent mean  $\pm$  s.e.m. (13/6 for the intact aortic rings and n=10/4 for the denuded rings).

#### **4.3.2.3 Relaxant effect of hibiscus or garcinia acid on contraction induced by L-type calcium channel activators**

Since hibiscus and garcinia acid relaxed the aorta pre-contracted with KCl, and the contraction induced by KCl is primarily dependent on the activation of VDCCs, one possible mechanism to explain their vasorelaxant activity is through inhibition of VDCCs. To examine this further, the effect of these substances on the contractions induced by Ca<sup>2+</sup> channel activators was examined. All of the tissues pre-contracted with a low concentration of KCl and either FPL 64176 or Bay K8644, showed an oscillatory type of contractile response. When the aorta was pre-contracted with FPL 64176 (30 µM), hibiscus acid (0.5 mg/ml) almost completely relaxed the tissue (95 ± 2% relaxation; n=4/4). A similar relaxant effect was observed when Bay K8644 (0.1 µM) was used to contract the aorta, although in this case a higher concentration of hibiscus acid (1 mg/ml) was required to produce a similar degree of relaxation (94 ± 4%; n=4/4) (**Figure 4.22**). The effect of garcinia acid (0.5 mg/ml) was very similar to that of hibiscus acid; producing 94 ± 4% (n=4/4) relaxation of the aorta pre-contracted with FPL 64176 and requiring a higher concentration (1 mg/ml) to almost completely relax the aorta (93 ± 2%; n=4/4) when pre-contracted with Bay K8644 (**Figure 4.22**).

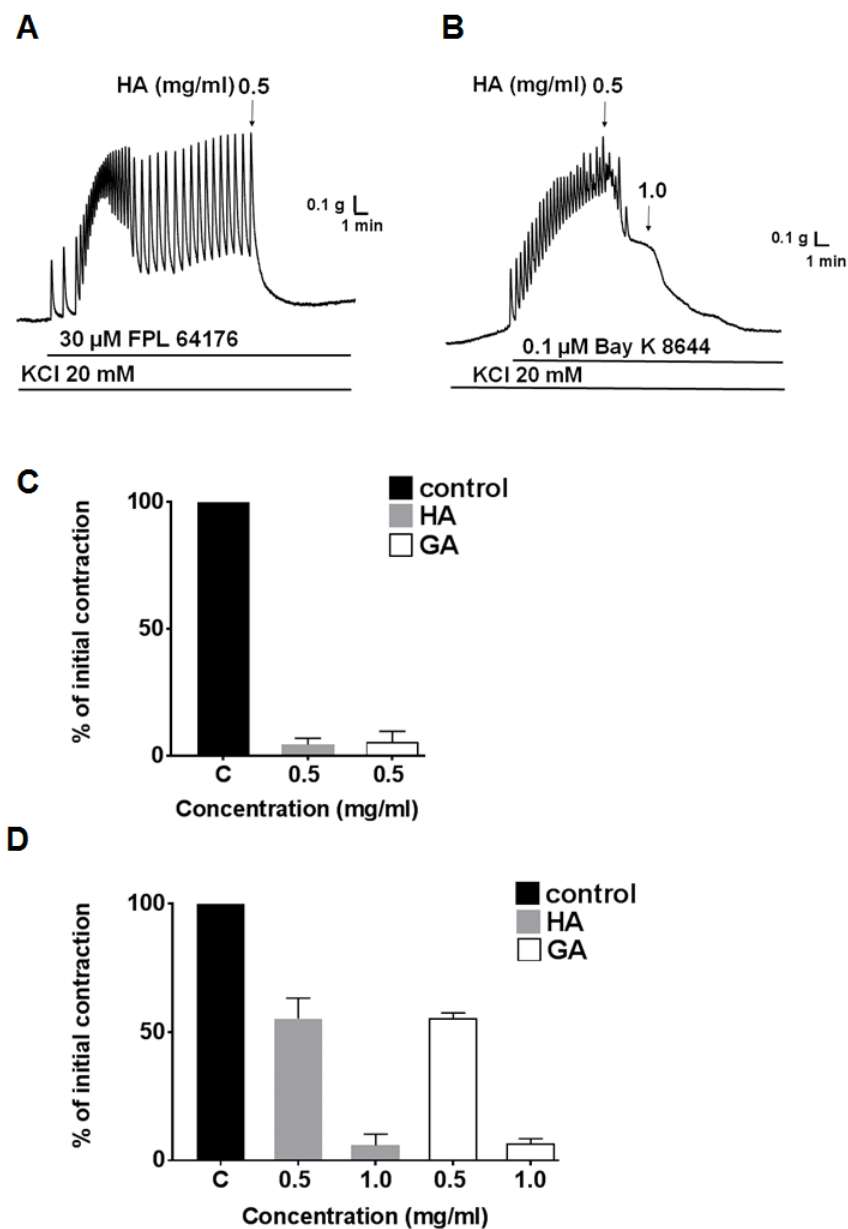


**Figure 4.22: Relaxant effect of hibiscus acid (HA) and garcinia acid (GA), on rat aorta pre-contracted with an L-type calcium channel activator.** Representative recording of the effect of HA (0.5-1 mg/ml) on the contraction induced by (A) 30  $\mu$ M FPL 64176 or (B) 0.1  $\mu$ M Bay K8644. Summary figures of the relaxant effect of HA and GA when the aorta was pre-contracted with either (C) FPL 64176 or (D) Bay K8644. Values represent mean  $\pm$  s.e.m. (n=4/4).

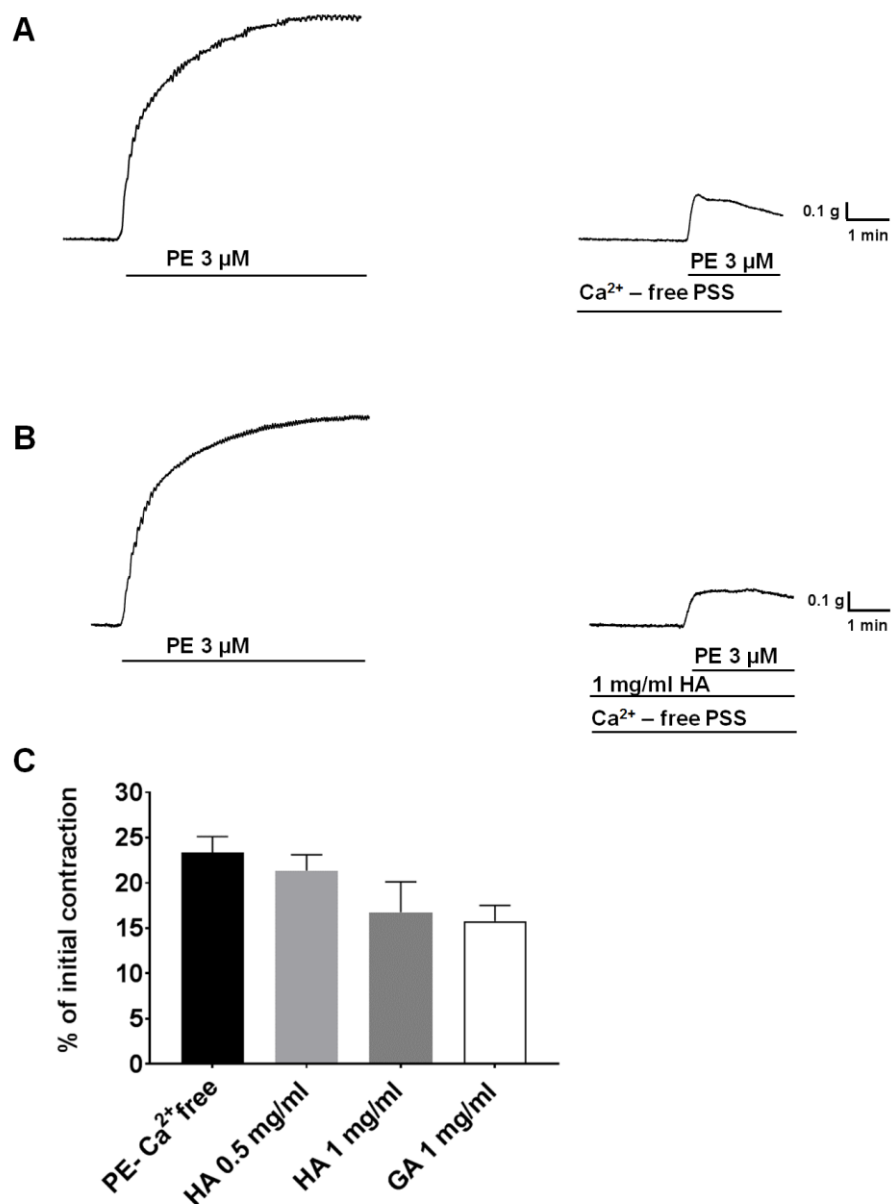
#### **4.3.2.4 Effect of hibiscus and garcinia acid on the phasic and tonic contractions induced by PE in the rat aorta**

In the absence of extracellular calcium, the phasic contraction of the aorta induced by PE is due to the release of calcium from intracellular stores (Nishimura *et al.*, 1991b). Under  $\text{Ca}^{2+}$ -free conditions, PE (3  $\mu\text{M}$ ) produced a transient contraction, which was  $23 \pm 1\%$  of the contraction produced in  $\text{Ca}^{2+}$  containing PSS (**Figure 4.23**). Neither hibiscus nor garcinia acid (1mg/ml) had any significant effect on the transient contraction to PE in  $\text{Ca}^{2+}$ -free PSS, being  $16 \pm 3\%$  and  $15 \pm 1\%$  in the presence of the respective acids (n=4/4) (**Figure 4.23**).

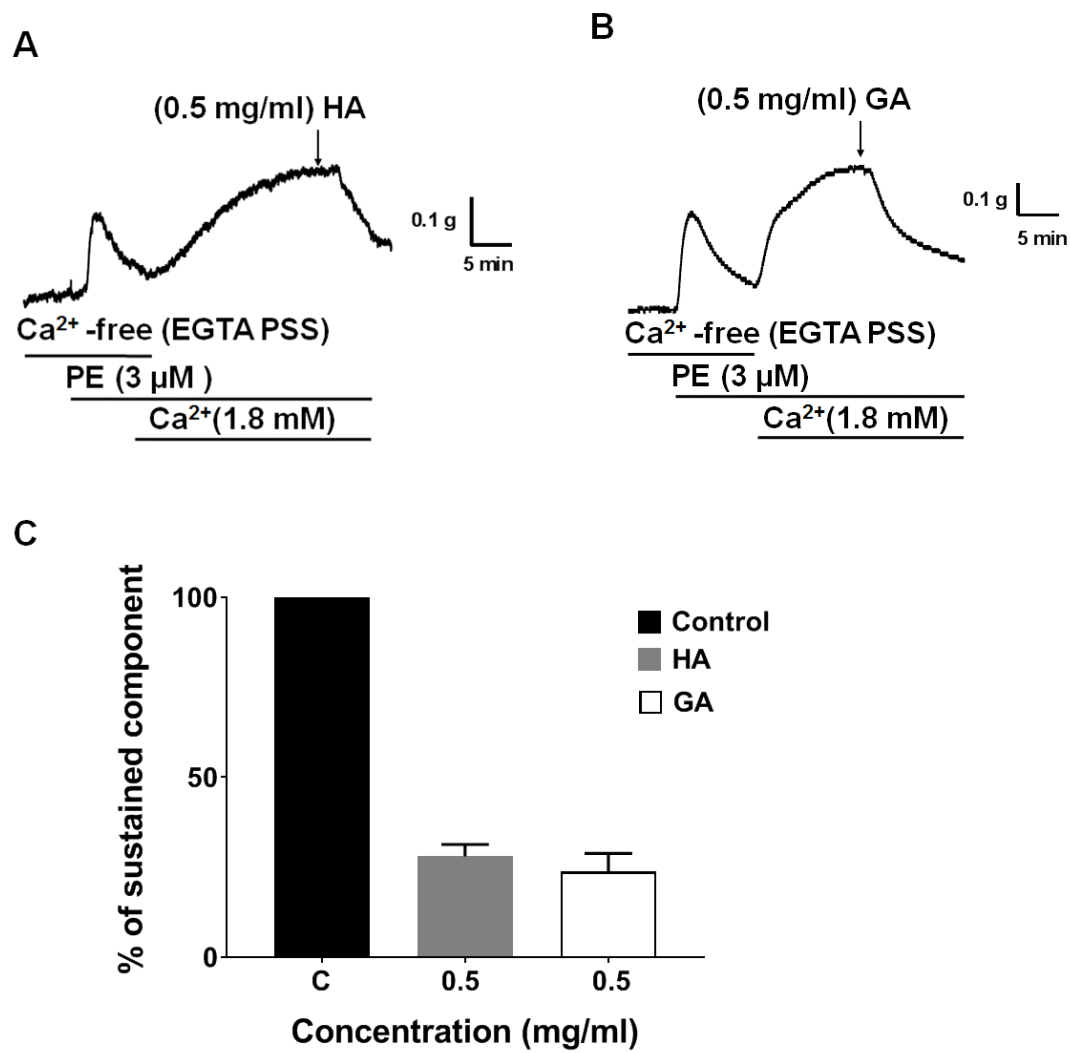
After an initial phasic contraction to PE (3  $\mu\text{M}$ ) was obtained in  $\text{Ca}^{2+}$ -free PSS, this developed into a sustained contraction following the subsequent re-addition of  $\text{Ca}^{2+}$  to the PSS. When hibiscus acid (**Figure 4.24**) or garcinia acid (**Figure 4.24**) was added during the sustained phase of the contraction, it caused a relaxation of  $71 \pm 3\%$  or  $76 \pm 5\%$ , respectively (n=4/4).

#### **4.3.2.5 Effect of potassium channel blockers on the relaxant effect of hibiscus and garcinia acid**

The involvement of  $\text{K}^+$  channels in the relaxant effect of hibiscus or garcinia acid was also examined, using the non-selective  $\text{K}^+$  channel blocker (TEA) and the selective  $\text{K}^+$  channel blocker (iberiotoxin, Ibtx). Pre-incubation of the aorta with either TEA (6 mM) or Ibtx (100 nM) increased the magnitude of the PE (3  $\mu\text{M}$ ) contraction by 35% (n=13/7) and 60% (n=15/5), respectively, when compared to that produced in absence of TEA or Ibtx.



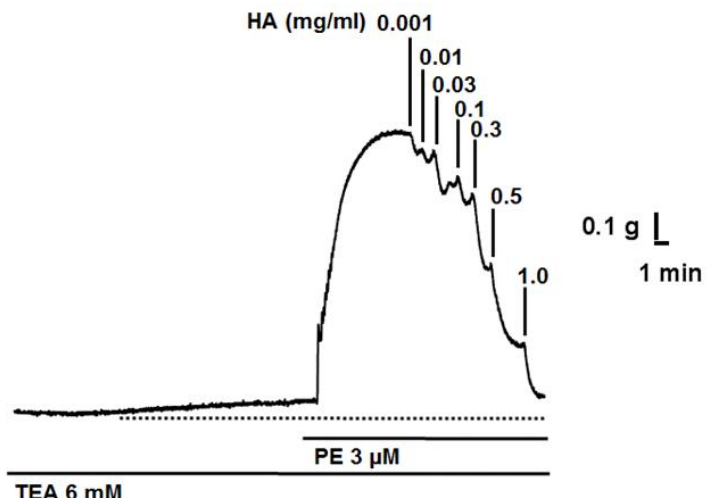
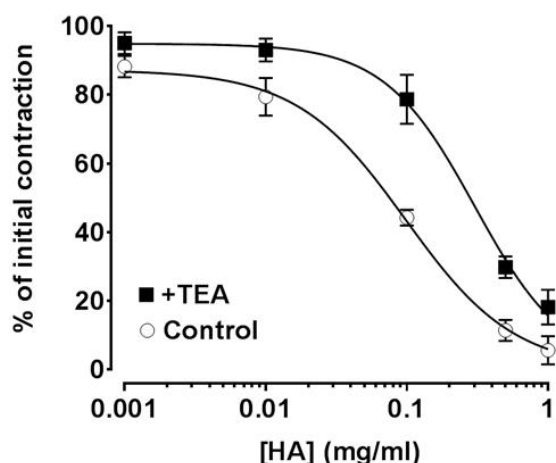
**Figure 4.23: Effect of hibiscus acid (HA) and garcinia acid (GA) on the phasic component of contraction induced by PE (3  $\mu$ M) in rat aorta.** (A) Representative recording of the PE-induced contraction in presence or absence of extracellular  $\text{Ca}^{2+}$ . (B) The same experimental protocol showing the effect of HA (1 mg/ml) on the PE-induced contraction in the absence of extracellular  $\text{Ca}^{2+}$ . (C) Summary figure showing the effects of HA (0.5 and 1 mg/ml) and GA (1 mg/ml) on the PE-induced transient contraction of aorta. Values represent mean  $\pm$  s.e.m. (n=4/4).



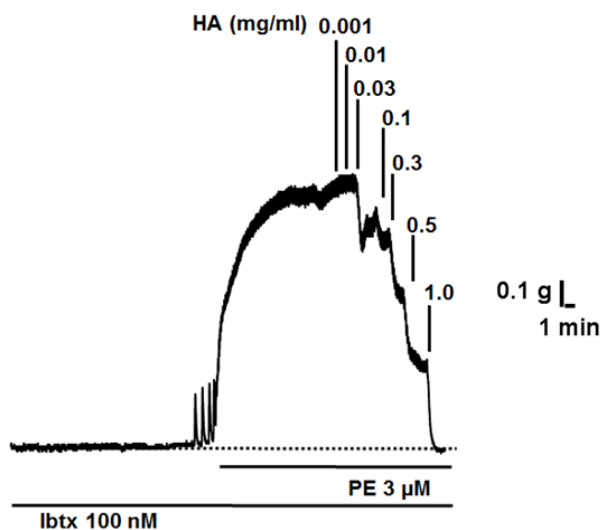
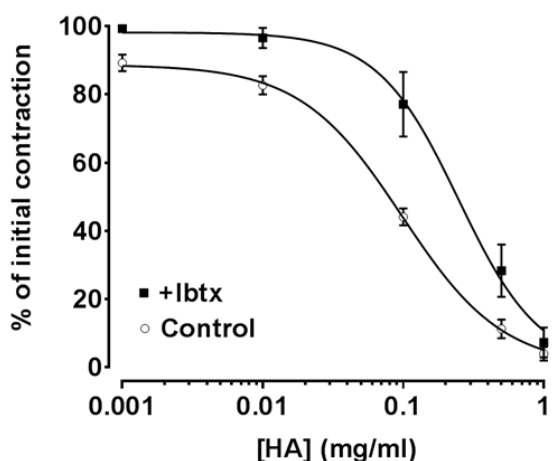
**Figure 4.24: Relaxant effect of hibiscus (HA) and garcinia acid (GA) on the sustained component of the PE-induced contraction.** Representative recordings showing the effect of (A) hibiscus acid and (B) garcinia acid on the tonic component of the PE-induced contraction, following the addition of 1.8 mM  $\text{Ca}^{2+}$ . The intracellular store was depleted by the application of PE in a  $\text{Ca}^{2+}$  free medium containing 1 mM EGTA and the re-addition of  $\text{Ca}^{2+}$  produced the tonic phase of contraction. (C) Summary figure illustrating the effects of HA and GA (0.5 mg/ml) on the tonic component of the PE-induced contraction. Values represent mean  $\pm$  s.e.m. ( $n=4/4$ ).

The IC<sub>50</sub> for the hibiscus acid induced relaxation of the PE pre-contracted aorta was significantly ( $P<0.05$ ) increased from  $0.09 \pm 0.01$  mg/ml for the control to  $0.3 \pm 0.04$  mg/ml in the presence of TEA, and the maximum relaxation was reduced (though not significantly) from  $95 \pm 4\%$  to  $82 \pm 5\%$  ( $n=6/6$ ;  $P>0.05$ ) (**Figure 4.25**). Similarly, the IC<sub>50</sub> was significantly increased when the aorta was treated with Ibx, being  $0.24 \pm 0.04$  mg/ml ( $P<0.05$ ), although the maximum relaxation was still almost complete ( $93 \pm 4\%$ ;  $n=8/6$ ) (**Figure 4.26**).

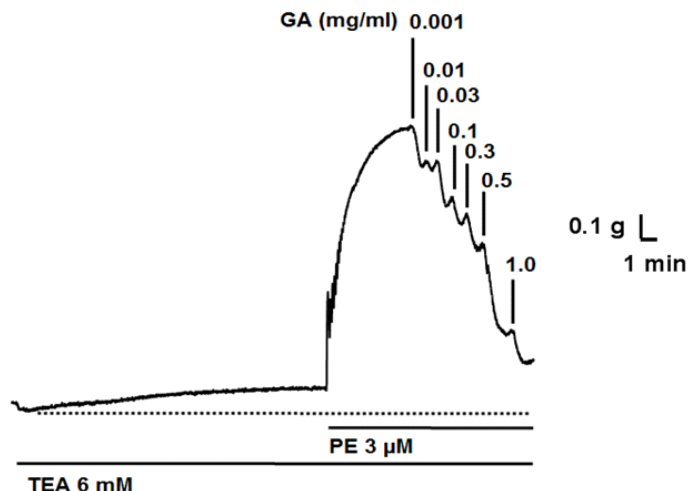
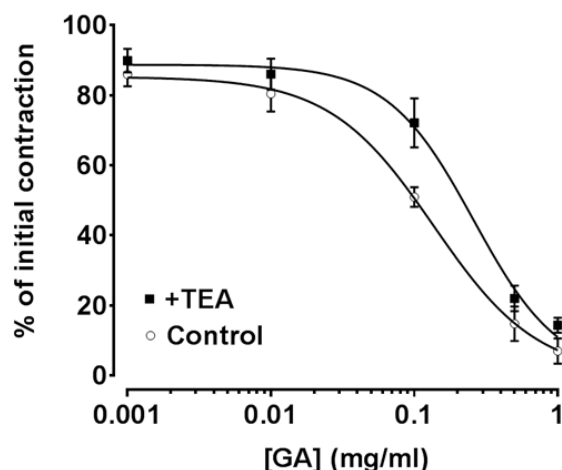
A similar effect was observed when garcinia acid was used as the vasorelaxant. Specifically, TEA significantly increased the IC<sub>50</sub> for garcinia acid from  $0.13 \pm 0.02$  mg/ml to  $0.25 \pm 0.03$  mg/ml and reduced the maximum relaxation from  $93 \pm 4\%$  to  $86 \pm 2\%$  ( $n=7/6$ ) ( $P<0.05$ ) (**Figure 4.27**). Similarly, the concentration-response curve for the relaxation induced by garcinia acid in PE pre-contracted aorta was shifted to the right in presence of Ibx (100 nM). The right shift of the curve is reflected by the significant increase in the IC<sub>50</sub> for garcinia acid to  $0.2 \pm 0.03$ . However, when compared to the control, Ibx (100 nM) had no effect on the magnitude of relaxation produced by garcinia acid, being  $89 \pm 4\%$ ;  $n=8/6$  (**Figure 4.28**).

**A****B**

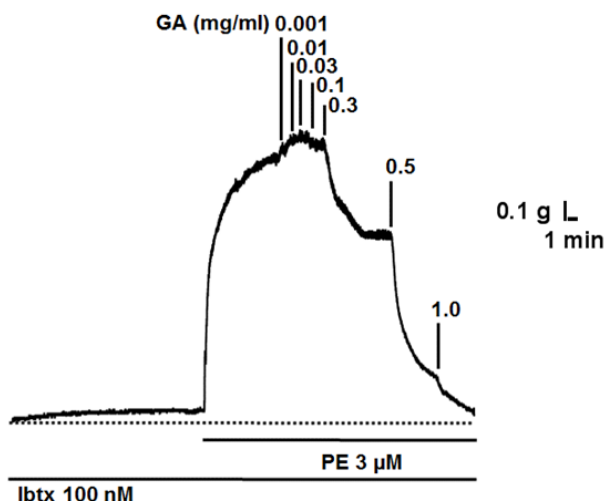
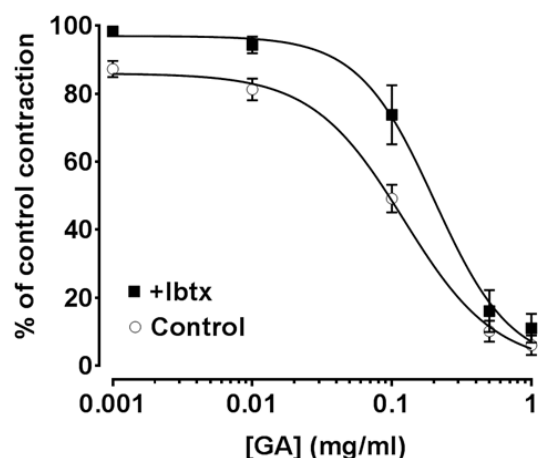
**Figure 4.25: The effect of potassium channel blockade on the relaxation induced by hibiscus acid (HA) on PE pre-contracted rat aorta.** (A) Representative recordings showing the relaxant effect of HA on the PE pre-contracted aorta in the presence of TEA (6 mM). (B) Summary figure illustrating the relaxant effect of HA in presence (square) or absence (circle) of TEA. The relaxant effect is expressed as a percentage of the initial contraction. Values represent mean  $\pm$  s.e.m. ( $n=6/6$ ).

**A****B**

**Figure 4.26: The effect of selective calcium activated potassium channel blockade on relaxation induced by hibiscus acid (HA) on PE pre-contracted rat aorta. (A) Representative recordings showing the relaxant effect of HA on the PE pre-contracted aorta in presence of 100 nM iberiotoxin (Ibtx). (B) Summary figure illustrating the relaxant effect of HA in presence (square) or absence (circle) of Ibtx. The relaxant effect is expressed as a percentage of the initial contraction. Values represent mean  $\pm$  s.e.m. ( $n=8/6$ ).**

**A****B**

**Figure 4.27: The effect of potassium channel blockade on relaxation induced by garcinia acid (GA) on PE pre-contracted rat aorta.** (A) Representative recordings showing the relaxant effect of GA on the PE pre-contracted endothelium-intact aorta in presence of TEA (6 mM). (B) Summary figure showing the relaxant effect of GA in concentrations (0.001-1 mg/ml) on the PE pre-contracted aorta in presence (square) or absence (circle) of TEA. The relaxant effect is expressed as a percentage of the initial contraction. Values represent mean  $\pm$  s.e.m. ( $n=7/6$ ).

**A****B**

**Figure 4.28:** The effect of selective calcium activated potassium channel blockade on relaxation induced by garcinia acid (GA) on PE pre-contracted rat aorta. **(A)** Representative recordings showing the relaxant effect of GA on the PE pre-contracted aorta in presence of 100 nM Ibtx. **(B)** Summary figure showing the relaxant effect of GA in concentrations (0.001-1 mg/ml) on the PE pre-contracted aorta in presence (square) or absence (circle) of Ibtx. The relaxant effect is expressed as a percentage of the initial contraction. Values represent mean  $\pm$  s.e.m. (n=8/6).

#### **4.3.2.6 Negative inotropic effects of hibiscus and garcinia acid on the left atrium**

As shown in **Figure 4.29** and **Figure 4.31A**, in the left rat atrium, the electrically induced contraction was reduced and ultimately abolished by hibiscus acid in a concentration-dependent manner. The lowest concentration of hibiscus acid (0.1 mg/ml) tested, produced a reduction of  $14 \pm 4\%$  ( $n=4/4$ ) in the force of atrial contraction when stimulated at 0.1 Hz. Increasing the concentration of hibiscus acid to 0.3 mg/ml caused greater inhibition (by  $38 \pm 5\%$ ), and the submaximal concentration of hibiscus acid (0.5 mg/ml), showed almost complete inhibition of the contraction; producing a reduction of  $83 \pm 9\%$ . Complete inhibition of the contraction (100% reduction) was achieved at the concentration (0.6 mg/ml). Similarly, garcinia acid also showed a negative inotropic effect in a concentration-dependent manner, and there was complete inhibition of the contraction (100% reduction;  $n=4/4$ ) upon application of 0.6 mg/ml (**Figure 4.30** and **Figure 4.31B**). The inhibitory activity of both compounds was maintained as long as they were applied to the tissue. This inhibitory effect was reversed when the tissue was washed, and complete recovery of the tissue was observed with regular washing out for 5 min with fresh PSS (**Figure 4.29E** and **Figure 4.30E**).

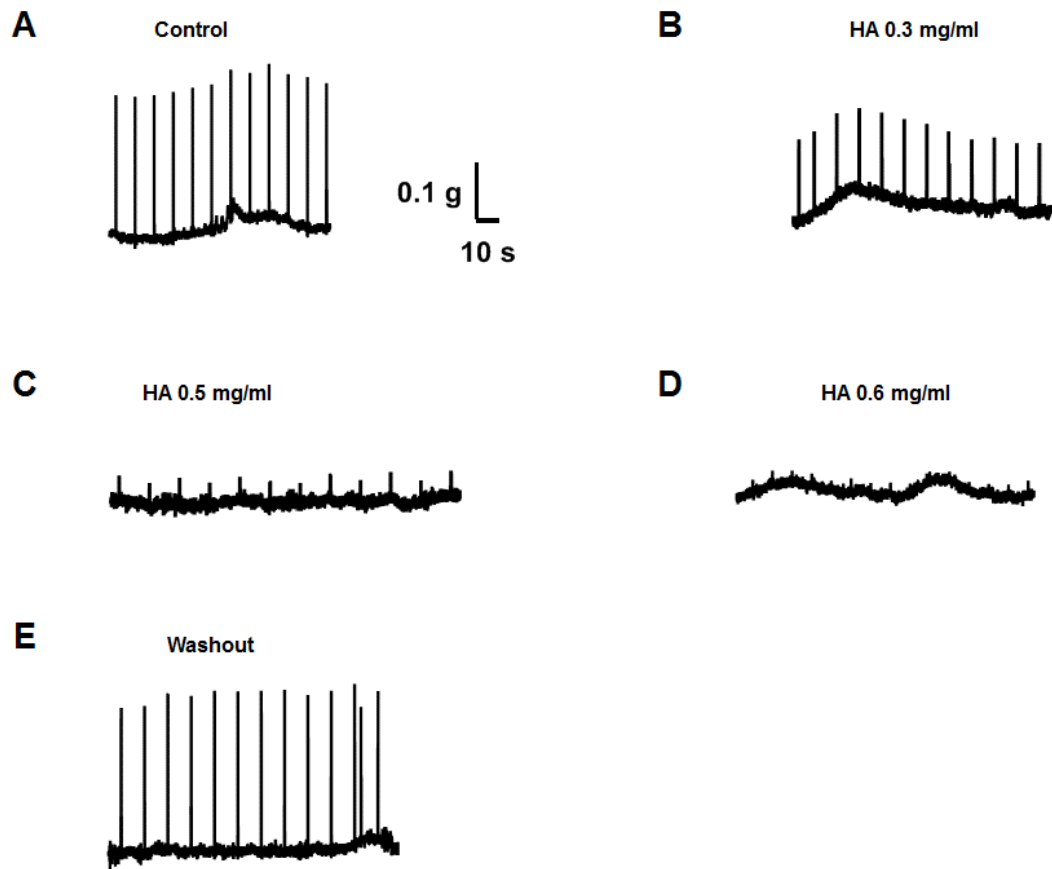


**Figure 4.29: Effect of hibiscus acid (HA) on the electrically stimulated rat left atrium.** Representative recording showing (A) control. (B) The negative inotropic effect of HA (0.3 mg/ml), and (C) (0.5 mg/ml) on the left atrium. (D) The complete inhibitory effect of HA (0.6 mg/ml). (E) The complete reversal of the inhibitory effect upon washout.

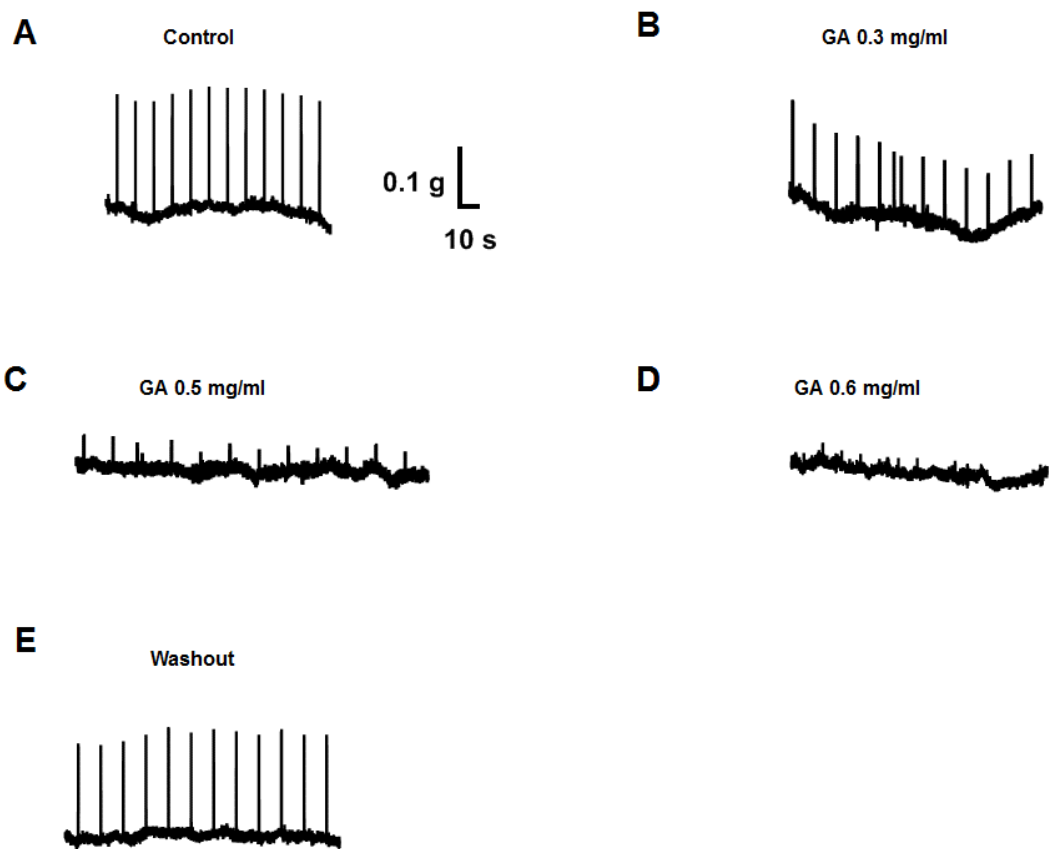
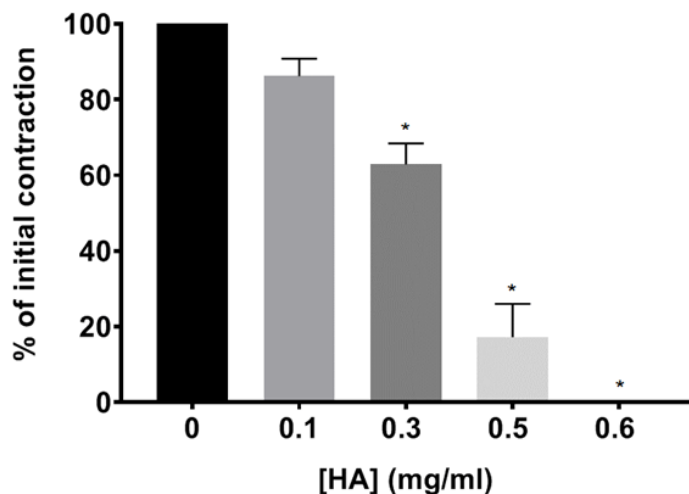


**Figure 4.30: Effect of garcinia acid (GA) on the electrically stimulated rat left atrium.** Representative recording showing (A) control. (B) The negative inotropic effect of GA (0.3 mg/ml), and (C) (0.5 mg/ml) on the left atrium. (D) The complete inhibitory effect of GA (0.6 mg/ml). (E) The complete abolishing of the inhibitory effect upon washout.

**A**



**B**

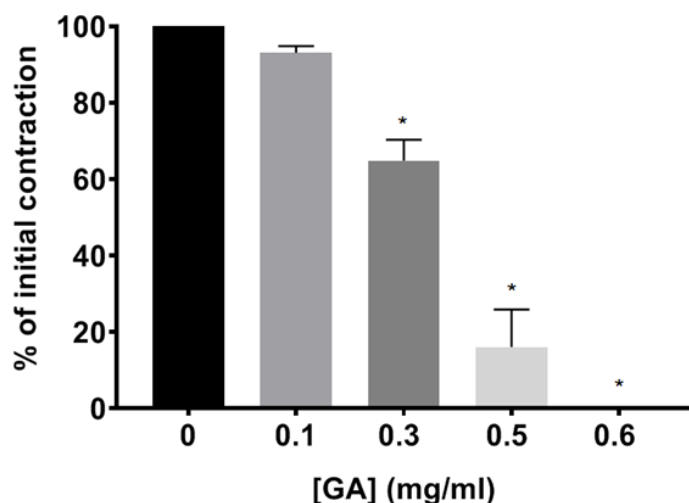


**Figure 4.31: Summary figure showing % inhibitory effect of (A) hibiscus acid (HA) and (B) garcinia acid (GA) on the electrically stimulated rat left atrium.** Statistical analysis was carried out using one-way ANOVA with Tukey's multiple comparisons test to compare with control. Values represent mean  $\pm$  s.e.m. ( $n= 4/4$  animals). \* represents  $P<0.05$ .

#### **4.3.2.7 Determining sensitivity of trachea to stimulating agonist and KCl**

Carbachol produced a concentration-dependent contraction of the rat trachea, which yielded an EC<sub>50</sub> of  $0.04 \pm 0.005 \mu\text{M}$ ; n=15/4 and a maximum contractile response of  $1.1 \pm 0.16 \text{ g}$  was achieved at  $3 \mu\text{M}$  of carbachol (**Figure 4.32**). A concentration-dependent contraction of the trachea was also produced upon cumulative addition of KCl (5-70 mM), yielding an EC<sub>50</sub> of  $23.19 \pm 0.38 \text{ mM}$ ; n=12/4. In this case, a maximum contraction of  $0.56 \pm 0.09 \text{ g}$  was achieved with 70 mM KCl (**Figure 4.33**).

#### **4.3.2.8 Effect of hibiscus and garcinia acid on the carbachol pre-contracted rat trachea**

Hibiscus acid caused a concentration-dependent relaxation of the rat trachea pre-contracted with carbachol ( $1 \mu\text{M}$ ). The IC<sub>50</sub> for hibiscus acid was  $0.18 \pm 0.02 \text{ mg/ml}$  (**Figure 4.34A** and **Figure 4.35A**) and the highest concentration tested ( $0.5 \text{ mg/ml}$ ) caused relaxation that fell below the resting tension the tissue were set at, being  $107 \pm 6\%$  (n=7/6). Garcinia acid was also found to have a similar effect to that of hibiscus acid. When the tissue was pre-contracted with carbachol, garcinia acid produced complete relaxation, being  $110 \pm 2\%$  at a concentration of  $0.5 \text{ mg/ml}$  (n=8/6) with an IC<sub>50</sub> of  $0.16 \pm 0.01 \text{ mg/ml}$  (**Figure 4.34B** and **Figure 4.34B**). The relaxation was maintained for as long as hibiscus or garcinia acid were present, and the tissue showed complete recovery after washing them out and allowing approximately 60 min for recovery. The time control for these experiments showed a slight relaxation ( $19 \pm 2\%$ ) in the carbachol-induced contraction, over the time course of the experiment (**Figure 4.34C**).

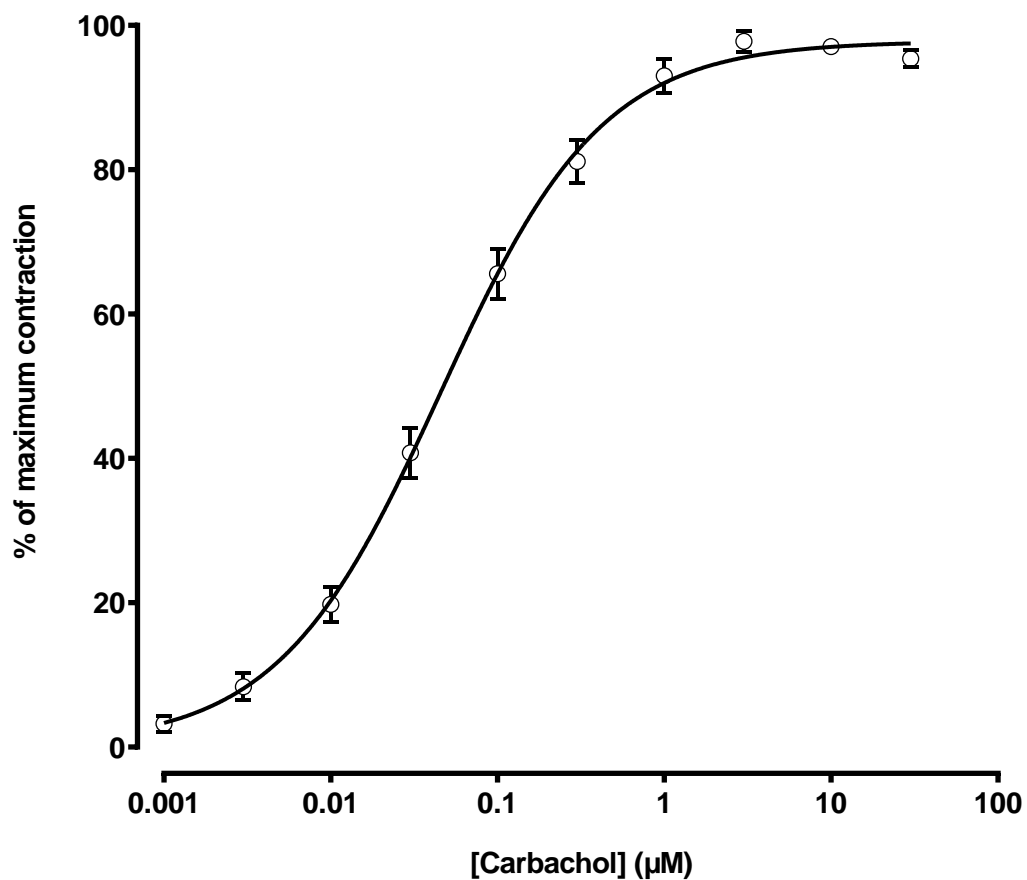


**Figure 4.32: Concentration-response curve to carbachol on the rat trachea.** Carbachol was added cumulatively in concentrations 1 nM to 30 μM. The responses are expressed as a percentage of the maximum contraction produced by carbachol and the data is fitted by four-parameter concentration-response curve. Each data point is shown as mean ± s.e.m., n=15/4.

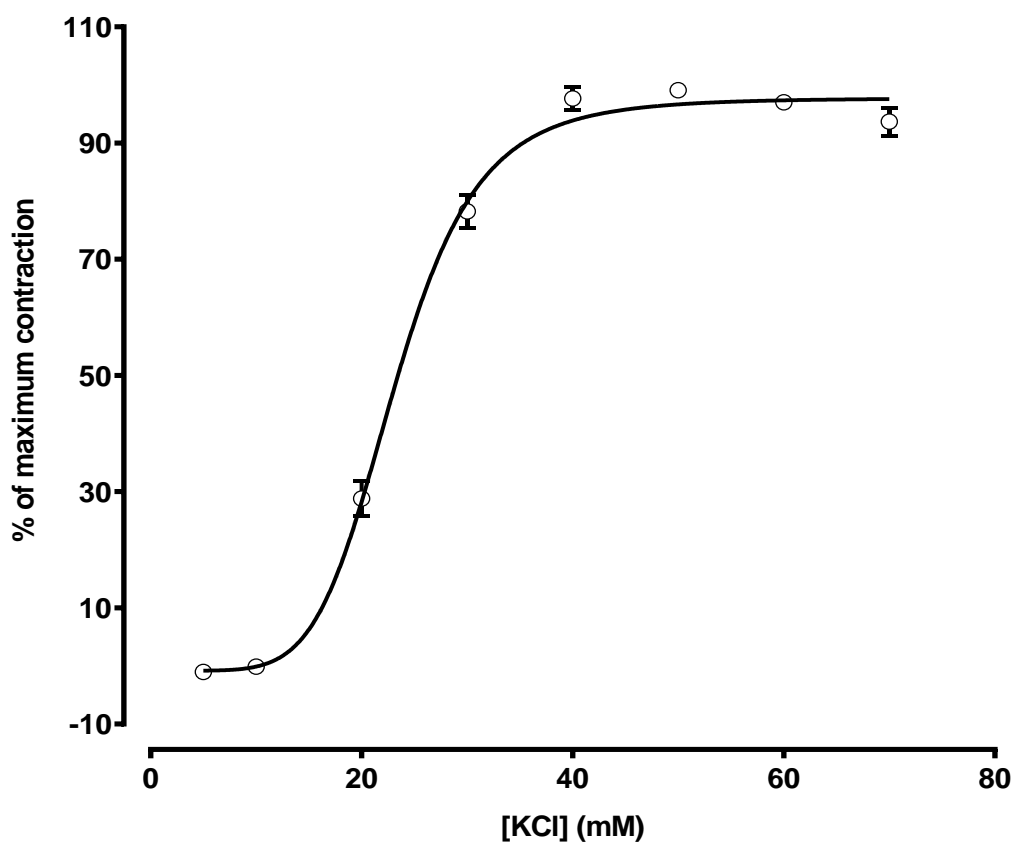


**Figure 4.33: Concentration-response curve to KCl on the rat trachea.** KCl was added cumulatively in concentrations 5 mM to 70 mM. The responses are expressed as a percentage of maximum contraction produced by KCl and the data fitted by a four-parameter dose-response curve. Each data point is shown as mean  $\pm$  s.e.m., n=12/4.

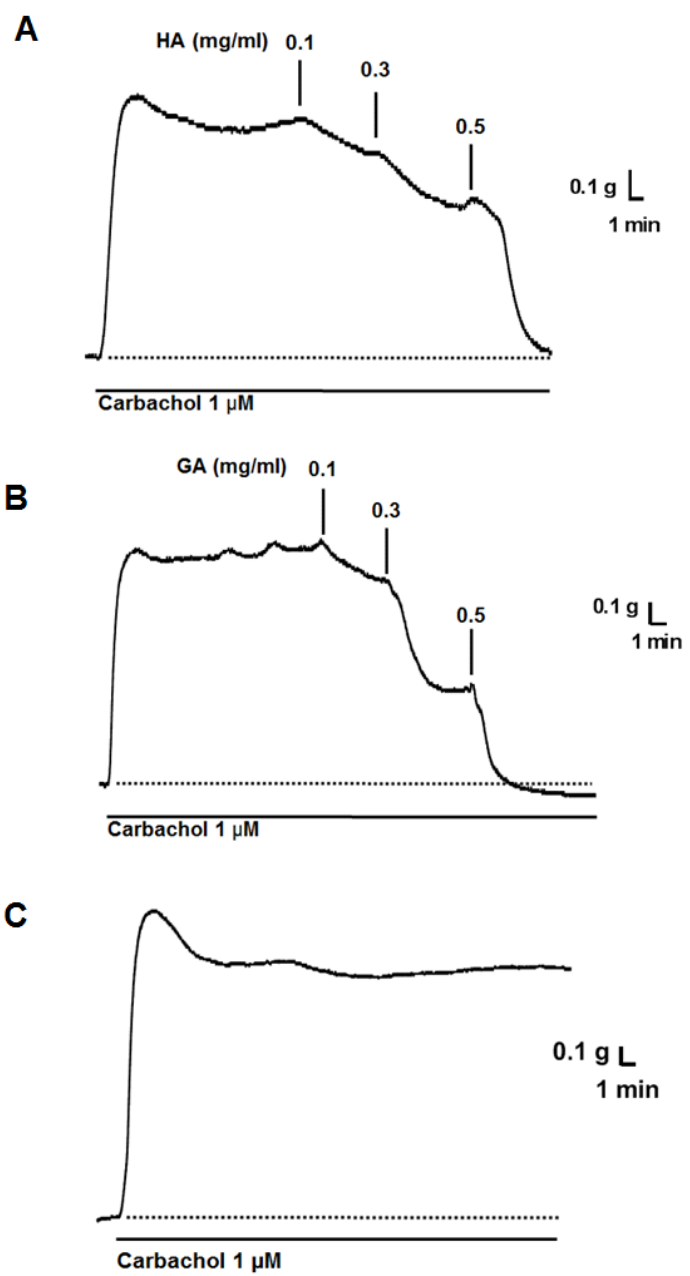
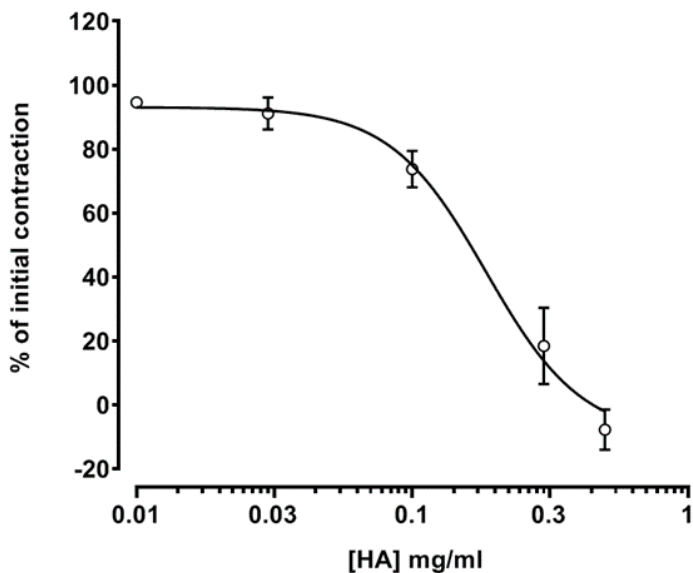


**Figure 4.34: Relaxant effect of hibiscus acid (HA) and garcinia acid (GA) on rat trachea pre-contracted with carbachol.** Representative recordings of the effect (A) of HA and (B) of GA on the trachea pre-contracted with carbachol (1  $\mu$ M). (C) Representative recordings of the time control, showing the stability of the contractile response during the course of the experiment.

A



B

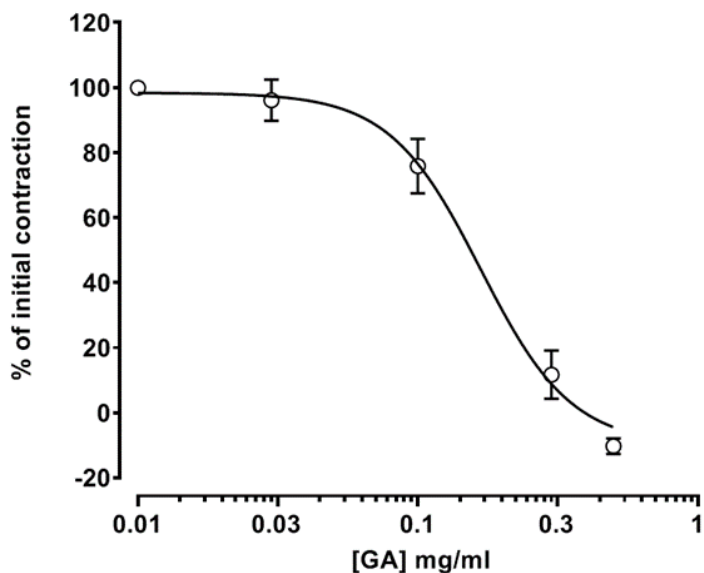


**Figure 4.35: Relaxant effect of hibiscus acid (HA) and garcinia acid (GA) on rat trachea pre-contracted with carbachol.** Relaxant effect (A) of HA and (B) of GA against carbachol ( $1 \mu\text{M}$ )-induced contractions in tracheal rings. The relaxant effect is expressed as a percentage of the initial contraction. Values represent mean  $\pm$  s.e.m. ( $n=7/6$  for HA and  $8/6$  for GA).

#### **4.3.2.9 Effect of hibiscus and garcinia acid on the KCl pre-contracted rat trachea**

The effect of hibiscus and garcinia acid were also investigated on the rat trachea following pre-contraction with KCl (60 mM). Under these condition, hibiscus acid produced relaxation in a concentration-dependent manner, and almost complete relaxation ( $97 \pm 4\%$ ;  $n=12/6$ ) was produced at concentration of 0.5 mg/ml (**Figure 4.36A** and **Figure 4.37A**). Application of higher concentrations of hibiscus acid (1 mg/ml) caused a relaxation below the resting tension at which the tissues were initially set, thus the overall relaxation was  $113 \pm 3\%$ , with an  $IC_{50}$  of  $0.32 \pm 0.01$  mg/ml. Garcinia acid also caused a concentration-dependent relaxation when applied on the KCl pre-contracted trachea. Like hibiscus acid, the  $IC_{50}$  for garcinia acid was  $0.33 \pm 0.01$  mg/ml, and a similar magnitude of relaxation ( $105 \pm 5\%$ ;  $n=11/6$ ) was obtained at the highest concentration of garcinia acid examined (1 mg/ml) (**Figure 4.36B** and **Figure 4.37B**). As showed in **Figure 4.36C**, the time control in the presence of KCl showed a marked increase of  $10 \pm 0.7\%$ .

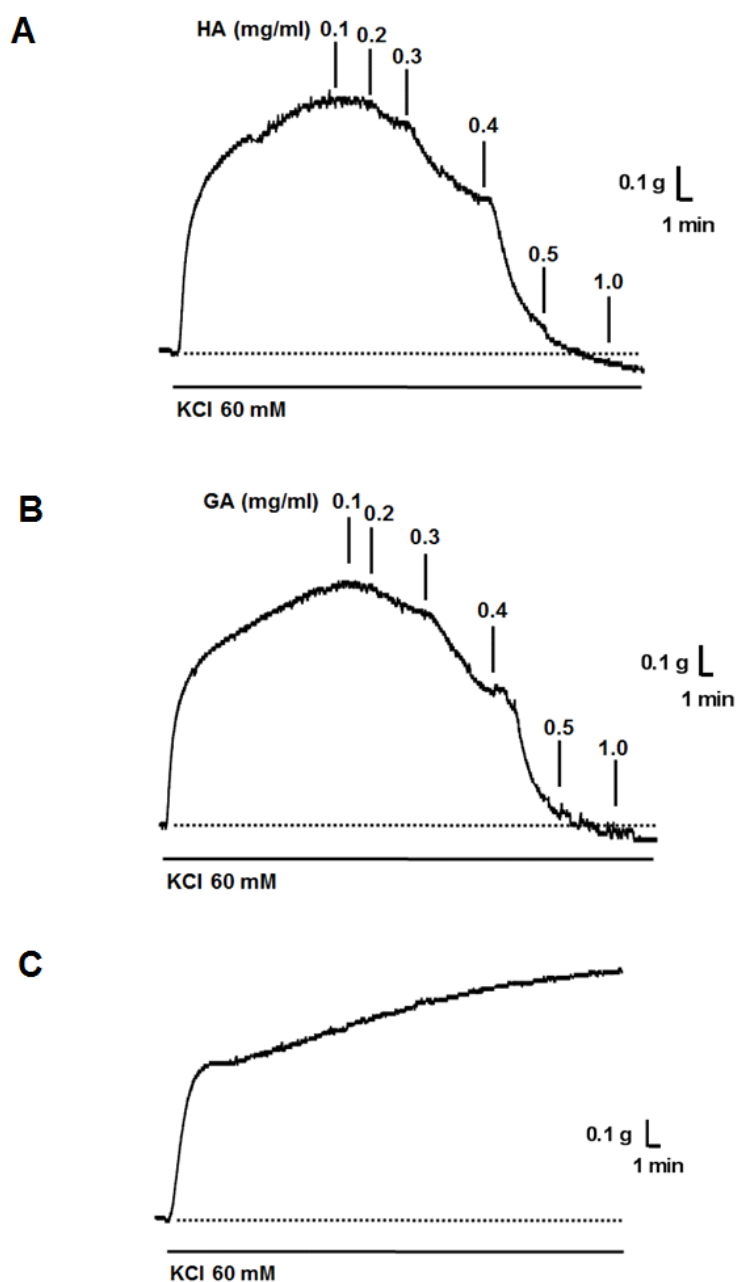


**Figure 4.36: Relaxant effect of hibiscus acid and garcinia acid on rat trachea pre-contracted with KCl.** Representative recording of the effect (A) of HA and (B) of GA on the trachea pre-contracted with KCl (60 mM). (C) Representative recordings of the time control, showing there was no contractile decline by the end of the experiment

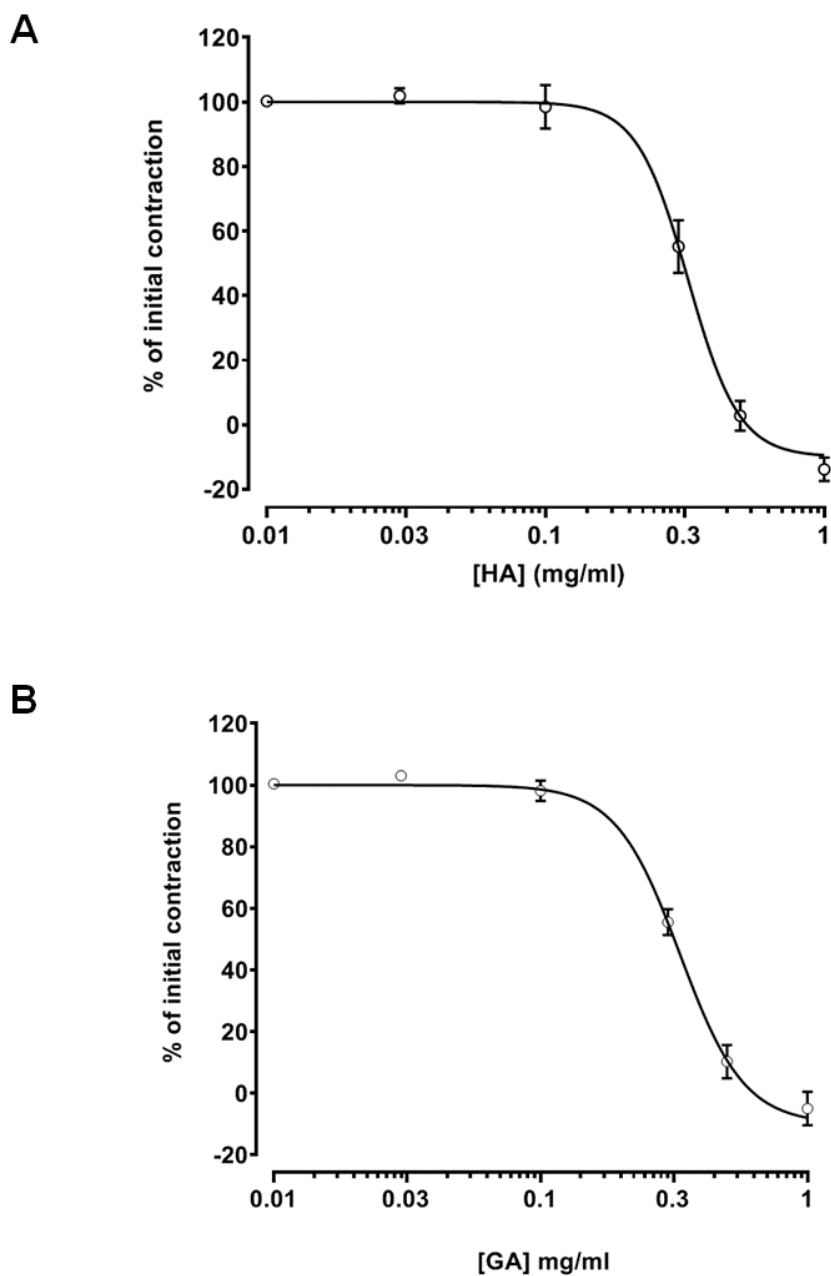


**Figure 4.37: Relaxant effect of hibiscus acid (HA) and garcinia acid (GA) on rat trachea pre-contracted with KCl.** Relaxant effect (A) of HA and (B) of GA against KCl (60 mM)-induced contractions of tracheal rings. The relaxant effect is expressed as a percentage of the initial contraction. Values represent mean  $\pm$  s.e.m. (n=12/6 for HA and 11/6 for GA).

#### **4.4 Discussion**

A variety of bioactive constituents have previously been identified in the calyces of *H. sabdariffa*, including phenolic acids, anthocyanins, and flavonoids (Da-Costa-Rocha *et al.*, 2014). However, very few studies have focussed on the pharmacological activities of the constituents identified.

In this chapter, hibiscus acid and its derivatives in their purified crystal forms have been isolated with significant yield with the aid of the conventional chromatographic methods, in particular GPC and VLC (Zheoat *et al.*, 2017). However, most of the previous studies have only focused on quantification of the compounds identified in *H. sabdariffa* extracts, with the aid of powerful chromatographic techniques such as reversed-phase high performance liquid chromatography (HPLC) and LC-Q-TOF-MS (Sindi *et al.*, 2014, Wang *et al.*, 2014).

All the samples for NMR testing were obtained through VLC and GPC of the crude methanolic extract of *H. sabdariffa*. NMR is a quantitative technique which enables the determination of functional groups, helps in confirming structures of compounds, and is used for structure elucidation. The absolute configuration of hibiscus acid and hibiscus acid dimethyl ester, were identified with the aid of X-ray crystallography.

Isolation and purification of the constituents of the methanolic extract of *H. sabdariffa* was carried out to enable biological tests to be carried out on the pure compounds. The structure and purity of hibiscus acid and hibiscus acid dimethyl ester were confirmed by spectroscopic analysis. In addition, the absolute configuration of

both compounds was elucidated by carrying out x-ray crystallography on the crystal forms. The absolute configuration found (2S,3R) agrees with that originally proposed by Boll *et al.* (1969) for hibiscus acid.

The  $^1\text{H}$  NMR spectrum of the crude ethyl acetate extract of *H. sabdariffa* showed the presence of hibiscus acid but not hibiscus acid derivatives. This can be observed by disappearance of the peaks of methoxy groups in the region between  $\delta_{\text{H}}$  3.5 to 3.83 have not appeared in the spectrum. Therefore, it could be that both hibiscus acid-6-methyl ester and hibiscus acid dimethyl ester are artefact compounds produced during the process of extraction with methanol. This result is in agreement with another published study (Hansawasdi *et al.*, 2000), who demonstrated that hibiscus acid-6-methyl ester is not actually synthesised by the plant, but is formed from hibiscus acid during the extraction process due to the methylation of one of the carboxylic groups, when methanol is used as a solvent.

The flavonoid (quercetin) was also isolated and purified from the methanolic extract with the help of a Sephadex column. The vasorelaxant activity of quercetin has been demonstrated previously in a number of *in vitro* studies (Duarte *et al.*, 1993, Ke Chen and Pace-Asciak, 1996, Roghani *et al.*, 2004, Hou *et al.*, 2014, Yuan *et al.*, 2018). It has been shown that quercetin at concentrations between 0.1  $\mu\text{M}$  and 1 mM caused a concentration-dependent relaxation of rat aorta pre-contracted with either adrenoceptor agonists (noradrenaline, and PE), or KCl (Duarte *et al.*, 1993, Ke Chen and Pace-Asciak, 1996, Roghani *et al.*, 2004). These studies also showed that the mechanism underlying the vasorelaxant activity of quercetin involved both

endothelium-dependent and endothelium-independent pathways. Furthermore, recent reports show that this compound exerts its vasorelaxant activity through blocking VDCCs, and also by releasing EDRFs (Hou *et al.*, 2014, Yuan *et al.*, 2018). As the vasorelaxant effect of quercetin has been extensively studied on the rat aorta, further investigation of this substance was not considered in the present study.

The results showed that the methanolic extract of *H. sabdariffa* relaxed, concentration-dependently, the aorta pre-contracted with PE and KCl, but with a significantly greater relaxant effect against the PE pre-contracted tissues. These findings are consistent with the observations, which have been reported by Ajay *et al.* (2007).

The results have also shown that hibiscus acid has a vasorelaxant effect on the rat aorta, which was more potent and effective in comparison to the activity of the crude extract of *H. sabdariffa*. This result is somewhat expected, knowing that hibiscus acid is one of the constituents present in the calyces of *H. sabdariffa* and its activity might be decreased by the presence of other (non-purified) phytochemical(s). The finding that commercially available garcinia acid, which is the main organic acid found in *G. cambogia*, had a very similar effect, provides further support for the notion that hibiscus acid has vasorelaxant activity. Both hibiscus and garcinia acid produced a concentration-dependent relaxation of the aorta when it was pre-contracted with either PE or KCl. Their effects were fully reversed upon their washout indicating that, over the concentration range used, they had no deleterious effect on the tissue.

Hibiscus and garcinia acids are diastereomeric  $\gamma$ -lactones derived from (2S, 3R) and (2S, 3S)-2-hydroxycitric acid, respectively (Boll *et al.*, 1969, Ibnusaud *et al.*, 2002). Only certain species of plants are known to be capable of synthesising hydroxycitric acid (Hida *et al.*, 2005); thus, hibiscus and garcinia acids are substances which are not found extensively in all plants. Hydroxycitric acid with the absolute configuration (2S, 3S), is a major acid component in the fruit rinds of garcinia species, including *G. cambogia*, *G. indica*, *G. Cowa*, and *G. atroviridis* (Lewis and Neelakantan, 1965, Lowenstein and Brunengraber, 1981, Jena *et al.*, 2002b, Jena *et al.*, 2002a). Whereas, hydroxycitric acid with the configuration (2S, 3R) is the hibiscus-type enantiomer, which is found predominantly in the calyces of *H. sabdariffa*, *H. cannabinus* and *H. rosa-sinensis* (Lewis and Neelakantan, 1965, Hida *et al.*, 2006, Yamada *et al.*, 2007). At present, details of the biosynthetic pathway for hydroxycitric acid and how it is regulated remain unclear (Yamada *et al.*, 2007). One hypothesis is that hydroxycitric acid is generated via a condensation reaction of oxaloacetate with glycolyl-CoA (Yamada *et al.*, 2007).

In agreement with the above findings of the crude extract, both hibiscus and garcinia acid were found to be significantly more potent in their relaxant effect when the tissue was pre-contracted with PE, in comparison to pre-contraction with KCl. Removal of the endothelium did not prevent the relaxation of the aorta to either hibiscus or garcinia acid in the PE pre-contracted aorta, with a similar degree of relaxation being achieved in endothelium-intact and endothelium-denuded tissues. Whilst this indicates that the relaxation to both these substances is endothelium- independent

there was nevertheless a slight rightward shift in the concentration-response curve to both hibiscus and garcinia acid after either removal of the endothelium or treatment with L-NAME. This may indicate a modulatory role of the endothelium in the response to either hibiscus or garcinia acid. However, it may also have been a consequence of the increased contraction produced by PE when the endothelium was removed, a finding that has previously been reported by others (Godfraind *et al.*, 1985). When the aorta was pre-contracted with KCl, there was no effect of removing the endothelium on the relaxation produced by either hibiscus or garcinia acid, and in this case the contractile response to KCl was not significantly affected by removal of the endothelium either. It should be noted that previous studies with the crude extracts of *H. sabdariffa* have found that the relaxation is significantly affected by removal of the endothelium or in presence of L-NAME (Obiefuna *et al.*, 1994, Ajay *et al.*, 2007, Sarr *et al.*, 2009), thus, it is clear that there may be additional constituents in the crude extract that are affecting vascular activity.

As both hibiscus and garcinia acid produced relaxation of the aorta pre-contracted with KCl, one possible explanation for their observed effect is that they are blocking  $\text{Ca}^{2+}$  channels. This is because the contraction induced by KCl predominantly involves depolarisation of the smooth muscle cell membrane and the resultant activation of VDCCs. Indeed, the relaxation of this type of contraction is frequently utilised when studying the effect of VDCC blockers (van Breemen *et al.*, 1981, Godfraind, 1983, Karaki and Weiss, 1984, Godfraind, 1986, Morel and Godfraind, 1991, Roy *et al.*, 1995, Okumura *et al.*, 1997). Further support for this mechanism of action is provided by the studies showing that hibiscus and garcinia acid relaxed the

aorta when it was pre-contracted with the selective L-type  $\text{Ca}^{2+}$  channel activator FPL 64176 or Bay K8644 (Yamamoto *et al.*, 1984, Rampe and Dage, 1992). The contraction induced by FPL 64176 was completely relaxed by lower concentrations of hibiscus or garcinia acid than was required when Bay K8644 was used to pre-contract the tissue. A possible explanation for the difference in sensitivity may be related to the agonistic properties of FPL 64176 and Bay K8644, as both L-type  $\text{Ca}^{2+}$  channel activators act via a mechanism and site of action that is unique for each (Zheng *et al.*, 1991, Rampe and Dage, 1992). The findings are nevertheless consistent with what has been observed previously with classical L-type  $\text{Ca}^{2+}$  channel blockers such as nifedipine, diltiazem, and verapamil (Auguet *et al.*, 1988, Zheng *et al.*, 1991). These selective L-type  $\text{Ca}^{2+}$  channel activators produced an oscillatory contractile response in the aorta, which is similar to what has been previously reported by Auguet *et al.* (1988). It also appeared that hibiscus and garcinia acid were more effective at relaxing the contractions induced by the  $\text{Ca}^{2+}$  channel activators compared to those induced by KCl. One possible reason could be that in these studies, KCl was applied in a hyperosmotic manner and it has been shown that a component of this contraction is independent of extracellular  $\text{Ca}^{2+}$  (Karaki *et al.*, 1983) and is somewhat insensitive to  $\text{Ca}^{2+}$  channel blockers. This may also explain why neither hibiscus nor garcinia acid caused complete relaxation of the aorta when it was pre-contracted with KCl. With regard to removal of the endothelium affecting the sensitivity of the aorta to hibiscus or garcinia acid, such an effect has also previously been observed with classical  $\text{Ca}^{2+}$  channel blockers (Kojda *et al.*, 1991) and this has been attributed to their ability to stimulate the endothelial cells to release nitric oxide (Günther *et al.*, 1992, Brovkovych *et al.*, 2001).

The contraction induced by PE involves both  $\text{Ca}^{2+}$  release from the SR and  $\text{Ca}^{2+}$  influx from the extracellular medium via ROCCs, and VDCCs (Bolton, 1979, Lee *et al.*, 2001). Given that neither hibiscus nor garcinia acid affected the phasic contraction produced by PE in the absence of extracellular  $\text{Ca}^{2+}$ , it seems unlikely that they are affecting  $\text{Ca}^{2+}$  release from the SR. The fact that this initial transient contraction was unaffected by either hibiscus or garcinia acid also indicates that these agents are unlikely to be affecting the biochemical sequence of events that links the increase in  $\text{Ca}^{2+}$  concentration to contraction (Miller-Hance *et al.*, 1988). Nevertheless, this is in contrast to what has been reported previously for the crude extract of *H. sabdariffa*, where there was ~30% reduction in the magnitude of the phasic contraction to noradrenaline (Owolabi *et al.*, 1995). Following the phasic response to PE, the re-addition of  $\text{Ca}^{2+}$  produced a sustained contraction that is due to the influx of extracellular  $\text{Ca}^{2+}$ . Both hibiscus and garcinia acids were found to produce relaxation of this tonic component, thereby further supporting their inhibitory effect upon  $\text{Ca}^{2+}$  influx.

While the above findings suggest that hibiscus and garcinia acid are producing vasorelaxation through inhibition of VDCCs, it is also possible that activation of  $\text{K}^+$  channels may be involved (Nelson and Quayle, 1995). However, the finding that both the non-selective  $\text{K}^+$  channel blocker TEA and the selective  $\text{K}^+$  channel blocker Ibtx, did not prevent the relaxation to either hibiscus or garcinia acid would argue against them having a major role. There was a slight, but significant rightward shift in the concentration-response curve to both hibiscus and garcinia acid in the presence of

either TEA or Ibtx, which reflects a decrease in the sensitivity of the aorta to the relaxant effects of both acids. This could be attributed to the noted additional contraction produced by TEA and Ibtx themselves. The decrease in potassium conductance caused by TEA, will result in depolarisation of the smooth muscle cell membrane, thereby producing a contraction (Nishio *et al.*, 1986). Typically when K<sup>+</sup> channels are responsible for a relaxant effect, TEA has been found to reduce the magnitude of the relaxation by >60% (Meisheri *et al.*, 1990, Meisheri *et al.*, 1991).

Data obtained on rat cardiac tissues shows that both hibiscus and garcinia acid produced a concentration-dependent negative inotropic effect on the isolated left atria when it was electrically stimulated. The contraction was completely abolished at the highest concentration examined. Moreover, a comparison between hibiscus acid and garcinia acid indicated that both acids have equal potency and efficacy in terms of their negative inotropic effect. As with the experiments on the aorta, their effects were fully reversible upon wash out and caused no deleterious effect on the atrial tissue over the range of concentrations used.

This appears to be the first study to show that hibiscus acid produces a negative inotropic effect and it is possible that this compound could be, at least in part, responsible for the negative inotropic effect of *H. sabdariffa*, which has been reported previously by Micucci *et al.* (2015). The ability of both hibiscus and garcinia acid to completely inhibit the electrically stimulated atrial tissues is similar to the effect of nifedipine (Refsum and Landmark, 1975), which was able to suppress the contraction evoked by electrical stimulation in a concentration-dependent manner. The present

results also accords with the ability of verapamil to inhibit the slow inward  $\text{Ca}^{2+}$  channels (L-type VDCCs) of atrial tissues (Linden and Brooker, 1980).

Excitation-contraction coupling links the electrical stimulation of cardiomyocytes to the contraction of these cells, and involves the activation of L-type VDCCs (Layland and Shah, 2002). The cross-bridge binding to actin can be strongly inhibited by troponin-tropomyosin in the absence of  $\text{Ca}^{2+}$ , in this case the inhibitory troponin (troponin I) is attached to actin (Tao *et al.*, 1990).  $\text{Ca}^{2+}$  entry triggers release of  $\text{Ca}^{2+}$  from SR, thereby raises the intracellular  $\text{Ca}^{2+}$  level. The ubiquitous second messenger ( $\text{Ca}^{2+}$ ) directly binds and activates the myofilament protein (troponin C), producing a conformational change in troponin complex. This change propagates along the actin filament by tropomyosin, enabling activation of actomyosin ATPase and contraction (Solaro and Rarick, 1998). Both hibiscus and garcinia acids have an inhibitory effect on both vascular and cardiac tissues, even though the mechanisms of contraction for both tissues are different. This fact provides further support for the earlier idea that these agents are unlikely to be affecting the biochemical sequence of events that links the increase in  $\text{Ca}^{2+}$  concentration to activation of the contractile machinery. Furthermore, this fact provides further support for what have been suggested that both hibiscus and garcinia acid are producing their relaxant effect through inhibition of VDCCs.

In the present study, both hibiscus and garcinia acid produced a concentration-dependent relaxation of the trachea when it was pre-contracted with either carbachol or KCl. Moreover, both acids were found to be significantly more potent in relaxing

carbachol-induced contraction, when compared to the KCl-induced contraction. However, it should be noted that the relaxation produced by either hibiscus or garcinia acid on the trachea was complete irrespective of the contraction caused by carbachol or KCl, such an effect is similar to what had been shown by nifedipine (Raeburn and Brown, 1991), and diltiazem (Matsuda *et al.*, 2000).

Since both hibiscus and garcinia acids relaxed the contraction induced by carbachol, similar to earlier suggestions, it seems that both acids act by inhibiting of  $\text{Ca}^{2+}$  influx. In airway smooth muscle cells, stimulation of M3/G<sub>q</sub>-coupled receptors by contractile agonist activates PLC $\beta$ , which cleaves PIP<sub>2</sub>, thus producing the second messengers, IP<sub>3</sub> and DAG. IP<sub>3</sub> diffuses in the cytosol and binds to the IP<sub>3</sub> receptors, which triggers  $\text{Ca}^{2+}$  release from SR to initiate contraction (Roux *et al.*, 1998). In addition, this release of intracellular  $\text{Ca}^{2+}$  may induce depolarisation of cell membrane by activation of a  $\text{Ca}^{2+}$ -activated Cl<sup>-</sup> currents (Janssen, 1996). This depolarising current leads to opening of the L-type VDCCs, causing influx of extracellular  $\text{Ca}^{2+}$  (Janssen, 1996). Whereas, DAG activates PKC, which also participate in the regulation of smooth muscle contraction by phosphorylation of several contractile proteins (Billington and Penn, 2003). The fact that both hibiscus and garcinia acids relaxed the contraction to KCl further supports the idea that both compounds act via blocking of VDCCs.

The present results are similar to that showed by the crude extract on the pre-contracted guinea-pig trachea (Ali *et al.*, 1991). Therefore, it could be at least in part

that hibiscus acid is responsible for the relaxant activity of *H. sabdariffa* on the non-vascular smooth muscles.

Both hibiscus and garcinia acids appear to have similar activity and potency with regard to their ability to cause vasorelaxation, negative inotropy, and relaxant effects in the trachea. This is somewhat unusual, since the majority of enantiomers often have unequal pharmacological properties. For example, S(-)-verapamil is more potent than the R(+)-verapamil enantiomer in terms of its vasodilatory effect, also the S (-) isomer is 15 times more potent in producing negative inotropic effect (Satoh *et al.*, 1980). Whilst diltiazem is a diastereomer with two pairs of enantiomers, only the 2S, 3S form is pharmacologically active (Nguyen *et al.*, 2006). Although rarer, there are nevertheless enantiomers that do have equal pharmacological activities; for example the antiarrhythmic flecainide and the antidepressant fluoxetine (Nguyen *et al.*, 2006, Grodner and Sitkiewicz, 2013).

# ***Chapter 5***

## **5 Phytochemical and pharmacological studies of *P. salicifolium***

### **5.1 Introduction**

The marshes of Iraq are considered as the largest ecosystem in the Middle East and Western Eurasia (Al-Mudaffar Fawzi *et al.*, 2016). More than one hundred species of aquatic and amphibious plants have been recorded in the marshes of Iraq and around 50% were re-collected in 2004-2005. Ancient Mesopotamians used a wide variety of plants for a range of medicinal and culinary purposes. In modern Mesopotamia, Marsh Arabs also used plants from the marshes for medicinal and healing purposes (Al-Mudaffar Fawzi *et al.*, 2016). *P. salicifolium* is a common species found in the wetlands and is an important food source for the local inhabitants (Hamdan *et al.*, 2010).

Studies with *P. salicifolium* indicated that flavonoid glycosides (Calis *et al.*, 1999), and flavonol glycosides (Hussein and Mohamed, 2013), are predominant in the aerial parts of this plant, and plants rich in these compounds have high antioxidant effects (Hussein and Mohamed, 2013). In particular, the antioxidant effect has been attributed to the presence of the flavonoid glycoside, apigenin-6-C-arabinopyranosyl-8-C-glucopyranoside (Hussein and Mohamed, 2013).

More recently, an antihypertensive effect of *P. hydropiper*, which is a plant from the family Polygonaceae was reported by Devarajan *et al.* (2018). They investigated the

effect of the extracts from the leaves of *P. hydropiper* in a mouse salt-induced hypertension model and found that the extract produced a significant reduction in blood pressure (Devarajan *et al.*, 2018).

Although local people living in the marshlands of Iraq use *P. salicifolium* as a preventive treatment for diabetes and cardiovascular disease; no scientific studies have investigated the antihypertensive activity of this plant. Therefore, the aim of this chapter was to characterise the phytochemical constituents of *P. salicifolium* and to determine whether the crude methanolic extract of this plant has any vasorelaxant activity.

## 5.2 Materials and Methods

### 5.2.1 Fractionation of the crude extracts of *P. salicifolium*

Ground material of the dried aerial parts of *P. salicifolium* (50 g) was extracted with n-hexane, EtOAc and then MeOH (500 ml each) using a Soxhlet apparatus (**Methods Section 2.4.1**). The extracts were dried at 40 °C using a rotary evaporator. The hexane extract (1g, 2% yield) was subjected to silica gel CC eluting gradient wise with solvents of increasing polarity starting with n-hexane, n-hexane/EtOAc and EtOAc. A total of 150 fractions (5 ml each) were collected from the CC of the hexane extract and based on TLC results similar fractions were combined into sub-fractions. Further purification of the compounds was carried out using PTLC with 30-70% EtOAc in n-hexane and 10% (v/v) MeOH in EtOAc (**Methods Section 2.5.2**). The methanol extract of *P. salicifolium* (7 g, 14% yield) was fractionated by VLC column.

Fractions of 12 fractions (500 ml each) (VLC F 1-12), were obtained and evaporated with the aid of a rotary evaporator. Furthermore, the methanol extract was also fractionated by GPC using a Sephadex LH-20 column eluted with methanol as the mobile phase (**Methods Section 2.5.3**). Fractions (vials 1 to 70; 5 ml each) were collected and left to evaporate in the fume cupboard. Preliminary assessment was achieved by visualisation of these fractions on TLC plates and fractions of similar profiles were pooled together, and 11 sub-fractions (PSM F1-11) were obtained.

### **5.2.2 Drugs, solvents and chemicals**

The crude methanolic extract of *P. salicifolium* was prepared as 20 mg/ml stock solution dissolved in PSS. R-(-)-phenylephrine hydrochloride and KCl were prepared as detailed earlier (**Methods Section 3.2.2**).

### **5.2.3 Effects of the crude methanolic extract of *P. salicifolium* on the rat**

#### **aorta**

A preliminary pharmacological screen was carried out by examining the vasorelaxant effect of the crude methanol extract of *P. salicifolium* (0.001- 0.1 mg/ml), when added cumulatively to endothelium-intact aorta pre-contracted with PE (3  $\mu$ M) (**Methods Section 3.2.3**). In order to find out whether the vasorelaxant activity is endothelium-dependent, further experiments were carried out, examining the effect of the crude methanolic extract on the endothelium-denuded aorta (**Methods Section 4.2.4**), where the concentration of the crude extract applied was increased up to 0.5 mg/ml. In a subset of experiments, the effect of the crude methanolic extract

of *P. salicifolium* (0.1-1.0 mg/ml) was also examined on the endothelium-intact aorta pre-contracted with KCl (60 mM).

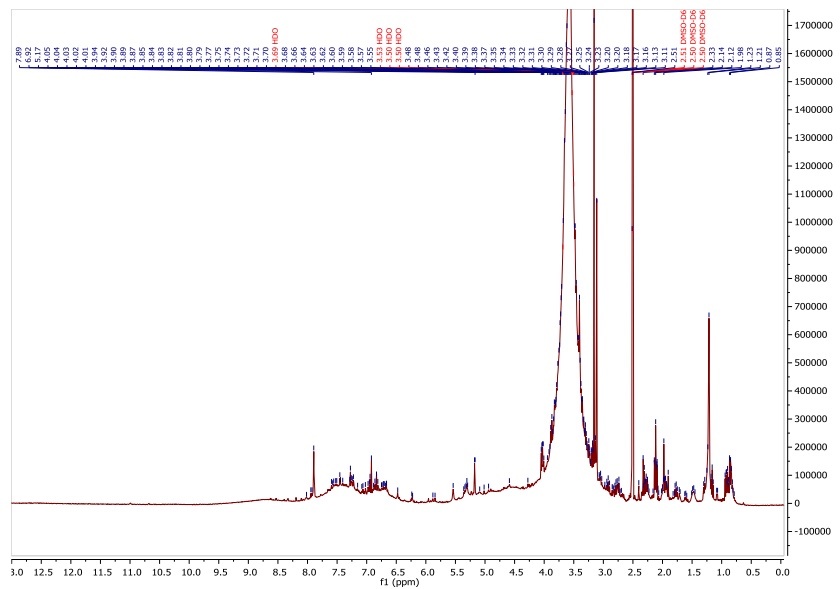
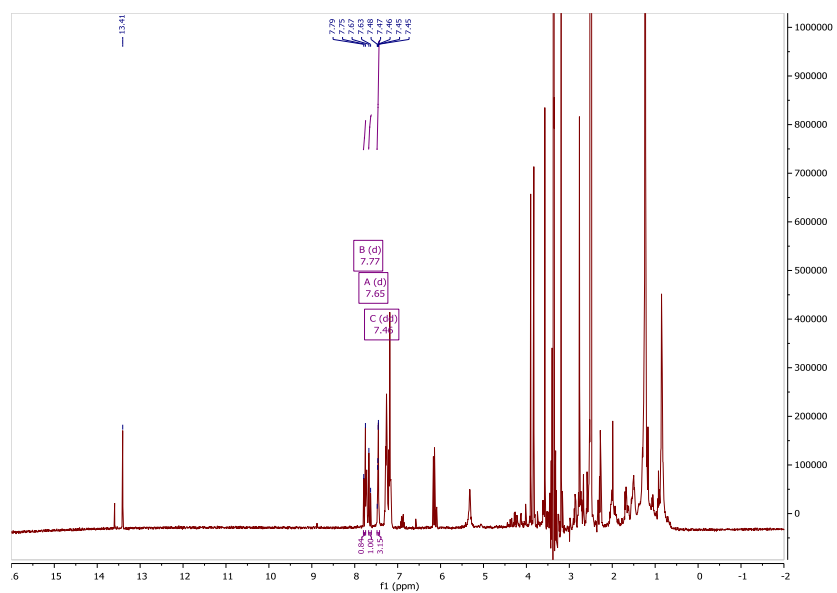
## 5.3 Results

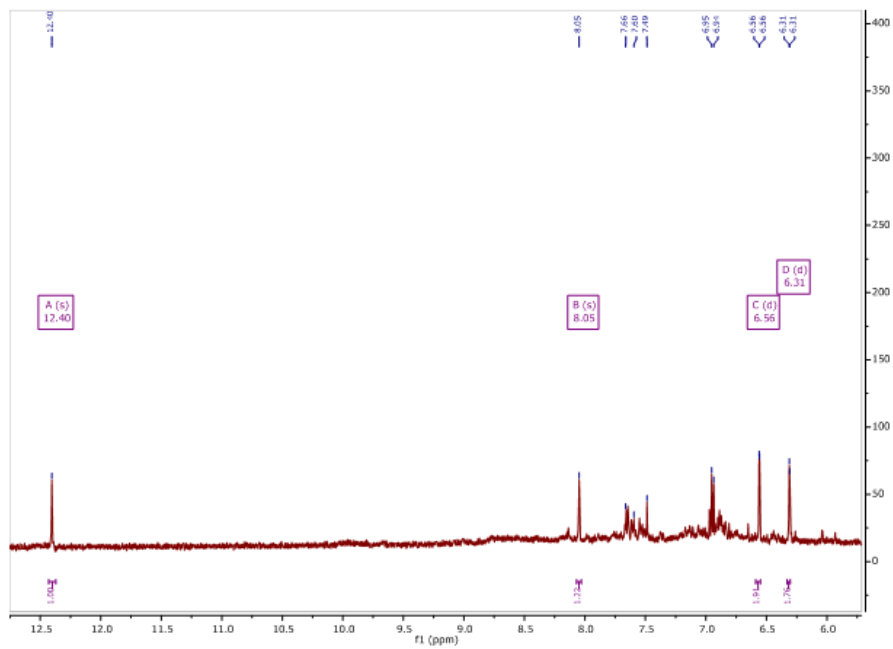
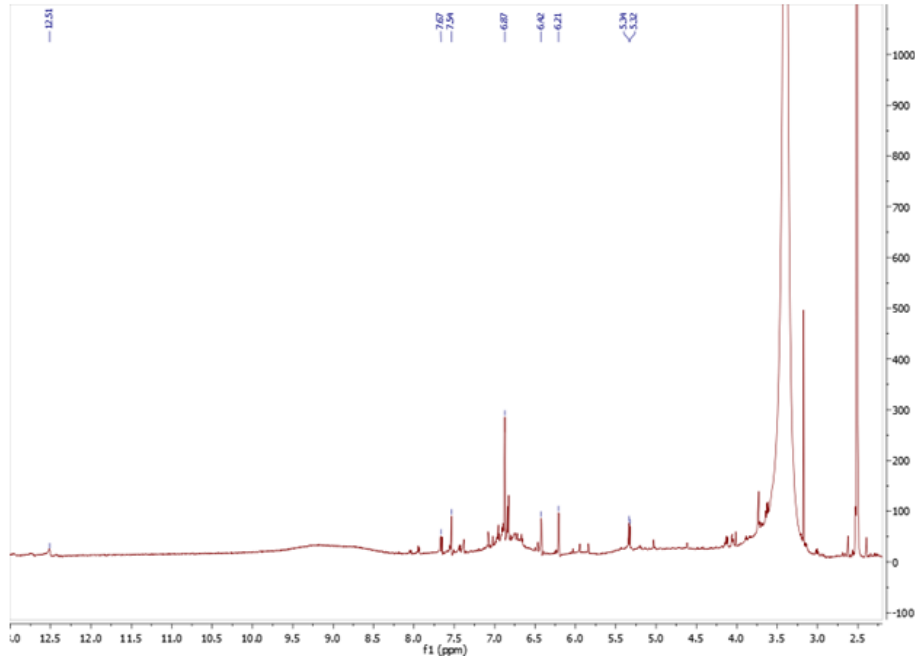
### 5.3.1 Phytochemical results

#### 5.3.1.1 Fractionation of *P. salicifolium* crude extracts

The  $^1\text{H}$  NMR spectra of the crude and sub-fractions of the crude methanolic extract of *P. salicifolium* showed peak signals in the aliphatic and aromatic regions indicating a mixture of fats, sugars and phenolic compounds, including flavonoids (**Spectrum 5.1**). The content of the collected sub-fractions obtained from the GPC of the methanol extract were investigated by  $^1\text{H}$  NMR spectroscopy to characterise the compounds of these sub-fractions. Sub-fraction PSM-F8 (vials 39-45; 0.05% yield) was identified as a mixture of flavonoids, while  $^1\text{H}$  NMR spectroscopy of the sub-fraction PSM-F9 (vials 46-54; 1.6% yield) showed the presence of an isoflavone as a major compound (**Spectrum 5.2A**). The compounds of sub-fraction PSM-F11 (vials 63-70; 1.5% yield) were identified as a mixture of flavonoid glycosides (**Spectrum 5.2B**).

Four compounds were separated from the fractionation of the crude hexane extract of *P. salicifolium*. The NMR experiments (1D and 2D), characterised these compounds as 2 chalcones (2',4'-dimethoxy-6'-hydroxychalcone, and 3',5'-dimethoxy-4',6'-dihydroxychalcone) and 2 flavanones (5,7-dimethoxyflavanone, and 5,8-dimethoxy-7-hydroxyflavanone).

**A****B**

**A****B**

**Spectrum 5.2:** <sup>1</sup>H NMR spectrum (400 MHz) of (A) sub-fraction (PSM-F9) of crude methanolic extract of *P. salicifolium* in Acetone-*d*<sub>6</sub>, and (B) sub-fraction 11 (PSM-F11) of crude methanolic extract of *P. salicifolium* in DMSO-*d*<sub>6</sub>.

### 5.3.1.1.1 Characterisation of 2',4'-dimethoxy-6'-hydroxychalcone (flavokawain B)

This compound (2',4'-dimethoxy-6'-hydroxychalcone) was separated from the combined fractions (9-11) of the hexane extract of *P. salicifolium*, using 30% (v/v) EtOAc in n-hexane as the mobile phase for PTLC (**Methods Section 2.5.2 and 5.2.1**). This compound (**Figure 5.1**) was obtained as a yellow solid with a yield of 50 mg (5%). On TLC, the compound appeared as a visible yellow spot, and when it was examined under the short UV light ( $\lambda$  254 nm), it appeared as a dark spot. However, the compound appeared as a brown spot after treatment with *p*-anisaldehyde-sulphuric acid and heating. The  $R_f$  value for this compound was 0.48 on normal silica gel when eluted with a mobile phase of 30% (v/v) EtOAc in n-hexane. Its molecular ion  $[M-H]^+$  at m/z 285 (Calc 285.5), suggesting the molecular formula of  $C_{17}H_{16}O_4$  (**Spectrum 5.3**).

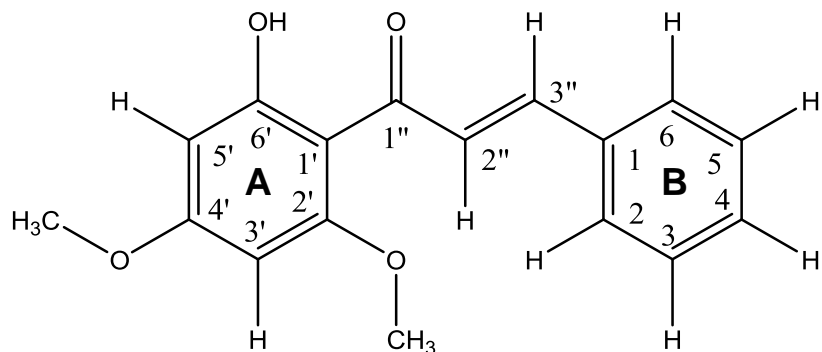
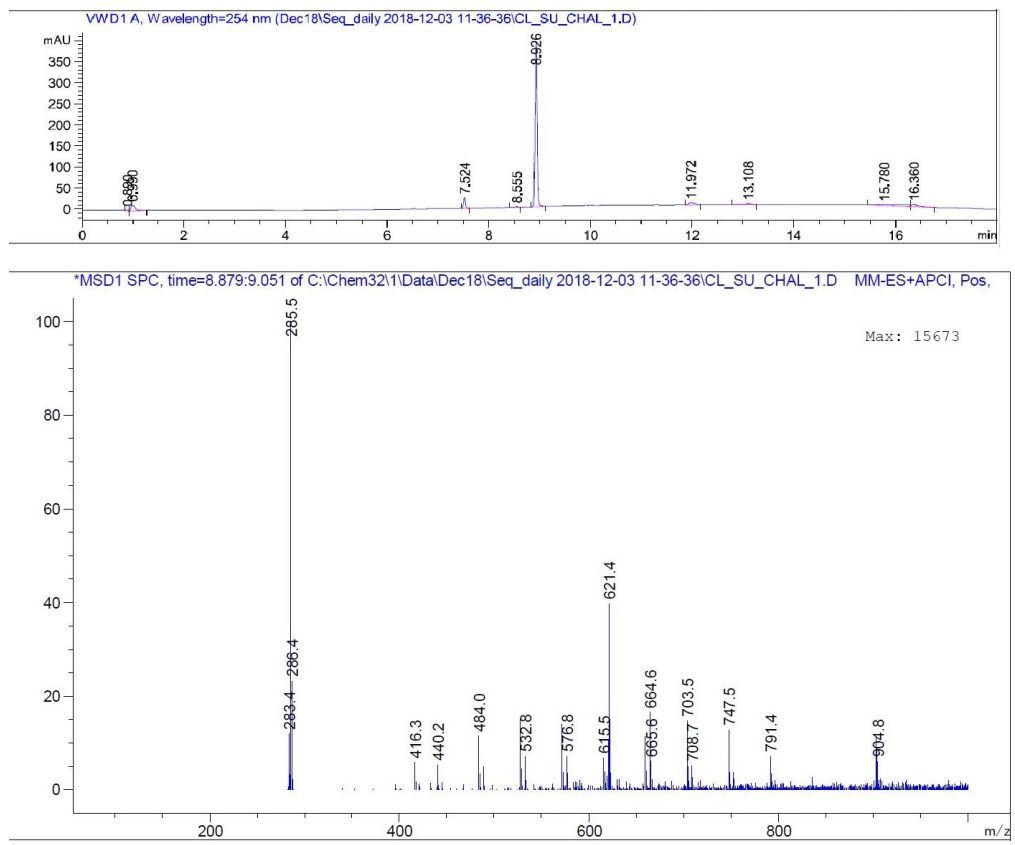


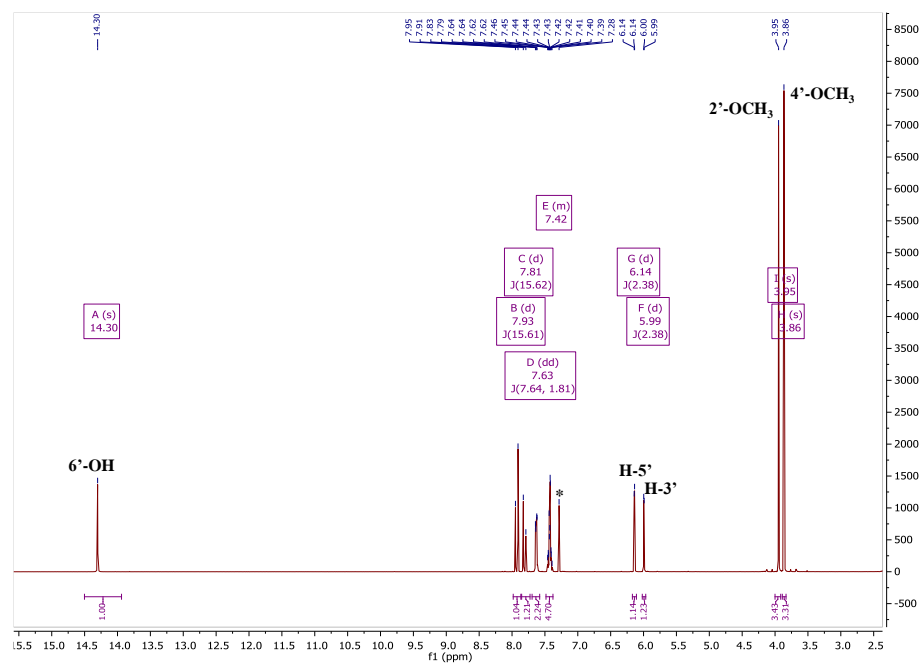
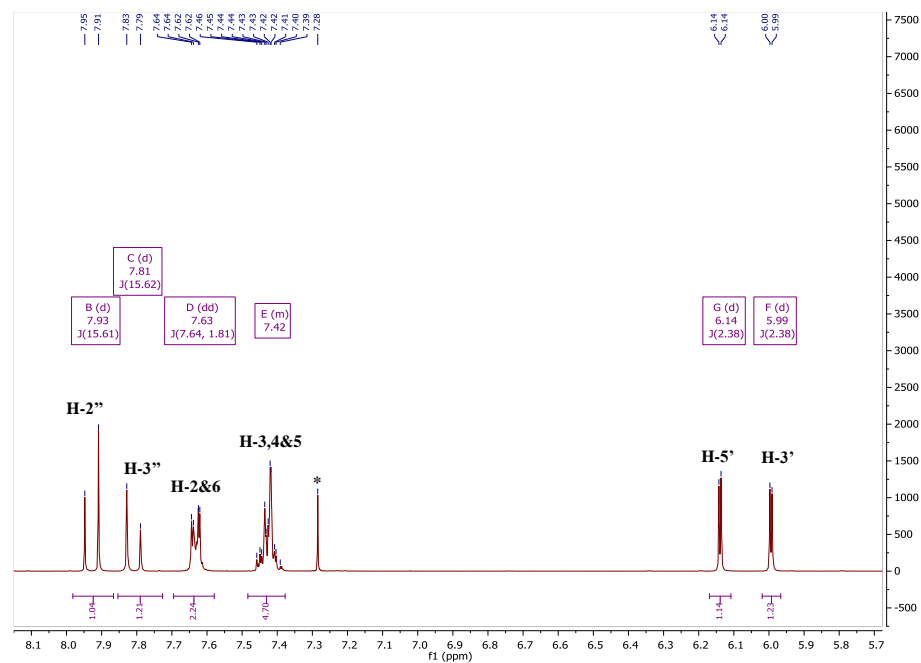
**Figure 5.1:** Chemical structure of 2',4'-dimethoxy-6'-hydroxychalcone.



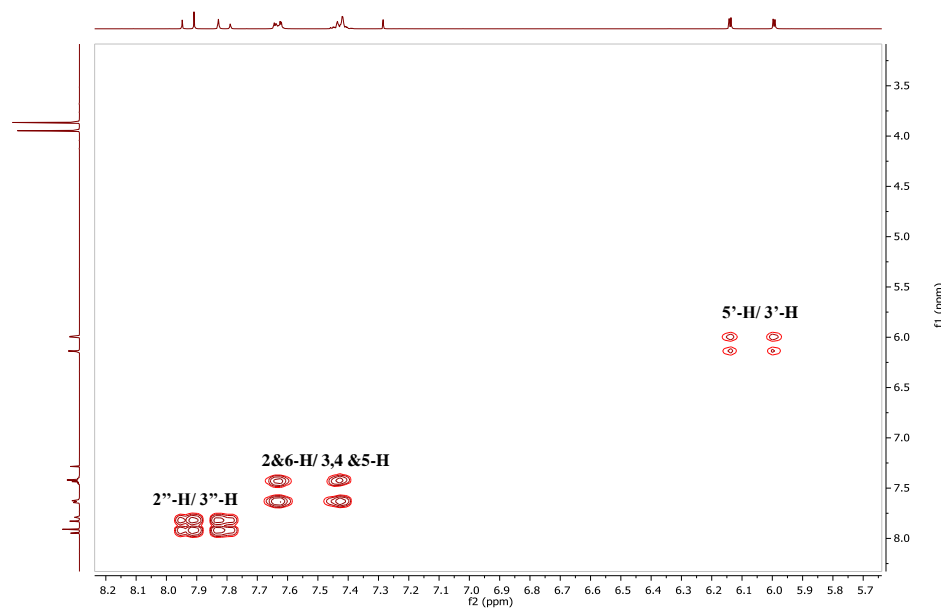
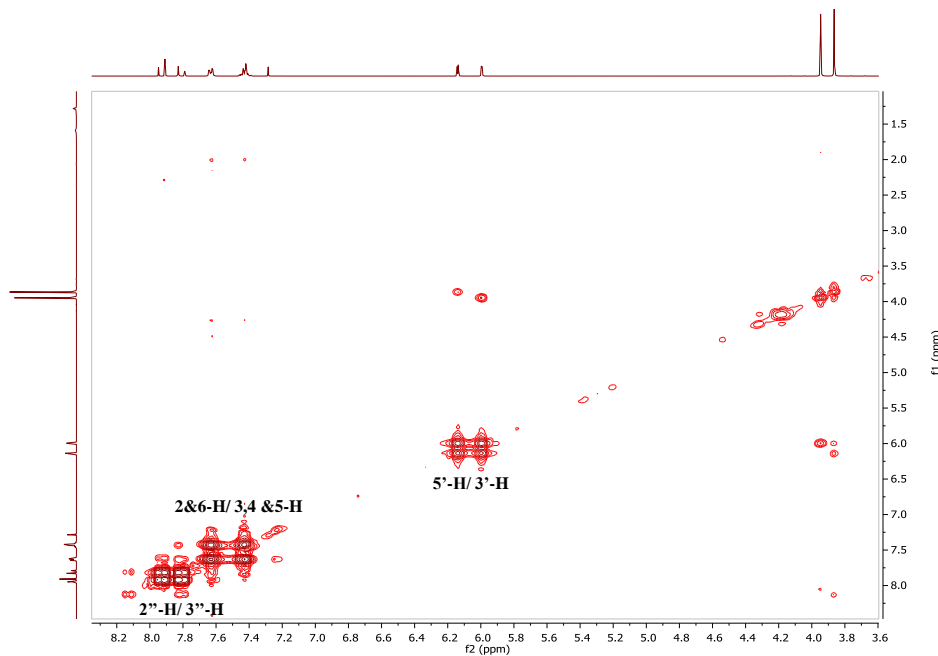
**Spectrum 5.3:** Molecular ion peak  $[M-H]^+$  spectrum of 2',4'-dimethoxy-6'-hydroxychalcone.

## NMR data analysis

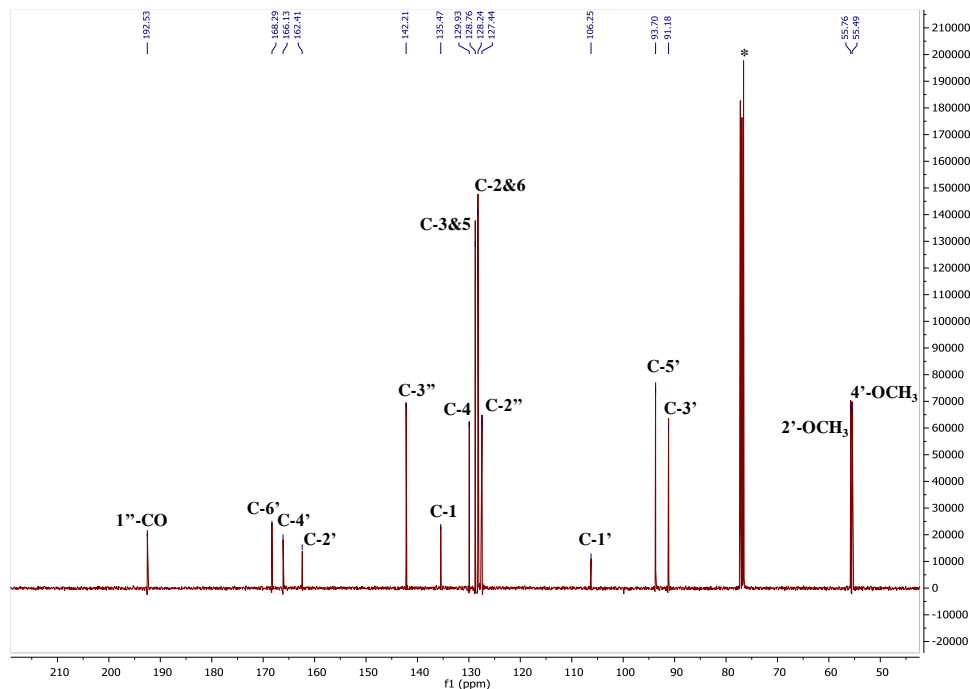
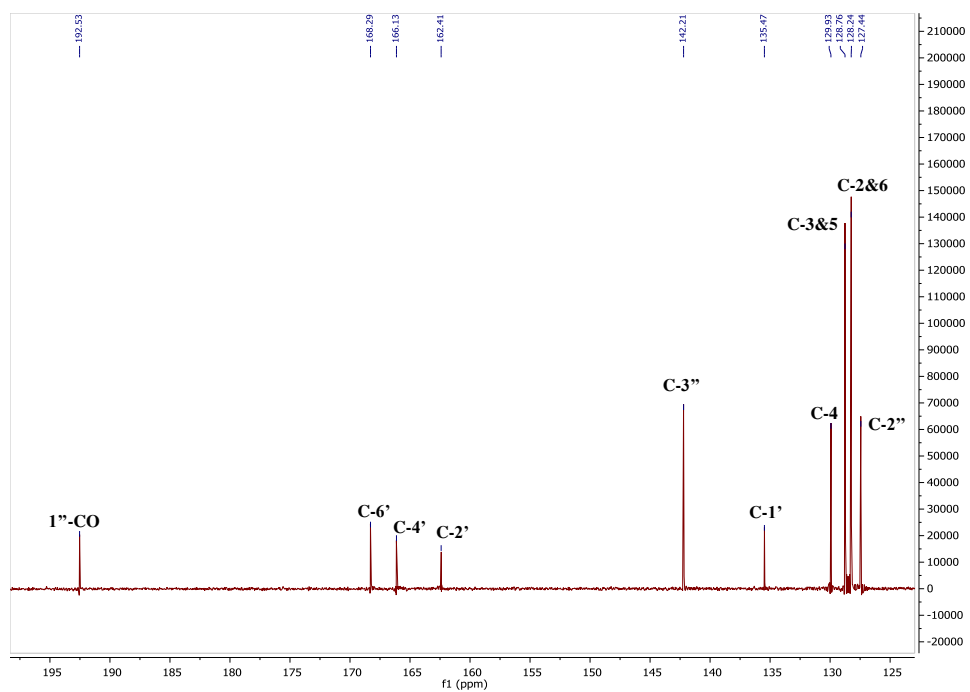
The proton spectrum indicated the presence of seven aromatic protons, which must be from two phenyl rings (**Spectrum 5.4**). Based on integration and  $^1\text{H}$ - $^1\text{H}$  couplings in the COSY spectrum, one of the rings is tetra and the other mono substituted (**Spectrum 5.5**). Protons H-3, H-4 and H-5 on the mono-substituted ring appeared as a multiplet between  $\delta_{\text{H}}$  7.37 and 7.43 ppm (3H, m) while protons H-2 and H-6 appeared as doublet of doublets at 7.63 (2H, dd,  $J=7.6, 1.8$ ). The signals at 3.86 (3H, s) and 3.95 (3H, s) were assigned to the 4'- and 2'-OCH<sub>3</sub>, respectively. While the one at  $\delta_{\text{H}}$  14.30 ppm was attributed to the H-bonded or chelated 6'-OH. The meta-coupled aromatic protons at 6.14 (1H, d,  $J=2.39$ ) and 5.99 (1H, d,  $J=2.39$ ) were assigned to H-5' and H-3' respectively. Two trans-coupled olefinic protons were observed at  $\delta$  7.91 (1H, d,  $J=15.6$ ,  $\alpha$ -H) and 7.83 (1H, d,  $J=15.6$ ,  $\beta$ -H). The carbon spectrum indicated the presence of 12 aromatic and two olefinic carbon signals (**Spectrum 5.6**). The signal at  $\delta_{\text{C}}$  192.5 was attributed to the carbonyl carbon of the chalcone while the signal at 127.4 ppm was assigned to the  $\alpha$ -olefinic carbon and the one at 142.2 to the  $\beta$ -olefinic carbon. The rest of the signals were for the aromatic ring carbons. These assignments were further supported by HMBC and HSQC spectra for the compound (**Spectrum 5.7** and **Spectrum 5.8**). The hydroxyl proton showed long range correlation ( $^3J$ ) to C-5' and C-1' and ( $^2J$ ) to C-6'. Hence, it must be attached at C-6'. The methoxy group protons at  $\delta_{\text{H}}$  3.95 and 3.86 showed long range correlations to the carbons at  $\delta_{\text{C}}$  162.4 (C-2') and 166.1 (C-4') respectively, hence they must be attached to these carbons also. The full chemical shift assignments are given in **Table 5.1**.

**A****B**

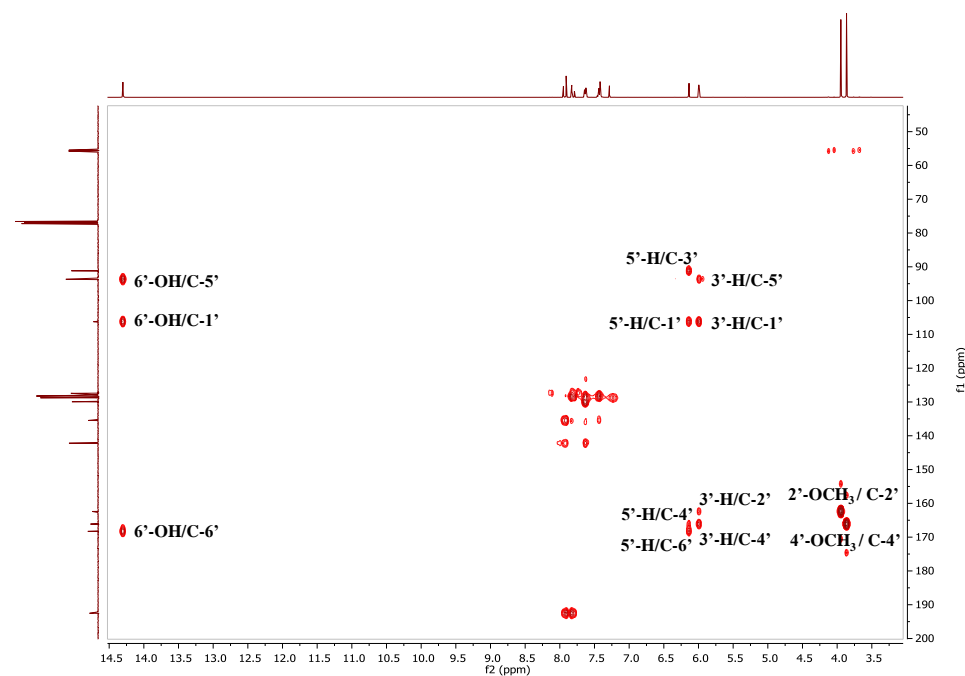
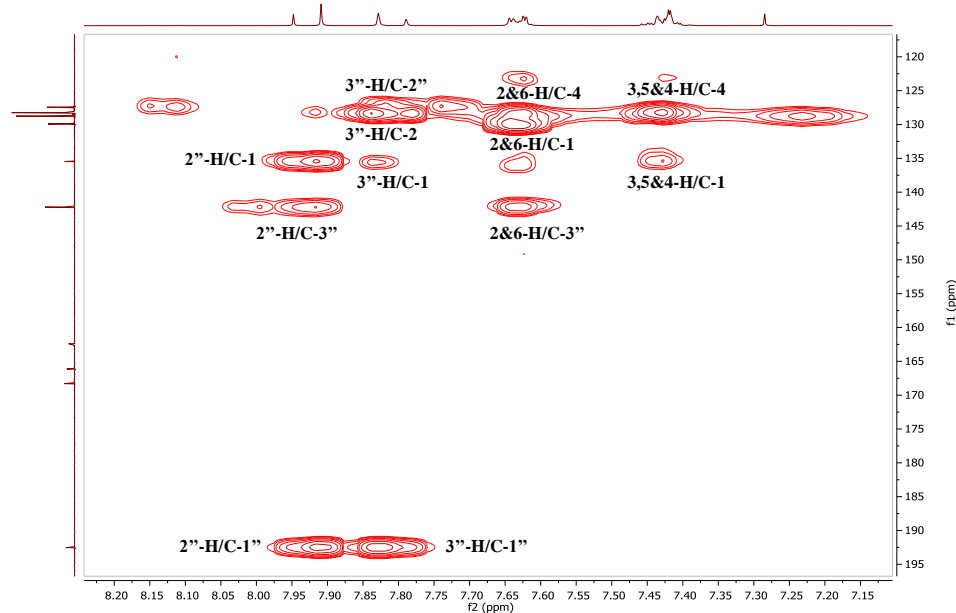
**Spectrum 5.4: (A) Full and (B) selected expansion of  $^1\text{H}$  NMR spectrum (400 MHz) of 2',4'-dimethoxy-6'-hydroxychalcone in Chloroform- $d$ .**

**A****B**

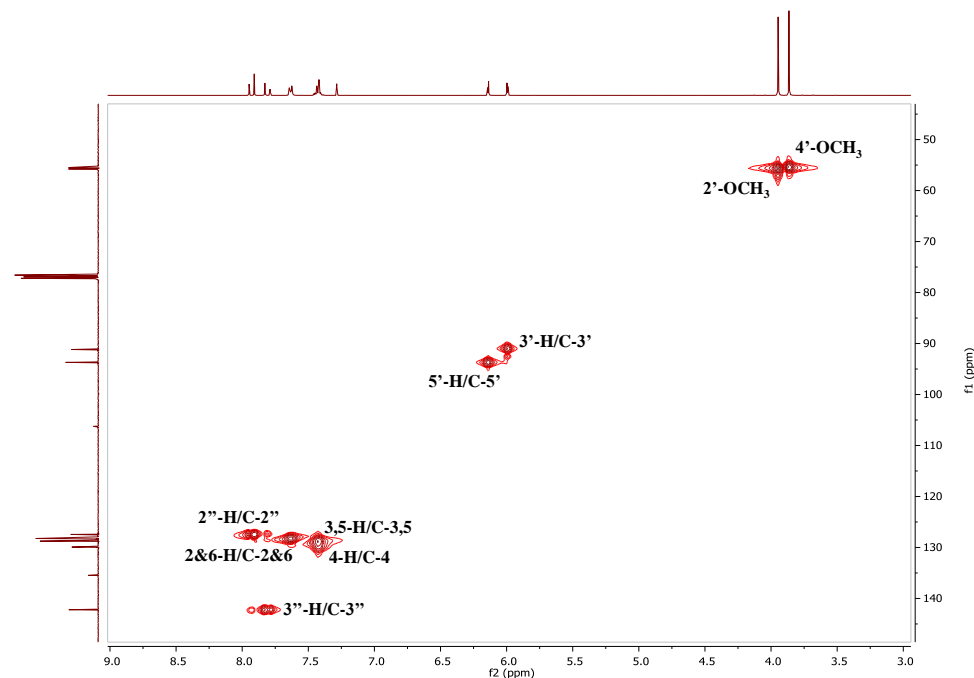
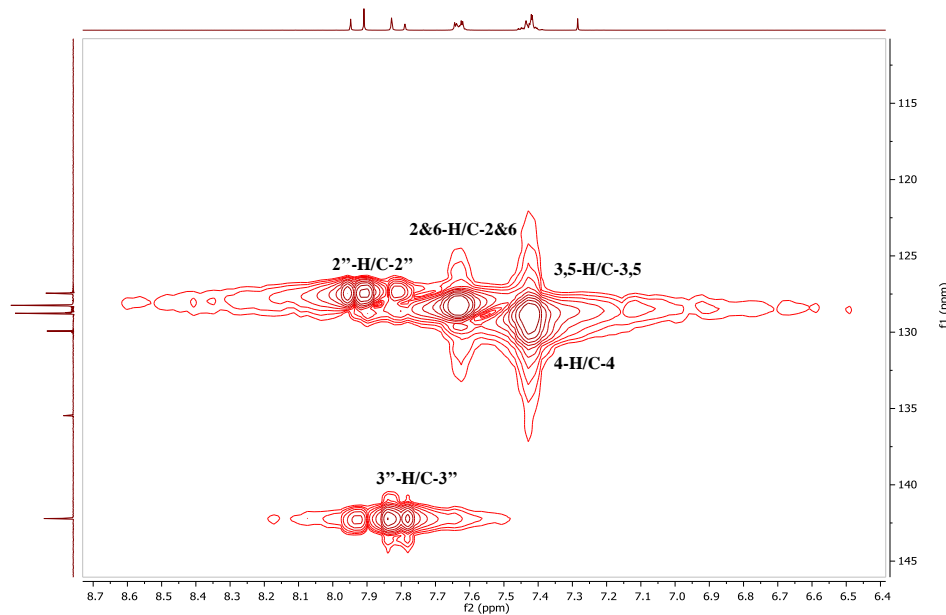
**Spectrum 5.5: (A) Full and (B) selected expansion of COSY spectrum (400 MHz) of 2',4'-dimethoxy-6'-hydroxychalcone in Chloroform-d.**

**A****B**

**Spectrum 5.6: (A) Full and (B) selected expansion of  $^{13}\text{C}$  NMR spectrum (100 MHz) of 2',4'-dimethoxy-6'-hydroxychalcone in Chloroform-*d*.**

**A****B**

**Spectrum 5.7: (A) Full and (B) selected expansion of HMBC spectrum (400 MHz) of 2',4'-dimethoxy-6'-hydroxychalcone in Chloroform-*d*.**

**A****B**

**Spectrum 5.8: (A) Full and (B) selected expansion of HSQC spectrum (400 MHz) of 2',4'-dimethoxy-6'-hydroxychalcone in Chloroform-d.**

**Table 5.1: NMR data for 2',4'-dimethoxy-6'-hydroxychalcone in Chloroform-*d***

Position	$\delta_{\text{H}}$ (mult, <i>J</i> (Hz))	$\delta_{\text{C}}$ (mult)	HMBC correlations
1	-	135.4	-
2, 6	7.63 (2H, dd, 7.6, 1.8)	128.2	C-1, C-4
3, 5, 4	7.42 (3H, m)	128.7 &129.9	C-1, C-4
$\alpha$ (2'')	7.91 (1H, d, 15.6)	127.4	C-1, C-3'', C-1''
$\beta$ (3'')	7.83 (1H, d, 15.6)	142.2	C-1, C-2, C-2'', C-1''
1'	-	106.2	-
6'	-	168.2	-
5'	6.14 (1H, d, 2.6)	93.7	C-1', C-6', C-4', C-3'
4'	-	166.1	-
3'	5.99 (1H, d, 2.6)	91.1	C-1', C-5', C-4', C-2'
2'	-	162.4	-
1''	-	192.5	-
6'-OH	14.30 (s)	-	C-1', C-6', C-5'
O-CH <sub>3</sub>	3.86 (3H, s)	55.4	C-4'
O-CH <sub>3</sub>	3.95 (3H, s)	55.7	C-2'

### 5.3.1.1.2 Characterisation of 2',5'-dimethoxy-4',6'-dihydroxychalcone

This compound (*2',5'-dimethoxy-4',6'-dihydroxychalcone*) was separated from the combined fractions (33-37) of the hexane extract of *P. salicifolium*, using 40% (v/v) EtOAc in n-hexane as the mobile phase for PTLC (**Methods Section 2.5.2 and 5.2.1**). This compound (**Figure 5.2**) was also obtained as a yellow solid with a yield of 40 mg (4%). Similar to *2',4'-dimethoxy-6'-hydroxychalcone*, this compound was visible to the eye and appeared as a yellow spot on the TLC. Under short UV ( $\lambda$  254 nm), it appeared as a dark spot, which turned to a brown spot after spraying with *p*-anisaldehyde- sulphuric acid followed by heating. The  $R_f$  value for this compound was 0.53 after elution of the TLC plate with a mobile phase of 40% EtOAc in n-hexane. The positive mode HRMS spectrum showed a molecular ion  $[M-H]^+$  at *m/z* 301 (Calc 301.11), suggesting the molecular formula of  $C_{17}H_{16}O_5$  (**Spectrum 5.9**).

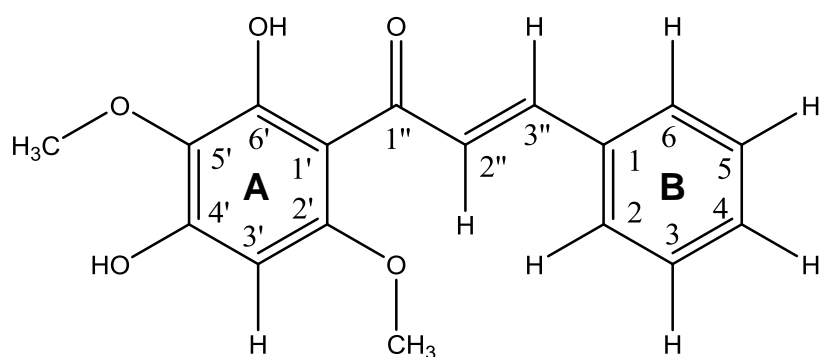
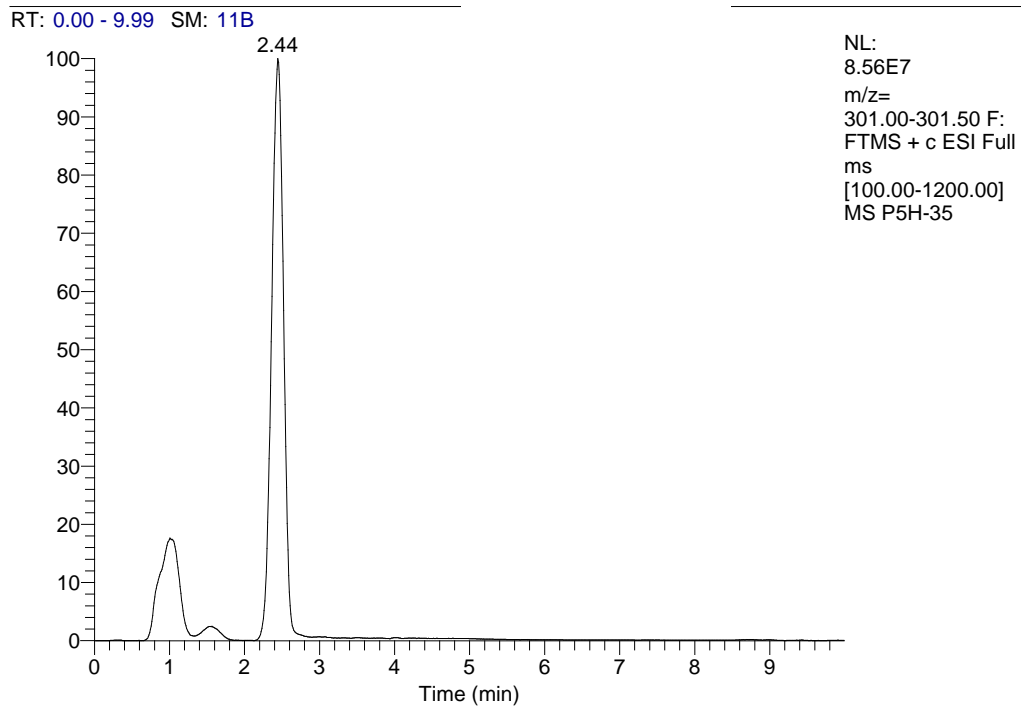
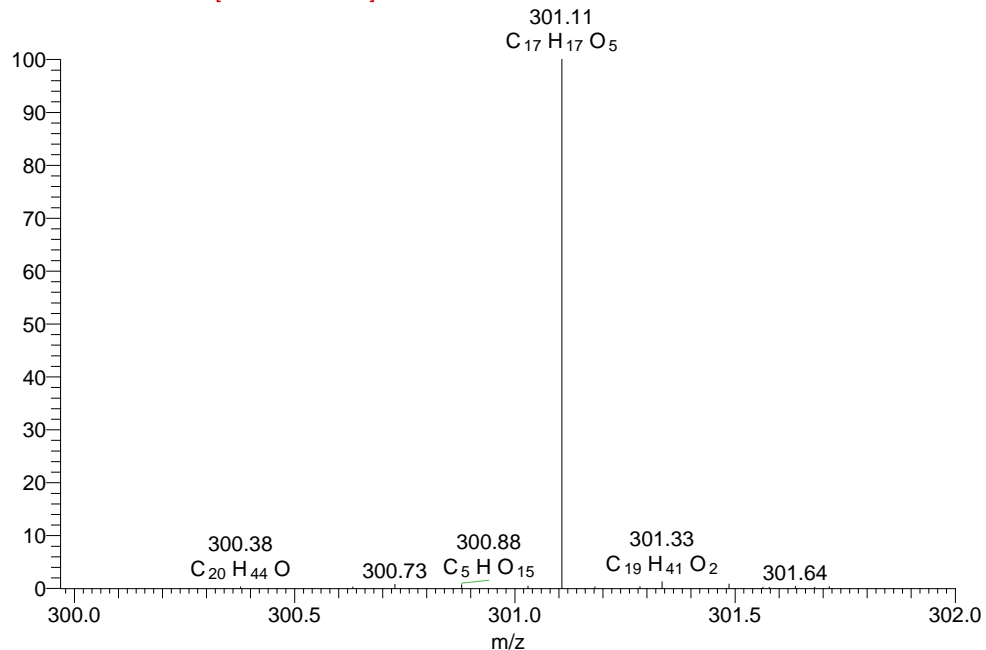


**Figure 5.2:** Chemical structure of 2',5'-dimethoxy-4',6'-dihydroxychalcone.



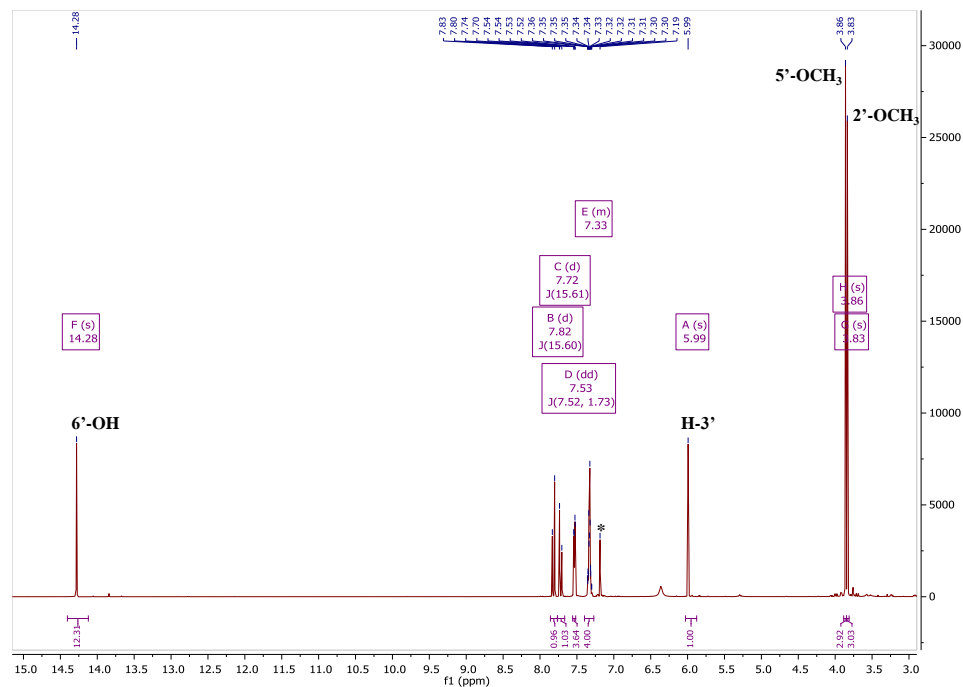
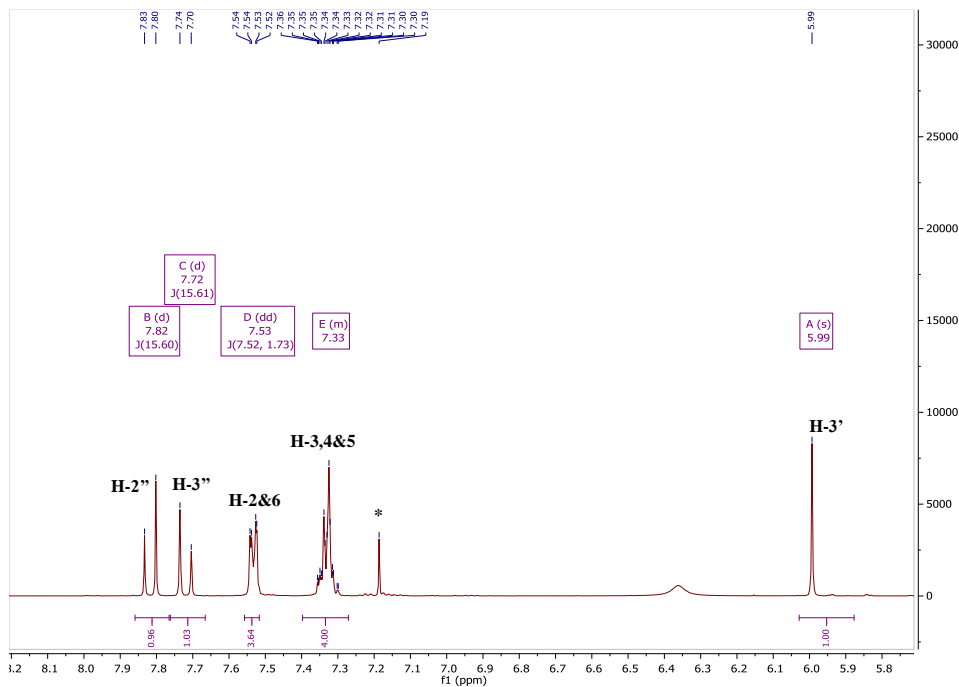
P5H-35 #253 RT: 2.43 AV: 1 NL: 9.13E7  
F: FTMS + c ESI Full ms [100.00-1200.00]



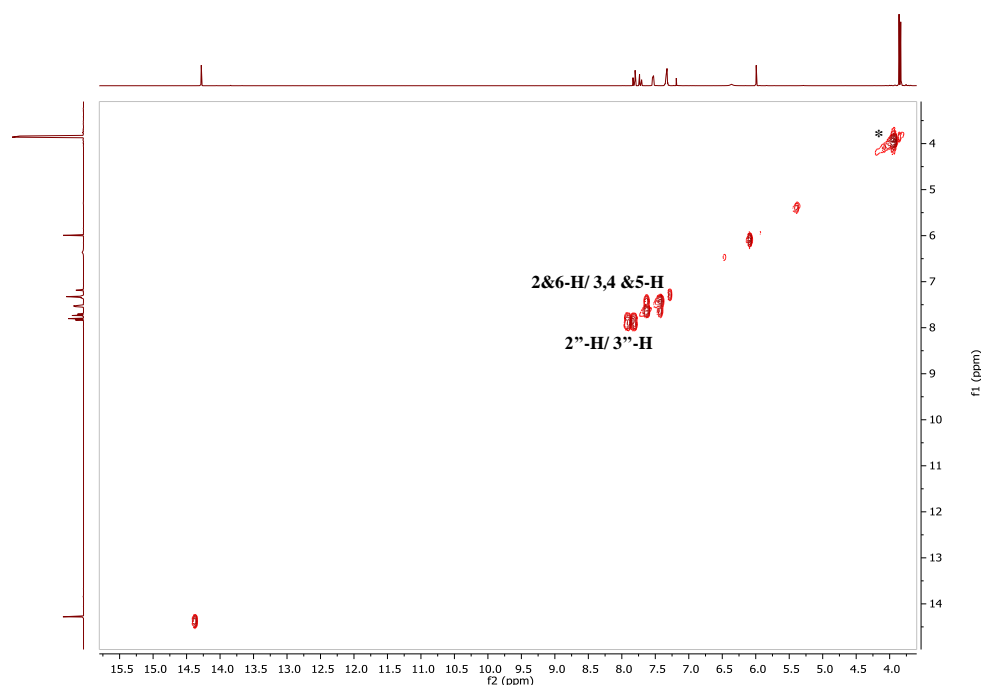
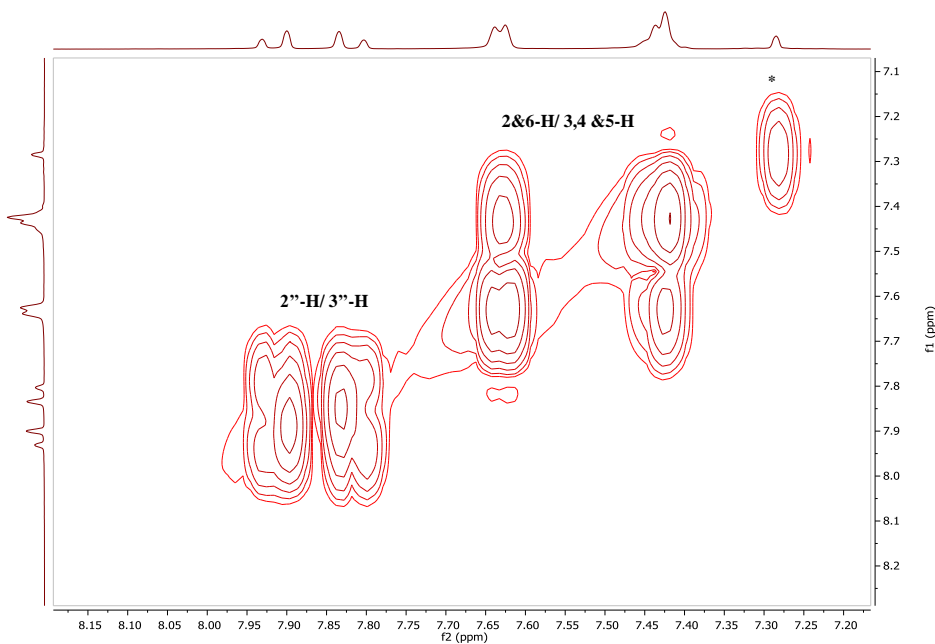
**Spectrum 5.9:** Molecular ion peak  $[M-H]^+$  spectrum of 2',5'-dimethoxy-4',6'-dihydroxychalcone.

## NMR data analysis

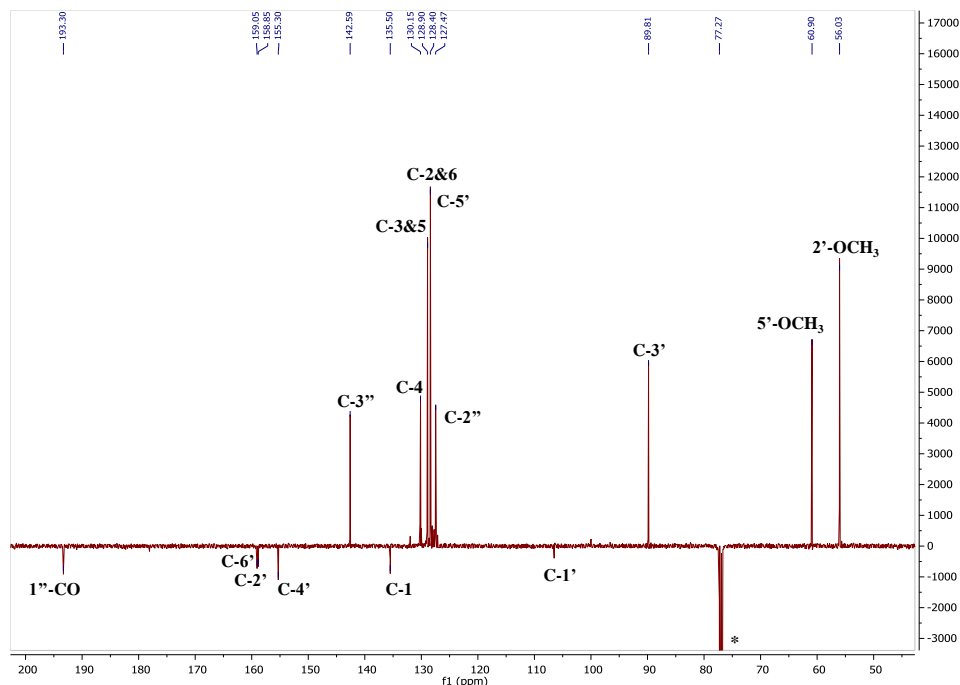
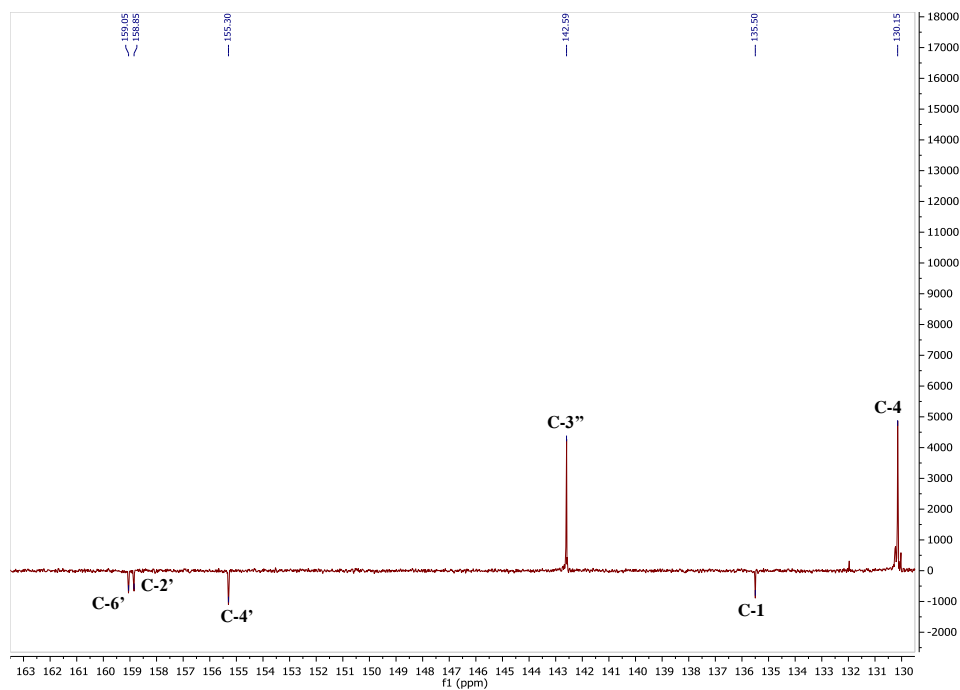
The proton spectrum was similar to that of 2',4'-dimethoxy-6'-hydroxychalcone, but showed six aromatic protons (**Spectrum 5.10**). The difference was due to an extra substitution in the tetra substituted ring as the mono-substituted ring protons were still identical. Based on integration and  $^1\text{H}$ - $^1\text{H}$  couplings in the COSY spectrum, this was confirmed by the disappearance of the meta-coupled protons in 2',4'-dimethoxy-6'-hydroxychalcone now replaced by a proton singlet in 2',5'-dimethoxy-4',6'-dihydroxychalcone (**Spectrum 5.11**). The two methoxy group signals appeared at  $\delta_{\text{H}}$  3.83 ppm (3H, s) and 3.86 ppm (3H, s), while the chelated 6'-OH was at 14.28 ppm. The aromatic singlet at  $\delta$  5.99 ppm (s) was assigned to H-3'. The trans-olefinic protons were also observed at  $\delta_{\text{H}}$  7.82 ppm (1H, d,  $J=15.6$ ,  $\alpha$ -H) and 7.72 (1H, d,  $J=15.6$ ,  $\beta$ -H). The  $^{13}\text{C}$  spectrum of this compound showed 17 signals made up of identical carbons but with one aromatic CH less and replaced by a quaternary carbon signal at 128.4 (**Spectrum 5.12**). Using the HMBC and HSQC spectra for the compound (**Spectrum 5.13** and **Spectrum 5.14**), the complete chemical shift assignments (**Table 5.2**) were made as follows: The hydroxyl proton at  $\delta_{\text{H}}$  14.2 ppm showed similar long range correlations to C1', C-6' and C-5'. The methoxy protons at 3.83 and 3.86 showed long range correlations to C-2' at  $\delta_{\text{C}}$  158.8 and C-5' at 128.4, respectively.

**A****B**

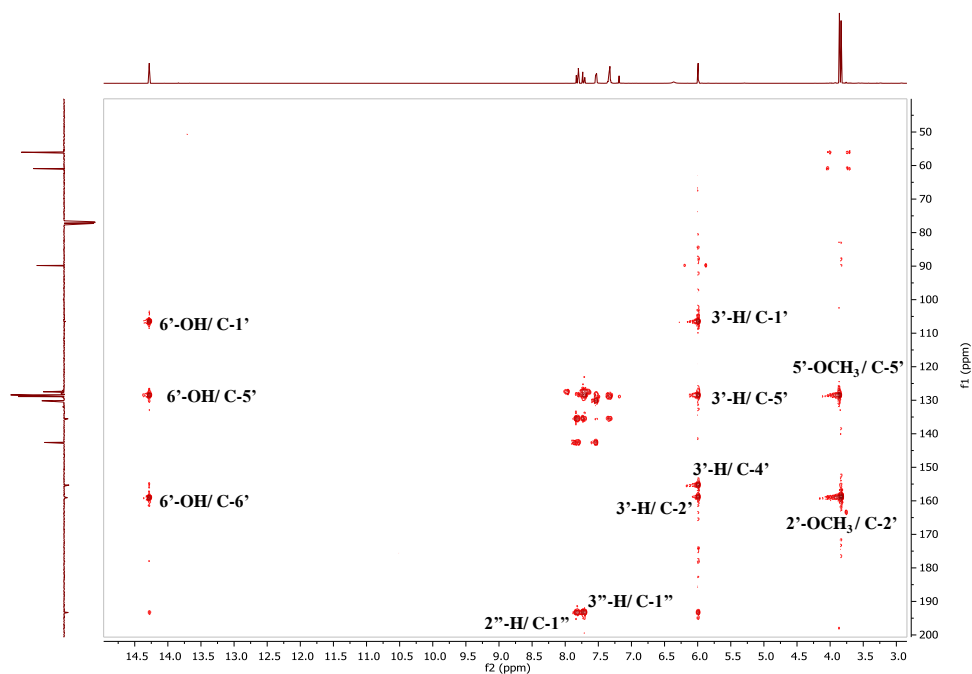
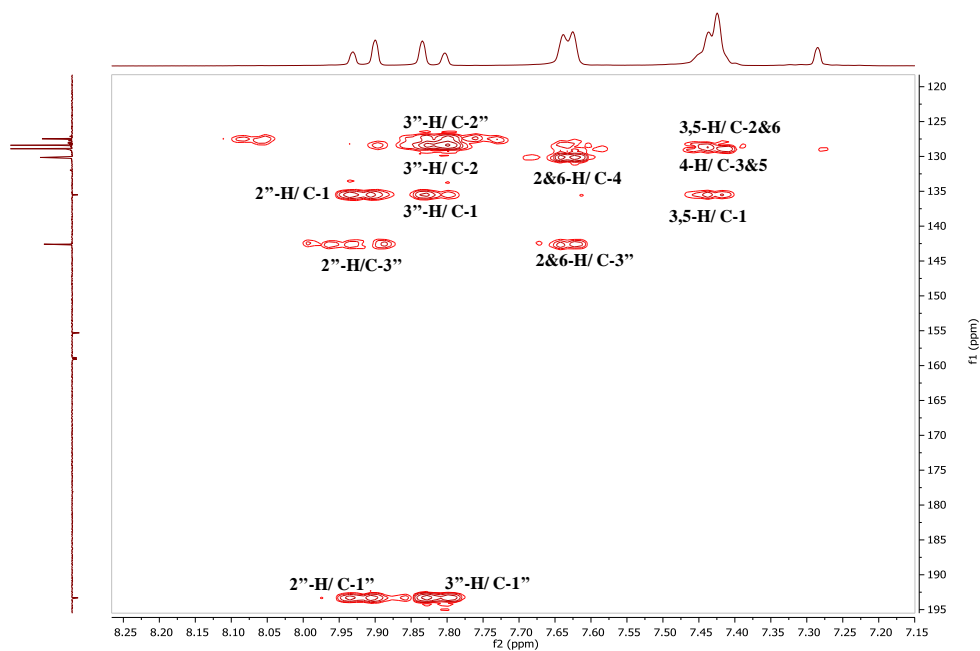
**Spectrum 5.10:** (A) Full  $^1\text{H}$  NMR spectrum (500 MHz) of 2',5'-dimethoxy-4',6'-dihydroxychalcone with (B) selected expansion of the aromatic region in Chloroform-*d*.

**A****B**

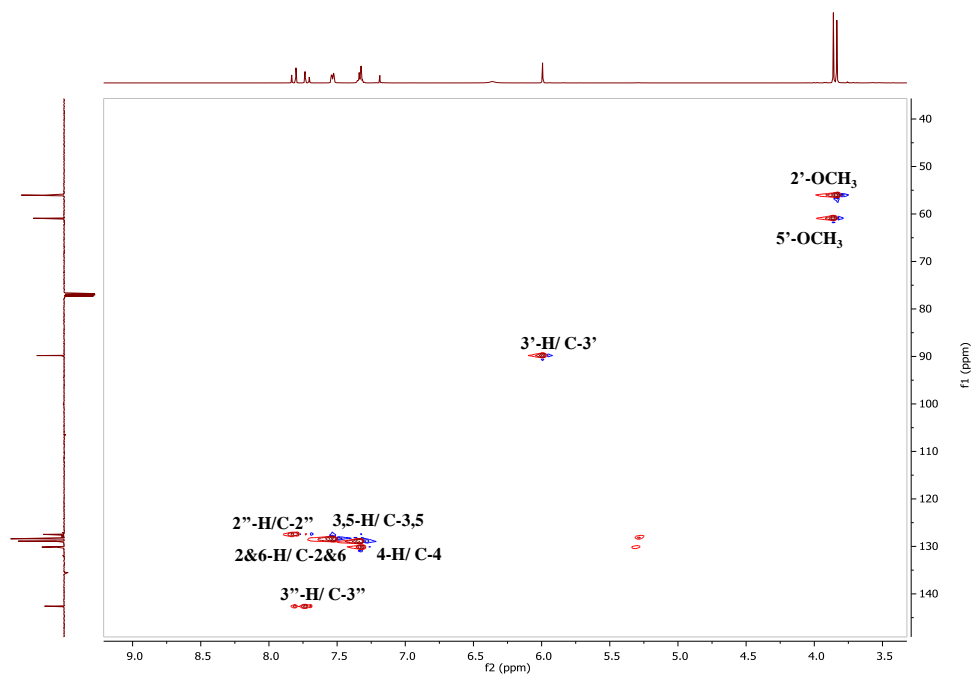
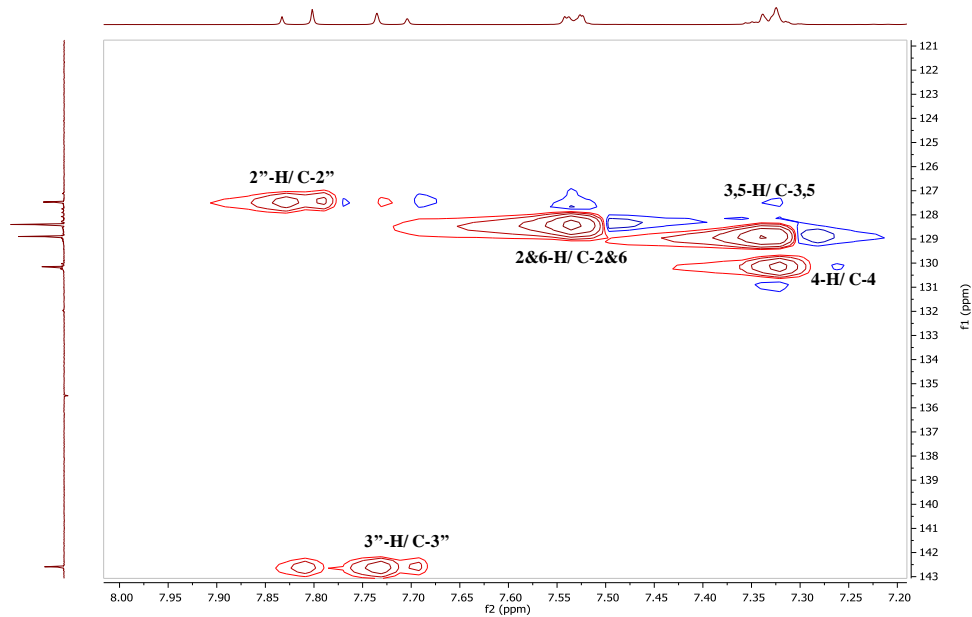
**Spectrum 5.11: (A) Full and (B) selected expansion of COSY spectrum (500 MHz) of 2',5'-dimethoxy-4',6'-dihydroxychalcone in Chloroform-d.**

**A****B**

**Spectrum 5.12: (A) Full and (B) selected expansion of DEPTq 135  $^{13}\text{C}$  NMR spectrum (100 MHz) of 2',5'-dimethoxy-4',6'-dihydroxychalcone in Chloroform-*d*.**

**A****B**

**Spectrum 5.13: (A) Full and (B) selected expansion of HMBC spectrum (500 MHz) of 2',5-dimethoxy-4',6'-dihydroxychalcone in Chloroform-d.**

**A****B**

**Spectrum 5.14: (A) Full and (B) selected expansion of HSQC spectrum (500 MHz) of 2',5'-dimethoxy-4',6'-dihydroxychalcone in Chloroform-d.**

**Table 5.2: NMR data for 2',5'-dimethoxy-4',6'-dihydroxychalcone in chloroform-*d***

Position	$\delta_H$ (mult, <i>J</i> (Hz))	$\delta_C$ (mult)	HMBC correlations
1	-	135.5	-
2, 6	7.53 (2H, dd, 7.5, 1.7)	128.4	C-1, C-3''
3, 5, 4	7.33 (3H, m)	128.9, 130.1	C-1, C4
$\alpha$ (2'')	7.82 (1H, d, 15.6)	127.4	C-1, C-1'', C-3''
$\beta$ (3'')	7.72 (1H, d, 15.6)	142.5	C-1, C-1'', C-2''
1'	-	106.5	-
6'	-	159.0	C-1', C-5', C-6'
2'	-	128.4	-
4'	-	155.3	-
3'	5.99 (1H, s)	89.8	C-1', C-2', C-4', C-5'
5'	-	158.8	-
1''	-	193.3	-
6'-OH	14.2 (s)	-	-
O-CH <sub>3</sub>	3.83 (3H, s)	60.09	C-2'
O-CH <sub>3</sub>	3.86 (3H, s)	56.03	C-5'

### 5.3.1.1.3 Characterisation of 5,7-dimethoxyflavanone (dimethyl pinocembrin)

The compound 5,7-dimethoxyflavanone was separated from the combined fractions (70-76) of the hexane extract of *P. salicifolium*, using 70% (v/v) EtOAc in n-hexane as the mobile phase for PTLC (**Methods Section 2.5.2 and 5.2.1**). This compound (**Figure 5.3**) was obtained as a yellow solid with a yield of 15 mg (1.5%). On TLC, it appeared as a dark spot when visualised under UV light ( $\lambda$  254 nm), and light blue under UV light ( $\lambda$  365 nm). The spot of the compound turned to a yellow spot after spraying with *p*-anisaldehyde-sulphuric acid reagent followed by heating. Its  $R_f$  was 0.37 when the silica gel eluted with the mobile phase of 70% (v/v) EtOAc in n-hexane. Its molecular ion  $[M-H]^+$  at m/z 285 (Calc 285.1), with a molecular formula of  $C_{17}H_{16}O_4$  (**Spectrum 5.15**).

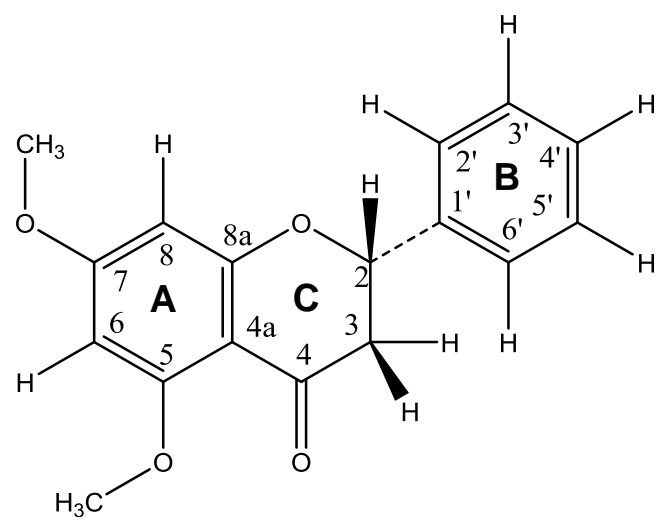
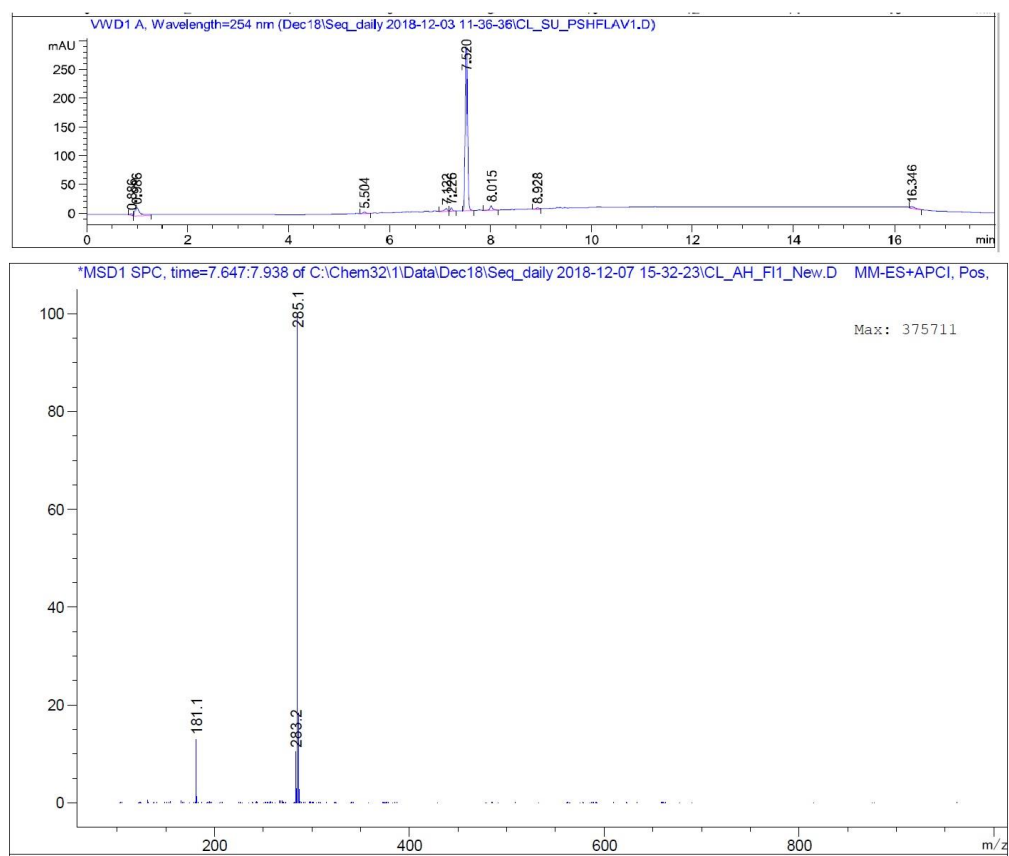


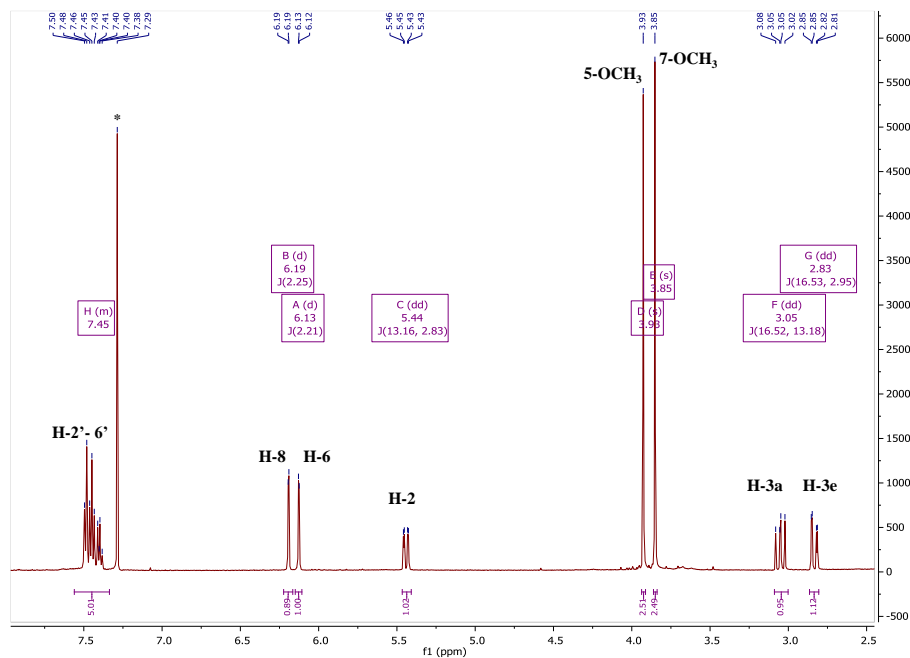
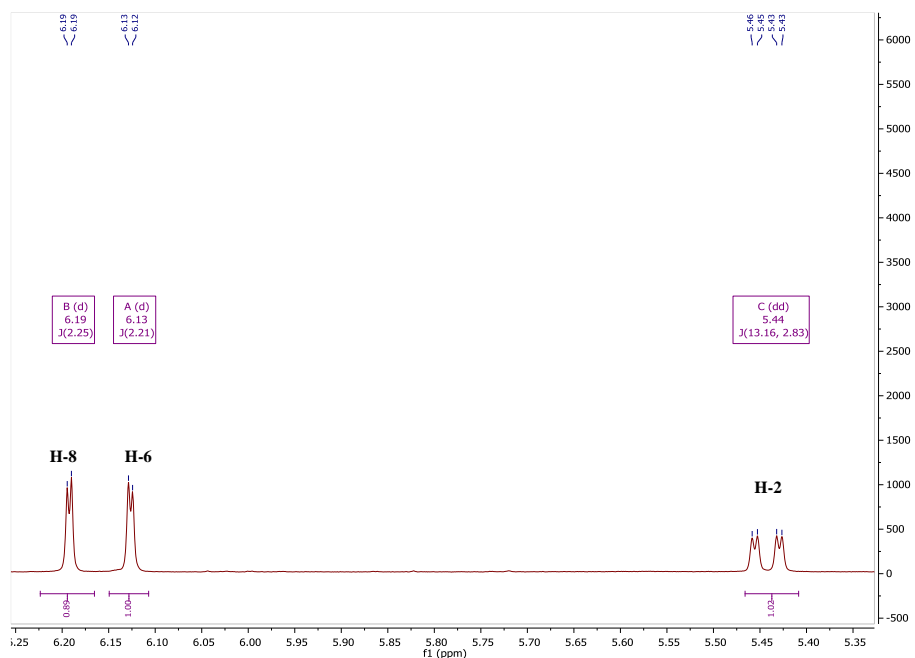
**Figure 5.3:** Chemical structure of 5,7-dimethoxyflavanone



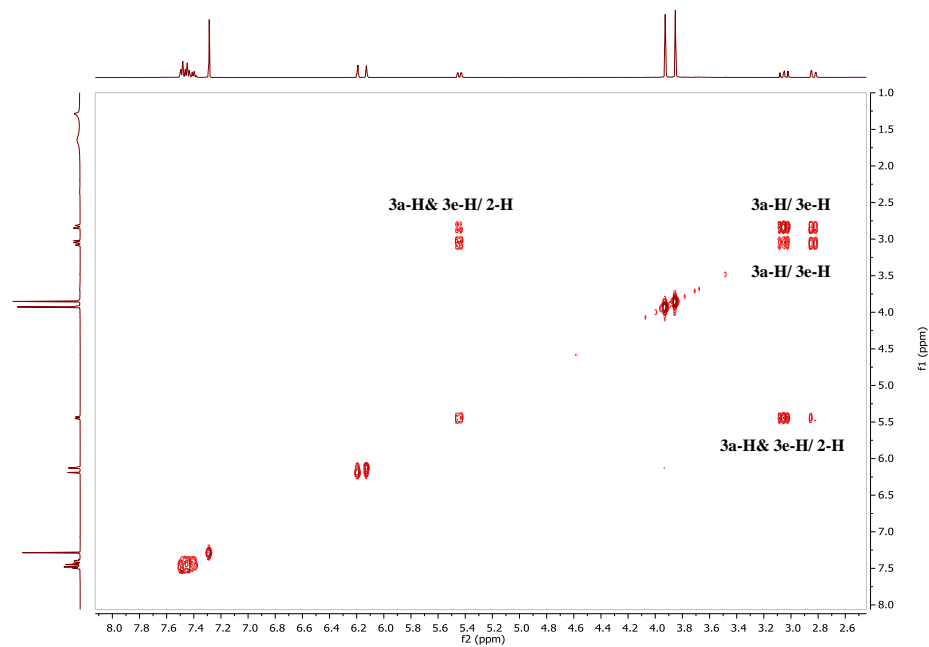
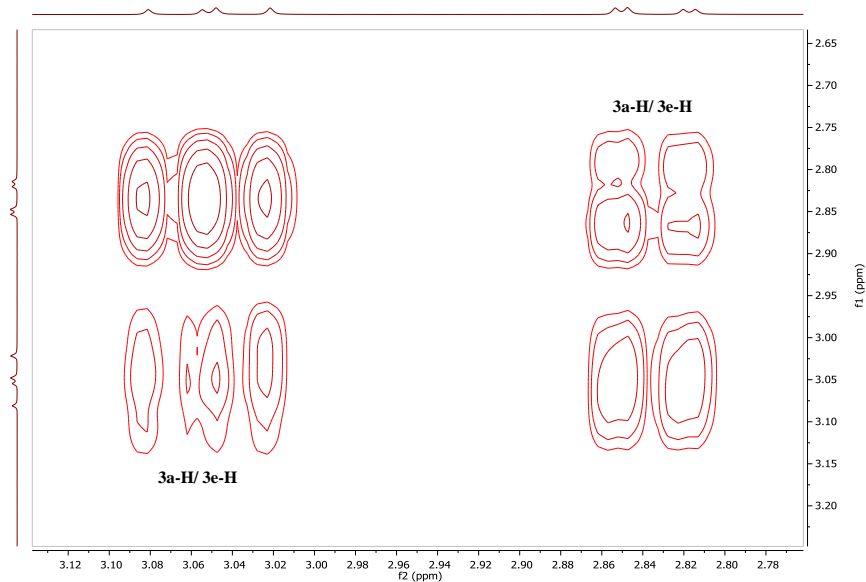
**Spectrum 5.15:** Molecular ion peak  $[M-H]^+$  spectrum of 5,7-dimethoxyflavone.

## NMR data analysis

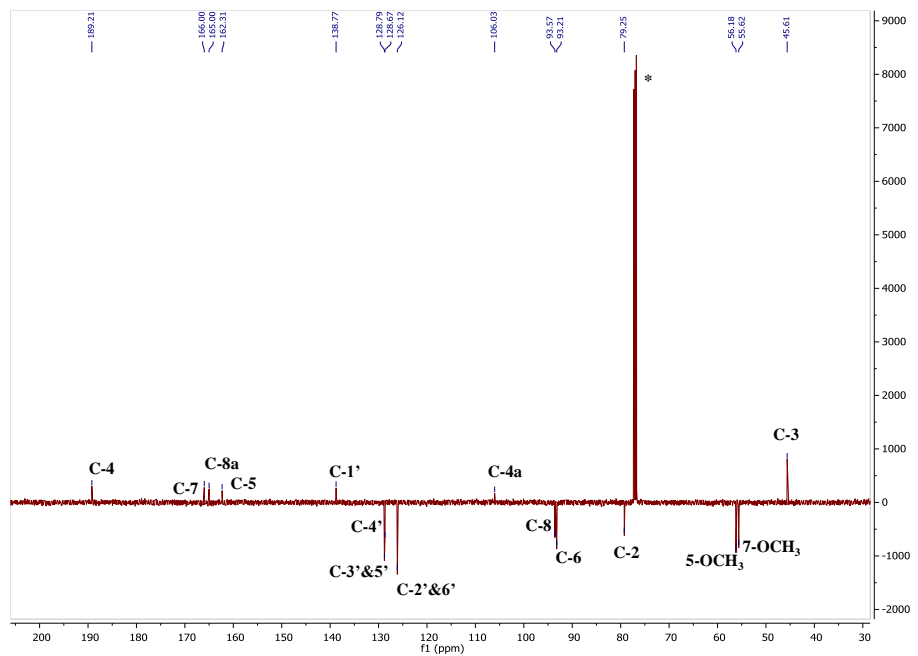
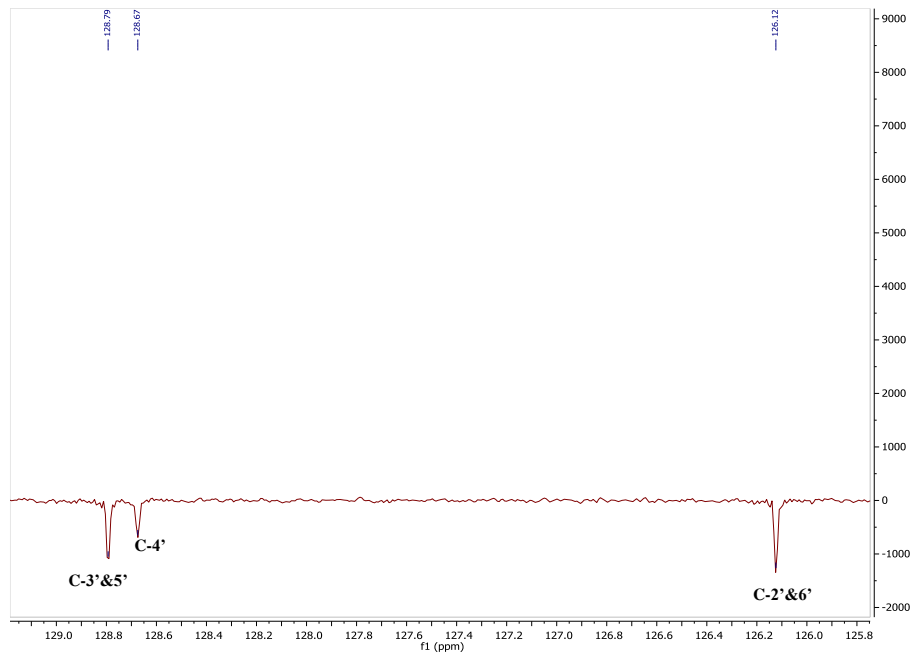
The proton spectrum showed the presence of seven aromatic protons (**Spectrum 5.16**), which was suggested to be from a flavanone nucleus. Based on integration and  $^1\text{H}$ - $^1\text{H}$  couplings (**Spectrum 5.17**) in the COSY spectrum, the proton signal at  $\delta_{\text{H}}$  5.44 ppm (1H, dd,  $J=13.1, 2.83$ ) shows the ABX spin pattern with the axial proton at  $\delta_{\text{H}}$  3.05 ppm (1H, dd,  $J=16.50, 13.18$ ) and with equatorial one at  $\delta_{\text{H}}$  2.83 ppm (1H, dd,  $J=16.50, 2.83$ ). Protons H-2', H-3', H-4', H-5' and H-6' on the mono-substituted ring-B appeared as a multiplet between  $\delta_{\text{H}}$  7.37 and 7.45 ppm (5H, m). The meta-coupled aromatic protons at  $\delta_{\text{H}}$  6.13 ppm (1H, d,  $J=2.25$ ) and 6.19 ppm (1H, d,  $J=2.25$ ) were assigned to H-6 and H-8, respectively. The signals at  $\delta$  3.85 ppm (3H, s) and 3.98 ppm (3H, s) were assigned to 7 and 5-OCH<sub>3</sub>, respectively. The  $^{13}\text{C}$  spectrum of this compound (**Spectrum 5.18**) showed the presence of 15 variable signals corresponding to carbon atoms of the flavanone structure and two meta-substituted methoxy groups. The S- configuration of ring-B at C-2 is corroborated depending on the trans-diaxial coupling (13.16) between H-2 and Ha-3. The methoxy group protons at  $\delta_{\text{H}}$  3.85 and 3.98 ppm showed long range correlations to the carbons at  $\delta_c$  at 166.0 (C-7) and 162.3 (C-5) respectively (**Spectrum 5.19** and **Spectrum 5.20**), hence they must be attached to these carbons also. These assignments were further supported by the HMBC spectrum for the compound and the full chemical shift assignments are given in **Table 5.3**.

**A****B**

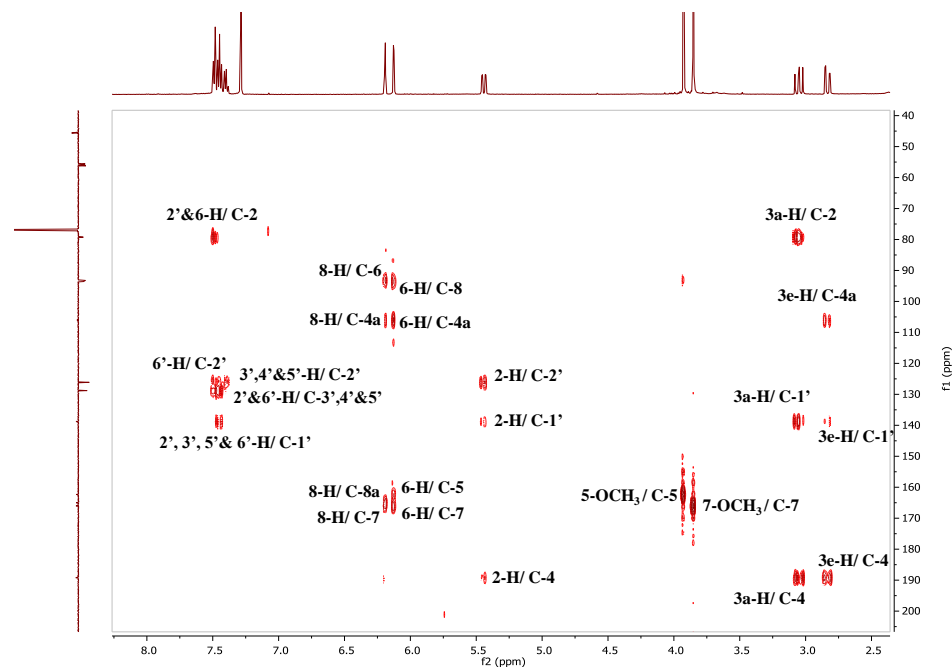
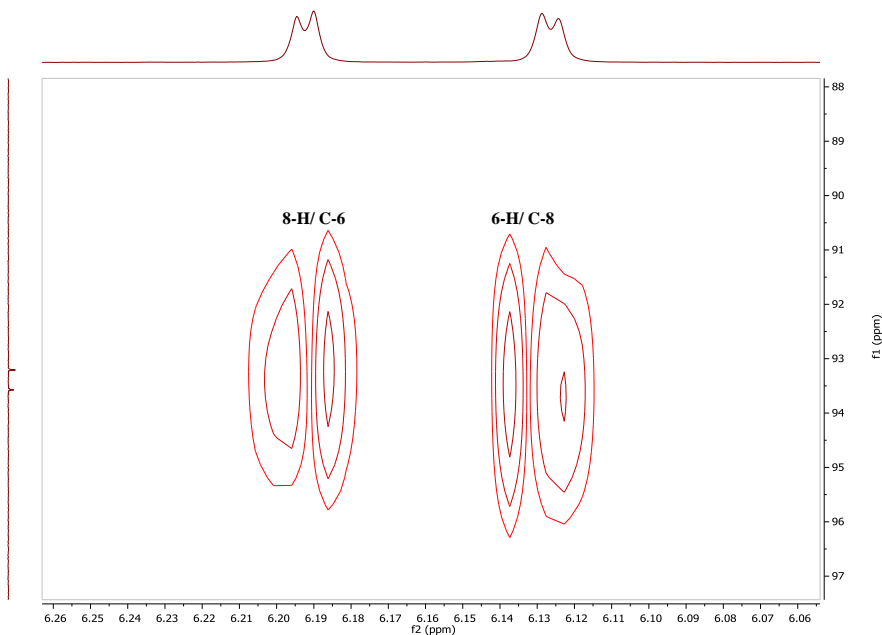
**Spectrum 5.16: (A) Full with (B) selected expansion of  $^1\text{H}$  NMR spectrum (400 MHz) of 5,7-dimethoxyflavanone in Chloroform-*d*.**

**A****B**

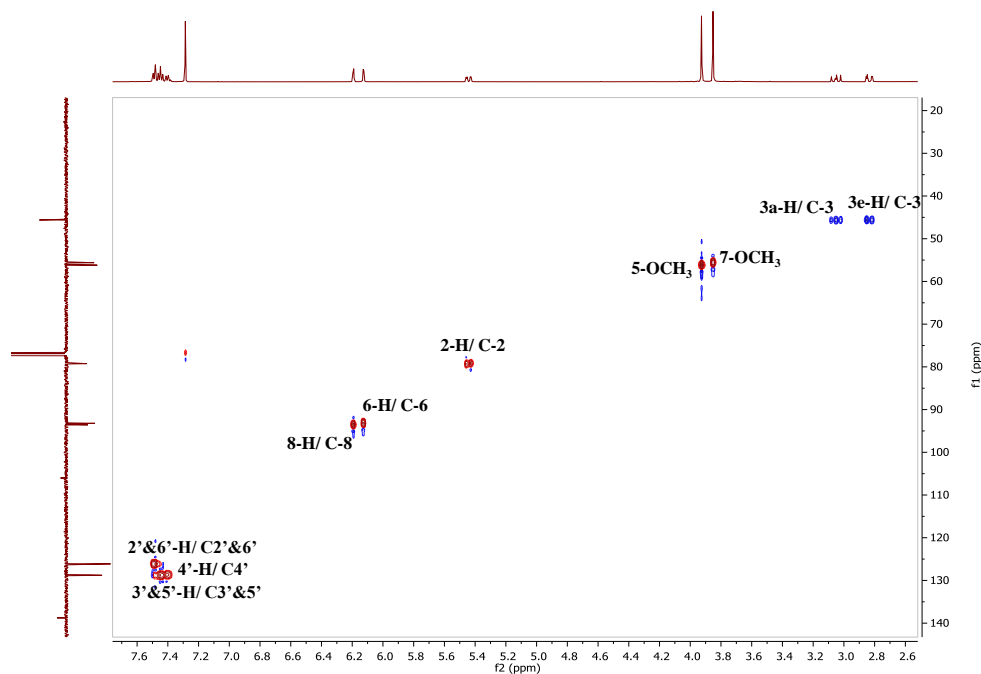
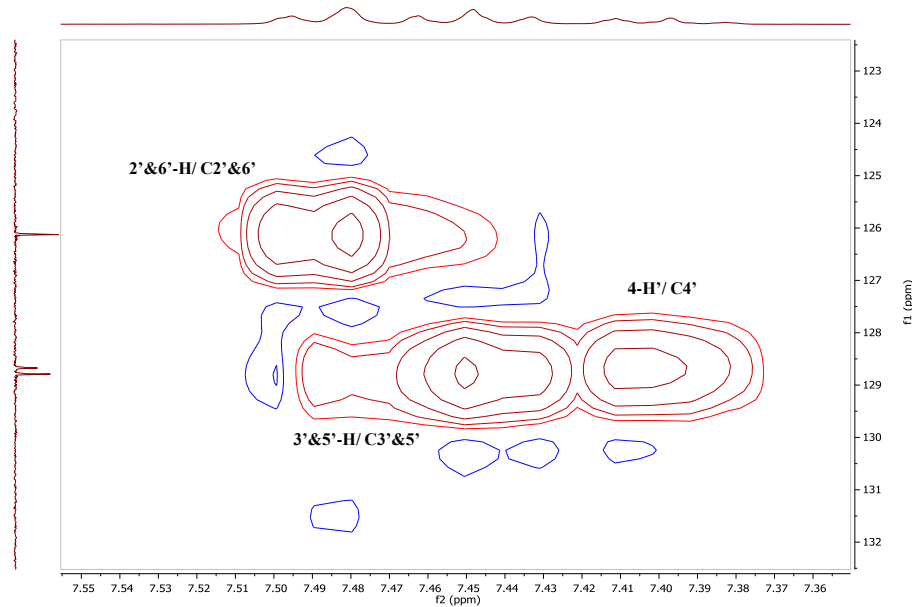
**Spectrum 5.17: (A) Full and (B) selected expansion of COSY spectrum (400 MHz) of 5,7-dimethoxyflavanone in Chloroform-*d*.**

**A****B**

**Spectrum 5.18: (A) Full and (B) selected expansion of DEPTq 135  $^{13}\text{C}$  NMR spectrum (100 MHz) of 5,7-dimethoxyflavanone in Chloroform-*d*.**

**A****B**

**Spectrum 5.19: (A) Full and (B) selected expansion of HMBC spectrum (400 MHz) of 5,7-dimethoxyflavanone in Chloroform-*d*.**

**A****B**

**Spectrum 5.20: (A) Full and (B) selected expansion of HSQC spectrum (400 MHz) of 5,7-dimethoxyflavanone in Chloroform-*d*.**

**Table 5.3: NMR data for 5,7-dimethoxyflavanone in chloroform-*d***

Position	$\delta_{\text{H}}$ (mult, <i>J</i> (Hz))	$\delta_{\text{C}}$ (mult)	HMBC correlations
2	5.44 (1H, dd, 13.1, 2.8)	79.2	C-2', C-1', Carbonyl
3	2.83 (1H, dd, 16.5, 2.8)	45.6	C-1', C-4a, Carbonyl
3	3.05 (1H, dd, 16.5, 13.1)	45.6	C-1', Carbonyl, C-2
4	-	189.2	-
4a	-	106.0	-
5	-	162.3	
O-CH <sub>3</sub>	3.98 (3H, s)	56.1	C-5
6	6.13 (1H, d, 2.2)	93.2	C-8, C-4a, C-7, C-5
7	-	166.0	-
O-CH <sub>3</sub>	3.85 (3H , s)	55.6	C-7
8	6.19 (1H, d, 2.2)	93.58	C-8a, C-4a , C-6
8a	-	165.0	-
1'	-	138.7	-
2' &6'	7.5 (2H)	126.1	C-2, C-3', C-4', C-5', C-1'
3', 4'&5'	7.38 (3H)	128.67 and 128.79	C-2', C-1'

#### 5.3.1.1.4 Characterisation of 5,8-dimethoxy-7-hydroxyflavanone

This compound (5,8-dimethoxy-7-hydroxyflavanone) was separated from the combined fractions (90-97) of the hexane extract of *P. salicifolium*, using 10% (v/v) MeOH in EtOAc as the mobile phase for PTLC. This compound (**Figure 5.4**) was obtained as a white solid with a yield of 10 mg (1%). On the TLC, it appeared as a dark spot under short UV light ( $\lambda$  254 nm), and a white spot under longer UV light ( $\lambda$  365 nm), which turned to a yellow spot upon spraying with *p*-anisaldehyde-sulphuric acid reagent followed by heating. Its  $R_f$  was 0.32 on silica gel when eluted with the mobile phase of 70% (v/v) EtOAc in n-hexane. Its molecular ion  $[M-H]^+$  at m/z 301 (Calc 301.2), suggesting the molecular formula of  $C_{17}H_{16}O_5$  (**Spectrum 5.21**).

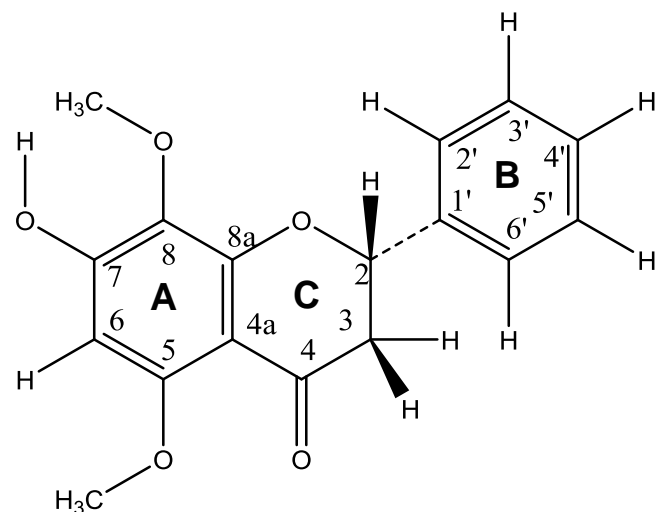
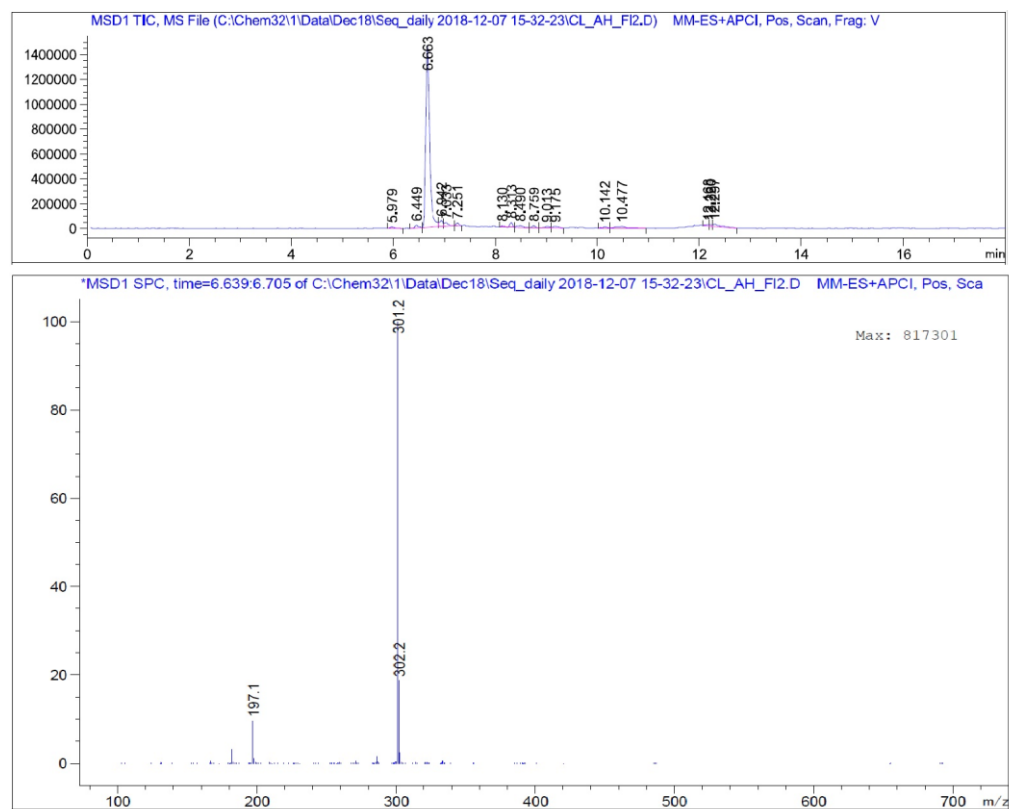


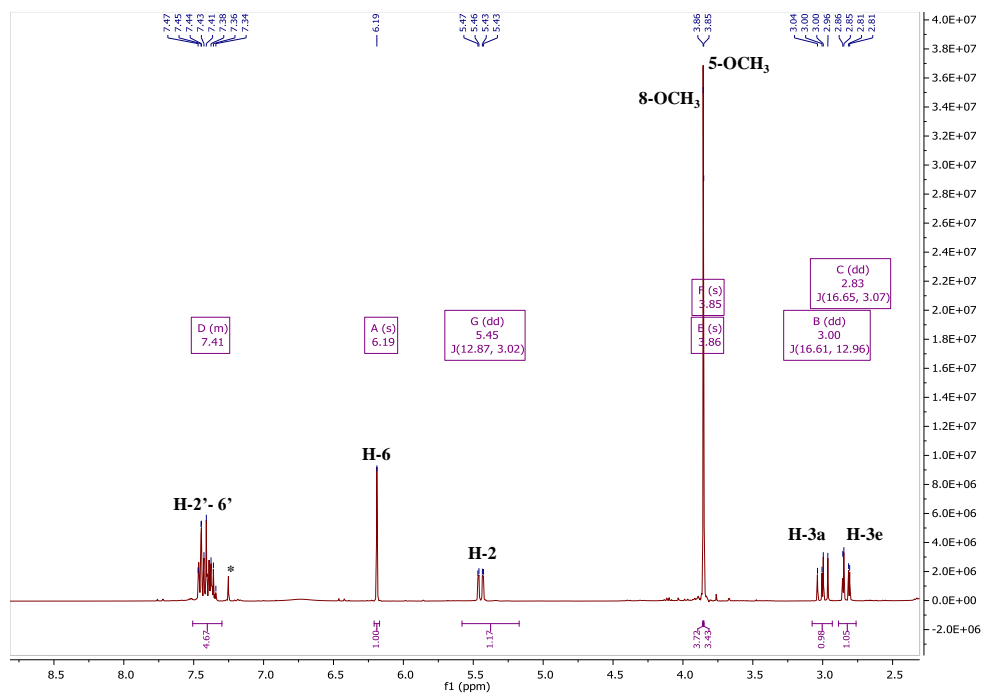
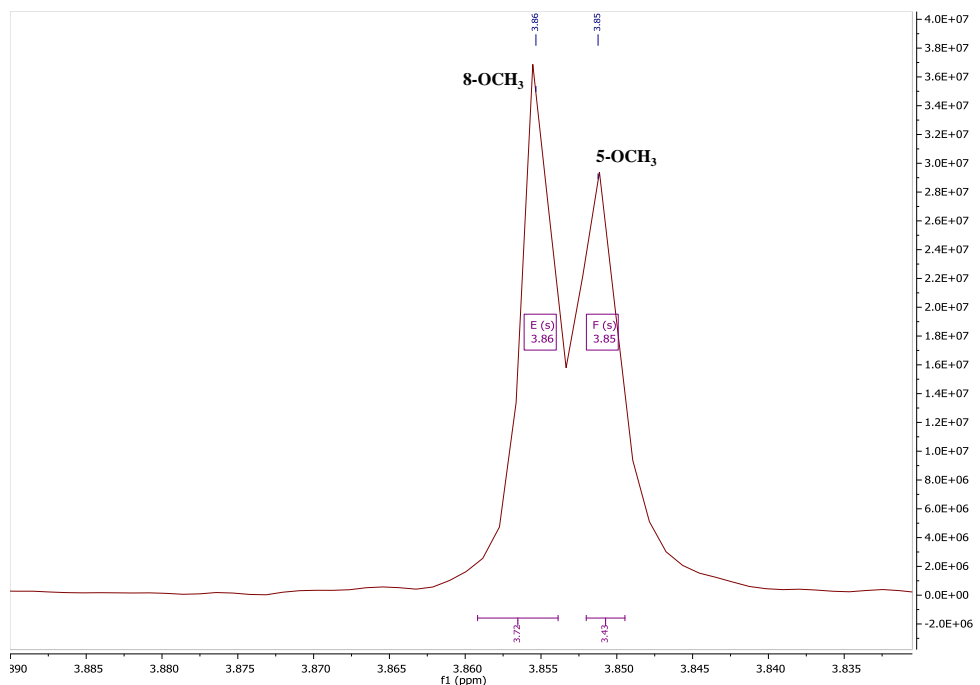
**Figure 5.4:** Chemical structure of 5,8-dimethoxy-7-hydroxyflavanone



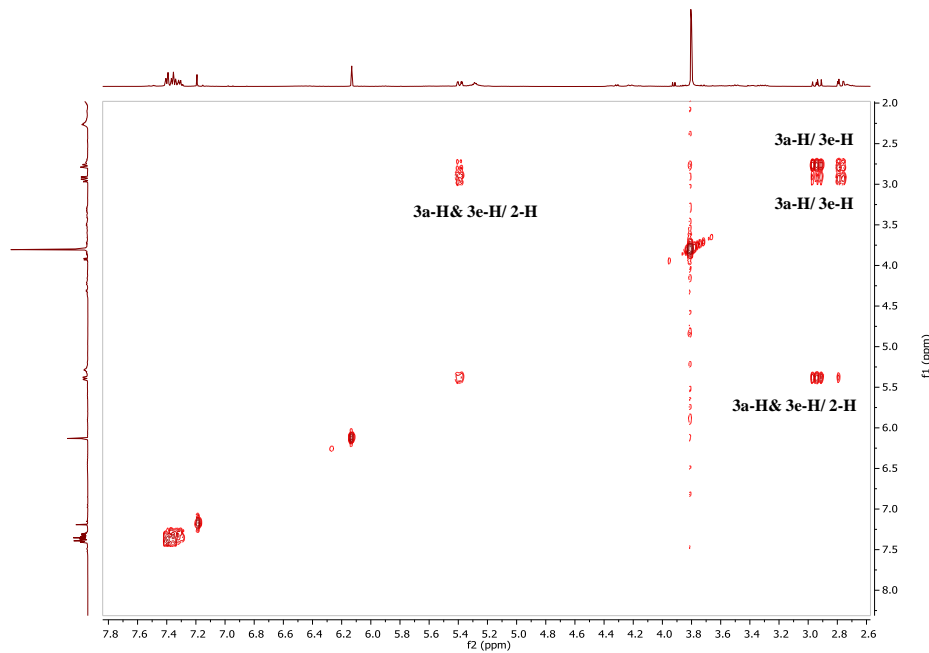
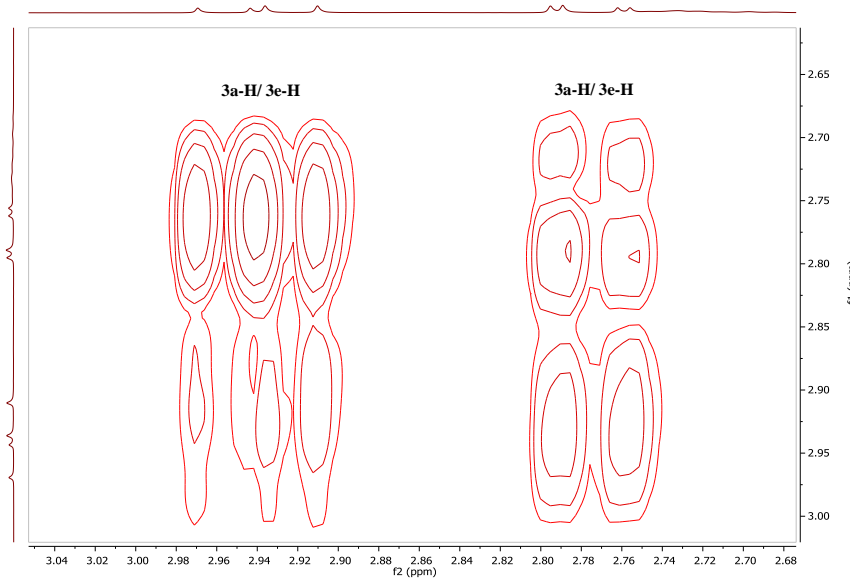
**Spectrum 5.21:** Molecular ion peak  $[M-H]^+$  spectrum of 5,8-dimethoxy-7-hydroxyflavanone.

## NMR data analysis

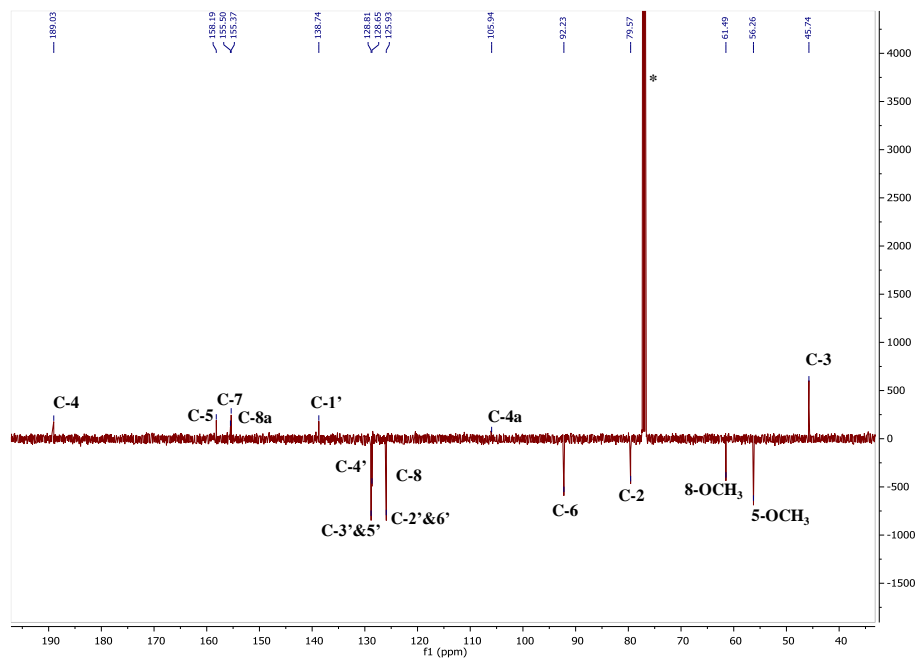
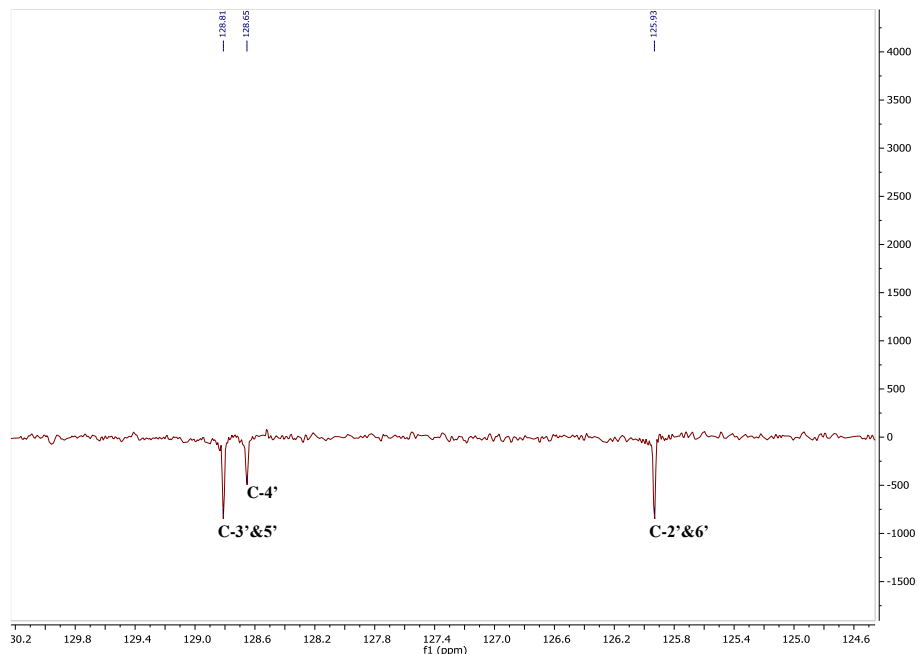
The proton spectrum was similar to that of 5,7-dimethoxy flavanone, but showed six aromatic protons (**Spectrum 5.22**). The difference was due to an extra substitution in the tetra-substituted ring whereas the mono-substituted ring protons were still identical. This was confirmed by the disappearance of the meta-coupled protons in 5,7-dimethoxyflavanone, now replaced by a proton singlet in 5,8-dimethoxy-7-hydroxyflavanone. The proton signal at  $\delta$  5.45 ppm (1H, dd,  $J=12.87, 3.02$ ) shows the ABX spin pattern with the axial proton at  $\delta_H$  3.0 ppm (1H, dd,  $J= 16.61, 12.96$ ) and with the equatorial one at  $\delta_H$  2.83 ppm (1H, dd,  $J=16.65, 3.07$ ) (**Spectrum 5.23**). The two methoxy groups appeared at  $\delta_H$  3.86 and 3.85 ppm. The appearance of the proton at  $\delta_H$  6.19 ppm as a singlet (1H, s) and the long range coupling with the carbon bearing hydroxyl group(C-7) and with the carbon bearing methoxy group (C-5) confirmed the penta substitution of ring-A. Signals between  $\delta_H$  7.35 and 7.47 ppm (5H, m) are attributed to the five protons of the unsubstituted ring-B. The signals at  $\delta_H$  3.85 ppm (3H, s) and 3.86 ppm (3H, s) were assigned to 5 and 8-OCH<sub>3</sub> respectively. The <sup>13</sup>C spectrum of this compound (**Spectrum 5.24**) showed the presence of 15 variable signals corresponding to carbon atoms of the flavanone structure and two para- substituted methoxy groups. Using the HMBC and HSQC spectra for the compound (**Spectrum 5.25** and **Spectrum 5.26**), the complete chemical shift assignments (**Table 5.4**) were made as follows: The methoxy protons at  $\delta_H$  3.85 and 3.86 ppm showed long range correlations to C-5 at  $\delta_c$  158.19 and C-8 at  $\delta_c$  128.65, respectively. The S- configuration of ring-B at C-2 is corroborated depending on the trans-diaxial coupling (12.96) between H-2 and Ha-3.

**A****B**

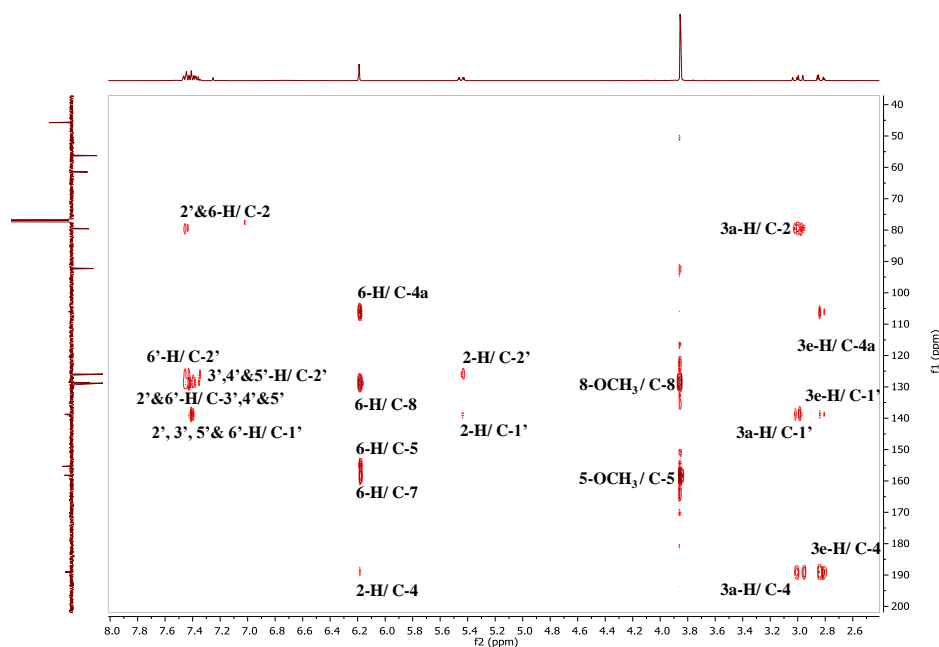
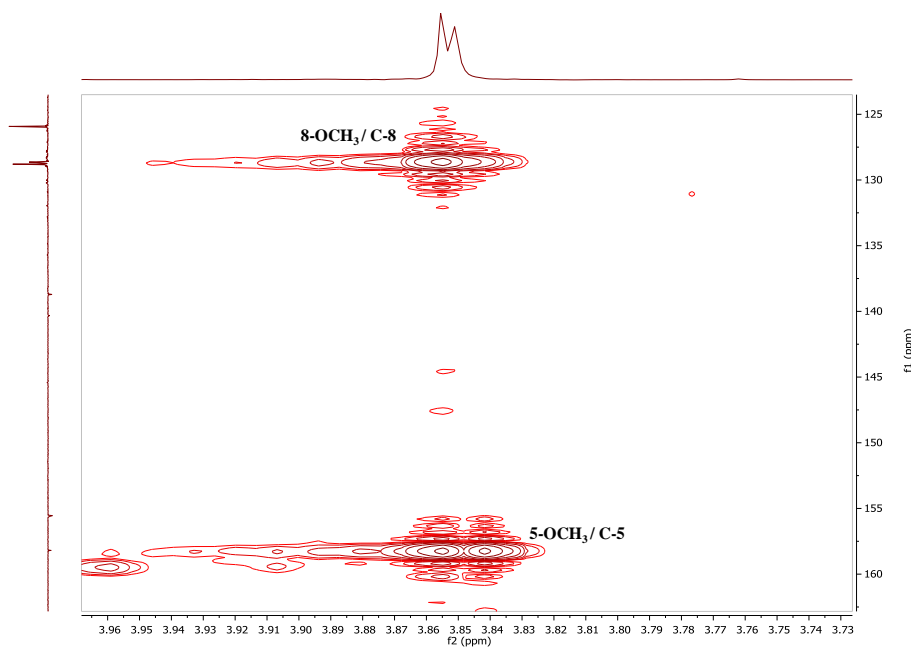
**Spectrum 5.22:** (A) Full <sup>1</sup>H NMR spectrum (400 MHz) of 5,8-dimethoxy-7-hydroxyflavanone and (B) selected expansion of the two methoxy region in Chloroform-*d*.

**A****B**

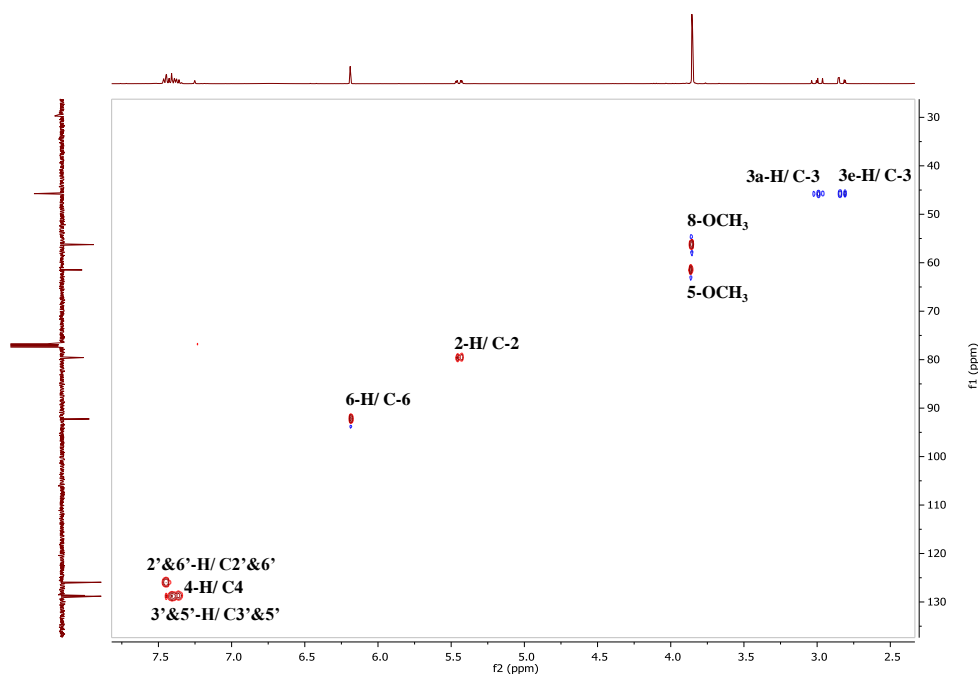
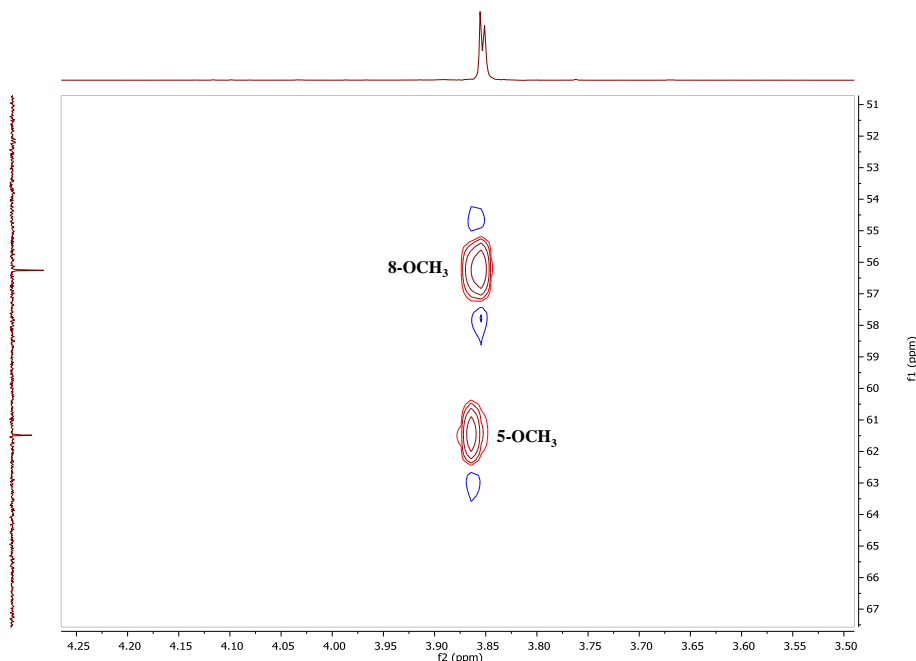
**Spectrum 5.23: (A) Full with (B) Selected expansion of COSY spectrum (400 MHz) of 5,8-dimethoxy-7-hydroxyflavanone in Chloroform-*d*.**

**A****B**

**Spectrum 5.24:** (A) Full DEPTq 135  $^{13}\text{C}$  NMR spectrum (100 MHz) of 5,8-dimethoxy-7-hydroxyflavanone with selected expansion of the ring-B in Chloroform-*d*.

**A****B**

**Spectrum 5.25: (A) Full HMBC spectrum (400 MHz) and (B) selected expansion of the methoxy peaks of 5,8-dimethoxy-7-hydroxyflavanone in Chloroform-*d*.**

**A****B**

**Spectrum 5.26: (A) Full and (B) selected expansion of HSQC spectrum (400 MHz) of 5,8-dimethoxy-7-hydroxyflavanone in Chloroform-*d*.**

**Table 5.4: NMR data for 5,8-dimethoxy-7-hydroxyflavanone in chloroform-*d***

Position	$\delta_{\text{H}}$ (mult, <i>J</i> (Hz))	$\delta_{\text{C}}$ (mult)	HMBC correlations
2	5.45 (1H, dd, 12.87, 3.02)	79.57	C-2', C-1', Carbonyl
3	2.83 (1H, dd, 16.65, 3.07)	45.74	C-4a, Carbonyl, C-1'
3	3.0 (1H, dd, 16.61, 12.96)	45.74	C-1', Carbonyl, C-2
4	-	189.0	-
4a	-	105.9	-
5	-	158.1	-
O-CH <sub>3</sub>	3.85 (3H, s)	56.1	C-5
6	6.20 (1H, s)	92.1	C-8, C-4a , C-7, C-5
7	OH	156.0	-
8	-	128.6	-
O-CH <sub>3</sub>	3.86 (3H , s)	61.4	C-8
8a	-	155.5	-
1'	-	138.7	-
2' &6'	7.47 (2H)	125.9	C-2, C-3', C-4', C-5'
3', 4'&5'	7.34 (3H)	128.8	C-2', C-1'

### **5.3.2 Vasorelaxant effects of the methanolic extract of *H. sabdariffa***

#### **5.3.2.1 Effect of the crude methanolic extract of *P. salicifolium* on rat aorta**

##### **5.3.2.1.1 Effect of the crude methanolic extract of *P. salicifolium* on the endothelium-intact rat aorta pre-contracted with PE**

The crude methanolic extract of *P. salicifolium* caused a concentration-dependent relaxation of the endothelium-intact aorta contracted with PE (3  $\mu$ M). The IC<sub>50</sub> for the extract was  $0.04 \pm 0.007$  mg/ml (**Figure 5.5** and **Figure 5.6**), and the highest concentration tested (0.1 mg/ml) almost completely relaxed the tissue ( $95 \pm 5\%$  relaxation) (n=7/3). The relaxation was maintained for as long as the extract was present, and the tissue showed complete recovery in its response to PE after washing out the extract and allowing approximately 60 min for recovery.

##### **5.3.2.1.2 Effect of the crude methanolic extract of *P. salicifolium* on the endothelium-denuded rat aorta pre-contracted with PE**

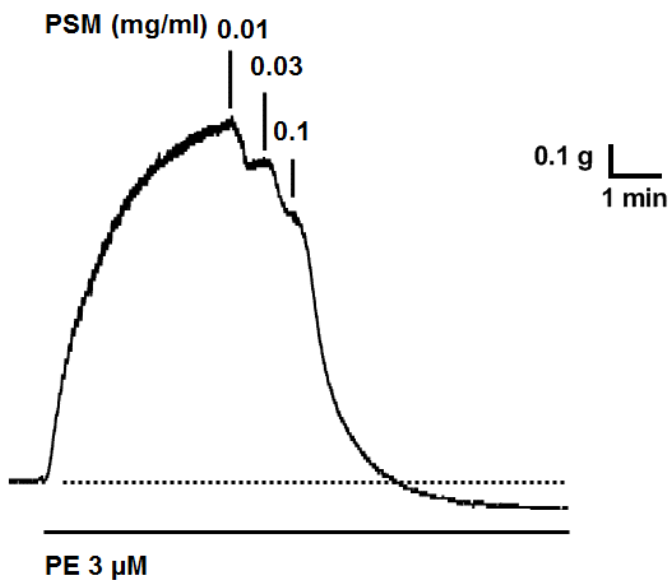
The relaxant effect of the crude methanolic extract of *P. salicifolium* (0.01-0.5 mg/ml), was also examined on endothelium-denuded aorta. In this situation, the relaxant activity of the extract was completely inhibited upon removal of the endothelium (**Figure 5.7**).

##### **5.3.2.1.3 Effect of the crude methanolic extract of *P. salicifolium* on the rat aorta pre-contracted with KCl**

The effect of the crude methanolic extract of *P. salicifolium* was also examined on the aorta pre-contracted with KCl (60 mM). There was no relaxant activity observed

when the crude methanolic extract of *P. salicifolium* was applied on the aorta pre-contracted with KCl, even at the highest concentration tested (1 mg/ml) (**Figure 5.8**)

**A**



**B**

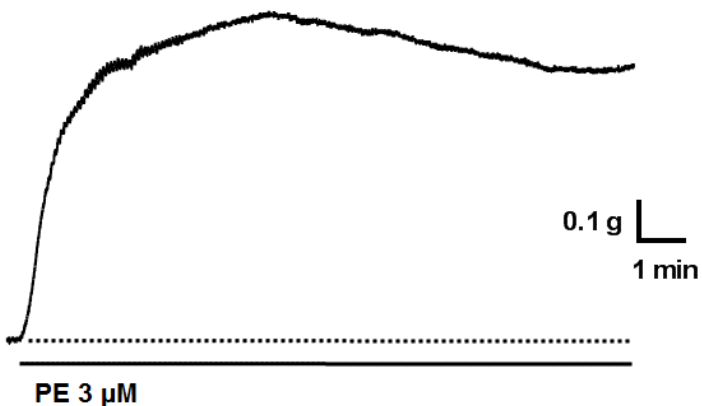


**Figure 5.5: Relaxant effect of the crude methanolic extract of *P. salicifolium* (PSM) on the endothelium-intact rat aorta pre-contracted with PE (3  $\mu$ M).** (A) Representative recordings of the effect of PSM on the endothelium-intact aorta pre-contracted with PE (3  $\mu$ M). (B) Representative recordings of the time control, showing slight decline in the contractile response by the end of the experiment.

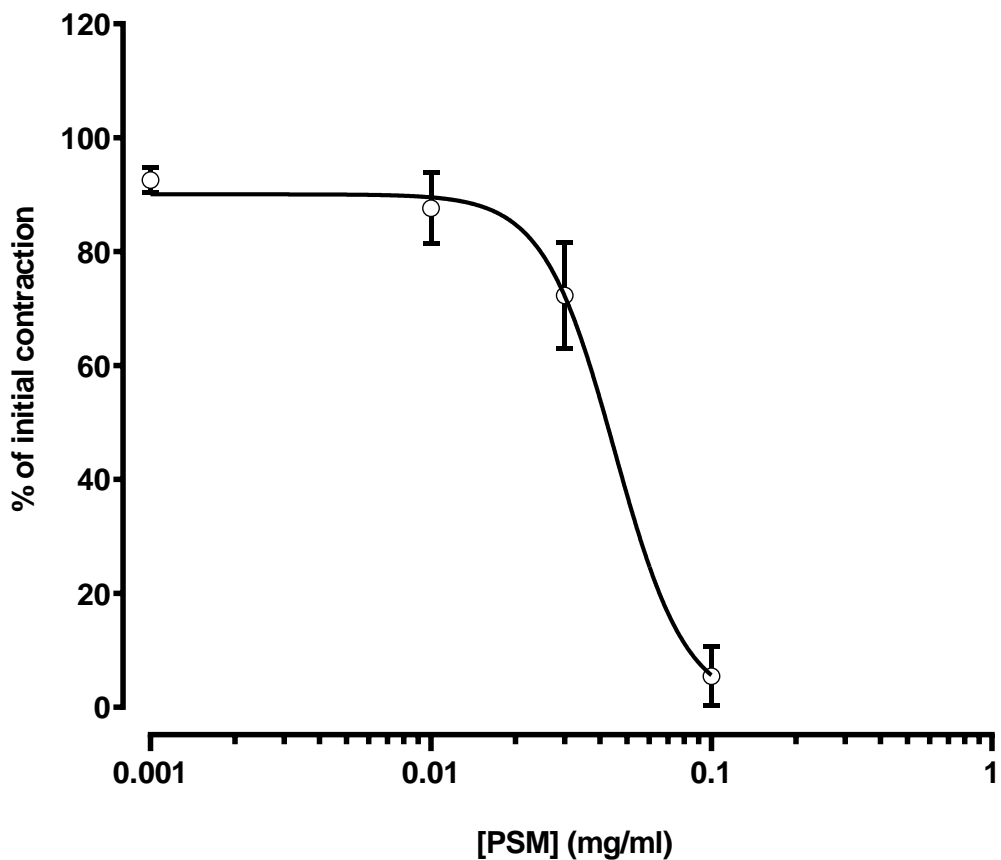


**Figure 5.6: Relaxant effect of the crude methanolic extract of *P. salicifolium* (PSM) on the endothelium-intact rat aorta pre-contracted with PE (3  $\mu$ M).** Summary figure showing the relaxant effect of PSM in concentrations (0.001-0.1 mg/ml) on the PE pre-contracted aorta. The relaxation is expressed as a percentage of the initial contraction. Data represent mean  $\pm$  s.e.m. (n=7/3).

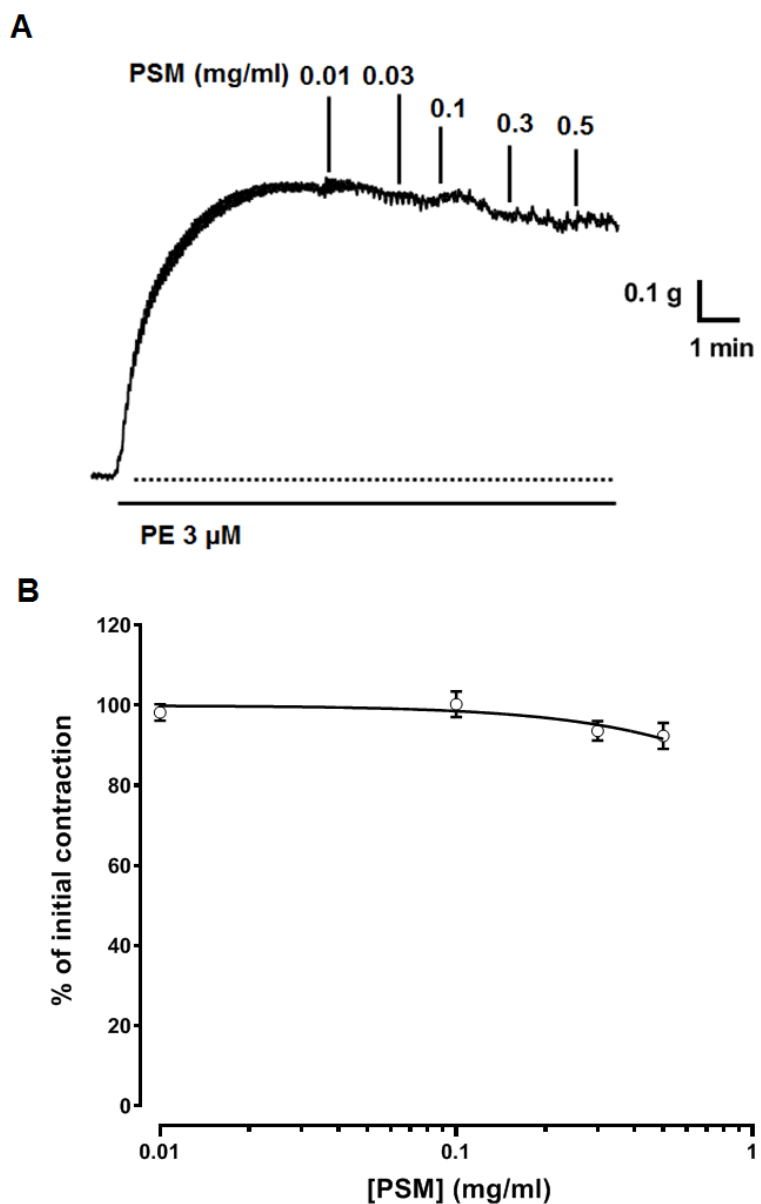


**Figure 5.7: Effect of the crude methanolic extract of *P. salicifolium* (PSM) on the endothelium-denuded rat aorta pre-contracted with PE.** (A) Representative recordings of the effect of PSM (0.01-0.5 mg/ml) on the endothelium-denuded aorta pre-contracted with PE (3  $\mu$ M). (B) Summary figure showing the absence of the relaxant effect of PSM in concentrations (0.01-0.5 mg/ml) on the PE pre-contracted aorta. The response is expressed as a percentage of the initial contraction. Data represent mean  $\pm$  s.e.m. (n=6/3).

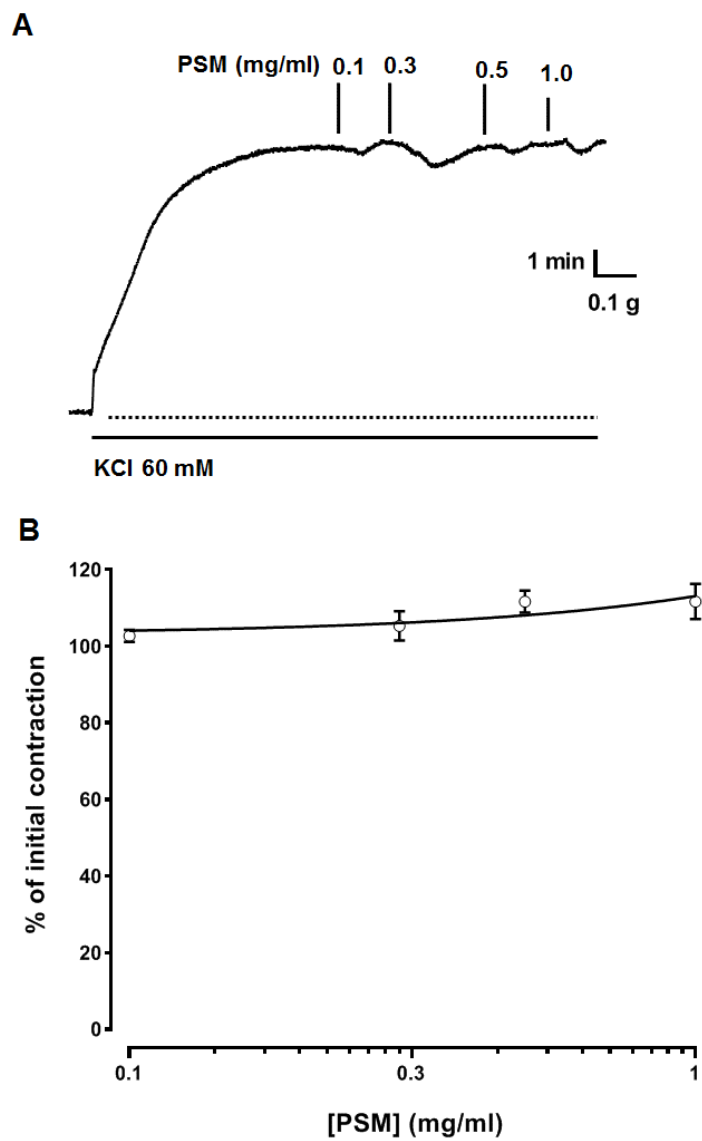


**Figure 5.8: Effect of the crude methanolic extract of *P. salicifolium* (PSM) on the rat aorta pre-contracted with KCl.** (A) Representative recordings of the effect of the PSM (0.1-1.0 mg/ml) on the aorta pre-contracted with KCl (60 mM). (B) Summary figure showing the absence of the relaxant effect of PSM in concentrations (0.1-1.0 mg/ml) on the KCl pre-contracted aorta. The response is expressed as a percentage of the initial contraction. Data represent mean  $\pm$  s.e.m. (n=7/3).

## 5.4 Discussion

The phytochemical studies of the hexane extract of *P. salicifolium* led to the isolation and purification of two chalcone compounds; 2',4'-dimethoxy-6'-hydroxychalcone, and 2',5'-dimethoxy-4',6'-dihydroxychalcone. Two flavanone compounds were also isolated and purified from the crude hexane extract; 5,7-dimethoxyflavanone, and 5,8-dimethoxy-7-hydroxyflavanone. These compounds have not been isolated before from this *Polygonum* species (*P. salicifolium*).

The chalcone, flavokawain B has previously been isolated from the kava root, and has been reported as a potent hepatocellular toxin, which induces cell death in Hep G<sub>2</sub> cells (Zhou *et al.*, 2010) and human osteosarcoma cells (Ji *et al.*, 2013). This compound has also been isolated from the herb, *Alpinia pricei* (Zingiberaceae), and found to be a potent anti-inflammatory (Lin *et al.*, 2009). Recently, flavokawain B was isolated from the seeds of the plant *Persicaria lapathifolia*, and shown to have antimicrobial and antifungal activities (Hailemariam *et al.*, 2018). The compound, 2',5'-dimethoxy-4',6'-dihydroxychalcone has previously been isolated from the leaves of *P. limbatum* and shown to have cytotoxic, antimicrobial, anti-inflammatory and anticholinesterase activities (Dzoyem *et al.*, 2012, Dzoyem *et al.*, 2017).

The compound 5,7-dimethoxyflavanone has previously been isolated from the kava root (Xuan *et al.*, 2008). This compound has also been synthesised by chemical modification of 5,7-dimethoxyflavone and demonstrated to cause moderate cytotoxicity in human small cell lung cancer (NCI-H187) cell lines (Yenjai and Wanich, 2010).

5,8-dimethoxy-7-hydroxyflavanone has previously been isolated from the aerial part of *P. senegalense* (Ogweno Midiwo *et al.*, 2002). There are no reported biological activities of this compound. Thus for future work, screening of this compound for various biological activities, including antimicrobial and anticancer effects could be carried out.

The phytochemical studies also showed the presence of a number of different polyphenolic compounds including; isoflavonoids, flavonoids, and glycosides of flavonoids in the crude methanolic extract of *P. salicifolium*. These findings are in agreement with the previous work of Calis *et al.* (1999), Hussein and Mohamed, (2013), and Hussein *et al.* (2017), who showed the presence of various polyphenolic compounds, for instance astragalin, quercitrin, luteolin, isoquercitrin, quercetin, hyperoside, and rutin in the aerial parts of *P. salicifolium*.

One of the aims of this chapter was to determine whether this plant (*P. salicifolium*) has any vasorelaxant activity. The crude methanolic extract of *P. salicifolium* was found to have vasorelaxant effect on the aorta, and, subsequent studies were carried out to determine the potential mechanisms for this vasorelaxant activity.

The crude extract relaxed, concentration-dependently, the endothelium-intact aorta pre-contracted with PE. The relaxant effect of the crude extract was completely abolished upon removal of the endothelium. Therefore, it seems that the vascular relaxant effect of this plant depends on the presence of the endothelium.

The fact that the relaxant activity of the crude extract was completely abolished when the aorta pre-contracted with KCl, strongly suggests that inhibition of  $\text{Ca}^{2+}$  influx is unlikely to be the mechanism underlying the vasorelaxation. In addition, this finding provides further support for the notion that this extract acts via the endothelium. In this regard, when endothelium-intact blood vessels are depolarised with KCl, the relaxation produced by EDRFs is impaired (Duarte *et al.*, 2004, Raffetto *et al.*, 2012). It is possible that the endothelium-dependent vasorelaxant activity of the crude methanolic extract of *P. salicifolium* is due to the presence of polyphenols, since these have previously been shown to have a vasorelaxant effect (Andriambeloson *et al.*, 1997, Andriambeloson *et al.*, 1998, Benito *et al.*, 2002, Ndiaye *et al.*, 2004, Duarte *et al.*, 2004).

# **Chapter 6**

## **6 General discussion**

The main objective of this study was to determine the bioactive compound(s) present in the calyces of *H. sabdariffa* (Malvaceae), which could be responsible for its antihypertensive effect (Ali *et al.*, 2005, Hopkins *et al.*, 2013). When tested for vasorelaxant activity on the pre-contracted aorta, the crude methanolic extract of *H. sabdariffa* calyces produced a concentration-dependent relaxation. These findings are consistent with what has been previously reported by Obiefuna *et al.* (1994), Ajay *et al.* (2007), and Sarr *et al.* (2009), who also showed that the crude extract produced its activity via both endothelium-dependent and endothelium-independent mechanisms (Ajay *et al.*, 2007, Sarr *et al.*, 2009). The crude extract relaxed the PE pre-contracted aorta by ~90% and the IC<sub>50</sub> was 0.3 mg/ml. This is very similar to what has previously been reported by Ajay *et al.* (2007) with regard to potency (~ 0.15 mg/ml) and efficacy (~90% maximum relaxation) of the crude extract.

Subsequent purification of the crude extract using different chromatographic techniques including TLC, NMR, and LC-MS, led to the isolation of steroids, organic acids, and polyphenolic compounds. Hibiscus acid was the main organic acid isolated from the methanol extract, and it was also identified in the ethyl acetate extract of the calyces. Other compounds such as β-sitosterol and stigmasterol were isolated from the ethyl acetate extract. The flavonoid, quercetin was also isolated from the methanolic extract of this plant. It has previously been shown that quercetin has a

vasorelaxant effect that is both endothelium-dependent and endothelium-independent (Hou *et al.*, 2014, Yuan *et al.*, 2018). Therefore, this substance was not considered as the main focus in the present investigation given that a number of studies have already examined its vasorelaxant activity (Duarte *et al.*, 1993, Ke Chen and Pace-Asciak, 1996, Roghani *et al.*, 2004, Hou *et al.*, 2014, Yuan *et al.*, 2018).

Bioactivity-led fractionation of the methanolic extract of *H. sabdariffa* showed that sub-fractions enriched with hibiscus acid and its derivatives produced vasorelaxation. The organic acid, hibiscus acid and its derivative, hibiscus acid dimethyl ester were purified and obtained in their pure crystal form. The structure of both compounds was elucidated with the aid of the NMR, LC-MS, and X-ray crystallographic techniques. The absolute configuration of hibiscus acid was found to be (2S,3R) 3-hydroxy-5-oxo-tetrahydrofuran-2,3-dicarboxylic acid.

Pure hibiscus acid produced a concentration-dependent relaxation when applied to the pre-contracted aorta. Hibiscus acid was approximately 3 times more potent than the crude extract in terms of its vasorelaxant effect. In parallel studies, the activity of the commercially available diastereomer, garcinia acid, which is unique to the fruit of *G. cambogia* (Clusiaceae) was examined. Garcinia acid was found to have an almost identical effect to that of hibiscus acid. With regard to their mechanism of action, it was found that both hibiscus and garcinia acid act by an endothelium-independent mechanism; most likely through inhibition of  $\text{Ca}^{2+}$  influx, i.e. via blocking of VDCCs.

Comparing the relaxant activity of both hibiscus and garcinia acids to the inhibitory effects of the classical  $\text{Ca}^{2+}$  channel blockers showed that there were significant differences with regard to their potency. The  $\text{Ca}^{2+}$  channel blockers, nifedipine and diltiazem relax the KCl pre-contracted rat aorta with  $\text{IC}_{50}$  values of  $4.5 \times 10^{-9}$  M, and  $1.6 \times 10^{-7}$  M respectively (Yoshiaki *et al.*, 1991), while verapamil has an  $\text{IC}_{50}$  of  $9 \times 10^{-9}$  M (Winslow *et al.*, 1986). These  $\text{Ca}^{2+}$  channel blockers are less potent when the aorta is pre-contracted with PE contraction. Under such conditions, the  $\text{IC}_{50}$  values were  $1.0 \times 10^{-6}$  M,  $4.3 \times 10^{-6}$  M, and  $0.05 \times 10^{-6}$  M for nifedipine, diltiazem, and verapamil respectively (Winslow *et al.*, 1986). Hibiscus acid, and similarly garcinia acid relaxed both the PE and KCl contractions with  $\text{IC}_{50}$  values of  $250 \times 10^{-6}$  M, and  $20 \times 10^{-4}$  M respectively. Thus, it is apparent that the potency of hibiscus and garcinia acids in relaxing the PE contraction is approximately 250, 60, and 500 times less when compared to nifedipine, diltiazem, and verapamil respectively. However, in this study, a maximum concentration of PE was used to induce the contraction of the aorta, and this may affect the potency of both hibiscus and garcinia acids. It has been reported that increasing the concentration of PE from 0.3 to 3  $\mu\text{M}$  decreases the potency of the vasodilator, sodium nitroprusside by 16-fold (Streefkerk *et al.*, 2002).

Both hibiscus and garcinia acids also relaxed the trachea pre-contracted with carbachol or KCl; although their potency was less than what has previously been reported for nifedipine (Raeburn and Brown, 1991). Furthermore, similar to nifedipine and diltiazem (Raeburn and Brown, 1991, Matsuda *et al.*, 2000), both hibiscus and garcinia acids showed some selectivity in relaxing vascular tissue when compared to their relaxant effect on the non-vascular tissues.

The ability of both hibiscus and garcinia acids to inhibit the contraction of the electrically stimulated atria lends further support to the suggestion that both compounds are  $\text{Ca}^{2+}$  channel blockers. It is believed that the cardiovascular activities of hibiscus and garcinia acids are new to literature, and with respect to their potency, it could be increased by chemical modification of their functional groups.

Regarding the plant *P. salicifolium*, the phytochemical investigation revealed the presence of various constituents. Analysis of the methanol extract showed the presence of different flavonoids and glycosides of the flavonoids. As, the methanol extract contains the most polar polyphenolic compounds.

The methanol extract of the aerial part of *P. salicifolium* was found to be active in terms of vasorelaxation, when applied to the endothelium-intact aorta pre-contracted with PE. However, the extract had no vasorelaxant activity when applied to the denuded aorta. Furthermore, the relaxant effect of the extract was completely inhibited when the aorta was pre-contracted with KCl. Therefore, it seems that this plant (*P. salicifolium*) acts through an endothelium-dependent mechanism to produce its vasorelaxant activity.

Further phytochemical investigation of the hexane extract of *P. salicifolium* was carried out, and a total of four compounds were isolated. Among them, two chalcones and two flavanones were identified and isolated, namely 2',4'-dimethoxy-6'-hydroxychalcone, 2',5'-dimethoxy-4',6'-dihydroxychalcone, 5,7-dimethoxy flavan-

one, and 5, 8-dimethoxy-7-hydroxyflavanone. Previous published studies have shown that these compounds have anticancer and antimicrobial properties (Zhou *et al.*, 2010, Dzoyem *et al.*, 2017, Yenjai and Wanich, 2010).

## 6.1 Recommendations for future work

It is strongly suggested that the mechanism by which hibiscus acid and garcinia acid produce their vasorelaxant effect, is by inhibiting  $\text{Ca}^{2+}$  influx via VDCCs. However, this interpretation awaits confirmation with more direct electrophysiological approaches, such as whole-cell patch-clamp recording. This would involve testing the effect of both hibiscus and garcinia acid on whole-cell  $\text{Ca}^{2+}$  currents in isolated smooth muscle cells.

This thesis has only examined the vasorelaxant activity of the crude methanolic extract of *P. salicifolium*. An attempt to purify and identify the constituents isolated from the crude methanolic extract was carried out, using VLC and GPC. It seems that the separation techniques that were used were not efficient, quantitatively, to be able to isolate these compounds in more purified forms. In addition, the small quantities of the polyphenolic mixtures precluded attempts to separate them, thus, this can be considered for the future, using more of the starting materials. Further work, particularly bioactivity-led fractionation will be required to be carried out on the methanolic extract, which exerted potent activity in an attempt to determine the compounds; which are responsible for the vasorelaxant effects of this plant. This could be done using advanced separation techniques such as Semi-Prep HPLC. In addition, further pharmacological work needs to be done on the endothelium to better

understand the exact mechanism by which these isolated bioactive compounds exert their vasorelaxation.

## 6.2 Conclusion

This thesis has reported the vasorelaxant effect of hibiscus acid, which could potentially explain, at least in part, the vasorelaxant activity of *H. sabdariffa*. This study has also shown a comparable vasorelaxant activity with the diastereomer, garcinia acid. Both acids appear to produce their vasorelaxant activity via blockade of VDCCs. Furthermore, this study provides support for the traditional use of the extracts or teas of *H. sabdariffa* as an antihypertensive natural product.

With respect to *P. salicifolium*, this thesis has characterised the phytochemical constituents in more detail, indicating the presence of various constituents such as chalcones, flavanones, flavonoids, and flavonoid glycosides. The findings have shown that *P. salicifolium* has vasorelaxant activity. This plant appears to produce its vasorelaxant activity through activation of the endothelium. The findings regarding the vasorelaxant activity of *P. salicifolium* are still in their infancy, yet they do support a potential therapeutic use for this plant as well.

## 7 References

- Abdul Hamid, Z., Lin Lin, W. H., Abdalla, B. J., Bee Yuen, O., Latif, E. S., Mohamed, J., Rajab, N. F., Paik Wah, C., Wak Harto, M. K. & Budin, S. B. (2014). The role of *Hibiscus sabdariffa* L. (Roselle) in maintenance of *ex vivo* murine bone marrow-derived hematopoietic stem cells. *Scientific World Journal*, 2014, 258192-258202.
- Abubakar, M., Ukwuani, A. & Mande, U. (2015). Antihypertensive Activity of *Hibiscus sabdariffa* aqueous calyx extract in Albino Rats. *Sky Journal of Biochemistry Research*, 4, 16-20.
- Adegunloye, B., Omoniyi, J., Owolabi, O., Ajagbonna, O., Sofola, O. & Coker, H. (1996). Mechanisms of the blood pressure lowering effect of the calyx extract of *Hibiscus sabdariffa* in rats. *African Journal of Medicine and Medical Sciences*, 25, 235-238.
- Ahmad, L., Semotiuk, A. J., Liu, Q.-R., Rashid, W., Mazari, P., Rahim, K. & Sadia, S. (2018). Anti-hypertensive plants of rural Pakistan: Current use and future potential. *Journal of Complementary Medicine Research*, 7, 138-153.
- Ajay, M., Chai, H., Mustafa, A., Gilani, A. H. & Mustafa, M. R. (2007). Mechanisms of the anti-hypertensive effect of *Hibiscus sabdariffa* L. calyces. *Journal of Ethnopharmacology*, 109, 388-393.
- Ajiboye, T. O., Salawu, N. A., Yakubu, M. T., Oladiji, A. T., Akanji, M. A. & Okogun, J. I. (2011). Antioxidant and drug detoxification potentials of *Hibiscus sabdariffa* anthocyanin extract. *Drug and Chemical Toxicology*, 34, 109-115.
- Al-Mudaffar Fawzi, N., Goodwin, K. P., Mahdi, B. A. & Stevens, M. L. (2016). Effects of Mesopotamian Marsh (Iraq) desiccation on the cultural knowledge and livelihood of Marsh Arab women. *Ecosystem Health and Sustainability*, 2, e01207.
- Alarcón-Alonso, J., Zamilpa, A., Aguilar, F. A., Herrera-Ruiz, M., Tortoriello, J. & Jimenez-Ferrer, E. (2012). Pharmacological characterization of the diuretic effect of *Hibiscus sabdariffa* Linn (Malvaceae) extract. *Journal of Ethnopharmacology*, 139, 751-756.
- Ali, B., Mousa, H. & El-Mougy, S. (2003). The effect of a water extract and anthocyanins of *Hibiscus sabdariffa* L. on paracetamol-induced hepatotoxicity in rats. *Phytotherapy Research*, 17, 56-59.
- Ali, B. H., Wabel, N. A. & Blunden, G. (2005). Phytochemical, pharmacological and toxicological aspects of *Hibiscus sabdariffa* L.: a review. *Phytotherapy Research*, 19, 369-375.
- Ali, M., Salih, W., Mohamed, A. & Homeida, A. (1991). Investigation of the antispasmodic potential of *Hibiscus sabdariffa* calyces. *Journal of Ethnopharmacology*, 31, 249-257.

Amano, M., Ito, M., Kimura, K., Fukata, Y., Chihara, K., Nakano, T., Matsuura, Y. & Kaibuchi, K. (1996). Phosphorylation and activation of myosin by Rho-associated kinase (Rho-kinase). *Journal of Biological Chemistry*, 271, 20246-20249.

Amano, M., Nakayama, M. & Kaibuchi, K. (2010). Rho-kinase/ROCK: a key regulator of the cytoskeleton and cell polarity. *Cytoskeleton*, 67, 545-554.

Amor, I. L.-B., Boubaker, J., Sgaier, M. B., Skandrani, I., Bhouri, W., Neffati, A., Kilani, S., Bouhlel, I., Ghedira, K. & Chekir-Ghedira, L. (2009). Phytochemistry and biological activities of *Phlomis* species. *Journal of Ethnopharmacology*, 125, 183-202.

Andriambeloson, E., Kleschyov, A. L., Muller, B., Beretz, A., Stoclet, J. C. & Andriantsitohaina, R. (1997). Nitric oxide production and endothelium-dependent vasorelaxation induced by wine polyphenols in rat aorta. *British Journal of Pharmacology*, 120, 1053-1058.

Andriambeloson, E., Magnier, C. L., Haan-Archipoff, G., Lobstein, A., Anton, R., Beretz, A., Stoclet, J. C. & Andriantsitohaina, R. (1998). Natural dietary polyphenolic compounds cause endothelium-dependent vasorelaxation in rat thoracic aorta. *The Journal of Nutrition*, 128, 2324-2333.

Archer, S. L., Huang, J., Hampl, V., Nelson, D. P., Shultz, P. J. & Weir, E. K. (1994). Nitric oxide and cGMP cause vasorelaxation by activation of a charybdotoxin-sensitive K channel by cGMP-dependent protein kinase. *Proceedings of the National Academy of Sciences*, 91, 7583-7587.

Auguet, M., Delaflotte, S., Chabrier, P.-E., Pirotzky, E., Clostre, F. & Braquet, P. (1988). Endothelin and  $\text{Ca}^{2+}$  agonist bay K 8644: Different vasoconstrictive properties. *Biochemical and Biophysical Research Communications*, 156, 186-192.

Bafana, A., Dutt, S., Kumar, A., Kumar, S. & Ahuja, P. S. (2011). The basic and applied aspects of superoxide dismutase. *Journal of Molecular Catalysis B: Enzymatic*, 68, 129-138.

Balogun, M. E., Nwachukwu, D. C., Iyare, E. E., Besong, E. E., Obimma, J. N. & Djobissie, S. F. (2016). Antihypertensive effect of methanolic extract from the leaves of *Hibiscus Sabdariffa* L. in rats. *Der Pharmacia Lettre*, 8, 473-484.

Bárány, M. (1996). *Biochemistry of smooth muscle contraction*, Elsevier.

Barron, J. T., Barany, M., Bárány, K. & Storti, R. V. (1980). Reversible phosphorylation and dephosphorylation of the 20,000-dalton light chain of myosin during the contraction-relaxation-contraction cycle of arterial smooth muscle. *Journal of Biological Chemistry*, 255, 6238-6244.

Beltran-Debon, R., Alonso-Villaverde, C., Aragones, G., Rodriguez-Medina, I., Rull, A., Micol, V., Segura-Carretero, A., Fernandez-Gutierrez, A., Camps, J. & Joven, J. (2010). The aqueous extract of *Hibiscus sabdariffa* calices modulates the production of monocyte chemoattractant protein-1 in humans. *Phytomedicine*, 17, 186-191.

Benito, S., Lopez, D., Sáiz, M. P., Buxaderas, S., Sánchez, J., Puig-Parellada, P. & Mitjavila, M. T. (2002). A flavonoid-rich diet increases nitric oxide production in rat aorta. *British Journal of Pharmacology*, 135, 910-916.

Berridge, M., Heslop, J., Irvine, R. & Brown, K. (1984). Inositol trisphosphate formation and calcium mobilization in Swiss 3T3 cells in response to platelet-derived growth factor. *Biochemical Journal*, 222, 195-201.

Bers, D. M. (2002). Cardiac excitation-contraction coupling. *Nature*, 415, 198.

Bers, D. M., Patton, C. W. & Nuccitelli, R. (2010). A practical guide to the preparation of  $\text{Ca}^{2+}$  buffers. *Methods in Cell Biology*, 99, 1-26.

Bers, D. M. & Perez-Reyes, E. (1999). Ca channels in cardiac myocytes: structure and function in Ca influx and intracellular Ca release. *Cardiovascular Research*, 42, 339-360.

Billington, C. K. & Penn, R. B. (2003). Signaling and regulation of G protein-coupled receptors in airway smooth muscle. *Respiratory Research*, 4, 2-2.

Bishop, A. L. & Alan, H. (2000). Rho GTPases and their effector proteins. *Biochemical Journal*, 348, 241-255.

Bolade, M., Oluwalana, I. & Ojo, O. (2009). Commercial practice of roselle (*Hibiscus sabdariffa* L.) beverage production: Optimization of hot water extraction and sweetness level. *World Journal of Agricultural Sciences*, 5, 126-131.

Boll, P. M., Sorensen, E. & Balieu, E. (1969). Naturally Occurring Lactones and Lactams. III. The absolute configuration of the hydroxycitric acid lactones; hibiscus acid and garcinia acid. *Acta Chemica Scandinavica*, 23, 286-293.

Bolotina, V. M., Najibi, S., Palacino, J. J., Pagano, P. J. & Cohen, R. A. (1994). Nitric oxide directly activates calcium-dependent potassium channels in vascular smooth muscle. *Nature*, 368, 850-853.

Bolton, T. B. (1979). Mechanisms of action of transmitters and other substances on smooth muscle. *Physiological Reviews*, 59, 606-718.

Bonnevier, J. & Arner, A. (2004). Actions downstream of cyclic GMP/protein kinase G can reverse protein kinase C-mediated phosphorylation of CPI-17 and  $\text{Ca}^{2+}$  sensitization in smooth muscle. *Journal of Biological Chemistry*, 279, 28998-29003.

Brovkovich, V. V., Kalinowski, L., Muller-Peddinghaus, R. & Malinski, T. (2001). Synergistic Antihypertensive Effects of Nifedipine on Endothelium : Concurrent Release of NO and Scavenging of Superoxide. *Hypertension*, 37, 34-39.

Brown, A. M. (1990). Regulation of heartbeat by G protein-coupled ion channels. *American Journal of Physiology-Heart and Circulatory Physiology*, 259, H1621-H1628.

Bülbring, E. & Tomita, T. (1987). Catecholamine action on smooth muscle. *Pharmacological Reviews*, 39, 49-96.

Calis, I., Kuruüzüm, A., Demirezer, L. Ö., Sticher, O., Gancı, W. & Rüedi, P. (1999). Phenylvaleric Acid and Flavonoid Glycosides from *Polygonum salicifolium*. *Journal of Natural Products*, 62, 1101-1105.

Carabelli, V., D'ascenzo, M., Carbone, E. & Grassi, C. (2002). Nitric oxide inhibits neuroendocrine Ca(V)1 L-channel gating via cGMP-dependent protein kinase in cell-attached patches of bovine chromaffin cells. *The Journal of Physiology*, 541, 351-366.

Carvajal-Zarrabal, O., Waliszewski, S. M., Barradas-Dermitz, D. M., Orta-Flores, Z., Hayward-Jones, P. M., Nolasco-Hipólito, C., Angulo-Guerrero, O., Sánchez-Ricaño, R., Infanzón, R. M. & Trujillo, P. R. (2005). The consumption of *Hibiscus sabdariffa* dried calyx ethanolic extract reduced lipid profile in rats. *Plant Foods for Human Nutrition*, 60, 153-159.

Carvajal, J. A., Germain, A. M., Huidobro-Toro, J. P. & Weiner, C. P. (2000). Molecular mechanism of cGMP-mediated smooth muscle relaxation. *Journal of Cellular Physiology*, 184, 409-420.

Chang, H. C., Peng, C. H., Yeh, D. M., Kao, E. S. & Wang, C. J. (2014). *Hibiscus sabdariffa* extract inhibits obesity and fat accumulation, and improves liver steatosis in humans. *Food & Function*, 5, 734-739.

Chang, Y.-C., Huang, K.-X., Huang, A.-C., Ho, Y.-C. & Wang, C.-J. (2006). Hibiscus anthocyanins-rich extract inhibited LDL oxidation and oxLDL-mediated macrophages apoptosis. *Food and Chemical Toxicology*, 44, 1015-1023.

Chen, C.-C., Chou, F.-P., Ho, Y.-C., Lin, W.-L., Wang, C.-P., Kao, E.-S., Huang, A.-C. & Wang, C.-J. (2004). Inhibitory effects of *Hibiscus sabdariffa* L extract on low-density lipoprotein oxidation and anti-hyperlipidemia in fructose-fed and cholesterol-fed rats. *Journal of the Science of Food and Agriculture*, 84, 1989-1996.

Chen, C.-C., Hsu, J.-D., Wang, S.-F., Chiang, H.-C., Yang, M.-Y., Kao, E.-S., Ho, Y.-C. & Wang, C.-J. (2003). *Hibiscus sabdariffa* extract inhibits the development of atherosclerosis in cholesterol-fed rabbits. *Journal of Agricultural and Food Chemistry*, 51, 5472-5477.

Cheng, H., Lederer, W. J. & Cannell, M. B. (1993). Calcium sparks: elementary events underlying excitation-contraction coupling in heart muscle. *Science*, 262, 740-744.

Compean, K. & Ynalvez, R. (2014). Antimicrobial activity of plant secondary metabolites: A review. *Research Journal of Medicinal Plants*, 8, 204-213.

Da-Costa-Rocha, I., Bonnlaender, B., Sievers, H., Pischel, I. & Heinrich, M. (2014). *Hibiscus sabdariffa* L.—A phytochemical and pharmacological review. *Food Chemistry*, 165, 424-443.

- Delmotte, P., Ressmeyer, A.-R., Bai, Y. & Sanderson, M. J. (2010). Mechanisms of airway smooth muscle relaxation induced by beta2-adrenergic agonists. *Frontiers in Bioscience*, 15, 750-764.
- Denninger, J. W. & Marletta, M. A. (1999). Guanylate cyclase and the ·NO/cGMP signaling pathway. *Biochimica et Biophysica Acta (BBA) - Bioenergetics*, 1411, 334-350.
- Devarajan, S., Yahiro, E., Uehara, Y., Kuroda, R., Hirano, Y., Nagata, K., Miura, S., Saku, K. & Urata, H. (2018). Depressor effect of the young leaves of *Polygonum hydropiper* Linn. in high-salt induced hypertensive mice. *Biomedicine & Pharmacotherapy*, 102, 1182-1187.
- Downes, P. & Michell, R. H. (1982). Phosphatidylinositol 4-phosphate and phosphatidylinositol 4, 5-bisphosphate: lipids in search of a function. *Cell Calcium*, 3, 467-502.
- Droogmans, G., Raeymaekers, L. & Casteels, R. (1977). Electro-and pharmacomechanical coupling in the smooth muscle cells of the rabbit ear artery. *The Journal of General Physiology*, 70, 129-148.
- Duarte, J., Andriambeloson, E., Diebolt, M. & Andriantsitohaina, R. (2004). Wine polyphenols stimulate superoxide anion production to promote calcium signaling and endothelial-dependent vasodilatation. *Physiological Research*, 53, 595-602.
- Duarte, J., Pérez-Vizcaíno, F., Zarzuelo, A., Jiménez, J. & Tamargo, J. (1993). Vasodilator effects of quercetin in isolated rat vascular smooth muscle. *European Journal of Pharmacology*, 239, 1-7.
- Dzoyem, J. P., Nkuete, A. H., Kuete, V., Tala, M. F., Wabo, H. K., Guru, S. K., Rajput, V. S., Sharma, A., Tane, P. & Khan, I. A. (2012). Cytotoxicity and antimicrobial activity of the methanol extract and compounds from *Polygonum limbatum*. *Planta Medica*, 78, 787-792.
- Dzoyem, J. P., Nkuete, A. H., Ngameni, B. & Eloff, J. N. (2017). Anti-inflammatory and anticholinesterase activity of six flavonoids isolated from *Polygonum* and *Dorstenia* species. *Archives of Pharmacal Research*, 40, 1129-1134.
- Eisner, D. A., Caldwell, J. L., Kistamás, K. & Trafford, A. W. (2017). Calcium and Excitation-Contraction Coupling in the Heart. *Circulation Research*, 121, 181-195.
- El-Anwar, R., Ibrahim, A., Abo El-Seoud, K. & Kabbask, A. (2016). Phytochemical and biological studies on *Persicaria salicifolia* Brouss. Ex Willd growing in Egypt. *International Research Journal of Pharmacy*, 7, 4-12.
- El-Saadany, S. S., Sitohy, M. Z., Labib, S. M. & El-Massry, R. A. (1991). Biochemical dynamics and hypocholesterolemic action of *Hibiscus sabdariffa* (Karkade). *Nahrung*, 35, 567-576.

Fabiato, A. (1983). Calcium-induced release of calcium from the cardiac sarcoplasmic reticulum. *American Journal of Physiology-Cell Physiology*, 245, C1-C14.

Faraji, M. H. & Tarkhani, A. H. (1999). The effect of sour tea (*Hibiscus sabdariffa*) on essential hypertension. *Journal of Ethnopharmacology*, 65, 231-236.

Farombi, E. & Ige, O. (2007). Hypolipidemic and antioxidant effects of ethanolic extract from dried calyx of *Hibiscus sabdariffa* in alloxan-induced diabetic rats. *Fundamental & Clinical Pharmacology*, 21, 601-609.

Fleischmann, B. K., Murray, R. K. & Kotlikoff, M. I. (1994). Voltage window for sustained elevation of cytosolic calcium in smooth muscle cells. *Proceedings of the National Academy of Sciences of the United States of America*, 91, 11914-11918.

Frank, T., Netzel, G., Kammerer, D. R., Carle, R., Kler, A., Kriesl, E., Bitsch, I., Bitsch, R. & Netzel, M. (2012). Consumption of *Hibiscus sabdariffa* L. aqueous extract and its impact on systemic antioxidant potential in healthy subjects. *Journal of the Science of Food and Agriculture*, 92, 2207-2218.

Furukawa, K., Tawada, Y. & Shigekawa, M. (1988). Regulation of the plasma membrane Ca<sup>2+</sup> pump by cyclic nucleotides in cultured vascular smooth muscle cells. *Journal of Biological Chemistry*, 263, 8058-8065.

Gerthoffer, W. T. & Larsen, J. K. (2000). Regulation of smooth muscle contraction. *Advances in Organ Biology*, 8, 49-80.

Godfraind, T. (1983). Actions of nifedipine on calcium fluxes and contraction in isolated rat arteries. *Journal of Pharmacology and Experimental Therapeutics*, 224, 443-450.

Godfraind, T. (1986). Calcium entry blockade and excitation contraction coupling in the cardiovascular system (with an attempt of pharmacological classification). *Acta Pharmacologica et Toxicologica*, 58 Suppl 2, 5-30.

Godfraind, T., Egleme, C. & Al Osachie, I. (1985). Role of endothelium in the contractile response of rat aorta to α-adrenoceptor agonists. *Clinical Science*, 68, 65s-71s.

Gosain, S., Ircchiaya, R., Sharma, P. C., Thareja, S., Kalra, A., Deep, A. & Bhardwaj, T. R. (2010). Hypolipidemic effect of ethanolic extract from the leaves of *Hibiscus sabdariffa* L. in hyperlipidemic rats. *Acta Poloniae Pharmaceutica*, 67, 179-184.

Grodner, B. & Sitkiewicz, D. (2013). [Enantiomers: a new problem in pharmacotherapy of depression?]. *Psychiatria polska*, 47, 511-518.

Günther, J., Dhein, S., Rösen, R., Klaus, W. & Fricke, U. (1992). Nitric oxide (EDRF) enhances the vasorelaxing effect of nitrendipine in various isolated arteries. *Basic Research in Cardiology*, 87, 452-460.

Gurrola-Diaz, C. M., Garcia-Lopez, P. M., Sanchez-Enriquez, S., Troyo-Sanroman, R., Andrade-Gonzalez, I. & Gomez-Leyva, J. F. (2010). Effects of *Hibiscus sabdariffa* extract powder and preventive treatment (diet) on the lipid profiles of patients with metabolic syndrome (MeSy). *Phytomedicine*, 17, 500-505.

Hailemariam, A., Feyera, M., Deyou, T. & Abdissa, N. (2018). Antimicrobial Chalcones from the Seeds of *Persicaria lapathifolia*. *Biochemistry & Pharmacology (Los Angel)*, 7, 2167-0501.

Halliwell, B. (1996). Antioxidants in human health and disease. *Annual Review of Nutrition*, 16, 33-50.

Hamdan, M. A., Asada, T., Hassan, F. M., Warner, B. G., Douabul, A., Al-Hilli, M. R. & Alwan, A. (2010). Vegetation response to re-flooding in the Mesopotamian Wetlands, Southern Iraq. *Wetlands*, 30, 177-188.

Hansawasdi, C., Kawabata, J. & Kasai, T. (2000).  $\alpha$ -Amylase inhibitors from roselle (*Hibiscus sabdariffa* Linn.) tea. *Bioscience, Biotechnology, and Biochemistry*, 64, 1041-1043.

Hartshorne, D. J. (1987). Biochemistry of the contractile process in smooth muscle. *Physiology of the Gastrointestinal Tract*, 423-482.

Herranz-Lopez, M., Fernandez-Arroyo, S., Perez-Sanchez, A., Barrajon-Catalan, E., Beltran-Debon, R., Menendez, J. A., Alonso-Villaverde, C., Segura-Carretero, A., Joven, J. & Micol, V. (2012). Synergism of plant-derived polyphenols in adipogenesis: perspectives and implications. *Phytomedicine*, 19, 253-261.

Herrera-Arellano, A., Flores-Romero, S., Chavez-Soto, M. A. & Tortoriello, J. (2004). Effectiveness and tolerability of a standardized extract from *Hibiscus sabdariffa* in patients with mild to moderate hypertension: a controlled and randomized clinical trial. *Phytomedicine*, 11, 375-382.

Herrera-Arellano, A., Miranda-Sánchez, J., Ávila-Castro, P., Herrera-Álvarez, S., Jiménez-Ferrer, J. E., Zamilpa, A., Román-Ramos, R., Ponce-Monter, H. & Tortoriello, J. (2007). Clinical effects produced by a standardized herbal medicinal product of *Hibiscus sabdariffa* on patients with hypertension. A randomized, double-blind, lisinopril-controlled clinical trial. *Planta Medica*, 73, 6-12.

Hida, H., Yamada, T. & Yamada, Y. (2005). Production of hydroxycitric acid by microorganisms. *Bioscience, Biotechnology, and Biochemistry*, 69, 1555-1561.

Hida, H., Yamada, T. & Yamada, Y. (2006). Absolute configuration of hydroxycitric acid produced by microorganisms. *Bioscience, Biotechnology, and Biochemistry*, 70, 1972-1974.

Hirata, K., Kikuchi, A., Sasaki, T., Kuroda, S., Kaibuchi, K., Matsuura, Y., Seki, H., Saida, K. & Takai, Y. (1992). Involvement of rho p21 in the GTP-enhanced calcium ion sensitivity of smooth muscle contraction. *Journal of Biological Chemistry*, 267, 8719-8722.

Hirunpanich, V., Utaipat, A., Morales, N. P., Bunyapraphatsara, N., Sato, H., Herunsale, A. & Suthisisang, C. (2006). Hypocholesterolemic and antioxidant effects of aqueous extracts from the dried calyx of *Hibiscus sabdariffa* L. in hypercholesterolemic rats. *Journal of Ethnopharmacology*, 103, 252-260.

Hopkins, A. L., Lamm, M. G., Funk, J. L. & Ritenbaugh, C. (2013). *Hibiscus sabdariffa* L. in the treatment of hypertension and hyperlipidemia: a comprehensive review of animal and human studies. *Fitoterapia*, 85, 84-94.

Hou, X., Liu, Y., Niu, L., Cui, L. & Zhang, M. (2014). Enhancement of voltage-gated K<sup>+</sup> channels and depression of voltage-gated Ca<sup>2+</sup> channels are involved in quercetin-induced vasorelaxation in rat coronary artery. *Planta Medica*, 80, 465-472.

Hussein, S., Usama, E.-M., Tantawy, M., Kawashty, S. & Saleh, N. (2017). Phenolics of selected species of Persicaria and Polygonum (Polygonaceae) in Egypt. *Arabian Journal of Chemistry*, 10, 76-81.

Hussein, S. R. & Mohamed, A. A. (2013). Antioxidant activity and phenolic profiling of two Egyptian medicinal herbs *Polygonum salicifolium* Brouss ex Wild and *Polygonum senegalense* Meisn. *Analele Universității din Oradea, Fascicula Biologie Tom*, 20, 59-63.

Ibnusaud, I., Thomas, P. T., Rani, R. N., Sasi, P. V., Beena, T. & Hisham, A. (2002). Chiral γ-butyrolactones related to optically active 2-hydroxycitric acids. *Tetrahedron*, 58, 4887-4892.

Ignarro, L. J., Buga, G. M., Wood, K. S., Byrns, R. E. & Chaudhuri, G. (1987). Endothelium-derived relaxing factor produced and released from artery and vein is nitric oxide. *Proceedings of the National Academy of Sciences*, 84, 9265-9269.

Inuwa, I., Ali, B. H., Al-Lawati, I., Beegam, S., Ziada, A. & Blunden, G. (2012). Long-term ingestion of *Hibiscus sabdariffa* calyx extract enhances myocardial capillarization in the spontaneously hypertensive rat. *Experimental Biology and Medicine*, 237, 563-569.

Janssen, L. J. (1996). Acetylcholine and caffeine activate Cl-and suppress K<sup>+</sup> conductances in human bronchial smooth muscle. *American Journal of Physiology-Lung Cellular and Molecular Physiology*, 270, L772-L781.

Jena, B., Jayaprakasha, G., Singh, R. & Sakariah, K. (2002a). Chemistry and biochemistry of (-)-hydroxycitric acid from Garcinia. *Journal of Agricultural and Food Chemistry*, 50, 10-22.

Jena, B. S., Jayaprakasha, G. K. & Sakariah, K. K. (2002b). Organic Acids from Leaves, Fruits, and Rinds of Garcinia cowa. *Journal of Agricultural and Food Chemistry*, 50, 3431-3434.

Ji, T., Lin, C., Krill, L. S., Eskander, R., Guo, Y., Zi, X. & Hoang, B. H. (2013). Flavokawain B, a kava chalcone, inhibits growth of human osteosarcoma cells through G2/M cell cycle arrest and apoptosis. *Molecular Cancer*, 12, 55-66.

Kamm, K. E. & Stull, J. T. (1985). The function of myosin and myosin light chain kinase phosphorylation in smooth muscle. *Annual Review of Pharmacology and Toxicology*, 25, 593-620.

Kao, E.-S., Tseng, T.-H., Lee, H.-J., Chan, K.-C. & Wang, C.-J. (2009). Anthocyanin extracted from Hibiscus attenuate oxidized LDL-mediated foam cell formation involving regulation of CD36 gene. *Chemico-Biological Interactions*, 179, 212-218.

Karaki, H., Ahn, H. Y. & Urakawa, N. (1983). Hyperosmotic applications of KCl induce vascular smooth muscle contraction which is independent of external Ca. *The Japanese Journal of Pharmacology*, 33, 246-248.

Karaki, H., Ozaki, H., Hori, M., Mitsui-Saito, M., Amano, K.-I., Harada, K.-I., Miyamoto, S., Nakazawa, H., Won, K.-J. & Sato, K. (1997). Calcium movements, distribution, and functions in smooth muscle. *Pharmacological Reviews*, 49, 157-230.

Karaki, H. & Weiss, G. B. (1984). Calcium channels in smooth muscle. *Gastroenterology*, 87, 960-970.

Kawasaki, M., Kanomata, T. & Yoshitama, K. (1986). Flavonoids in the leaves of twenty-eight polygonaceous plants. *Botanical Society of Japan*, 99, 63-74.

Ke Chen, C. & Pace-Asciak, C. R. (1996). Vasorelaxing activity of resveratrol and quercetin in isolated rat aorta. *General Pharmacology: The Vascular System*, 27, 363-366.

Khodakhah, K., Melishchuk, A. & Armstrong, C. M. (1997). Killing K channels with TEA<sup>+</sup>. *Proceedings of the National Academy of Sciences*, 94, 13335-13338.

Knox, A. J. & Tattersfield, A. E. (1995). Airway smooth muscle relaxation. *Thorax*, 50, 894-901.

Kobirumaki-Shimozawa, F., Inoue, T., Shintani, S. A., Oyama, K., Terui, T., Minamisawa, S., Ishiwata, S. I. & Fukuda, N. (2014). Cardiac thin filament regulation and the Frank-Starling mechanism. *The Journal of Physiological Sciences*, 64, 221-232.

Kojda, G., Klaus, W., Werner, G. & Fricke, U. (1991). The influence of endothelium on the action of PGF 2α, and some dihydropyridine-type calcium antagonists in porcine basilar arteries. *Basic Research in Cardiology*, 86, 254-265.

Koyama, M., Ito, M., Feng, J., Seko, T., Shiraki, K., Takase, K., Hartshorne, D. J. & Nakano, T. (2000). Phosphorylation of CPI-17, an inhibitory phosphoprotein of smooth muscle myosin phosphatase, by Rho-kinase. *FEBS Letters*, 475, 197-200.

Kuriyama, H., Kitamura, K., Itoh, T. & Inoue, R. (1998). Physiological features of visceral smooth muscle cells, with special reference to receptors and ion channels. *Physiological Reviews*, 78, 811-920.

Kuriyan, R., Kumar, D. R., Rajendran, R. & Kurpad, A. V. (2010). An evaluation of the hypolipidemic effect of an extract of *Hibiscus Sabdariffa* leaves in hyperlipidemic Indians: a double blind, placebo controlled trial. *BMC Complementary and Alternative Medicine*, 10, 27-35.

Lanerolle, P. D. & Paul, R. J. (1991). Myosin phosphorylation/dephosphorylation and regulation of airway smooth muscle contractility. *American Journal of Physiology-Lung Cellular and Molecular Physiology*, 261, L1-L14.

Layland, J. & Shah, A. M. (2002). Biochemistry and Physiology of Cardiac Muscle. *Medicine*, 30, 51-53.

Lee, C. H., Poburko, D., Sahota, P., Sandhu, J., Ruehlmann, D. O. & Van Breemen, C. (2001). The mechanism of phenylephrine-mediated  $[Ca^{2+}]_i$  oscillations underlying tonic contraction in the rabbit inferior vena cava. *The Journal of Physiology*, 534, 641-650.

Lee, W.-C., Wang, C.-J., Chen, Y.-H., Hsu, J.-D., Cheng, S.-Y., Chen, H.-C. & Lee, H.-J. (2009). Polyphenol extracts from *Hibiscus sabdariffa* Linnaeus attenuate nephropathy in experimental type 1 diabetes. *Journal of Agricultural and Food Chemistry*, 57, 2206-2210.

Lewis, Y. S. & Neelakantan, S. (1965). (–)-Hydroxycitric acid—the principal acid in the fruits of *Garcinia cambogia* desr. *Phytochemistry*, 4, 619-625.

Lim, Y. C., Budin, S. B., Othman, F., Latip, J. & Zainalabidin, S. (2017). Roselle Polyphenols Exert Potent Negative Inotropic Effects via Modulation of Intracellular Calcium Regulatory Channels in Isolated Rat Heart. *Cardiovascular Toxicology*, 17, 251-259.

Lin, C.-T., Senthil Kumar, K. J., Tseng, Y.-H., Wang, Z.-J., Pan, M.-Y., Xiao, J.-H., Chien, S.-C. & Wang, S.-Y. (2009). Anti-inflammatory Activity of Flavokawain B from *Alpinia pricei* Hayata. *Journal of Agricultural and Food Chemistry*, 57, 6060-6065.

Lin, T.-L., Lin, H.-H., Chen, C.-C., Lin, M.-C., Chou, M.-C. & Wang, C.-J. (2007). *Hibiscus sabdariffa* extract reduces serum cholesterol in men and women. *Nutrition Research*, 27, 140-145.

Lin, W. L., Hsieh, Y. J., Chou, F. P., Wang, C. J., Cheng, M. T. & Tseng, T. H. (2003). Hibiscus protocatechuic acid inhibits lipopolysaccharide-induced rat hepatic damage. *Archives of Toxicology*, 77, 42-47.

Linden, J. & Brooker, G. (1980). The influence of resting membrane potential on the effect of verapamil on atria. *Journal of Molecular and Cellular Cardiology*, 12, 325-331.

Lopez, S. N., Sierra, M. G., Gattuso, S. J., Furlán, R. L. & Zacchino, S. A. (2006). An unusual homoisoflavanone and a structurally-related dihydrochalcone from *Polygonum ferrugineum* (Polygonaceae). *Phytochemistry*, 67, 2152-2158.

Lowenstein, J. M. & Brunengraber, H. (1981). Hydroxycitrate. *Methods in Enzymology*, 72, 486-497.

Mathur, S. & Hoskins, C. (2017). Drug Development: Lessons from Nature. *Biomedical Reports*, 6, 612-614.

Matsuda, F., Sugahara, K., Sugita, M., Sadohara, T., Kiyota, T. & Terasaki, H. (2000). Comparative effect of amrinone, aminophylline and diltiazem on rat airway smooth muscle. *Acta Anaesthesiologica Scandinavica*, 44, 763-766.

Mcchesney, J. D., Venkataraman, S. K. & Henri, J. T. (2007). Plant natural products: Back to the future or into extinction? *Phytochemistry*, 68, 2015-2022.

McDonald, T. F., Pelzer, S., Trautwein, W. & Pelzer, D. J. (1994). Regulation and modulation of calcium channels in cardiac, skeletal, and smooth muscle cells. *Physiological Reviews*, 74, 365-507.

Mckay, D. L., Chen, C. O., Saltzman, E. & Blumberg, J. B. (2009). *Hibiscus sabdariffa* L. tea (tisane) lowers blood pressure in prehypertensive and mildly hypertensive adults. *The Journal of Nutrition*, 140, 298-303.

Meisheri, K. D., Dubray, L. a. C. & Oleynek, J. J. (1990). A sensitive *in vitro* functional assay to detect K<sup>+</sup> channel-dependent vasodilators. *Journal of Pharmacological Methods*, 24, 251-261.

Meisheri, K. D., Swirtz, M. A., Purohit, S. S., Cipkus-Dubray, L. A., Khan, S. A. & Oleynek, J. J. (1991). Characterization of K<sup>+</sup> channel-dependent as well as - independent components of pinacidil-induced vasodilation. *Journal of Pharmacology and Experimental Therapeutics*, 256, 492-499.

Micucci, M., Malaguti, M., Gallina Toschi, T., Di Lecce, G., Aldini, R., Angeletti, A., Chiarini, A., Budriesi, R. & Hrelia, S. (2015). Cardiac and Vascular Synergic Protective Effect of *Olea europea* L. Leaves and *Hibiscus sabdariffa* L. Flower Extracts. *Oxidative Medicine and Cellular Longevity*, 2015, 318125.

Mikawa, K., Kume, H. & Takagi, K. (1998). Effects of atrial natriuretic peptide and 8-brom cyclic guanosine monophosphate on human tracheal smooth muscle. *Arzneimittel-Forschung*, 48, 914-918.

Miller-Hance, W., Miller, J., Wells, J., Stull, J. & Kamm, K. (1988). Biochemical events associated with activation of smooth muscle contraction. *Journal of Biological Chemistry*, 263, 13979-13982.

Mohagheghi, A., Maghsoud, S., Khashayar, P. & Ghazi-Khansari, M. (2011). The effect of *Hibiscus sabdariffa* on lipid profile, creatinine, and serum electrolytes: a randomized clinical trial. *ISRN Gastroenterology*, 2011, 976019.

Mohamed, J., Shing, S. W., Idris, M. H. M., Budin, S. B. & Zainalabidin, S. (2013). The protective effect of aqueous extracts of roselle (*Hibiscus sabdariffa* L. UKMR-

2) against red blood cell membrane oxidative stress in rats with streptozotocin-induced diabetes. *Clinics*, 68, 1358-1363.

Mohd-Esa, N., Hern, F. S., Ismail, A. & Yee, C. L. (2010). Antioxidant activity in different parts of roselle (*Hibiscus sabdariffa* L.) extracts and potential exploitation of the seeds. *Food Chemistry*, 122, 1055-1060.

Mojiminiyi, F. B., Dikko, M., Muhammad, B. Y., Ojobor, P. D., Ajagbonna, O. P., Okolo, R. U., Igboekwe, U. V., Mojiminiyi, U. E., Fagbemi, M. A., Bello, S. O. & Anga, T. J. (2007). Antihypertensive effect of an aqueous extract of the calyx of *Hibiscus sabdariffa*. *Fitoterapia*, 78, 292-297.

Moncada, S., Palmer, R. M. & Higgs, E. A. (1988). The discovery of nitric oxide as the endogenous nitrovasodilator. *Hypertension*, 12, 365-372.

Morel, N. & Godfraind, T. (1991). Characterization in rat aorta of the binding sites responsible for blockade of noradrenaline-evoked calcium entry by nisoldipine. *British Journal of Pharmacology*, 102, 467-477.

Morgan, K. G. (1990). The role of calcium in the control of vascular tone as assessed by the  $\text{Ca}^{2+}$  indicator aequorin. *Cardiovascular Drugs and Therapy*, 4, 1355-1362.

Mozaffari-Khosravi, H., Ahadi, Z. & Barzegar, K. (2013). The effect of green tea and sour tea on blood pressure of patients with type 2 diabetes: a randomized clinical trial. *Journal of Dietary Supplements*, 10, 105-115.

Mozaffari-Khosravi, H., Jalali-Khanabadi, B.-A., Afkhami-Ardekani, M. & Fatehi, F. (2009a). Effects of sour tea (*Hibiscus sabdariffa*) on lipid profile and lipoproteins in patients with type II diabetes. *The Journal of Alternative and Complementary Medicine*, 15, 899-903.

Mozaffari-Khosravi, H., Jalali-Khanabadi, B., Afkhami-Ardekani, M., Fatehi, F. & Noori-Shakham, M. (2009b). The effects of sour tea (*Hibiscus sabdariffa*) on hypertension in patients with type II diabetes. *Journal of Human Hypertension*, 23, 48-54.

Murray, K. J. (1990). Cyclic amp and mechanisms of vasolidation. *Pharmacology & Therapeutics*, 47, 329-345.

Ndiaye, M., Chataigneau, T., Chataigneau, M. & Schini-Kerth, V. B. (2004). Red wine polyphenols induce EDHF-mediated relaxations in porcine coronary arteries through the redox-sensitive activation of the PI3-kinase/Akt pathway. *British Journal of Pharmacology*, 142, 1131-1136.

Nelson, M. T. & Quayle, J. M. (1995). Physiological roles and properties of potassium channels in arterial smooth muscle. *American Journal of Physiology-Cell Physiology*, 268, C799-C822.

Nguyen, L. A., He, H. & Pham-Huy, C. (2006). Chiral Drugs: An Overview. *International Journal of Biomedical Science : IJBS*, 2, 85-100.

Nishimura, K., Ota, M. & Ito, K. (1991). Existence of two components in the tonic contraction of rat aorta mediated by  $\alpha$ 1-adrenoceptor activation. *British Journal of Pharmacology*, 102, 215-221.

Nishio, M., Kigoshi, S. & Muramatsu, I. (1986). Mechanisms of tetraethylammonium-induced contraction in the canine coronary artery. *Pharmacology*, 33, 256-265.

Nwachukwu, D., Aneke, E., Nwachukwu, N., Obika, L., Nwagha, U. & Eze, A. (2015). Effect of *Hibiscus sabdariffa* on blood pressure and electrolyte profile of mild to moderate hypertensive Nigerians: A comparative study with hydrochlorothiazide. *Nigerian Journal of Clinical Practice*, 18, 762-770.

Obiefuna, P. C. M., Owolabi, O. A., Adegunloye, B. J., Obiefuna, I. P. & Sofola, O. A. (1994). The Petal Extract of *Hibiscus sabdariffa* Produces Relaxation of Isolated Rat Aorta. *International Journal of Pharmacognosy*, 32, 69-74.

Ochani, P. C. & D'mello, P. (2009). Antioxidant and antihyperlipidemic activity of *Hibiscus sabdariffa* Linn. leaves and calyces extracts in rats. *Indian Journal of Experimental Biology*, 47, 276-282.

Odigie, I., Ettarh, R. & Adigun, S. (2003). Chronic administration of aqueous extract of *Hibiscus sabdariffa* attenuates hypertension and reverses cardiac hypertrophy in 2K-1C hypertensive rats. *Journal of Ethnopharmacology*, 86, 181-185.

Ogweno Midiwo, J., Yenesew, A., Juma, B. F., Derese, S., Ayoo, J. A., Aluoch, A. O. & Guchu, S. (2002). Bioactive compounds from some Kenyan ethnomedicinal plants: Myrsinaceae, Polygonaceae and Psiadia punctulata. *Phytochemistry Reviews*, 1, 311-323.

Okumura, K., Ichihara, K. & Nagasaka, M. (1997). Effects of Aranidipine, a Novel Calcium Channel Blocker, on Mechanical Responses of the Isolated Rat Portal Vein: Comparison with Typical Calcium Channel Blockers and Potassium Channel Openers. *Journal of Cardiovascular Pharmacology*, 29, 209-215.

Olatunji, L. A., Adebayo, J. O., Oguntoye, O. B., Olatunde, N. O., Olatunji, V. A. & Soladoye, A. O. (2005). Effects of aqueous extracts of petals of red and green *Hibiscus sabdariffa*. on plasma lipid and hematological variables in rats. *Pharmaceutical Biology*, 43, 471-474.

Onyenekwe, P. C., Ajani, E. O., Ameh, D. A. & Gamaniel, K. S. (1999). Antihypertensive effect of roselle (*Hibiscus sabdariffa*) calyx infusion in spontaneously hypertensive rats and a comparison of its toxicity with that in Wistar rats. *Cell Biochemistry & Function*, 17, 199-206.

Owens, G. K. (1995). Regulation of differentiation of vascular smooth muscle cells. *Physiological Reviews*, 75, 487-517.

Owolabi, O. A., Adegunloye, B. J., Ajagbona, O. P., Sofola, O. A. & Obiefuna, P. C. M. (1995). Mechanism of Relaxant Effect Mediated by an Aqueous Extract of

*Hibiscus sabdariffa* Petals in Isolated Rat Aorta. *International Journal of Pharmacognosy*, 33, 210-214.

Palmer, R. M., Ferrige, A. G. & Moncada, S. (1987). Nitric oxide release accounts for the biological activity of endothelium-derived relaxing factor. *Nature*, 327, 524-526.

Parsons, S., Flack, H. D. & Wagner, T. (2013). Use of intensity quotients and differences in absolute structure refinement. *Acta Crystallographica Section B*, 69, 249-259.

Peng, C.-H., Chyau, C.-C., Chan, K.-C., Chan, T.-H., Wang, C.-J. & Huang, C.-N. (2011). *Hibiscus sabdariffa* polyphenolic extract inhibits hyperglycemia, hyperlipidemia, and glycation-oxidative stress while improving insulin resistance. *Journal of Agricultural and Food Chemistry*, 59, 9901-9909.

Quignard, J. F., Frapier, J. M., Harricane, M. C., Albat, B., Nargeot, J. & Richard, S. (1997). Voltage-gated calcium channel currents in human coronary myocytes. Regulation by cyclic GMP and nitric oxide. *The Journal of Clinical Investigation*, 99, 185-193.

Raeburn, D. & Brown, T. J. (1991). RP 49356 and cromakalim relax airway smooth muscle *in vitro* by opening a sulphonylurea-sensitive K<sup>+</sup> channel: A comparison with nifedipine. *Journal of Pharmacology and Experimental Therapeutics*, 256, 480-485.

Raffetto, J. D., Yu, P., Reslan, O. M., Xia, Y. & Khalil, R. A. (2012). Endothelium-dependent nitric oxide and hyperpolarization-mediated venous relaxation pathways in rat inferior vena cava. *Journal of Vascular Surgery*, 55, 1716-1725.

Ramakrishna, V. & Jailkhani, R. (2007). Evaluation of oxidative stress in Insulin Dependent Diabetes Mellitus (IDDM) patients. *Diagnostic Pathology*, 2, 22-28.

Rampe, D. & Dage, R. C. (1992). Functional interactions between two Ca<sup>2+</sup> channel activators,(S)-Bay K 8644 and FPL 64176, in smooth muscle. *Molecular Pharmacology*, 41, 599-602.

Refsum, H. & Landmark, K. (1975). The effect of a calcium-antagonistic drug, nifedipine, on the mechanical and electrical activity of the isolated rat atrium. *Acta Pharmacologica et Toxicologica*, 37, 369-376.

Robertson, B. E., Schubert, R., Hescheler, J. & Nelson, M. T. (1993). cGMP-dependent protein kinase activates Ca-activated K channels in cerebral artery smooth muscle cells. *American Journal of Physiology-Cell Physiology*, 265, C299-C303.

Roghani, M., Baluchnejadmojarad, T., Vaez-Mahdavi, M. R. & Roghani-Dehkordi, F. (2004). Mechanisms underlying quercetin-induced vasorelaxation in aorta of subchronic diabetic rats: an *in vitro* study. *Vascular Pharmacology*, 42, 31-35.

Roux, E., Molimard, M. & Marthan, R. (1998). Muscarinic stimulation of airway smooth muscle cells. *General Pharmacology: The Vascular System*, 31, 349-356.

Roy, B., Sicotte, B., Brochu, M. & St-Louis, J. (1995). Effects of nifedipine and Bay K 8644 on myotropic responses in aortic rings of pregnant rats. *European Journal of Pharmacology*, 280, 1-9.

Salah, A., Gathumbi, J. & Vierling, W. (2002). Inhibition of intestinal motility by methanol extracts of *Hibiscus sabdariffa* L.(Malvaceae) in rats. *Phytotherapy Research*, 16, 283-285.

Sarr, M., Ngom, S., Kane, M. O., Wele, A., Diop, D., Sarr, B., Gueye, L., Andriantsitohaina, R. & Diallo, A. S. (2009). *In vitro* vasorelaxation mechanisms of bioactive compounds extracted from *Hibiscus sabdariffa* on rat thoracic aorta. *Nutrition & Metabolism*, 6, 45-57.

Satoh, K., Yanagisawa, T. & Taira, N. (1980). Coronary vasodilator and cardiac effects of optical isomers of verapamil in the dog. *Journal of Cardiovascular Pharmacology*, 2, 309-318.

Savithramma, N., Linga, R. M. & Ankanna, S. (2011). Screening of traditional medicinal plants for secondary metabolites. *International Journal of Research in Pharmaceutical Sciences*, 4, 634-647

Segura-Carretero, A., Puertas-Mejia, M. A., Cortacero-Ramirez, S., Beltran, R., Alonso-Villaverde, C., Joven, J., Dinelli, G. & Fernandez-Gutierrez, A. (2008). Selective extraction, separation, and identification of anthocyanins from *Hibiscus sabdariffa* L. using solid phase extraction-capillary electrophoresis-mass spectrometry (time-of-flight /ion trap). *Electrophoresis*, 29, 2852-2861.

Seko, T., Ito, M., Kureishi, Y., Okamoto, R., Moriki, N., Onishi, K., Isaka, N., Hartshorne, D. J. & Nakano, T. (2003). Activation of RhoA and inhibition of myosin phosphatase as important components in hypertension in vascular smooth muscle. *Circulation Research*, 92, 411-418.

Serban, C., Sahebkar, A., Ursoniu, S., Andrica, F. & Banach, M. (2015). Effect of sour tea (*Hibiscus sabdariffa* L.) on arterial hypertension: a systematic review and meta-analysis of randomized controlled trials. *Journal of Hypertension*, 33, 1119-1127.

Sheldrick, G. M. (2015). Crystal structure refinement with SHELXL. *Acta Crystallographica Section C: Structural Chemistry*, 71, 3-8.

Sindi, H. A., Marshall, L. J. & Morgan, M. R. (2014). Comparative chemical and biochemical analysis of extracts of *Hibiscus sabdariffa*. *Food Chemistry*, 164, 23-29.

Sireeratawong, S., Itharat, A., Khonsung, P., Lertprasertsuke, N. & Jaijoy, K. (2013). Toxicity studies of the water extract from the calyces of *Hibiscus sabdariffa* L. in rats. *African Journal of Traditional, Complementary, and Alternative Medicines : AJTCAM*, 10, 122-127.

- Solaro, R. J. & Rarick, H. M. (1998). Troponin and tropomyosin: proteins that switch on and tune in the activity of cardiac myofilaments. *Circulation Research*, 83, 471-480.
- Somlyo, A., Walker, J., Goldman, Y., Trentham, D. R., Kobayashi, S., Kitazawa, T. & Somlyo, A. V. (1988). Inositol trisphosphate, calcium and muscle contraction. *Philosophical Transactions of the Royal Society of London. B, Biological Sciences*, 320, 399-414.
- Somlyo, A. P. & Somlyo, A. V. (1994). Signal transduction and regulation in smooth muscle. *Nature*, 372, 231-236.
- Somlyo, A. P., Wu, X., Walker, L. A. & Somlyo, A. V. (1999). Pharmacomechanical coupling: the role of calcium, G-proteins, kinases and phosphatases. *Reviews of Physiology, Biochemistry and Pharmacology*, 134, 201-234.
- Somlyo, A. V. & Somlyo, A. P. (1968). Electromechanical and pharmacomechanical coupling in vascular smooth muscle. *Journal of Pharmacology and Experimental Therapeutics*, 159, 129-145.
- Stankevičius, E., Dalsgaard, T., Kroigaard, C., Beck, L., Boedtkjer, E., Misfeldt, M. W., Nielsen, G., Schjorring, O., Hughes, A. & Simonsen, U. (2011). Opening of Small and Intermediate Calcium-Activated Potassium Channels Induces Relaxation Mainly Mediated by Nitric-Oxide Release in Large Arteries and Endothelium-Derived Hyperpolarizing Factor in Small Arteries from Rat. *Journal of Pharmacology and Experimental Therapeutics*, 339, 842-850.
- Stiles, G. L., Caron, M. G. & Lefkowitz, R. J. (1984). Beta-adrenergic receptors: biochemical mechanisms of physiological regulation. *Physiological Reviews*, 64, 661-743.
- Streefkerk, J. O., De Groot, A. A., Pfaffendorf, M. & Van Zwieten, P. A. (2002). Influence of the nature of pre-contraction on the responses to commonly employed vasodilator agents in rat-isolated aortic rings. *Fundamental & Clinical Pharmacology*, 16, 485-494.
- Tanaka, Y., Aida, M., Tanaka, H., Shigenobu, K. & Toro, L. (1998). Involvement of maxi-K<sub>Ca</sub> channel activation in atrial natriuretic peptide-induced vasorelaxation. *Naunyn-Schmiedeberg's Archives of Pharmacology*, 357, 705-708.
- Tao, T., Gong, B.-J. & Leavis, P. C. (1990). Calcium-induced movement of troponin-I relative to actin in skeletal muscle thin filaments. *Science*, 247, 1339-1341.
- Tewari, K. & Simard, J. M. (1997). Sodium nitroprusside and cGMP decrease Ca<sup>2+</sup> channel availability in basilar artery smooth muscle cells. *Pflugers Archiv : European Journal of Physiology*, 433, 304-311.
- Thomas, G., Chung, M. & Cohen, C. J. (1985). A dihydropyridine (Bay k 8644) that enhances calcium currents in guinea pig and calf myocardial cells. A new type of positive inotropic agent. *Circulation Research*, 56, 87-96.

Triggle, C. R. (2012). The endothelium: influencing vascular smooth muscle in many ways. *Canadian Journal of Physiology & Pharmacology*, 90, 713-739.

Tseng, T.-H., Kao, E.-S., Chu, C.-Y., Chou, F.-P., Wu, H.-W. L. & Wang, C.-J. (1997). Protective effects of dried flower extracts of *Hibiscus sabdariffa* L. against oxidative stress in rat primary hepatocytes. *Food and Chemical Toxicology*, 35, 1159-1164.

Tseng, T.-H., Wang, C.-J. & Kao, E.-S. (1996). Hibiscus protocatechuic acid protects against oxidative damage induced by tert-butylhydroperoxide in rat primary hepatocytes. *Chemico-Biological Interactions*, 101, 137-148.

Uehata, M., Ishizaki, T., Satoh, H., Ono, T., Kawahara, T., Morishita, T., Tamakawa, H., Yamagami, K., Inui, J. & Maekawa, M. (1997). Calcium sensitization of smooth muscle mediated by a Rho-associated protein kinase in hypertension. *Nature*, 389, 990-994.

Usoh, I., Akpan, E., Etim, E. & Farombi, E. (2005). Antioxidant actions of dried flower extracts of *Hibiscus sabdariffa* L. on sodium arsenite-induced oxidative stress in rats. *Pakistan Journal of Nutrition*, 4, 135-141.

Van Breemen, C., Hwang, O. & Meisher, K. D. (1981). The mechanism of inhibitory action of diltiazem on vascular smooth muscle contractility. *Journal of Pharmacology and Experimental Therapeutics*, 218, 459-463.

Vaughan-Jones, R. (1986). Excitation and contraction in heart: the role of calcium. *British Medical Bulletin*, 42, 413-420.

Wang, C.-J., Wang, J.-M., Lin, W.-L., Chu, C.-Y., Chou, F.-P. & Tseng, T.-H. (2000). Protective effect of Hibiscus anthocyanins against tert-butyl hydroperoxide-induced hepatic toxicity in rats. *Food and Chemical Toxicology*, 38, 411-416.

Wang, J., Cao, X., Jiang, H., Qi, Y., Chin, K. L. & Yue, Y. (2014). Antioxidant activity of leaf extracts from different *Hibiscus sabdariffa* accessions and simultaneous determination five major antioxidant compounds by LC-Q-TOF-MS. *Molecules*, 19, 21226-21238.

Webb, R. C. (2003). Smooth muscle contraction and relaxation. *Advances in Physiology Education*, 27, 201-206.

Winslow, E., Farmer, S., Martorana, M. & Marshall, R. J. (1986). The effects of bepridil compared with calcium antagonists on rat and rabbit aorta. *European Journal of Pharmacology*, 131, 219-228.

Wong, P. K., Yusof, S., Ghazali, H. M. & Che Man, Y. B. (2002). Physico-chemical characteristics of roselle (*Hibiscus sabdariffa* L.). *Nutrition & Food Science*, 32, 68-73.

Woodsome, T. P., Polzin, A., Kitazawa, K., Eto, M. & Kitazawa, T. (2006). Agonist- and depolarization-induced signals for myosin light chain phosphorylation and force

generation of cultured vascular smooth muscle cells. *Journal of Cell Science*, 119, 1769-1780.

Wynne, B. M., Chiao, C.-W. & Webb, R. C. (2009). Vascular Smooth Muscle Cell Signaling Mechanisms for Contraction to Angiotensin II and Endothelin-1. *Journal of the American Society of Hypertension : JASH*, 3, 84-95.

Xuan, T. D., Fukuta, M., Wei, A. C., Elzaawely, A. A., Khanh, T. D. & Tawata, S. (2008). Efficacy of extracting solvents to chemical components of kava (*Piper methysticum*) roots. *Journal of Natural Medicines*, 62, 188-194.

Yamada, T., Hida, H. & Yamada, Y. (2007). Chemistry, physiological properties, and microbial production of hydroxycitric acid. *Applied Microbiology and Biotechnology*, 75, 977-982.

Yamakage, M., Hirshman, C. A. & Croxton, T. L. (1996). Sodium nitroprusside stimulates  $\text{Ca}^{2+}$ -activated  $\text{K}^+$  channels in porcine tracheal smooth muscle cells. *American Journal of Physiology-Lung Cellular and Molecular Physiology*, 270, L338-L345.

Yamamoto, H., Hwang, O. & Van Breeman, C. (1984). Bay K8644 differentiates between potential and receptor operated  $\text{Ca}^{2+}$  channels. *European Journal of Pharmacology*, 102, 555-557.

Yang, M.-Y., Peng, C.-H., Chan, K.-C., Yang, Y.-S., Huang, C.-N. & Wang, C.-J. (2009). The hypolipidemic effect of *Hibiscus sabdariffa* polyphenols via inhibiting lipogenesis and promoting hepatic lipid clearance. *Journal of Agricultural and Food Chemistry*, 58, 850-859.

Yenjai, C. & Wanich, S. (2010). Cytotoxicity against KB and NCI-H187 cell lines of modified flavonoids from *Kaempferia parviflora*. *Bioorganic & Medicinal Chemistry Letters*, 20, 2821-2823.

Yoshiaki, O., Tadashi, K., Kumiko, A., Hirohumi, T., Toru, T. & Tatsuyuki, N. (1991). Effect of TC-81, a new dihydropyridine derivative, on  $\text{K}^+$ -induced contraction in rat aorta. *European Journal of Pharmacology*, 205, 49-54.

Yoshida, Y., Sun, H.-T., Cai, J.-Q. & Imai, S. (1991). Cyclic GMP-dependent protein kinase stimulates the plasma membrane  $\text{Ca}^{2+}$  pump ATPase of vascular smooth muscle via phosphorylation of a 240-kDa protein. *Journal of Biological Chemistry*, 266, 19819-19825.

Yuan, T.-Y., Niu, Z.-R., Chen, D., Chen, Y.-C., Zhang, H.-F., Fang, L.-H. & Du, G.-H. (2018). Vasorelaxant effect of quercetin on cerebral basilar artery *in vitro* and the underlying mechanisms study. *Journal of Asian Natural Products Research*, 20, 477-487.

Zheng, W., Rampe, D. & Triggle, D. J. (1991). Pharmacological, radioligand binding, and electrophysiological characteristics of FPL 64176, a novel

nondihydropyridine  $\text{Ca}^{2+}$  channel activator, in cardiac and vascular preparations. *Molecular Pharmacology*, 40, 734-741.

Zheoat, A. M., Gray, A. I., Igoli, J. O., Kennedy, A. R. & Ferro, V. A. (2017). Crystal structures of hibiscus acid and hibiscus acid dimethyl ester isolated from *Hibiscus sabdariffa* (Malvaceae). *Acta Crystallographica Section E: Crystallographic Communications*, 73, 1368-1371.

Zhou, P., Gross, S., Liu, J.-H., Yu, B.-Y., Feng, L.-L., Nolta, J., Sharma, V., Piwnica-Worms, D. & Qiu, S. X. (2010). Flavokawain B, the hepatotoxic constituent from kava root, induces GSH-sensitive oxidative stress through modulation of IKK/NF-kappaB and MAPK signaling pathways. *The FASEB Journal*, 24, 4722-4732.

Zhou, W., Wei, L., Xiao, T., Lai, C., Peng, M., Xu, L., Luo, X., Deng, S. & Zhang, F. (2017). Diabetogenic agent alloxan is a proteasome inhibitor. *Biochemical and Biophysical Research Communications*, 488, 400-406.

Zhou, X.-B., Ruth, P., Schlossmann, J., Hofmann, F. & Korth, M. (1996). Protein phosphatase 2A is essential for the activation of  $\text{Ca}^{2+}$ -activated  $\text{K}^+$  currents by cGMP-dependent protein kinase in tracheal smooth muscle and Chinese hamster ovary cells. *Journal of Biological Chemistry*, 271, 19760-19767.